In vitro and *in vivo* characterization of histone deacetylase inhibitors as potential therapeutics for autosomal recessive proximal spinal muscular atrophy (SMA)

Inaugural-Dissertation
zur
Erlangung des Doktorgrades
der Mathematisch-Naturwissenschaftlichen Fakultät
der Universität zu Köln

vorgelegt von
Markus Rießland
aus Köln

Köln
2009

The Doctoral Thesis "*In vitro* and *in vivo* characterization of histone deacetylase inhibitors as potential therapeutics for autosomal recessive proximal spinal muscular atrophy (SMA)" was performed at the Institute of Human Genetics, Institute of Genetics and Centre for Molecular Medicine Cologne (CMMC) of the University of Cologne from July 2005 to 2009.

Berichterstatter/in Prof. Dr. rer. nat. Brunhilde Wirth
Prof. Dr. rer. nat. Manolis Pasparakis

Tag der letzten mündlichen Prüfung: 20.11.2009

Für meine Eltern

ACKNOWLEDGEMENTS

First, I wish to thank my supervisor Professor Dr. Brunhilde Wirth, for giving me the opportunity to work on various very interesting projects, for helpful discussions and encouragement, and for generous support to attend scientific congresses and further education. I appreciate that I could perform my thesis in Brunhilde Wirth´s laboratory.

I thank my examiners, Prof. Dr. Manolis Pasparakis and Prof. Dr. Ansgar Büschges.

A very big “Thank You!” to all past and present members of the Institute for Human Genetics and especially of the “SMA group” for ever being nice colleagues. I would like to thank Anja Förster for her excellent technical support and for always being motivated and interested. I thank Lutz Garbes for very helpful discussions about virtually everything and for carefully reading this manuscript. I thank Irmgard Hölker for staying by my left side since a quite long time and for her helpfulness. I thank Bastian Ackermann and Sandra Kröber, for always being nice and helpful. With you it was never boring in the lab! Thank You! A big “Thank You!” to Ylva Mende and Miriam Jakubik, for their nice and patient way to introduce me into “mouse-work”. Moreover, I thank Lars Brichta for all that he taught me at the beginning of my scientific carreer.

I am very grateful to Dr. Eric Hahnen for various helpful discussions, his help with the “Erlangen-project” and supplying me with new HDACis. I thank Jan Hauke and Sebastian Seufert for being always helpful in the lab.
I thank Karin Boß for carefully reading the manuscript.

I thank Darius Zlotos for synthesizing SAHA. I thank Prof. Sendtner for supplying us with SMA-like mice. A big thank to J.J. Buggy and Gloucester pharmaceuticals for supplying us with PCI-34051 and FK228. I thank Christian Tränkle for performing the *in vitro* HDAC activity test.

I thank Christoph Patsch for motivating discussions, being a perfect fellow student and being a good friend.

I wish to thank Sandra Stelter for her great support in everything and for just being there.

I thank parents and my grandmother. Without their everlasting support, it would never have been possible to study biology or to perform this work. Thank you! I thank Sonja Antweiler for being the best big sister one can imagine.

Table of contents

List of abbreviations

A	adenine
APS	ammonium persulfate
bp	base pair
BSA	bovine serum albumin
C	cytosine
CD	cluster of differentiation
cDNA	complementary DNA
cen	centromeric
CK	creatine kinase
cM	centimorgan
cm	centimeter
CNS	central nervous system
DEPC	diethylpyrocarbonate
D-MEM	Dulbecco's modified Eagle medium
DMSO	dimethylsulfoxide
DNA	deoxyribonucleic acid
EBV	Epstein-Barr virus
EDTA	ethylenediaminetetraacetic acid
e.g.	exempli gratia
EMG	electromyography
ESE	exonic splicing enhancer
ESS	exonic splicing silencer
et al.	et alii
FCS	fetal calf serum
FDA	Food and Drug Administration
FITC	fluorescein isothiocyanate
FL	full length
G	guanine
G	acceleration due to gravity
h	hours
HAT	histone acetyltransferase
HDAC	histone deacetylase
HMT	histone methyltransferase
HP-β-CD	hydroxypropyl-β-cyclodextrin

i.e.	id est
ISS	intronic splicing silencer
kb	kilobases
kDa	kilodalton
l	liter
LAT	lysine acetyltransferase
LLN	lower limit of normal
M	molar
m	milli-
Mb	megabases
MDa	megadalton
min	minutes
ml	milliliter
mm	millimeter
mM	millimolar
mRNA	messenger RNA
NCV	nerve conduction velocity
n.d.	not determined
ng	nanogram
nm	nanometer
nM	nanomolar
nmol	nanomol
n.s.	not significant
OHSC	organotypic hippocampal slice culture
OMIM	Online Mendelian Inheritance in Man
P	postnatal day
p	probability (statistical significance)
PAA	polyacrylamide
PAGE	polyacrylamide gel electrophoresis
PBS	phosphate-buffered saline
PCR	polymerase chain reaction
pH	power of hydrogen
pmol	picomol
RNA	ribonucleic acid
RNAi	RNA interference
rpm	revolutions per minute
RT	reverse transcription

SAHA	suberoylanilide hydroxamide acid
s.c.	subcutaneous
SD	standard deviation
SDS	sodium dodecyl sulfate
SEM	standard error of the mean
siRNA	small interfering RNA
SMA	autosomal recessive spinal muscular atrophy
SMN	survival motor neuron
T	thymidine
TEMED	N,N,N',N'-tetramethylethylenediamine
ter	telomeric
UV	ultraviolet
VPA	valproic acid
µ	micro-
µg	microgram
µl	microliter
µM	micromolar
µm	micrometer
#	number

1 Introduction

1.1 The clinical picture and diagnosis of proximal spinal muscular atrophy

Spinal muscular atrophies (SMA) present as a broad spectrum of diverse clinical pictures. All spinal muscular atrophies are caused by the loss of lower motor neurons in the spinal cord, resulting in denervation of especially voluntary muscles leading to muscle weakness and atrophy as main symptoms of the disease. The occurrence of the atrophy may differ between proximal or distal, symmetrical or asymmetrical muscle atrophy. Also a wide mode of inheritance is found, ranging from sporadic occurrence over X-chromosome linked to recessive or dominant heredity. Possible forms of spinal muscular atrophies include X-linked disease (XL-SMA), spinal muscular atrophy with respiratory distress (*SMARD*), spinal and bulbar muscular atrophy (*Kennedy's disease*), and distal spinal muscular atrophy.

A*utosomal recessive proximal spinal muscular atrophy* is the most common form of spinal muscular atrophies and, therefore, is simply referred to as "SMA". It is the subject of this thesis and, unless mentioned otherwise, the term "SMA" used herein refers to the autosomal recessive proximal from of spinal muscular atrophies.

With an occurring incidence in the western European population of 1 in 6,000 to 10,000 life-births and a carrier frequency of 1:35 (Czeizel and Hamula 1989; Feldkotter et al. 2002; Pearn et al. 1978), SMA is the second most frequent autosomal recessive disorder in humans and the leading genetic cause of infant death today (Montes et al. 2009).

The major characteristic hallmark of SMA is the degeneration of α-motor neurons in the anterior horns of the spinal cord, leading to hypotonia and muscle weakness finally resulting in muscle atrophy. Other neurological systems (including brain and sensory nerves) usually display no dysfunction and affected individuals show normal intelligence. Muscular weakness starts at the voluntary muscles of the proximal limbs, such as upper arms and legs, rather than in the distal ones, like hands or feet. The atrophy is more pronounced and begins earlier in the legs than in the arms. SMA is a progressive disease starting from muscle weakness and resulting in atrophy of the muscles. SMA patients show further symptoms, like tremor of the hands and an explicit decrease of deep reflexes. Furthermore, fasciculations of the tongue are observable in SMA patients. Muscle groups in the face and in the eyes are typically not involved.

The serum level of the creatine kinase (CK) activity is a common and very sensitive marker of increased muscle membrane permeability. Elevated CK activity points towards a muscle damage (Schlattner et al. 2006). CK activity is a common diagnostic tool for

myocardial infarction or muscular dystrophy. While in these cases the CK activity level is highly increased (10-fold and more above the normal level), in SMA patients only a mild elevation can be detected. Therefore, a highly augmented CK amount is a criterion of exclusion for SMA diagnosis.

Nowadays, one of the main diagnostic tools for SMA is electromyography (EMG). Electromyography is a technique for evaluating and recording the activation signal of muscles. With the help of an apparatus called “electromyograph” EMG is performed and the results are recorded in an electromyogram. By the use of this apparatus it is possible to detect the electrical potential generated by myoblasts in an active and in an inactive state. Electromyographic investigations in affected SMA patients show a typical pattern of denervation, normally without sensory involvement. Additionally, SMA patients reveal specific EMG characteristics, such as spontaneous muscle activity with fibrillations and fasciculations of single muscle fibers and motor units. The nerve conduction velocity (NCV) in SMA patients is normal or mildly reduced, but not lower than 70% compared to healthy individuals.

As a guideline for the diagnosis of SMA, in 1992 the SMA Consortium defined the following list of major exclusion criteria for SMA (Munsat and Davies 1992):

- CNS dysfunction
- arthrogryposis
- involvement of other neurologic systems or other organs (e.g. hearing, cardiac or vision)
- sensory loss
- eye muscle weakness
- marked facial weakness
- marked increase in creatine kinase (CK) activity levels.

Still, in very rare SMA cases it has been observed that the disease may sometimes associate with arthrogryposis, CNS involvement, increased CK values or heart defects (Rudnik-Schoneborn et al. 1996). Nevertheless, it remains elusive, whether these observations are true causal associations or just random findings.

To screen out the misdiagnosis of muscular dystrophy or other neuromuscular disorders and to verify the diagnosis for SMA, muscle biopsy of patients is an established means. These histological samples are evaluated histochemically, and may allow distinguishing SMA from other denervating diseases. There are two types of muscle fibers. Muscle fibers of the type I have a red appearance, because they contain

the oxygen binding protein myoglobin and they show slow fatigue since they generate ATP by oxidative metabolism, and therefore are suited for endurance. Due to the absence of myoglobin, type II fibers appear white. Besides the oxidative metabolism type II fibers make use of the anaerobic metabolism, hence they are faster to fatigue, but they are efficient for short bursts of speed and power. In a muscle biopsy from a typical chronic SMA patient groups of atrophic and hypertrophic fibers or fiber-type grouping are most often found (see Figure 1). Moreover, SMA skeletal muscle usually shows atrophic fibers with islands of group hypertrophy (Buchthal and Olsen 1970). Furthermore, evidence of skeletal muscle denervation can be observed.

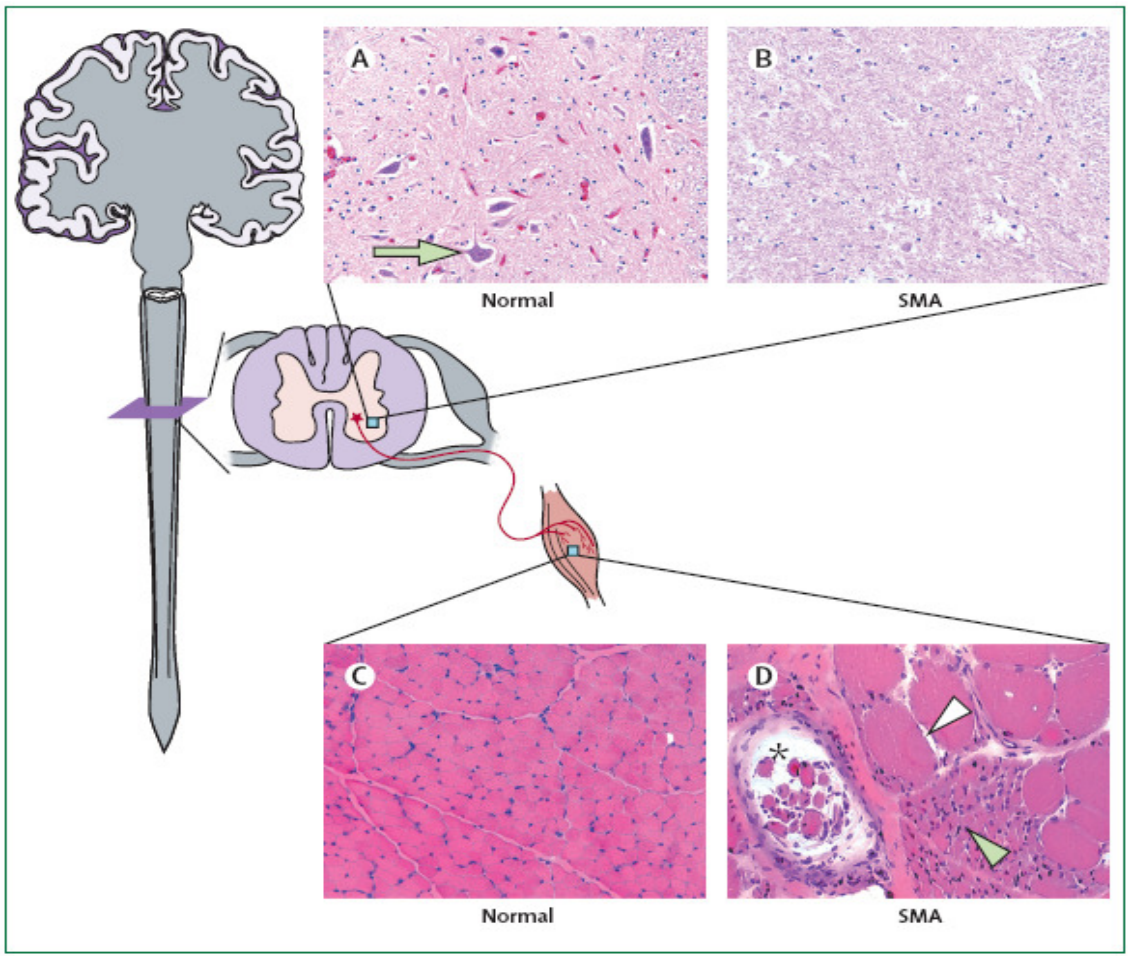

Figure 1 Histopathology of spinal muscular atrophy
Motor commands generated in the cerebral cortex are transmitted through spinal cord α-motor neurons (red cell in spinal cord anterior horn and green arrow in (**A**)). The spinal cord anterior horn region shows an absence of motor neurons in a patient (**B**) compared with those in the healthy control (**A**). Skeletal muscle of a patient (**D**) shows hypertrophic fibers (hollow arrowhead) surrounded by group atrophy (green arrowhead) compared with healthy fibers with uniform morphology in normal infantile muscle (**C**). Despite the atrophy of muscle fibers in spinal muscular atrophy, muscle spindles (black asterisk) are not affected and become more conspicuous (**D**). All slides are stained with haematoxylin and eosin. (Taken from (Lunn and Wang 2008))

Besides the atrophy of both muscle fiber types, an additional distinctive feature is the presence of a small number of scattered hypertrophic type I fibers presumably resulting

from physiologic hypertrophy. Nevertheless, normal-appearing fibers may be present. Although the muscle biopsies of SMA patients show neither, significant necrosis, degeneration, regeneration, lipid accumulation, nor connective tissue proliferation, some of these features may sometimes occur in older chronic SMA patients, suggesting a secondary myopathic process.

In the year 1995 Lefebvre and colleagues identified the SMA disease determining gene, called *survival of motor neuron 1* gene (Lefebvre et al. 1995). Since then it has been possible to confirm the clinical diagnosis of SMA by molecular genetic testing. To verify the clinical diagnosis of SMA, the *SMN1* gene on chromosome 5q is screened for specific mutations (deletions/gene conversions of exon 7 or exon 7 and 8). Furthermore, this highly important diagnostic tool may also be applied in prenatal diagnosis and carrier testing. The gain of knowledge regarding SMA led to the modification of the primary diagnostic criteria proposed by the International SMA Consortium (Munsat and Davies 1992) by Zerres and Davies in 1999 (Zerres and Davies 1999). In 2008, Lunn and Wang proposed another guideline for proper SMA diagnostics shown in Figure 2.

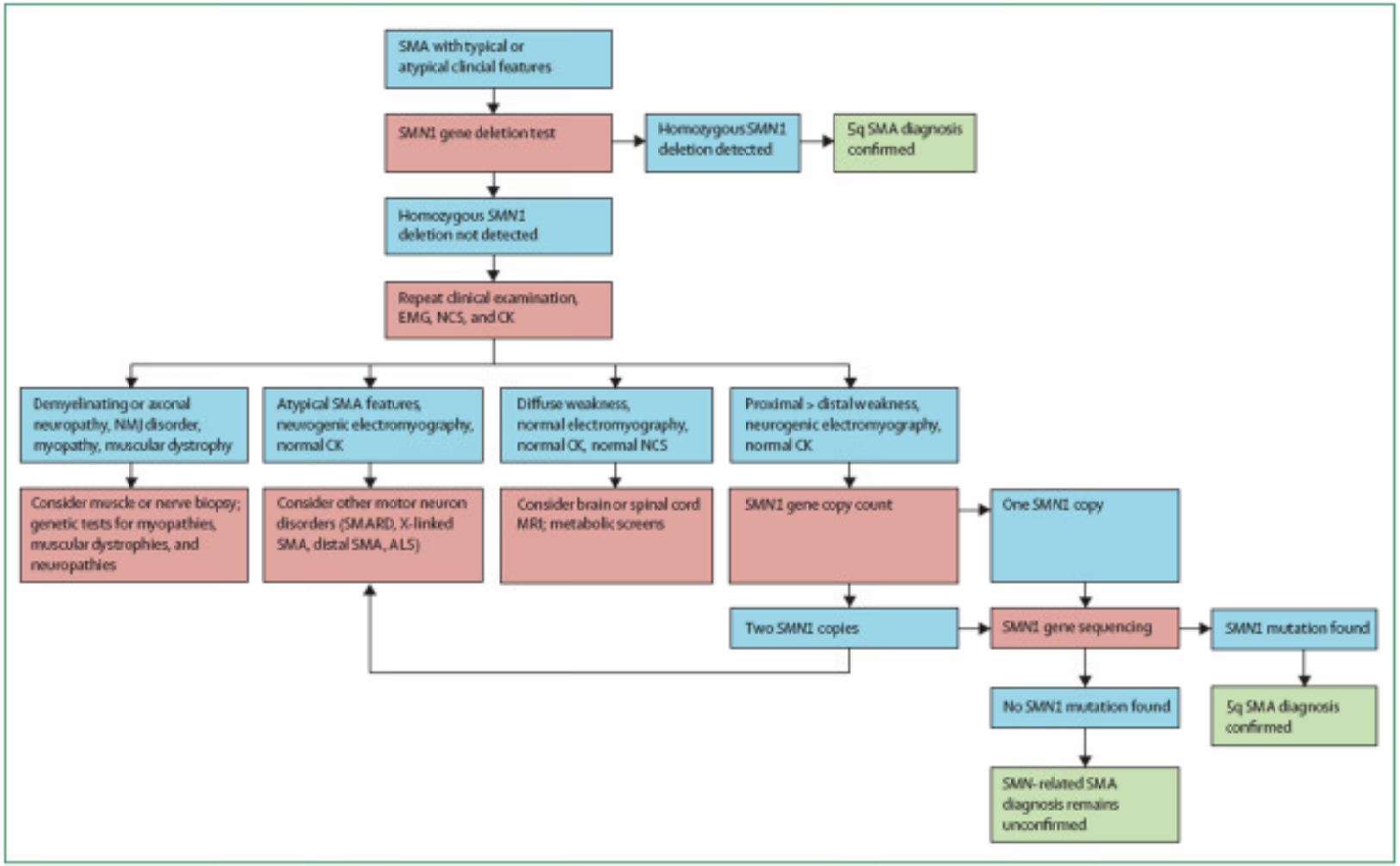

Figure 2 Diagnostic algorithm for spinal muscular atrophy Every patient presenting with clinical symptoms resembling spinal muscular atrophy (SMA) should be tested for homozygous deletion of *SMN1*, which would confirm the diagnosis of SMN-associated SMA (5q SMA). A negative *SMN1* test should be followed by a repeat clinical examination for atypical clinical features (e.g., contractures, eventration of hemidiaphragms, congenital absence of muscles) and laboratory testing for creatine kinase (CK) and electrophysiological studies such as EMG and a nerve conduction study (NCS). If lower motor neuron disease is suggested by EMG, *SMN1* copy number will establish if *SMN1* sequencing is indicated to identify intragenic mutations in patients with a single *SMN1* copy. If two *SMN1* copies are detected, then investigation should be directed towards other motor neuron diseases by further diagnostic work-up such as muscle or nerve biopsy, imaging studies, metabolic screens, and genetic testing. ALS=amyotrophic lateral sclerosis. NMJ=neuromuscular junction. SMARD=SMA with respiratory distress. Red boxes=diagnostic assessments. Blue boxes=physical and laboratory findings. Green boxes=final diagnoses. Taken from (Lunn and Wang 2008).

1.1.1 Classification of proximal SMA

Based on different motor functions and on the age of onset, spinal muscular atrophy has been divided into four clinical types: severe type I; intermediate type II; mild type III and adult-onset type IV as a very mild form (Munsat and Davies 1992; Zerres and Rudnik-Schoneborn 1995).

1.1.1.1 SMA type I (*Werdnig-Hoffmann disease*, MIM #253300)

This type of SMA is the most severe form and is also called acute SMA. The clinical picture of SMA type I was first described by Werdnig in 1891 (Werdnig 1891) and independently by Hoffmann in 1893 (Hoffmann 1893).

Usually type I SMA is diagnosed within the first 6 months of life. The onset of the disease is before the age of 6 months and death occurs within the first two years of life. Recent data suggest a mean age of survival of ~7 months for an SMA type I patient (Rudnik-Schoneborn et al. 2009, *in press*). In rare cases, the symptoms may begin prenatally (in the third trimester). Werdnig-Hoffmann disease is the most common form of SMA and accounts for about 50% of patients diagnosed with spinal muscular atrophy (Markowitz et al. 2004). Besides a generalized muscle weakness ("*floppy infants*") the affected children suffer from hypotonia and are never able to sit unaided. The patients show symmetrical flaccid paralysis and no control of head movement. Typical for SMA type I patients is the paradoxical breathing (inward bony thorax movement with outward abdominal movement during inspiration) and a bell-shaped upper torso, which is due to their spared diaphragm, combined with weakened intercostal muscles. The bulbar denervation results in characteristic tongue fasciculation and weakness with poor suck and problems in swallowing. The increased risk of aspiration pneumonia is an important cause of morbidity and mortality. In 1995, it was postulated that 8% of affected children reach the tenth year of life (Zerres and Rudnik-Schoneborn 1995). However, that study might have included non *SMN1*-linked patients, since at that time *SMN1* had not yet been identified.

1.1.1.2 SMA type II (intermediate form, MIM #253550)

Affected children with SMA type II show first disease symptoms after six, but before 18 months of life. SMA type II is of intermediate severity and patients are able to sit independently but never learn to walk and need support to stand. Life expectancy is reduced, but usually children do not die before the age of two years and more than 70% grow older than 20 years. Surgical or orthotic intervention is required to correct the often

developing kyphoscoliosis. Frequent symptoms are also fine tremors with digit extension or hand grips. Comparable to patients with type I disease, clearing of tracheal secretions and coughing might become difficult because of poor bulbar function and weak intercostal muscles. A very frequent cause of death during adolescence is respiratory insufficiency.

1.1.1.3 SMA type III (*Kugelberg-Welander*, MIM #253400)

A less severe form of SMA was for the first time reported in the year 1956 by Kugelberg and Welander (Kugelberg and Welander 1956).

The so called juvenile SMA is quite variable in its age of onset, but generally first symptoms of SMA type III occur after the 18th month of life. Depending on the exact age of onset, SMA type III is divided into two subtypes: if first symptoms are diagnosed before the age of three years, the disease is called type IIIa, if the patient is older than three years he or she SMA bears type IIIb (Zerres and Rudnik-Schoneborn 1995). This juvenile form of SMA is very heterogeneous as some affected individuals may need wheelchair assistance in childhood, whereas others may continue to walk throughout their whole lives. A quiet common orthopedic feature of this progressive form is the development of scoliosis.

1.1.1.4 SMA type IV (adult SMA, MIM #271150)

The first symptoms of this adult form of SMA typically occur in the second or third decade of life (Wirth 2002). The patients are comparatively mildly affected and have a normal life expectancy. No respiratory problems are observed and affected individuals are able to walk in adult years.

1.2 The molecular basis of proximal spinal muscular atrophy (SMA)

The identification of the SMA disease causing gene started in the year 1990, when scientists succeeded in mapping SMA patients of type I, II, and III by linkage analysis to a region of about 10 cM on chromosome 5q11.2 - q13.3 (Brzustowicz et al. 1990; Gilliam et al. 1990; Melki et al. 1990). A few years later the development of many new polymorphic markers enabled the researchers to narrow down the initial quite large interval to a critical disease region of less than 1 Mb (DiDonato et al. 1994; Melki et al. 1993; Melki et al. 1994; Soares et al. 1993; Wirth et al. 1995; Wirth et al. 1994). This newly identified region contained a highly complex unstable sub-region of about 500 kb, which was subjected to intrachromosomal rearrangements, including gene duplications, gene conversions, and *de novo* deletions (Lefebvre et al. 1995). This complex genomic organization considerably hindered the researches to construct a uniform physical map (Lefebvre et al. 1995; Melki et al. 1994; Roy et al. 1995a; Roy et al. 1995b; Thompson et al. 1993).

Finally in the year 1995, the *survival motor neuron gene* (*SMN*) was identified as the disease-causing gene by the use of a human fetal brain cDNA library (Lefebvre et al. 1995).

Today it is well-known that the genomic SMA region is prone to *de novo* rearrangements, including unequal crossovers, intrachromosomal rearrangements, and gene conversions (Melki et al. 1994; Wirth et al. 1997). In this critical 500 kb SMA segment five genes have been identified: the *survival of motor neuron gene* (*SMN*); the *BIRC1* (*baculoviral IAP repeat-containing 1*) gene, also known as *NAIP* (*neuronal apoptosis inhibitory protein*); the *SERF1* (*small EDRK-rich factor 1*) gene, also known as *H4F5,* the *GTF2H2* (*general transcription factor IIH*) gene or *p44*; and the *OCLN* (*occludin*) gene (Lefebvre et al. 1995; Schmutz et al. 2004) (see Figure 3). This dynamic 500 kb genomic SMA region can be present in 0 to 4 copies per chromosome 5 and is flanked by the single-copy genes *RAD17* (proximal) and *BDP1* (also known as *TFNR*) (distal) (Kelter et al. 2000; von Deimling et al. 1999).

Figure 3 Schematic overview of the genomic SMA region on chromosome 5q13. Many genes in the vicinity of the SMN genes are duplicated and inverted.

1.2.1 The *SMN* gene

Lefebvre and colleagues identified the SMA disease-determining gene called *survival motor neuron gene* (*SMN)* in the year 1995 (Lefebvre et al. 1995). Two copies of the *SMN* gene are located in the genomic SMA candidate region: the telomeric (*SMN1*) and the centromeric (*SMN2*) duplicate (Lefebvre et al. 1995). These gene copies are almost identical except for five silent nucleotide differences not affecting the amino acid sequence: one each in exon 7 (840C→T, codon 280, nt position 27141), exon 8 (nt position 27869) and intron 6 (nt position 27092) and another two in intron 7 (nt positions 27289 and 27404), respectively (see Figure 4) (Burglen et al. 1996; Lefebvre et al. 1995). To date there have several other gene variants been described, but discrimination between *SMN1* and *SMN2* has not been possible, since these variants have been found in both gene copies (Brahe et al. 1996; Hahnen and Wirth 1996; Monani et al. 1999).

The *SMN* gene has a size of 28 kb on genomic level and consists of 9 exons (1, 2a, 2b-8) and 8 introns with an open reading frame of 882 bp (294 codons) (Chen et al. 1998; Lefebvre et al. 1995). The ~1.5 kb *SMN* transcripts are expressed in all somatic tissues and encode a 294 amino acid protein of 38 kDa (Lefebvre et al. 1995). The expression level is ~50-fold to 100-fold higher in spinal cord as compared to other tissues (Coovert et al. 1997; Lefebvre et al. 1997). Interestingly, the SMN protein is very highly conserved from yeast to man (Miguel-Aliaga et al. 1999; Paushkin et al. 2000; Schrank et al. 1997). On an evolutionary background, the *SMN* gene duplication occurred for the first time in primates and therefore took place after the split of primates from rodents, since mice and rats have only one copy namely *Smn*. Nevertheless, the gene copy *SMN2* is unique to humans, since chimpanzees never carry this converted gene despite having multiple *SMN* gene copies in their genome (Rochette et al. 2001).

Over 98% of patients with spinal muscular atrophy have a homozygous *SMN1* deletion, rearrangement, or mutation (Hahnen et al. 1995; Lefebvre et al. 1995). All these patients, however, retain at least one copy of *SMN2*, which undergoes alternative splicing and produces mainly a truncated mRNA isoform, which lacks exon 7 (major product) or exon 5, or both (see 1.2.2). In these individuals the loss of the *SMN1* gene causes SMA, while the severity of the SMA phenotype inversely correlates with the number of *SMN2* copies (Lefebvre et al. 1995; Wirth 2000). In very rare cases some individuals are protected from developing SMA, although they lack *SMN1.* These persons express the only known fully protective modifier of SMA, namely Plastin 3 (Oprea et al. 2008).

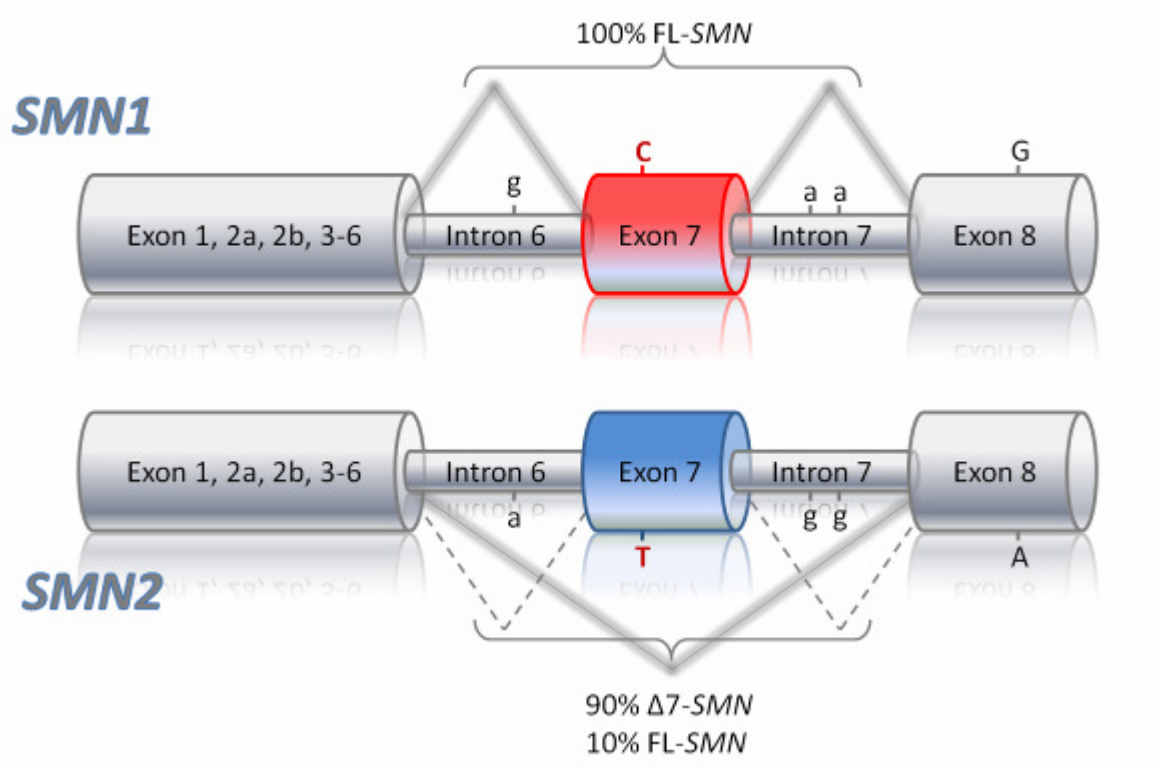

Figure 4 Schematic representation of the genomic structure, nucleotide and splicing differences between *SMN1* and *SMN2*. The *SMN* gene copies can be distinguished by 5 nucleotide exchanges of which only the C → T transition in exon 7 (marked in red) lies within the coding region. The nucleotide exchange in exon 7 is a translationally silent mutation. Therefore full-length *SMN1* and *SMN2* mRNA encode identical proteins of 294 amino acids. However, the C→T transition affects an exonic splicing enhancer and/or silencer causing alternative splicing of *SMN2* pre-mRNA. *SMN2*Δ7 transcripts produce a truncated and unstable protein.

1.2.2 The *SMN* transcript

Although the *SMN1* and the *SMN2* gene encode for an identical protein, they differ in 5 nucleotide exchanges, all of which are translationally silent. *SMN1* produces almost exclusively full length transcripts, whereas because of the C to T transition at position +6 in exon 7 of *SMN2,* 90% of the *SMN2* transcripts are alternatively spliced lacking exon 7 (Δ7-SMN2). Only 10% of *SMN2* pre-mRNA produce full length transcripts (FL-SMN2). The first stop codon of the FL-transcripts is located at the end of exon 7; hence these transcripts are translated into a FL-SMN protein consisting of 294 amino acids. The Δ7-*SMN2* transcripts lack exon 7 and therefore encode a truncated SMN protein of only 282 amino acids. The skipping of exon 7 leads to the use of an alternative stop codon located in exon 8, therefore a truncated protein is generated, which C-terminally lacks 16 amino acids encoded by exon 7 but instead contains four amino acids encoded by exon 8. This shortening of the protein reduces its oligomerization capacity and decreases its stability. Thus, the appropriate protein function of SMN is severely reduced (Lorson and Androphy 2000; Lorson et al. 1998).

Furthermore, it has been shown that both *SMN* genes are able to produce three more transcripts. One alternative transcript is the Δ3-*SMN,* which lacks exon 3, another one is Δ5-*SMN* lacking exon 5 and, additionally, there are *SMN* mRNA occurring which lack both, exon 5 and exon 7 (Δ5,7-SMN) (Chang et al. 2001; Gennarelli et al. 1995; Singh et al. 2006).

At a closer look on the splicing function of the SMN protein, the Δ3-SMN protein reveals an interesting feature of the *Tudor domain,* which is located in exon 3 of SMN. Researchers have proven that the disruption of this respective domain reduces the ability of SMN to interact with the Sm (*Smith antigen*) proteins, which is essential for the splicing involvement of the SMN protein (Buhler et al. 1999; Mohaghegh et al. 1999; Sun et al. 2005) (see also protein function of SMN chapter 1.2.3.1).

Focusing on the *SMN* pre-mRNA splicing, it is necessary to mention the C to T transition in *SMN2* exon 7 again. This particular nucleotide exchange lies directly within an exonic splicing enhancer (ESE) (Lorson and Androphy 2000; Lorson et al. 1999). It destroys a heptamer motive, which is normally (in the case of *SMN1*) recognized by the splicing factor SF2/ASF (splicing factor 2 (SF2), a positive splicing factor that is also known as the alternative splicing factor (ASF)) (Cartegni and Krainer 2002). The hence resulting alternative splicing produces a transcript lacking exon 7. A concurring hypothesis instead postulates that the C to T transition forms a new exonic splicing silencer (ESS), which recruits the splicing factor hnRNP A1, and that this leads to the exclusion of exon 7 (Kashima and Manley 2003).

The splicing pattern of the *SMN2*-pre-mRNA is subjected to the influence of different splicing factors. It has been shown in *in vivo* splicing experiments that the SR-like splicing factor SFRS10 (Serine/Arginine rich splicing factor 10; formally known as hTra2-β1, the human homolog of transformer-2 from *Drosophila melanogaster*) specifically binds to a GA-rich region, a second ESE in the central part of *SMN* exon 7. Overexpression of SFRS10 restores the alternative splicing pattern of *SMN2*, so that 80% of full length transcripts are produced (Hofmann et al. 2000).

Both splicing factors SF2/ASF and SFRS10 interact specifically and directly with exon 7 of the *SMN* pre-mRNA (Cartegni and Krainer 2002; Hofmann et al. 2000). Splicing factors like SRp30 and hnRNP-G act on the exon 7 inclusion via binding to SFRS10 (Bose et al. 2008; Helmken and Wirth 2000; Hofmann and Wirth 2002; Young et al. 2002). The splicing factor SF2/ASF is interacting with the U2 class of small nuclear ribonuclear protein (U2 snRNP) and its auxiliary factor (U2AF) at the branch point located in intron six to support removal of the intron and successful pre-mRNA splicing during *SMN1* transcription (Cartegni and Krainer 2002). A detailed description of the splicing process of SMN pre-mRNA is given in Figure 5.

Furthermore, several chemical compounds were found to influence the splicing pattern of *SMN2.* Previously it was shown in a lymphoblastoid cell line for sodium butyrate to increase the FL-*SMN2* level 4-fold by forcing the inclusion of exon 7 (Chang et al. 2001). In the following years the capability to boost full-length levels of transcripts was proven in fibroblast cultures for Aclarubicin (Andreassi et al. 2001) and in our laboratory for valproate (Brichta et al. 2003).

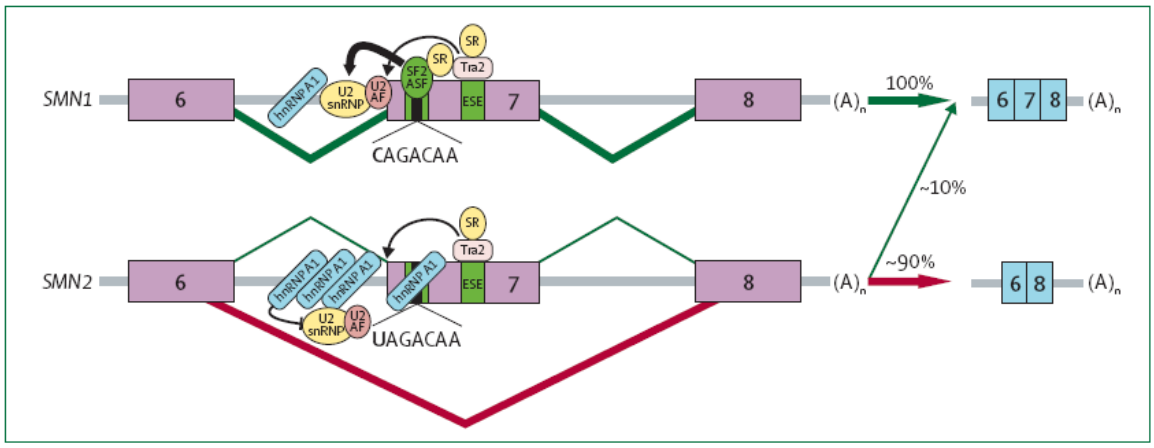

Figure 5 Pre-mRNA splicing of *SMN1* and *SMN2*
In *SMN1*, an exonic splicing enhancer (ESE), which contains the nucleotide cytosine (C) at position six in exon seven (Ex7+6), is recognised by splicing factor 2 or alternative splicing factor (SF2/ASF), which interacts (thick black arrow) with the U2 class of small nuclear ribonuclear protein (U2 snRNP) to remove intron six. Other splicing factors (e.g. SFRS10) determine splicing through interactions (thin black arrow) with ESE elements found centrally within exon seven. Serine and arginine (SR)-rich proteins might also exert a positive splicing effect. In *SMN2*, the ribonucleotide uridine (transcribed from thymidine) at Ex7+6 favours exon seven exclusion by binding to heterogeneous nuclear ribonuclear protein (hnRNP) A1, a negative splicing factor. Moreover, SF2/ASF no longer recognises this sequence motif. Binding of hnRNP A1 is also believed to prohibit U2 snRNP binding to the branch point, which results in about 90% of *SMN2* final mRNA transcripts with no exon seven. The positive splicing factors downstream (thin black arrow) are functioning and could account for exon 7 inclusion in about 10% of *SMN2* transcripts. (taken from (Lunn and Wang 2008))

1.2.3 The SMN protein

The SMN protein, 38 kDa in size, consists of 294 amino acid and is found in virtually all cells of the human body (Carvalho et al. 1999; Lefebvre et al. 1995; Liu and Dreyfuss 1996; Young et al. 2001; Young et al. 2000). The full-length SMN protein localizes both in the nucleus and the cytoplasm. Immunostaining of various cell types revealed a diffuse cytoplasmic distribution of SMN, while it is found in bright dot-like structures in the nucleus (Burlet et al. 1998; Coovert et al. 1997; Liu and Dreyfuss 1996). These SMN-containing structures are often observed in close proximity to or completely overlapping with the coiled bodies [also Cajal bodies; nuclear domains that are enriched in spliceosomal U snRNPs (Fakan et al. 1984)], and therefore are termed gemini of coiled bodies (gems) (Liu and Dreyfuss 1996; Liu et al. 1997; Young et al. 2000).

Another isoform of SMN consisting only of exons 1-3 and a part of intron 3 is only observed in axons (aSMN) (Setola et al. 2007).

Since the SMN protein possesses diverse functions in many different environments, its functions are subsequently subdivided into a) housekeeping functions, b) neuron specific functions and c) muscle specific functions:

1.2.3.1 Housekeeping functions of SMN

- **Biogenesis of snRNPs (pre-mRNA splicing)**

The so called small nuclear ribonucleoproteins (snRNPs) play an important role in every cell. The snRNPs are active in recognizing and removing introns from pre-mRNAs in the nucleus. Every snRNP is comprised of a small nuclear RNA (snRNA) and a protein part. The protein part is made of a number of specific proteins that are unique for each snRNP and the so called Sm (Smith antigen) proteins. The Sm proteins are essential for the splicing process. SMN plays here an important role in assembling Sm proteins onto the snRNAs to produce an active snRNP particle (Eggert et al. 2006; Gubitz et al. 2004; Pellizzoni 2007; Raker et al. 1999). Therefore, the SMN protein acts in an active complex in the cytoplasm of every cell. This so called “SMN complex” is composed of SMN, GEMIN2–8 and UNR-interacting protein (UNRIP). SMN protein itself is acting as an oligomer as it has been found to self-associate, and it has been suggested that oligomerization is crucial for SMN function (Lorson et al. 1998; Pellizzoni et al. 1999). The exact numbers of SMN monomers in an SMN complex is unknown, it has been shown to form higher-order complexes ranging from 20S to 80S and has been proven to

be impaired in SMN mutants of SMA patients (Lorson et al. 1998; Paushkin et al. 2002; Pellizzoni 2007; Pellizzoni et al. 1999).

- **Transcription**

The SMN protein was shown to interact with its exon 6 with mSin3a (Zou et al. 2004). mSin3a is a well known transcription corepressor that is involved in histone deacetylation and chromatin remodelling. SMN and the mSin3a protein are involved in the formation of a protein supra-complex exceeding 40,000 kDa in size (Zou et al. 2004). Since mSin3a associates with histone deacetylases and methytransferases and other proteins known to regulate chromatin remodelling (Yang et al. 2003), it has been postulated that SMN might be involved in the transcriptional repression of critical genes in motor neurons, via mSin3 associated histone modification enzymes (Zou et al. 2004).

- **Stress response**

If a cell is exposed to environmental stress such as heat shock, exposure to relevant chemical compounds or to UV irradiation, it starts a protective cellular process called “stress response“. While specific stress-induced genes are activated in response to stress most other genes are silenced. It has been shown that ~50% of total mRNA transcripts are actively recruited and dynamically sorted into cytosolic compartments forming the so-called stress granules (SGs) (Kedersha et al. 1999). This process has been shown to be dependent on the eukaryotic initiation factor (eIF) 2α and its phosphorylation status (Clemens 2001a, b). The SGs have been proven to serve as transient local storage compartment for mRNAs under stress conditions (Nover et al. 1989). Interestingly, it has been observed that the SMN protein co-localizes and interacts with T-cell internal antigen-1 (TIA-1) and TIAR (TIA-1-related protein), which are known RNA-binding proteins that accumulate in SGs (Hua and Zhou 2004). It has been stated that SMN granules can be seen as stress granules (Hua and Zhou 2004). This suggests that SMN contributes to formation and function of SGs.

- **Translation regulation**

Since SMN is known to be involved in mRNA localization and transport along the axons, SMN is widely discussed to be involved in translational regulation. It has been shown that the fragile X mental retardation syndrome protein (FMRP), which plays an important role in transport of mRNPs and in their translation, interacts with SMN. Therefore, it has been discussed that SMN may have a specific function in regulating translation in neurons (Piazzon et al. 2008).

1.2.3.2 Neuron specific functions of SMN

- **Axonal mRNA transport**

For the C-terminal exon 7 of SMN was shown that it contains a sequence motif, which is responsible for the cytoplasmic localization of the SMN protein. The overexpression of an exon-7 deletion mutant was characterized by nuclear accumulation of SMN and reduced neurite outgrowth. An active transport of SMN granules to developing neurites and growth cones was observed, indicating an involvement of SMN in axonal transport of mRNA and mRNA binding proteins (Zhang et al. 2003). Recently, a novel isoform of SMN was identified, called a-SMN (axonal SMN). This isoform consists of exons 1-3 and a part of intron 3 of *SMN* and is exclusively found in axons of motor neurons (Setola et al. 2007). a-SMN, preferentially encoded by *SMN1*, stimulates motor neuron axonogenesis and induces axonal-like growth in non-neuronal cells (Setola et al. 2007).

- **Neurite outgrowth**

Not only the axonal isoform of SMN (a-SMN) plays an important role in neurite outgrowth (see chapter above), but also the selective overexpression of the SMN C-terminal domain has been shown to induce neurite outgrowth similar to full length protein and could rescue SMN knock-down effects. Furthermore, it has been stated that knock-down of endogenous SMN led to a significant change in the G-/F-actin ratio, indicating a role for SMN in actin dynamics. In regard to these observations, SMN might be involved in microfilament metabolism in axons of motor neurons (van Bergeijk et al. 2007).

Moreover, the knock-down of Smn in zebrafish embryos has been shown to lead to an earlier branching of axons, underlining the important role of Smn in motor axon–specific pathfinding and in motor axon development (McWhorter et al. 2003). Overexpression of the recently identified protective modifier of SMA, Plastin-3, has been observed to rescue this axonal phenotype by restoring the axonal length of motor axons (Oprea et al. 2008).

- **Neuromuscular junction formation**

Neuromuscular junctions (NMJ) are the synapses of the axon terminal of a motor neuron with the motor endplate of a muscle. The neurotransmitter acetylcholine passes the signal through the neuromuscular junction to the motor endplate. In an SMA mouse model in which Smn protein levels are severely reduced, the maturation of the NMJs was shown to be seriously impaired. Reduced Smn level has been shown to lead to an impairment of the maturation of acetylcholine receptor (AChR) clusters into pretzel-like

structures. Furthermore, pre-synaptic defects, such as poor terminal arborization have been observed. The described NMJ malformations have been postulated to lead to functional deficits at the NMJ characterized by intermittent neurotransmission failures (Kariya et al. 2008). Moreover, a recent publication indicated a severely disturbed synaptic vesicle release at NMJs in an SMA-like mouse model (Kong et al. 2009).

1.2.3.3 Muscle specific functions of SMN

- **Myoblast fusion, sarcomeric Z-disc localization**

Although SMA is a neuromuscular disease affecting primarily the motor neurons and, as a secondary effect, the muscles leading to atrophy, features like scattered hypertrophic type I fibers, significant necrosis, lipid accumulation or connective tissue proliferation, are rarely found in older SMA patients, suggesting a secondary myopathic process.

Therefore, several studies searched for a muscle specific role of SMN. Indeed, some functions may be specific for this tissue, but these findings are still subject to discussions. One work has proven that the knock-down of *Smn* in myoblasts led to severe defects in myoblast fusion and an abnormal myotube morphology (Shafey et al. 2005). Another publication revealed that the whole Smn protein complex is localized to the sarcomeric Z-disc and is a direct target of calpain-3-mediated proteolytic cleavage (Walker et al. 2008).

Noteworthily, the hypothesis that SMA might be caused by a muscle specific reduction of SMN was rebutted by the finding that neuronal specific expression of SMN in a Smn knock-out mouse rescues the phenotype, whereas the muscle specific expression does not (Gavrilina et al. 2008a).

1.3 SMA animal models

Since humans are the only known species carrying an *SMN2* gene copy, all animals used to model SMA have only one endogenous *Smn* gene that is equivalent to *SMN1.* Supporting the importance of *SMN,* in all organisms, loss of *Smn* leads to lethality. Nevertheless, the levels of maternal Smn (Smn derived from the mother's *Smn* gene as opposed to the embryo's) defines the time point of lethality. In *Smn* knock-out mice for example, there is only a minimal amount of maternal Smn leading to an early embryonic lethality (Schrank et al. 1997). In contrast to mice, in the egg-laying animal *D. melanogaster* death occurs later, when the maternal Smn level drops below a crucial point (Chan et al. 2003). The resulting hypothesis that loss of *SMN* in a specific tissue in conditional *Smn* mutants results in the death of that tissue was proven by different approaches (see chapter 1.3.1.3) (Cifuentes-Diaz et al. 2001; Frugier et al. 2000; Vitte et al. 2004).

1.3.1 SMA mouse models

To analyze the pathomechanism of SMA, many different SMA mouse models have been generated over the past years. Mice carry only one *Smn* gene, which is equivalent to the human *SMN1,* and lack another copy comparable to the human *SMN2* (DiDonato et al. 1999; DiDonato et al. 1997; Viollet et al. 1997). In the following chapters, different SMA mouse models will be highlighted.

1.3.1.1 Classic knock-out of murine *Smn*

Already in 1997, Schrank and co-workers described the first classical knock-out of the murine *Smn* gene. The researches disrupted exons 2-4 of the *Smn* gene and observed early embryonic lethality before implantation between day E2.5 and E3.5. The analyzed blastocysts and morulae have revealed a disorganized, multicystic structure with extensive cellular degeneration (Schrank et al. 1997).

In the year 2000, the group of Li genetically replaced a 1.6 kb fragment of the *Smn* gene including exon 7 with a HPRT (hypoxanthine phosphoribosyltransferase) cassette and observed normal embryos at E3.5 but not at E6.5, indicating an essential role of Smn in the embryonic development (Hsieh-Li et al. 2000).

Heterozygous $Smn^{+/-}$-mice showed no symptomatic muscle atrophy, but a ~50% reduction of the Smn protein level and a resulting degeneration of the α-motor neurons after 6 months of life (Jablonka et al. 2000).

1.3.1.2 *SMN2* transgenic mice modeling an SMA phenotype

Since the homozygous ubiquitous knock-out of the endogenous *Smn* gene leads to early embryonic lethality, researchers tried to mimic SMA in mice by additionally integrating copies of the human *SMN2* gene. In the year 2000, two independent groups managed to generate an SMA-like phenotype in mice. Monani and co-workers integrated a 34 kb large BamHI fragment of human *SMN2,* isolated from a cosmid clone into the mouse genome. Mice with an $Smn^{-/-}$;$SMN2^{tg/tg}$ genotype represent an SMA-like phenotype, with degeneration of α-motor neurons and resulting muscle atrophy. Comparable to SMA patients, the severity of the disease correlates inversely with the *SMN2* copy number. While $Smn^{-/-}$;$SMN2^{tg/tg}$-mice, carrying one *SMN2* copy per integrate, die between 1-8 days, $Smn^{-/-}$;$SMN2^{tg/tg}$-mice with 8-16 *SMN2* copies show a complete rescue of the phenotype (Monani et al. 2000). Hsieh-Li and co-workers integrated a BAC clone containing the human *SMN2* gene into the murine DNA. The resulting $Smn^{-/-}$;$SMN2^{tg/tg}$-mice carry 4 *SMN2* copies (two per integrate), are fertile and live for about one year (Hsieh-Li et al. 2000). $Smn^{-/-}$;$SMN2^{tg/wt}$-mice show a severe form of SMA and survive for about 9.9 days (own observation).

Another mouse model resembling a milder form of SMA (SMA type III mice) is based on the already mentioned Monani-SMA mouse model. In a study by Arthur Burghes´ laboratory, researchers have introduced a transgene carrying a missense (A2G) mutation in exon 1 of the *SMN* gene into the severe SMA genetic background. $Smn^{-/-}$;$SMN2^{tg/tg}$;$SMN^{A2Gtg/wt}$-mice exhibited many of the clinical and pathological characteristics of type III (mild) SMA, suggesting a stabilization-capacity of the truncated SMN protein for the low expressed full-length SMN protein amount. These mice suffer from motor neuron degeneration and its associated effects. They include evidence of motor axon degeneration, loss and sprouting, muscle atrophy, and abnormal EMG patterns (Monani et al. 2003). Moreover, researchers could recently show that a previously human *SMN1* mutation (*SMN*(A111G)) (Sun et al. 2005), an allele capable of snRNP assembly, can rescue mice that lack *Smn* and contain either one or two copies of *SMN2* (SMA mice). However, the SMN^{A111G} transgene has been proven not to be able to rescue the SMA phenotype alone. Moreover, the normal survival of *SMNA111G*-high-expressing $Smn^{-/-}$;$SMN2^{tg/tg}$;$SMN^{A111Gtg/wt}$-mice has directly been correlated with snRNP assembly activity in spinal cord and the correction of snRNA levels (Workman et al. 2009).

Furthermore, the transgene expression of the truncated *SMN2Δ7* cDNA on a $Smn^{-/-}$;$SMN2^{tg/tg}$ background was observed to increase the lifespan of SMA-like animals from 5 to 14 days. This was an *in vivo* proof that the SMNΔ7-protein has the capability to

associate with the SMN-protein and to stabilize the whole SMN-complex and that SMNΔ7 has no detrimental effect on the SMA animals (Le et al. 2005).

1.3.1.3 Conditional *Smn* knock-out mice

To investigate tissue specific functions of Smn, several Cre/LoxP mediated conditional knock-out strains were generated.

With the help of a neuron-specific enolase promoter driven Cre-recombinase (NSE-Cre) Frugier and colleagues disrupted the endogenous *Smn* in neurons of mice. Profound motor axon but no cell body loss and muscle paralysis of neurologic origin was detected, the mean age of these SMA-like animals was 25 days (Frugier et al. 2000).

The important role of *Smn* in the skeletal musculature was proven by the finding that an α-skeletal actin promoter (HSA-Cre) driven Cre, causing a muscle specific deletion of *Smn* exon 7, which leads to muscle paralysis after 3 weeks, resulting in a progressive myopathy and finally death after a mean age of 33 days (Cifuentes-Diaz et al. 2001).

A liver specific deletion of *Smn* exon 7 led to massive iron overload in the liver of E16 mice, dramatic liver atrophy, dysfunction and lack of regeneration, culminating in late embryonic lethality (Vitte et al. 2004).

Neuron specific overexpression driven by a prion promoter could rescue the SMA phenotype in a severe SMA mouse model (genotype: $Smn^{-/-}$;$SMN2^{tg/tg}$, mean survival 5 days), whereas the muscle specific expression (HAS promoter) could not (Gavrilina et al. 2008a). This reflects the finding that SMA results from SMN depletion-mediated degeneration of motor neurons and is not caused by a primary muscular defect.

1.3.2 Further SMA animal models

The essential housekeeping function of *Smn* was highlighted by the finding that loss of *Smn* by gene disruption in a relatively simple organism like *Schizosaccharomyces pombe* is lethal (Owen et al. 2000; Paushkin et al. 2000).

RNA interference (RNAi) and knock-out experiments in the nematode (roundworm) *Caenorhabditis elegans* led to embryonic lethality and developmental defects or to movement defects with later knock-down of *Smn* in adult animals (Burt et al. 2006; Miguel-Aliaga et al. 1999).

In the genetic model organism *Drosophila melanogaster* it was shown that mutations of *Smn* which disrupt its self-organization and which therefore can be considered equivalent to null alleles, lead to larval lethality or embryonic lethality if maternal Smn was removed (Chan et al. 2003). A mutation that causes loss of *Smn* in the adult thorax of the fly led to loss of ability to fly and jump (Rajendra et al. 2007),

whereas different small interfering RNA knock-down approaches of *Smn* resulted in lethality at different stages, depending on different knockdown attempts (Chang et al. 2008).

Antisense morpholino knock-down of *Smn* in Zebrafish (*Danio rerio*) resulted in abnormal axon patterning and death (McWhorter et al. 2003).

1.4 SMA therapy

To date, there is no cure for SMA available. Symptomatic treatment like physical therapy to maintain joint mobility and to decrease the incidence of contractures and respiratory drainage are very important. Due to the gain of knowledge about the molecular basis of SMA, its underlying pathomechanism is well understood. Thus, the development of therapeutic approaches underwent a boost in the past years. A major aim is to prevent potential SMA patients from developing the disease. Besides so-called non-targeted strategies, which aim at the development of neuroprotective or neurotrophic agents that are able to protect α-motor neurons from degeneration, the unique feature of SMA, that every patient possesses at least one *SMN2* copy-gene, capable of ameliorating the phenotype, is a further target of a prospective therapy.

An overview of the therapeutic approaches for SMA, which have been established until now is given in Figure 6.

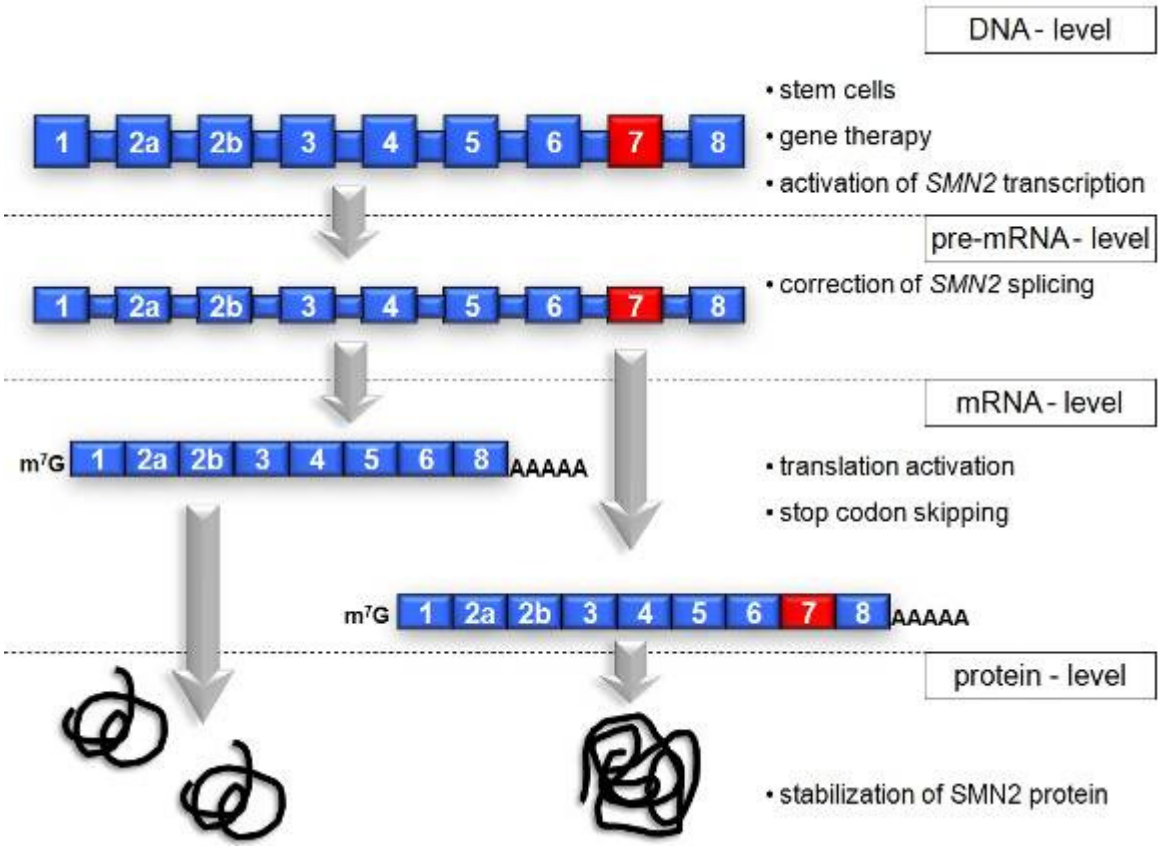

Figure 6 Strategies for potential spinal muscular atrophy therapy

On DNA level, mainly four approaches for SMA therapy are imaginable. The growing field of stem cell research might one day make embryonic stem cell transfer of healthy donor cells a concrete opportunity (Andreassi et al. 2001; Ebert et al. 2009; Zhang et al. 2001). Furthermore, introduction of an *SMN1* gene copy by gene therapy into the α-motor neurons could prevent neuronal degeneration. Since recently the SMA modifying factor Plastin 3 has been identified, a potential activation of this factor might also be a prospective therapeutic approach (Oprea et al. 2008). One variant, which takes advantage from the clinical benefit that SMA patients retain *SMN2* copies, is to activate the expression of *SMN2* by transcriptional activation, for example by the use of histone deacetylase inhibitors (Brichta et al. 2003; Garbes et al. 2009; Riessland et al. 2006) (see chapter 1.5.6).

On pre-mRNA-level, the correction of the *SMN2* transcript splicing is the main attempt to produce higher amounts of full-length *SMN2.* The inclusion of *SMN2* exon 7 would lead to the production of fully functional SMN protein (Andreassi et al. 2001; Ebert et al. 2009; Zhang et al. 2001).

One discussed intervention on mRNA level is skipping of the stop codon in exon 8 of the Δ7-*SMN2* transcripts, which leads to the synthesis of a protein containing additional amino acids at the C-terminus, which could increase stability and oligomerization ability of the Δ7-SMN2 protein. Additionally, activation of the translation machinery would lead to higher amounts of Δ7-SMN2, which is known to stabilize the low-level FL-SMN2 protein (Mattis et al. 2006; Wolstencroft et al. 2005).

Another idea is to elevate the activity or to biochemically stabilize the functional FL-SMN2 protein remaining in SMA patients to improve the efficacy of processes catalyzed by SMN, e.g. the assembly of snRNPs and axonal mRNA trafficking (Chang et al. 2004; Garbes et al. 2009).

1.5 Epigenetic chromatin modifications

The deoxyribonucleic acid (DNA), which comprises the genetic material and possesses the long-term storage function of information, exists in the nucleus as a complex with proteins, the so called *chromatin*. The DNA is tightly packed in the chromatin. The DNA-double helix which has a diameter of 2 nm is in ~200 bp (base pairs) wrapped around a histone-octamere; this resembles the 10 nm fiber. If a histone H1 attaches to this fiber, the DNA becomes more densely packed and the 30 nm fiber is built. The 30 nm fiber is in turn attached to a protein matrix, which forms a further condensed chromatin structure (overview of the DNA packaging is given in Figure 7).

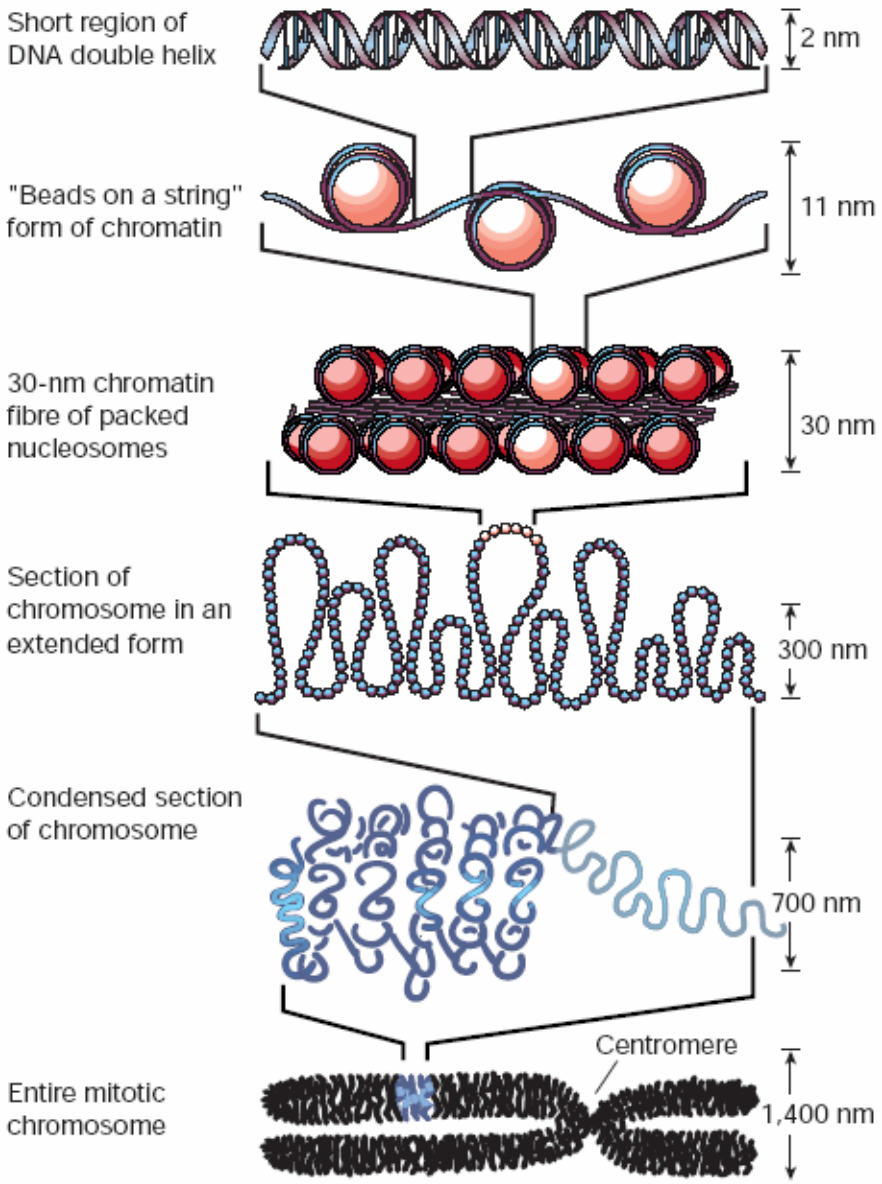

Figure 7 Eukaryotic packaging of DNA in the nucleus. DNA is associated with histone and non-histone proteins to form a highly folded, complex structure called chromatin (Felsenfeld and Groudine 2003).

The already mentioned histone proteins play a crucial role in the DNA packaging process. Histones are basic proteins which exist in mainly five different types in each animal or plant cell: H1, H2A, H2B, H3 and H4. In principle, each histone resembles a similar structure. Histones possess a central globular domain and a flexible aminoterminal and frequently a carboxyterminal tail. A characteristic feature of the histone amino acid-sequence is its high frequency of the basic amino acids lysine and arginine. Histones H2A and H2B form dimers with themselves, which in turn assemble with a tetramer consisting of two H3 and two H4 proteins, resulting in the formation of a histone-octamer. Because of its negatively charged phosphate-backbone, the DNA attaches tightly to the histone-octamers and forms a so-called nucleosome. When the nucleosome assembles with the histone H1 the above described 30 nm fiber is formed (Gruss and Knippers 1996; Kornberg and Klug 1981; Kornberg and Lorch 1999).

There is a series of posttranslational modifications of histones such as phosphorylation, methylation, ubiquitylation or acetylation, which generate the dynamic state of chromatin. In the following, the histone-acetylation will be described in more detail. Specific enzymes, the histone acetyltransferases (HAT), are able to attach acetyl-groups derived from acetyl-coenzyme A to up to four lysine-residues of the histones H2A, H2B, H3 and H4. The acetyl-group is transferred to the positively charged ε-amino group of the side chain of lysine residues of histone tails. Thus, the charge is neutralized and the affinity of the DNA to the histones is severely reduced. Hence the chromatin packaging is loosened and the DNA is accessible for protein factors involved in transcription, replication, recombination or repair processes (Eberharter and Becker 2002; Kornberg and Lorch 1999). The antagonists of the histone acetyltransferases (HAT), which activate transcription are the histone deacetylases (HDAC), which remove the acetyl-groups from lysine groups of the histones and therefore repress the gene transcription (see Figure 8).

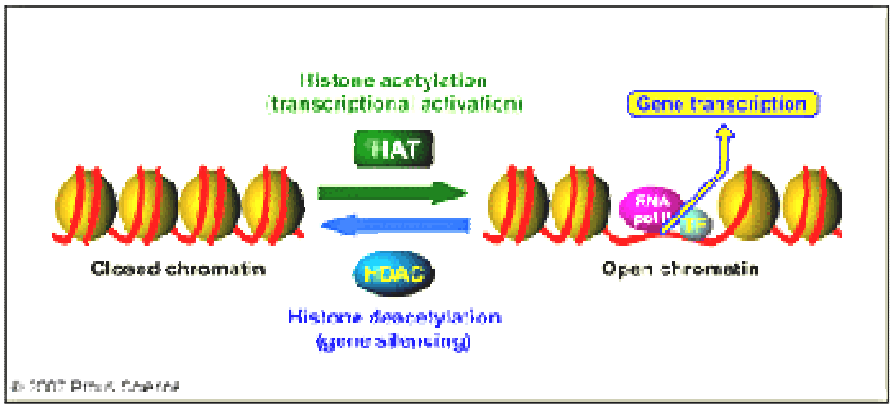

Figure 8 The antagonistic functions of histone acetyltransferases and histone deacetylases (adapted from (Graul et al. 2007)).

Based on their sequence homology to yeast orthologues Rpd3 (reduced potassium dependency 3), HdaI (histone deacetylase A) and Sir2 (Silent mating type Information Regulation-2), respectively, mammalian HDACs are grouped into class I, class II, class III and class IV (de Ruijter et al. 2003; Gregoretti et al. 2004). The so-called ‘‘classical” HDACs comprise 11 family members of class I, II, and IV (see Figure 9), whereas class III members are named sirtuins (Gregoretti et al. 2004). The sirtuins and the classical HDACs mainly differ in their catalytic mechanisms. While classical HDACs are Zn^{2+}-dependent enzymes harboring a catalytic pocket with a Zn^{2+} ion at its base, sirtuins have a different mechanism of action requiring NAD^{+} as an essential cofactor (de Ruijter et al. 2003).

As previously described, high HDAC activity is associated with condensed, transcriptionally inactive chromatin. In addition to this epigenetic function of HDACs, it has recently been recognized that certain HDACs also exhibit important cytoplasmatic function by controlling the acetylation status and function of numerous cytoplasmatic proteins and transcription factors. Thus, the more precise term for these respective enzymes would be ‘‘lysine deacetylases” to indicate that their substrates are not restricted to histone proteins (Yang and Seto 2008).

Since HDACs and the chemical inhibition of these enzymes are the major topic of this work, the different classes of classical HDACs will be discussed in detail in the following.

1.5.1 Class I histone deacetylases

Class I includes HDACs 1, 2, 3, and 8. These enzymes are related to yeast deacetylase RPD3 (reduced potassium dependency 3) and show homologous catalytic sites. HDAC1, 2 and 3 are known to be part of multiprotein nuclear complexes that are involved in transcriptional repression. HDAC1 and 2 are observed to be components of the co-rest complex, which inactivates the expression of neuronal genes in non-neuronal tissues (Huang et al. 1999). Since HDAC3 was found within the N-COR and SMRT repressor complex, this family member is clearly involved in controlling gene expression (Wen et al. 2000). So far class I member HDAC8 has not been found to be a component of any repressor complex, although it possesses similar biological attributes (e.g. domain organization etc.) suggesting a particular function for this class I HDAC. The selective inhibition of HDAC8 was recently shown to induce apoptosis in T-cell lymphoma or leukemia cell lines and to induce neuronal differentiation, inhibition of proliferation, and decreased clonogenic growth in neuroblastoma cells (Balasubramanian et al. 2008; Krennhrubec et al. 2007).

1.5.2 Class IIA histone deacetylases

Class IIA HDACs possess only one catalytic domain, whereas family members from class IIB possess two. Class IIA consists of the family members HDAC4, 5, 7, 9, which typically incorporate a large, functionally important N-terminal domain, which is involved in nuclear-cytoplasmic shuttling and specific DNA-binding. Each HDAC from class IIA contains three conserved 14-3-3 binding sites, additionally the endogenous nuclear import and export signals control the cellular trafficking of these HDACs. If the 14-3-3 proteins bind to these respective HDACs, their cytoplasmatic retention or nuclear export is phosphorylation dependently stimulated. This process in turn can regulate the activity of transcription factors like the myocyte enhancing factor-2 (MEF2) (Yang and Seto 2008).

1.5.3 Class IIB histone deacetylases

As already mentioned in contrast to the class IIA enzymes, HDACs of class IIB carry two tandem deacetylase domains and a C-terminal zinc finger. The two members of class IIB are HDAC6 and HDAC10. Interestingly, HDAC6 seems to play important roles in deacetylating cytoplasmic targets such as α-tubulin (Hubbert et al. 2002) or heat shock protein 90 (HSP90) (Kovacs et al. 2005). Involved in these functions it was shown that HDAC6 can influence cell adhesion, motility and chaperone function. Besides its deacetylase activity, HDAC6 may function by binding to ubiquitin via its zinc finger domain and therefore regulate aggresome function, autophagy, heat shock factor-1 (HSF-1) and the function of platelet derived growth factor (PDGF) (Kawaguchi et al. 2003; Pandey et al. 2007). Although HDAC10 is structurally closely related to HDAC6, there is not much known about its function.

1.5.4 Class IV histone deacetylase

The only family member of class IV is HDAC11. This HDAC is structurally related to discussed classes, class I and II. Very little is known about its expression profile and its cellular function.

1.5.5 Histone acetyltransferases (HATs)

Compared with the HDACs, proteins with histone acetyltransferase (HAT) activity show a higher diversity (Carrozza et al. 2003; Roth et al. 2001). Like the deacetylation function of HDACs, which is not restricted to histones, also some HATs are able to acetylate non-histone proteins (Kouzarides 2000; Sterner and Berger 2000). This finding was first described in 1997 when p53 was found to be acetylated at specific lysine residues in its

C-terminus (Gu and Roeder 1997). On the other hand, not all of the proteins which possess lysine acetyltransferase activity are able to acetylate histones (Yang 2004), therefore those enzymes are more generally termed lysine acetyltransferases (LATs). The classification of HATs led to the subdivision into the following families: Hat1, Gcn5/PCAF, p300/CBP, MYST, p160, CIITA, ATFII; $TAF_{II}250$, TFIIIC, Elp3, CDY, TFIIB, MCM3AP, Eco1, and ARD1 (Yang 2004). Nevertheless, the vast majority of proteins known to be modified by LATs are histones and transcriptional regulators. However, many different cellular proteins have been shown to be acetylated by LATs, these substrates include the signaling regulator Smad7 (Gronroos et al. 2002), DNA metabolic enzymes (Hasan et al. 2001; Tini et al. 2002), and α-tubulin (Doenecke and Gallwitz 1982). Since HATs may act in different mulitprotein-complexes the mode of LAT function is quite complex and not completely understood (Yang 2004).

1.5.6 Histone deacetylase inhibitors

Since the activity of HDACs in general reduces the transcription rate, it is evident that the inhibition of HDACs could up-regulate the transcription level. Inhibition of HDACs would lead to acetylation of histones, thus the affinity of the DNA to the histones is reduced and the chromatin structure loosened up and so-called *ATP-dependent chromatin remodelling complexes* have access to the DNA. These protein complexes uncover promoter regions of the DNA, at which the transcription finally starts (Eberharter and Becker 2002).

It was shown that some chemical compounds are capable of inhibiting the activity of HDACs. Thus, these compounds were named histone deacetylase inhibitors (HDACi). Since it was proven that HDACis are indeed able to up-regulate the transcription level (Strahl and Allis 2000), and that HATs and HDACs play an important role in the dynamic regulation of genes which are involved in cell proliferation and differentiation (Glass and Rosenfeld 2000; Kouzarides 2000), efforts were increased in finding new HDACis as potential therapeutics for genetic disorders (Pazin and Kadonaga 1997). But complete understanding of the mechanism which controls the transcriptional changes after HDAC inhibition remains still elusive. Whereas the inhibition of HDACs in a cell based transcription assay, by trichostatin A (TSA), only 2% of the 340 investigated genes were found to be differentially regulated (Van Lint et al. 1996), a more recent microarray approach revealed that transcription of up to 22% of genes can be altered by other pan-HDAC inhibitors (Peart et al. 2005). The complexity of the HDACi dependent transcription control was underlined by subsequent studies which showed that the inhibition of HDAC enzymes can differentially serve to up- or down regulation of

expression patterns with little predictive value. Hence, these experimental results suggest that HDAC inhibition may up-regulate the expression of other regulatory enzymes and co-factors, which subsequently behave as activators or repressors of gene activity.

Some of the substances which have histone deacetylase properties are categorized in the following (Marks et al. 2000):

1) Short-chain fatty acids:	- Phenylbutyrate (PB)
	- Sodium Butyrate (SB)
	- Valproic acid (VPA)
2) Hydroxamates:	- Trichostatin A (TSA)
	- Suberoylanilide hydroxamic acid (SAHA)
	- Suberic bishydroxamic acid (SBHA)
	- m-carboxycinnamic acid bishydroxamide (CBHA)
	- PCI-34051 (HDAC8 specific)
	- LBH589 (Panobinostat)
3) Bezamides:	- M344
	- MS-275
4) Cyclic tetrapeptides:	- Trapoxin A
	- Apicidin
5) Bicyclic tetrapeptide	- Depsipeptide (FK228)

The HDACis bind in the catalytic pocket of the respective HDACs and thereby inhibit their function.

In 2001, the first publication of an HDACi treatment study for a prospective SMA therapy was issued. The researchers made use of the unique feature of SMA, namely the presence of the modifying gene copy *SMN2,* and targeted its expression by HDACi treatment. Hence, the treatment of Epstein-Barr-Virus transformed lymphoblastoid cell lines derived from SMA type I, II, and III patients with sodium butyrate indeed revealed increased full-length *SMN2* transcript and SMN protein levels (Chang et al. 2001). Moreover, in an *in vivo* model, when sodium butyrate was administered to pregnant mothers of SMA transgenic mice (*Smn*$^{-/-}$; *SMN2*^{tg}), it improved survival in their offspring. Since this first study suggested that HDAC inhibitors might be able to exert an effect on *SMN2* expression, many attempts to up-regulate the *SMN2* expression and to revert the splicing pattern of *SMN2* followed.

It was shown that also the well-known epilepsy drug valproic acid (VPA) is able to up-regulate the FL-*SMN2* transcription level and protein level in fibroblasts derived from SMA patients (Brichta et al. 2003). Comparable results were published on the second-generation HDACi Suberoylanilide hydroxamic acid (SAHA), which revealed a favourable effect on SMN2 protein levels and expression levels in cell lines and in rat hippocampal slices (Hahnen et al. 2006c).

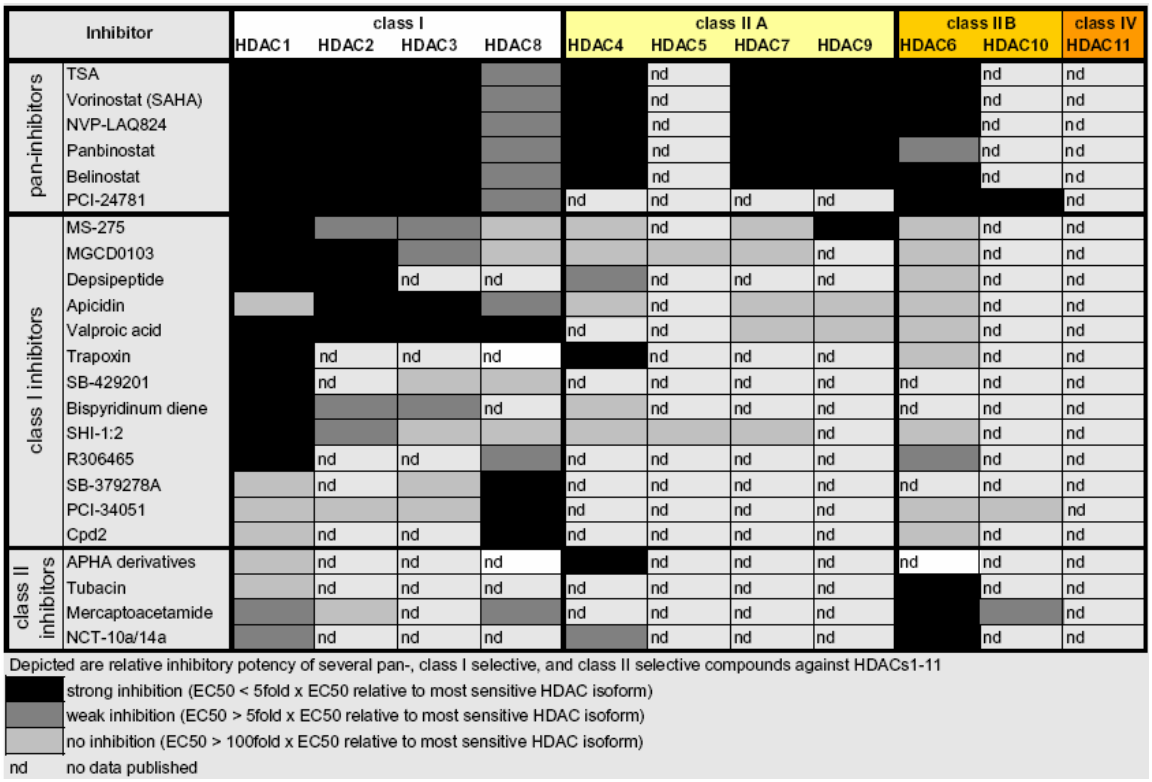

Figure 9 Inhibitory profile of pan- and class-selective HDAC inhibitors (taken from (Witt et al. 2009))

Since sodium butyrate and SAHA are so called pan-HDACis ("pan-": Greek πᾶν, pan, "of everything", "involving members" of a group) and VPA predominantly inhibits unspecifically all HDAC members from HDAC family I, the expression of many genes may be regulated by their functions. Thus, it is quite obvious that pan-HDAC treatment in patients leads to frequent unfavorable side effects (e.g. for VPA known side effects are GI intolerance, sedation, tremor, asymptomatic reduction in platelet count, severe hepatic dysfunction, hemorrhagic pancreatitis, and agranulocytosis. Other serious side effects include neural-tube defects with first-trimester exposure and death from overdose. Platelet dysfunction, coagulopathies, and edema occur infrequently. Increased appetite, weight gain, and transient hair loss may occur (reviewed in (Gerstner et al. 2008))). Furthermore, a clinical trial has recently shown that SMA patients respond

differentially to VPA treatment. It was observed that, for yet unknown reasons, only one third of VPA treated SMA patients responded by an up-regulation of SMN expression, whereas one third responded by a down-regulation and the last third revealed no change in the SMN expression level (Brichta et al. 2006a).

The two previously described facts support the urgent need for more HDACi which are capable in up-regulating the *SMN2* expression in SMA patients. Moreover, the identification of a specific HDAC which regulates the *SMN2* expression might reduce common side effects of pan-HDACis in a prospective SMA therapy. The development of HDAC isoenzyme specific inhibitors is currently ongoing and of wide interest. For an overview of the specificity of the respective compounds, see Figure 9.

2 Aims

Proximal spinal muscular atrophy is the leading genetic cause of death in early childhood. Until now, no cure is available. The *survival motor neuron gene 1* (*SMN1*) is the disease determining gene. While the disease gene *SMN1* produces full length transcripts only (FL-*SMN*), the majority of transcripts derived from the copy gene *SMN2* lack exon 7 due to alternative splicing. Even though the amount of *SMN2*-derived FL-SMN protein is not sufficient to countervail the loss of *SMN1* and to prevent disease onset, *SMN2* has shown to be the main disease modifying gene. Due to its disease modifying property, which could be confirmed using transgenic models, *SMN2* became an interesting therapeutic target.

Since transcriptional *SMN2* activation or modulation of its splicing pattern to increase FL-*SMN* levels is likely to slow down disease progression, the main aim of this was to identify chemical compounds, namely histone deacetylase inhibitors (HDACis), to act in this way.

In the first place, this work was concentrated on the *in vitro* investigation of newly identified second generation HDAC inhibitors. To evaluate if the new compounds are able to exert an effect on the human *SMN2* gene *in vitro*, it was made use of a treatment-assay, based on cell lines derived from SMA patients. Potential effects of the HDACis should be characterized in detail by analysis of *SMN2* RNA and protein levels in the treated cell lines.

Moreover the identification of the respective histone deacetylase, which controls the expression of *SMN2* was another aspired goal of this work. The potential identification of a specific HDAC would raise the question for a respective specific inhibitor, which then should also be assessed.

Finally, since our group has previously shown that the FDA-approved drug suberoylanilide hydroxamic acid (SAHA) is a potent and non-toxic candidate drug for SMA treatment, this work focussed on the *in vivo* characterization of this compound. Therefore two different SMA-mouse models were chosen and treated with SAHA. After finding the best treatment regimen for these animals, different outcome measurements, like survival time, motor abilities, SMN expression levels and histological changes in tissues such as motor neurons, neuromuscular junctions and muscles should be evaluated.

3 Materials and Methods

3.1 Fibroblasts derived from SMA patients

For all human fibroblast cell lines used in this work, a genetic analysis was carried out and informed written consent was given by the respective subjects or their legal guardians. All SMA type I, II, and III patients who donated human material fulfilled the diagnostic criteria for SMA (Munsat and Davies 1992) and carry homozygous deletions of *SMN1* as determined by routine molecular diagnostic testing. The number of genomic *SMN2* copies (SMA type I, II, and III patients; see Table 1) was determined in DNA isolated from an EDTA blood sample, which has been collected from the respective donor (for details regarding the quantitative analysis of *SMN1* and *SMN2* copies, see also chapter 3.11.11).

Table 1 Human fibroblast cell lines derived from SMA patients, used in this work.

Name of the cell line	SMA type	SMN1 gene copies	SMN2 gene copies
ML12	III	-	3
ML16	I	-	3
ML17	I	-	2
ML20	II	-	2

3.2 Mouse inbred strains

Two different SMA model mouse inbred strains were used in this project: 1.) FVB.Cg-Tg(SMN2)2Hung Smn1^{tm1Hung}/J, subsequently entitled **SMA_H mouse model** (purchased from Jackson´s Laboratory; Stock Number: 005058) In this mouse model the *Smn* gene was disrupted by the deletion of a 1.6-kb fragment at the *Smn* locus, including *Smn* exon 7. The *SMN2* transgene of this mouse model is located in a 115 kb large integrated BAC-clone-fragment (derived from clone C7). Importantly, the SMA_H mice carry 2 SMN2 copies per integrate. 2.) FVB.Cg-Tg(SMN2)89Ahmb *Smn1*^{tm1Msd}/J (kindly provided from the group of Michael Sendtner (Würzburg); available at Jackson´s Laboratory, Stock Number: 005024), subsequently abbreviated as **SMA_B mouse model**. In this mouse model the *Smn* gene was disrupted by the insertion of the targeting vector into exon 2 of the *Smn* gene. The *SMN2* transgene of this mouse model is located in a 35.5 kb large integrated PAC-clone-fragment (derived from clone 215P15). Importantly, the used SMA_B mice carry 1 *SMN2* copies per integrate. As a wild-type strain, the inbred strain FVB/NJ (Jackson´s Laboratory, Stock Number: 001800) was used.

The SMA_H mice were housed in micro-isolation chambers in the mouse facilty of the Institute of Genetics, Cologne. Breeding pairs consisted of one mouse that was homozygous for the transgene and the knock-out (*SMN2*$^{tg/tg}$*; Smn*$^{-/-}$) allele and the other mouse was heterozygous for the knock-out (*Smn*$^{-/+}$) allele, which resulted in pups that display the SMA phenotype and control littermates. All mice were humanely euthanized according to protocols set forth by the "Landesamt für Natur, Umwelt und Verbraucherschutz NRW".

The animal breeding and all mouse experiments were approved by the local animal protection committee. The animal experiment application form was confirmed. All in vivo experiments were performed under the reference number 9.93.2.10.31.07.292.

The SMAB mice were kept under the same conditions, but in the "Franz-Penzoldt-Zentrum" in Erlangen. The reference number for the animal experiments performed in Erlangen was: 621-2531.31-18/05.

3.3 Cell lines derived from SMA patients

In the institute for Human Genetics in Cologne, the laboratory of Professor Dr. Brunhilde Wirth has access to a collection of more than 100 primary fibroblast cell lines derived from SMA patients, SMA carriers and controls. All fibroblast lines were obtained from skin biopsies. Confirmed consent is available and was approved by the local ethnic committee.

3.4 Equipment and Chemicals

Centrifuges:
- Allegra X22-R, *Beckman Coulter*
- 5415 D, Eppendorf
- 5415 R, Eppendorf

Microplate reader:
- Safire^2, *Tecan*

Ultrasonic waterbath:
- Bioruptor, *Diagenode*

Heating block:
- HTMR-133, *HLC*

Spectrophotometer:
- BioPhotometer, *Eppendorf*
- NanoDrop ND-1000, *Peqlab*

Cuvettes:
UV-Vette, Eppendorf

Thermocycler:
GeneAmp 9600, *Perkin Elmer*
GeneAmp 9700, Applied Biosystems

Realtime thermocycler:
LightCycler 1.5, *Roche*
Taqman 7500, Applied Biosystems

Agarose gel electrophoresis chamber:
SGE-020-02, CBS Scientific

pH meter:
pH Level 1, *inoLab*

SDS gel electrophoresis chamber:
Mini-Protean 3 Cell, *Biorad*

Tissue culture hood:
Hera Safe, *Heraeus*

Microscopes:
Leica DMIL (inverted microscope for cell culture), *Leica*
Leica TCS-SP (confocal microscope), *Leica*
Axioplan 2 imaging microscop, *Zeiss*

Power supplies:
PowerPac 1000, *Biorad*
PowerPac HC, *Biorad*
High Voltage Power Pac P30, *Biometra*

Shaker:
3015, *GFL*
VS.R23, Grant BOEKEL

Imaging systems:
Chemidoc XRS, *Biorad*
Gel Doc 2000, *Biorad*

Western Blot transfer chamber:
Mini Trans-Blot Cell, *Biorad*

Autoradiography cassette:
Developer Cassette 18x24cm, *Siemens*

Developer machine:
CURIX 60, *Agfa*

Imaging system:
ChemiDoc XRS, *Biorad*

Incubator:
Hera Cell 150, *Heraeus*

Vibratome:
Vibratome® Series 1000, *Pelco*

Infiltration System
Infiltrationsautomat Leica TP 1020, *Leica*

Transfection apparatus
Nucleofector, *Lonza*

Neubauer counting chamber, *Optik-Labor*

Concentrator 5301, *Eppendorf*

3.4.1 Chemicals

Whenever possible, only chemicals with the purity grade "pro analysis" were used for the experiments described in this work. All standard chemicals and organic solvents were purchased from the following companies: *Roche Molecular Biochemicals*, Mannheim; *Invitrogen*, Niederlande, BV, Leek (Netherlands); *Merk*, Darmstadt; *MWG*, Ebersberg; *Amersham*, Freiburg; *Diagenode* Liège (Belgium); *Promega*, Mannheim; *Sigma Chemie*, Taufkirchen; *Serva*, Heidelberg; *Stratagene*, La Jolla (USA); *Applichem*, Darmstadt; *Roth*, Karlsruhe. For RNA isolation and analysis, only chemicals free of RNases have been used.

3.4.2 Kits

Custom Superscript ds-cDNA synthesis Kit, *Invitrogen*
ChargeSwitch® gDNA Mini Tissue Kit, *Invitrogen*
LowCell# ChIP kit, *Diagenode*
Qiaex II Gel Extraction Kit, *Qiagen*
QuantiTect Rev. Transcription Kit, *Qiagen*

QIAshredder, *Qiagen*
RNase-Free DNase Set, *Qiagen*
Quant-iT™ RiboGreen® RNA Assay Kit, *Invitrogen*
Quant-iT™ PicoGreen® dsDNA Assay Kit, *Invitrogen*
QIAquick PCR Purification Kit, *Qiagen*
RNeasy MinElute Cleanup Kit, *Qiagen*
EndoFree Plasmid Maxi Kit, *Qiagen*
RNeasy Mini Kit, *Qiagen*
SuperScript First-Strand Synthesis System for RT-PCR Kit, *Invitrogen*
SuperSignal West Pico Chemiluminiscent Substrate Kit, *Pierce*
Power SYBR® Green PCR Master Mix, *Applied Biosystems*
LightCycler® FastStart DNA Master SYBR Green I, *Roche*
Basic Nucleofector® Kit for Primary Mammalian Fibroblasts, *Lonza*

3.4.3 Reagents, enzymes and additional supplies for cell culture procedures

3.4.3.1 Reagents

Oligo d(T) primers, # SP230, *Operon*
100 bp DNA Ladder, # 15628-050, *Invitrogen*
1 kb DNA Ladder, # 15615-016, *Invitrogen*
Precision Plus Protein All Blue Standards, # 161-0373, *Bio-Rad*
Dimethylsulfate, # D5279-05, *Sigm*a
Hydroypropyl-β-cyclodextran (HP-β-CD), *AppliChem*
DAPI, # H-1200, Vector Laboratories Inc
Thiazolyl blue tetrazolium bromide (MTT), *Sigma*
M344 (4-Dimethylamino-N-(6-hydroxycarbamoylhexyl)-benzamide), *Axxora*
SAHA, synthesized by D. Zlotos, Intitue for Pharmakology University Bonn
FK228, kindly provided by *Gloucester Pharmaceuticals*
PCI-34051, kindly provided by J.J. Buggy, *AXYS Pharmaceuticals*, San Francisco
Amphotericin B, *Gibco*
Dulbecco´s Modified Eagle Medium, *Gibco (Invitrogen)*
Dimethylsulfoxide, *Sigma*
Deoxycholacid, *Sigma*
Milk powder (Instant Nonfat Dry Milk), *Stop&Shop*
Fetal Calf Serum, *Biochrom AG*
IGEPAL, *Sigma*

2-Propanol, *Roth*
Sodiumchloride, *AppliChem*
PBS: Phophate buffered saline Dulbecco, *Gibco (Invitrogen)*
PenStrep (Penicillin Streptomycin), *Roche*
Trypsin-EDTA soultion (1x), *Sigma*
Sodiumdodecylsulfate (SDS), *AppliChem*
Acrylamide: Acrylamide/Bisacrylamide 29:1 (30%), *Biorad*
Ammoniumpersulfat, *AppliChem*
Bromphenolblue, *AppliChem*
Bovine Serum Albumin, *Sigma*
SuperSignal West Pico Chemiluminescent Substrate, *Pierce*
Coomassie Brilliantblau R-250, *AppliChem*
Ethanol, *Roth*
Gycerin 99%, *AppliChem*
Glycin, *AppliChem*
Methanol, *Roth*
Ponceau S, *Sigma*
Precision Plus Protein All Blue Standard, *Biorad*
Stripping Puffer: Restore Western Blot Stripping Buffer, *Pierce*
TEMED: N,N,N',N' – Tetramethyl-Ethylendiamin, *AppliChem*
Tris: Tris-(hydroxymethyl)-Aminomethan, *Roth*
Tris-Base: Tris-(hydroxymethyl)-Aminomethan, *Sigma*
Tween 20: Polysorbat 20, *Caelo*
β-Mercaptoethanol, *AppliChem*

3.4.3.2 Enzymes

RQ1 RNase-Free DNase, # M6101, *Promega*
Taq DNA Polymerase Recombinant, cat. # 10342020, *Invitrogen*

3.4.3.3 Additional materials for cell culture procedures

DharmaFECT™ 1 Transfection Reagent, T-2001-03, *Dharmacon*
DharmaFECT™ 4 Transfection Reagent, T-2004-03, *Dharmacon*
DMSO, # D2650, *Sigma*
OPTIMEM® I, # 31985, *Invitrogen*
Disposable Filter Unit 0.45 µm FP30/0.45 CA-S, # 10462100, *Whatman*
Disposable Filter Unit 0.2 µm FP30/0.2 CA-S, # 10462200, *Whatman*

3.4.3.4 Additional materials for laboratory mouse in vivo procedures

Animal feeding needles 24x1'', *Harvard Apparatus*
BD Micro-Fine + U-40 Insulin syringe, *BD Medical*
Hydroxypropyl-β-cyclodextrin, *AppliChem*

3.4.3.5 Purchased human cDNA clones

ORF clone of human HDAC8 #RC208390, *OriGene*
clone of human HDAC2 #SC110918, *OriGene*
clone of human HDAC11 #SC123846, *OriGene*

3.5 Antibodies

3.5.1 Primary antibodies

α-SMN, monoclonal IgG1, # S55920, (*BD Transduction Laboratories)*
α-β-tubulin, monoclonal IgG1, # T4026, (*Sigma)*
α-β-actin, monoclonal IgG2a, (*Sigma)*
c-MYC (9E11), Mouse Monoclonal Antibody – UNCONJ (*Invitrogen)*
anti-SF2/ASF, monoclonal mouse (kindly provided by A. Krainer, Cold Spring Harbor Laboratories)
anti β-Actin, monoclonal mouse (*Sigma*)
anti-SRp20, monoclonal mouse (*Santa Cruz*)
anti-SMN, monoclonal mouse (*BD Transduction Laboratories*)
anti-Htra2-β1, polyclonal rabbit
anti-cMYC, monoclonal mouse (*Invitrogen*)
anti-HDAC2 (*Santa Cruz*)
anti-HDAC8 polyclonal rabbit (*MBL*)
anti-acetyl Histone H3 K9, monoclonal mouse (*Upstate*)
anti-β-Tubulin, (*Sigma*)
anti-H3K9ac polyclonal rabbit (*Diagenode*)
α-bungarotoxin labeled with rhodamine (*Invitrogen*)
anti-Neurofilament M (145kDa) rabbit
anti-GADD45α monoclonal mouse (*Abnova*)

3.5.2 Secondary antibodies

Horseradish peroxidase conjugated goat anti-mouse IgG, # 115-035-000, *Dianova*
Horseradish peroxidase conjugated goat anti-rabbit IgG, # 31460, *Pierce*
donkey anti-rabbit Cy2 (*Dianova*)

3.6 Solutions and Media

3.6.1 Frequently used buffers and solutions

Ammonium Persulfate (APS) solution (10%):	for 10 ml:
APS	1.0 g
deionized H2O	to a final volume of 10 ml
	store at -20°C
Blocking solution (6%):	for 100 ml:
Nonfat dry milk	6 g
TBS Tween buffer	to a final volume of 100 ml
Bradford solution:	for 1l:
Coomassie Brilliant Blue G250	100 mg
H3PO4 (85%)	100 ml
Ethanol (95%)	50 ml
deionized H2O	to a final volume of 1 l
	store at 4°C
Diethylpyrocarbonate (DEPC) treated H2O:	for 1 l:
DEPC	1 ml
deionized H2O	to a final volume of 1 l
	mix overnight and autoclave
(other solutions can be treated with DEPC in a similar way, except for Tris solutions)	
DNA loading buffer (10 x):	for 50 ml:
100 mM EDTA (pH 7.2-8.5)	10 ml 0.5 M EDTA (pH 7.2-8.5)
1% SDS	2.5 ml 20% SDS
50% Glycerol	28.7 ml 87% Glycerol
0.1% Bromphenol Blue	0.05 g
deionized H2O	to a final volume of 50 ml
dNTP mix:	for 1 ml:
dNTP (100 mM)	12.5 µl of each dNTP (total volume: 50 µl)
deionized H2O	to a final volume of 1000 µl

Electrophoresis buffer (10 x):	for 1 l:
Tris-Base	30.29 g
Glycine	144.13 g
SDS	10.0 g
deionized H2O	to a final volume of 1 l

Ethidium bromide solution (1%):	for 100 ml:
Ethidium bromide	1.0 g
deionized H2O	to a final volume of 100 ml
store at 4°C in the dark	

Laemmli buffer for SDS PAGE (2x):	for 100 ml:
Tris-Base	0.757 g
Glycerol	20 ml
Bromphenol Blue	10 mg
SDS	6 g
(prior to use: β-Mercaptoethanol	10 ml)
deionized H2O	to a final volume of 90 ml without β-Mercaptoethanol, store at RT

(100 ml with β-Mercaptoethanol, store at 4°C and use not longer than 2 weeks)

Lysis buffer (pH 7.4):	for 500 ml:
155 mM NH4Cl	77.5 ml 1 M NH4Cl
10 mM KHCO3	5 ml 1 M KHCO3
0.1 mM EDTA	100 µl 0.5 M EDTA
deionized H2O	400 ml
adjust pH to 7.4 with HCl	
deionized H2O	to a final volume of 500 ml
store at 4°C	

PCR buffer (10 x):	for 500 ml:
500 mM KCl	250 ml 1 M KCl
100 mM Tris-HCl (pH 8.3)	50 ml 1 M Tris (pH 8.3)
15 mM MgCl2	7.5 ml 1 M MgCl2
0.1% gelatin	0.5 g gelatin
deionized water	to a final volume of 500 ml

adjust to pH 8.3, sterile filtration

Phosphate buffered saline (PBS) (10 x):	for 1000 ml:
NaCl	80.0 g
KCl	2.0 g
Na2HPO4	14.4 g
KH2PO4 (pH 7.3)	2.4 g
deionized H2O	to a volume of 800 ml
adjust pH to 7.4	
deionized H2O	to a final volume of 1000 ml, autoclave

Ponceau solution:	for 100 ml:
0.5% Ponceau S	0.5 g
1% Acetic acid glacial	1 ml
deionized H2O	to a final volume of 100 ml

RIPA buffer:	for 50 ml:
150 mM NaCl	1.5 ml 5 M NaCl
1% IGEPAL	5 ml 10% IGEPAL
0.5% DOC (Deoxycholic acid)	2.5 ml 10% DOC
0.1% SDS (Sodium Dodecyl Sulfate)	0.5 ml 10% SDS
50 mM Tris (pH 8.6)	2.5 ml 1 M Tris (pH 8.6)
deionized H2O deionized H2O	to a final volume of 50 ml

RT mix:	for 1000 µl:
5 x buffer (supplied with reverse transcriptase)	400 µl
DTT (100 mM)	200 µl
dNTP (100 mM)	25 µl of each dNTP (total volume: 100 µl)
DEPC treated deionized H2O	300 µl

Separation gel for SDS PAGE 12%:	for 1 gel:
deionized H2O	1.7 ml
acrylamide-bisacrylamide mix (29:1, 30%)	2.0 ml
Tris (1.5M, pH 8.8)	1.3 ml
SDS (10%)	0.05 ml
APS (10%)	0.05 ml
TEMED	0.002 ml

Sodium Dodecyl Sulfate (SDS) solution 10%:	for 100 ml:
SDS	10.0 g
deionized H2O	to a final volume of 100 ml
dilute at 65°C, store at room temperature	

Stacking gel for SDS PAGE:	for 1 gel:
deionized H2O	0.68 ml
acrylamide-bisacrylamide mix (29:1, 30%)	0.17 ml
Tris (1 M, pH 6.8)	0.13 ml
SDS (10%)	0.01 ml
APS (10%)	0.01 ml
TEMED	0.001 ml

TBE buffer (5 x):	for 1 l:
445 mM Tris base	54 g Tris base
445 mM Borate	27.5 g Boric acid
10 mM EDTA	20 ml 0.5 M EDTA (pH 8.0)
deionized H2O	to a final volume of 1000 ml

TBS Tween buffer:	for 5 l:
20 mM Tris	12.1 g Tris
137 mM NaCl	40.0 g NaCl
0.5% Tween 20	25 ml Tween 20
deionized H2O deionized H2O	to a final volume of 5 l
adjust to pH 7.56	

TE^{-4} buffer:	for 100 ml:
Tris (1 M, pH 8.0)	1 ml
EDTA (0.5 M, pH 8.0)	20 µl
deionized H2O	to a final volume of 100 ml

Transfer buffer:	for 5 l:
Tris-Base	12.1 g
Glycine	56.3 g
Methanol	1000 ml
deionized H2O	to a final volume of 5 l

Tris-HCl (1 M, pH 6.8):	for 400 ml:
Tris-HCl	60.0 g
deionized H2O	to a final volume of 400 ml
adjust pH to 6.8 with concentrated HCl	

Tris-HCl (1.5 M, pH 8.8):	for 400 ml:
Tris-HCl	90.5 g
deionized H2O	to a final volume of 400 ml
adjust pH	to 8.8 with concentrated HCl

3.6.2 Media for eukaryotic cell and tissue culture procedures

Medium for human fibroblasts: for 556.4 ml:
D-MEM with 4500 mg/l Glucose, L-Glutamine,
Pyruvate (#41966-029, *Invitrogen*) 500.0 ml
Fetal calf serum (*Biochrom*) 50.0 ml
Penicillin-Streptomycin (*Invitrogen*) 5.0 ml
Amphotericin B (*PromoCell*) 1.4 ml of a stock with the concentration 250 µg/ml

Media for siRNA transfection of human fibroblasts:
OptiMEM I (#31985-047, Invitrogen)

PBS Dulbecco w/o Ca^{2+}, Mg^{2+} low endotoxin (*Biochrom AG*)

3.7 Primers and siRNAs

All primer were individually designed and purchased from the company Metabion. Every primer was delivered in lyophilized form and subsequently diluted in deionized, autoclaved H_2O to achieve primer stock solutions with a concentration of 100 pmol/µl. Stock solutions were stored at -20°C and served for the preparation of working solutions with the concentration 10 pmol/µl.

Table 2 Overview over the pre-designed primer assays used in quantitative real-time PCR experiments in Taqman (*Applied Biosystems*). * = this primer pair was not used for quantification of recombinant expression of *HDAC8,* because it is located in the 3' UTR region.

Transcript	**QuantiTect Primer Assay (*Qiagen*)**	**Catalogue #**	**Amplicon length**
Actin, beta	Mm_Actb_2_SG	QT01136772	77 bp
ACTIN, beta	Hs_ACTB_2_SG	QT01680476	104 bp
SMN1/SMN2	Hs_SMN2_2_SG	QT01673679	97 bp
HDAC1	Hs_HDAC1_1_SG	QT00015239	140 bp
HDAC2	Hs_HDAC2_1_SG	QT00001890	127 bp
HDAC3	Hs_HDAC3_1_SG	QT00093730	100 bp
HDAC4	Hs_HDAC4_1_SG	QT00005810	86 bp
HDAC5	Hs_HDAC5_1_SG	QT00060585	145 bp
HDAC6	Hs_HDAC6_1_SG	QT00002709	64 bp
HDAC7	Hs_HDAC7_1_SG	QT00031822	121 bp
HDAC8	Hs_HDAC8_1_SG *	QT00049630	91 bp
HDAC9	Hs_HDAC9_1_SG	QT00039333	92 bp
HDAC10	Hs_HDAC10_1_SG	QT00007252	161 bp
HDAC11	Hs_HDAC11_2_SG	QT01674617	65 bp

Table 3 siRNA assays used in the respective experiments

Target Transcript	**Name of the siRNA assay**	**Catalogue #**
HDAC1	Hs_HDAC1_6 HP	SI02663472 *Qiagen*
HDAC2	Hs_HDAC2_1 HP	SI00434952 *Qiagen*
HDAC3	Hs_HDAC3_1 HP	SI00057316 *Qiagen*
HDAC4	Hs_HDAC4_3 HP	SI00083951 *Qiagen*
HDAC5	Hs_HDAC5_1 HP	SI00077714 *Qiagen*

HDAC6	Hs_HDAC6_5 HP	SI02663808 *Qiagen*
HDAC7	Hs_HDAC7A_5 HP	SI02777719 *Qiagen*
HDAC8	Hs_HDAC8_2 HP	SI00122066 *Qiagen*
HDAC9	Hs_HDAC9_1 HP	SI00148372 *Qiagen*
HDAC10	Hs_HDAC10_1 HP	SI00141736 *Qiagen*
HDAC11	Hs_HDAC11_5 HP	SI03039085 *Qiagen*
siTOX	Transfection Control	*Dharmacon* (siRNA to check transfection efficiency) D-001500-01-05
AllStars Negative Control siRNA	Non-Targeting siRNA	*Qiagen* (control siRNA) 1027280

Table 4 Specifically designed primer for genotyping

Primer #	Name	Gene/Transcript	Sequence (5' to 3')	Annealing temperature	Amplicon size [bp]
3370	Hung WT fw	*Wt Smn*	ATA ACA CCA CCA CTC TTA CTC	55°C	KO=950 WT=1050
3371	Hung KO fw	*Smn KO*	GTA GCC GTG ATG CCA TTG TCA		
3372	Hung WT_KO rev	*Wt Smn*	AGC CTG AAG AAC GAG ATC AGC		
3373	HungSMA_mouse_tgSMN2_fw_1F	*transgenic 5'-UTR of SMN2*	ACT GCA ACC TCC TGG GTT CAA GTG	58°C	172
3374	HungSMA_mouse_tgSMN2_rev_1B	*transgenic 5'UTR of SMN2*	CAG TTC GAG ACC AGC CTG ACC AAT		
3375	HungSMA_mouse_tgSMN2_fw_2F	*10kb upstream of the SMN2 coding region (transgene)*	CGA ATC ACT TGA GGG CAG GAG TTT G	58°C	479
3376	HungSMA_mouse_tgSMN2_rev_2B	*10kb upstream of the SMN2 coding region*	AAC TGG TGG ACA TGG CTG TTC ATT G		
3377	HungSMA_mouse_tgSMN2_fw_3F	*centromeric NAIP region of the BAC clone (transgene)*	AAA CCA GTC GGG CAC AAT ACC TAG C	58°C	720
3378	HungSMA_mouse_tgSMN2_rev_3B	*centromeric region of the BAC clone (transgene)*	TAT GCT GAT TGA AGG GAG GGG TGC		
2649	m_smn forw	*Smn*	CCG GGA TAT TGG GAT TGT AG	55°C	782
2650	m_smn rev	*Smn*	TTC TTT TGG CTT TTA TTC TTC TTG		

Table 5 Specifically designed primer for copy number determination and expression studies

Primer #	Name	Gene/Transcript	Sequence (5' to 3')	Annealing temperature	Amplicon size [bp]
1449	SMN Ex 5 for	*SMN-FL_Δ7*	CCA CCA CCC CAC TTA CTA TCA	FL-SMN=62°C Δ7-SMN=61°C	FL-SMN=236 Δ7-SMN=182
1450	SMN Ex 6/8 rev	*SMN-Δ7*	GCT CTA TGC CAG CAT TTC CAT A		
3054	SMN_Ex7/8_rev 1	*SMN-FL*	GCT CTA TGC CAG CAT TTC TCC T		
3887	hum_HDAC8_fw	*HDAC8*	TGA CGG AAT GTG CAA AGT AGC	53°C	107
3888	hum_HDAC8_rev	*HDAC8*	ATA TTC CCA GGA CAG CAT CAT T		
2952	Intron4 fw hum	*SMN2*	AAA TGC TCA AGA GGT AAG GAT ACA A	55°C	111
2953	Intron2b rev hum	*SMN2*	GAA GTT AAA TCT CAA CAT TTT AAA T		
158(eh)	ApoB fwd	*ApoB*	CAC GTG GGC TCC AGC ATT	55°C	73
159(eh)	ApoB rev	*ApoB*	TCA CCA GTC ATT TCT GCC TTT G		

All siRNAs were pre-designed by the respective company. The siRNAs purchased from Qiagen were delivered in lyophilized form. To obtain a 20 µM stock solution, 250 µl siRNA Suspension Buffer (*Qiagen*) were added to 5 nmol siRNA. Subsequently, the dilution was incubated at 90°C for 1 min and at 37°C for another 60 min according to the manufacturer's protocol to disrupt higher aggregates.

Stocks were stored at -20°C and further diluted with siRNA Suspension Buffer to obtain 1 µM working dilutions prior to use.

The siRNAs purchased from Dharmacon were also delivered in lyophilized form and dissolved in 1 x siRNA Buffer (*Dharmacon*) to obtain a stock dilution of 20 µM. Stocks were stored at -20°C. Prior to transfection of fibroblasts, stocks were further diluted with siRNA Buffer to obtain working dilutions with a concentration of 1 µM.

3.8 Software, internet programs, and databases

Microsoft® Office Professional Edition 2003, *Microsoft Corporation* (word processing, data analysis and preparation of presentations)

Adobe Photoshop 8.0.1, *Adobe Systems Inc.* (image editing)

EndNote 9, *Thomson ResearchSoft* (organization of references)

SigmaPlot 9.0, *Systat Software, Inc.* (creation of graphs)

OneDScan, *Scanalytics* (densitometric analysis of PAA gels and western blots)

Quantity One 4.5.1, *Biorad* (scanning and densitometric analysis of gels and western blots)

Editseq/PrimerSelect/SeqBuilder, *DNASTAR Inc.* (DNA/protein sequence analysis, primer selection)

LightCycler Software, *Roche* (documentation/analysis of real-time PCR data)
Sequence Detection Software, *Applied Biosystems* (documentation/analysis of real-time PCR data)
Multi-Analyst Version 1.1, *Biorad* (scanning and densitometric analysis of gels and western blots)
XFluor4SafireII software, *Tecan* (analysis of absorption/fluorescence using microtiter plates)
AxioVision Rel.4.7 computer software (*Zeiss*)

NCBI, www.ncbi.nlm.nih.gov
Genecards, www.genecards.org
ENSEMBL, www.ensembl.org
UCSC Genome Browser, www.genome.ucsc.edu/cgi-bin/hgGateway
Medline, www.ncbi.nlm.gov/PubMed
OMIM, www.ncbi.nlm.nih.gov/entrez/query.fcgi?db=OMIM
Gene Expression Atlas database, expression.gnf.org

3.9 Cell culture procedures

Whenever cell culture work was performed it was done under sterile conditions in order to avoid any contaminations with fungi or bacteria. Sterile conditions were guaranteed by the use of a laminar flow tissue culture hood and sterile solutions and materials. Additionally, always amphotericin B and penicillin and streptomycin were added to culture media. Both, human and murine embryonic fibroblasts were grown in the same culture medium.

3.9.1 Cell culture of primary fibroblasts derived from SMA patients

All used fibroblast cell lines were grown as adherent cultures in D-MEM medium containing 10% FCS, amphotericin B and penicillin and streptomycin (for detailed medium description see chapter 3.6.2). Fibroblasts were grown as monolayer in tissue culture flask of either 25 cm^2 or 75 cm^2 surfaces and kept in a sterile cell incubator at normal cultivation growing conditions of an atmosphere with 5% CO2 at 37°C. Humidity in the incubator was warranted by evaporation of water from a special water reservoir. Depending on the cell division rate of the respective fibroblast line the medium was either changed by default once or twice a week or when a cell line showed a very rapid growth or metabolism, the metabolic products changed the pH within the medium so that the indicator in the standard D-MEM turned the color from red to yellow indicating the necessity of a medium change. Each time a cell line was grown ~70-80% confluent, the

cells were splitted into new flasks, following the subsequent steps. First, the fibroblast monolayer was washed with PBS (w/o Ca^{2+}, Mg^{2+}), then Trypsin-EDTA was added to the cells and incubated for 5 minutes in the cell incubator. After that the trypsinization was stopped by addition of fresh culture medium and cells were split into several new flasks. To keep the growth of the cells dense but not confluent, cells were split, depending on the division rate of the respective cell line from one 75 cm² flask in two to three new 75 cm² flasks.

For the longtime storage of the fibroblasts, cells were first pelleted after trypsinization in a centrifugation step for 8 min at 1200 rpm at 4°C. Then the pellet was resuspended in a sterile-filtered solution of FCS (90%) and DMSO (10%). The resuspended cells in the freezing medium were stored over night at -80°C and then transferred to -196°C liquid nitrogen and kept there for longtime storage. At any time, these aliquots can be thawn again and cells can be brought back to culture conditions.

3.9.2 Stimulation of primary fibroblast cell lines with chemical substances

To treat fibroblasts with the respective chemical compound, the monolayer was first grown to a maximum confluency of 80% then the cells were trypsinized and after cell concentration determination, a homogenous mixture of $2x10^5$ fibroblasts in 8 ml medium was transferred onto 10 cm² petri dishes. In order to let the cells attach to the petri dish ground, the cells were pre-incubated for at least 4 h. For each experiment one dish served as a control and was treated only with the respective drug solvent (DMSO). To exclude passage specific effects, every HDACi treatment experiment was always repeated at least twice with different passages of the respective fibroblast cell line and the final results are given as mean ± SEM.

Substance	Concentrations	treatment time period
M344	0.5, 5, 10, 30, 50, 100 µM	64 h
SAHA	0.1, 1, 5, 10, 50 µM	48 h
FK228	10, 50, 100, 250, 500 nM	64h (human), 48h (murine)
PCI-34051	1, 5, 10, 25, 50, 100 µM	6 h

3.9.3 MTT assay

Thiazolyl blue tetrazolium bromide (MTT) is converted into violet formazan crystals by living cells, but not by dead cells. The absorption maxima of MTT and formazan are different. Thus, MTT can be added to cell cultures treated with a respective chemical substance (e.g. HDAC inhibitor), and subsequent photometric measurement of the newly

synthesized formazan can give evidence of cell survival under drug treatment and the cytotoxicity of the drug (Mosmann 1983).

Some 8000 fibroblasts in 250 µl medium in each well of a 96-well plate were treated with the different concentrations of the respective HDACi as described above in the respective experiments and incubated for 64 h at 5% CO2 and 37°C. For each concentration eight wells were used, to avoid major errors. For the mock even sixteen wells were included. After incubation the old medium was removed and replaced by 225 µl fresh medium and 25 µl MTT-stock-solution (50 mg MTT (*Sigma*) in 10 ml PBS (*Gibco*)). Again the cells were incubated for 3 h, to start the crystal-production. After replacing the old medium by 100 µl iso-stock (50 ml Isopropanol (100%) + 165 µl HCl 37%) the photometric absorption was measured in a plate-reader (*Tecan*). The absorption gives evidence for the cell-viability after the respective HDACi treatment. All resulting data are given as mean values (± SEM).

3.9.4 Transient transfection of primary human fibroblasts

In order to knock down the expression of a specific gene small interfering RNAs (siRNA) were used. The siRNA stocks (chapter 3.7) were first diluted to a final concentration of 1 µM in siRNA suspension buffer. The lipofection substance Dharmafect 1 (*Dharmacon*) was used for all siRNA transfection experiments. The transfection experiments were performed according to the manufacturer´s protocol. Beside the siRNA regarding the respective target gene, siTOX (*Dharmacon*) siRNA served as a transfection control and AllStars Negative Control siRNA (*Qiagen*) served as a negative control. All cells transfected with siTOX induced apoptosis. Subsequently to the respective incubation time, cells were harvested for RNA (see 3.11.5) or protein isolation (see 3.12.2). Every knock-down experiment was performed in triplicates.

Since primary fibroblasts are not easy to transfect with plasmids in order to over-express the respective cloned gene (for used plasmid see 3.4.3.5), the method of electroporation was used. With the help of the Nucleofector (*Lonza*) it is possible to transfect plasmid directly into the nucleus of fibroblasts (see internet-page: http://www.lonzabio.com/technology/nucleofector/ as reference). The Basic Nucleofector® Kit for Primary Mammalian Fibroblasts (*Lonza*) was used to transfect SMA fibroblast cell lines, following its manual.

In summary, fibroblasts were trypsinized, counted, and a volume containing the required amount of cells was centrifuged at 1200 rpm for 10 min. For each single transfection reaction, a number of 0.5 x 10^6 cells were used. The cell pellet was suspended in Nucleofector Solution (100 µl for each 0.5 x 10^6 cells), and after addition of 2 µg pmaxGFP expression vector (*Lonza*), which served as a transfection control, for

each 0.5 x 10^6 cells, aliquots of 100 µl were transferred to cuvettes and electropored with the program U21. After electroporation in cuvettes, aliquots were added to 1.5 ml of culture medium, which was pre-warmed in 6-well plates and incubated in the cell incubator for the respective time-period.

3.10 Animal breeding and characterization of SMA-like mice

3.10.1 Animal breeding

All mice used in this thesis were housed in micro-isolation chambers in the mouse facilty of the Institute of Genetics, Cologne or in the Franz-Penzoldt-Zentrum in Erlangen, respectively (SMA_B). In order to generate SMA_H-like mice, breeding pairs consisted of one mouse that was homozygous for the human *SMN2* transgene and the *Smn* knock-out (*SMN2*$^{tg/tg}$; *Smn*$^{-/-}$) allele and the other mouse was heterozygous for the knock-out (*Smn*$^{-/+}$) allele, which resulted in pups that all were heterozygous for the transgene and to 50% either homozygous or heterozygous for the knock-out allele. The *Smn*$^{-/-}$;*SMN2*$^{tg/wt}$ mice develop a severe SMA-like phenotype, whereas the Smn$^{+/-}$;SMN2$^{tg/wt}$ develop normal and were used as contol littermates. The normal rhythm of light and dark periods was set to 12h-12h intervals. Animal bedding, cages, water and feed was regularly changed every week by the animal keepers. When the mice reached an age of three weeks, tail-tips were taken for genotyping and ear-tags were set. SMA-like animals and their respective littermates were marked soon after birth by a water-resistant marker labelling on the chest. Genotyping of SMA-like animals was performed after death.

3.10.2 Motor ability test and determination of weight progression of mice

To measure the motor ability of SMA-like mice and their respective littermates, the so-called tube test was performed (El-Khodor et al. 2008). The great advantage of the tube test is that it can be performed with neonates. To perform a tube test, first the whole litter was taken together with some bedding into an adequate vessel to separate it from the mother. Next, each pup was placed one by one headfirst into a vertical 50 ml reaction tube. The pups were placed into the tube in that way that they could hold themselves by their muscular strength of their hind limbs (see Figure 10). If a mouse was able to hold itself for a while (>20 sec.) and if the hind limbs were spread, it was scored to the highest tube score of 4. Depending on the spreading of the hind limbs, each mouse was rated from 4 (best score wide spreading) to 1 (bad score, hind limbs in a clasped position). A mouse was rated with the worst score of 0 when it was not able to hold onto the tube. The tube test was performed daily starting from P0 in the morning between 9:00 h and 10:30 h a.m.

Additionally, the weight of each mouse was determined in parallel. Therefore, the upright 50 ml plastic reaction tube was placed onto a balance. During the time when a mouse was performing a tube test, its weight was noted. Thus, the weighing was

performed like the tube test daily starting from P0 in the morning between 9:00 h and 10:30 h a.m.

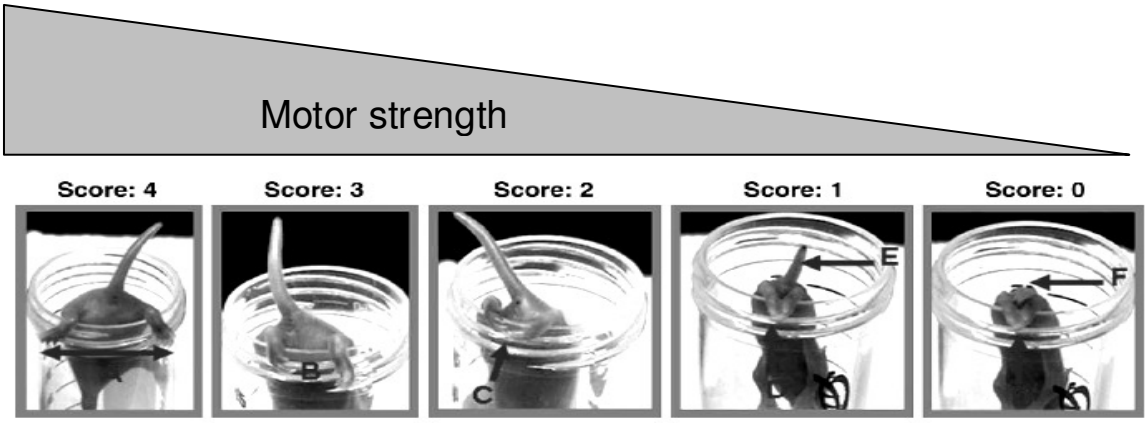

Figure 10 The tube test and the scoring criteria for tube score. Mice were suspended by their hind limbs from the lip of a standard 50 ml plastic centrifuge tube. The posture adopted was scored according to the following criteria: score of 4 indicates normal hind-limb separation with tail raised (A); score of 3, weakness is apparent and hind limbs are closer together but they seldom touch each other (B); score of 2, hind limbs are close to each other and often touching (C); score of 1, weakness apparent and the hind limbs are almost always in a clasped position (D) with the tail raised (E); a score of 0 indicates constant clasping of the hind limbs (D) with the tail lowered (F) or failure to hold onto the tube. (Taken from (El-Khodor et al. 2008)).

3.10.3 Treatment of mice with test substances

Three different methods of application were chosen to treat the SMA-like mice and their littermates with the test substances. First, in the case of SMA_B mice, which were observed to be severely affected, the mother animals were treated with 200 mg/kg/day of SAHA. Therefore, 1.33g of SAHA was solved in 1L water (supplemented with 18g hydroypropyl-β-cyclodextran (HP-β-CD)). This respective solution was given to the mother mouse instead of normal drinking water. Thus, given the fact that a 20g mouse drinks 3 ml water per day, this dosage equals 200 mg SAHA per kg body weight per day. However, the expected SMA-like pups were then treated with SAHA by suckling of the mother milk.

The second method used to apply the test substance to the SMA-like mice, was a direct subcutaneous injection of the respective substance. Each treatment concentration was diluted in that way that one injection of 12.5 µl of the solution into the neck of the mouse equalled the respective mg/kg dosage (e.g. 25 mg/kg SAHA).

The third application method was the oral treatment. Therefore, each mouse was fed with 12.5 µl of the substance with the respective concentration. To feed a mouse, it was held at the neck and the tip of a blunt-ended syringe was placed into its mouth and

12.5 µl of the treatment solution was slowly released. It was always paid attention to the swallowing behaviour of each mouse. The speed of application was accordingly adapted. Individual treatment methods, the subcutaneous and the oral treatment were performed twice daily. The first treatment took place in the morning after the performance of the tube test and the weighing (see chapter 3.10.2) between 9:00 h and 10:30 h a.m. The second treatment was performed between 17:00 h and 18:30 h.

3.10.4 Generation of murine embryonic fibroblasts

Primary embryonic fibroblasts were obtained from E13.5 old embryos. The mice with the relevant genotype were bred and it was checked for pregnancy according to the presence of a vaginal plug. 13 days after the plug-check, plug-positive mice were sacrificed. Subsequently, the embryos were removed from the uterus and washed in PBS under sterile conditions. Additionally, head, heart and liver were removed and the head was used for subsequent verification of the expected genotype. Each embryo was homogenized by pressing it with the help of a 10 ml syringe plunger through a cell sieve. The sieve was then rinsed with 10 ml MEF-medium and the flow-through was collected in a 50 ml reaction tube. The lysate was centrifuged for 5 min at 1200 rpm. The supernatant was discarded and the pellet was resuspended in 6 ml MEF-medium and plated out onto 6 cm dishes. At the following day the medium was exchanged to get rid of cell debris.

Table 6 Murine embryonic fibroblast cell lines used in this thesis

Name of the cell line	genotype	SMA inbred strain	Inbred strain	SMN2 gene copies
MEF14	*SMN2$^{tg/tg}$; Smn$^{-/-}$*	SMA-Burghes (SMAB)	C57BL/6	2
MEF5	*SMN2$^{tg/tg}$; Smn$^{-/-}$*	SMA-Hung (SMAH)	FVB/N	4 (2 per integrate)

3.10.5 Preparation of mouse organs

For the preparation of mouse organs, the respective mouse was sacrificed by decapitation either at day P5 or P10. Subsequently, the mouse was fixed onto a operating table and its body was opened by abdominal incision.

For the subsequent RNA or protein preparation of organs (see chapters 3.11.4 and 3.12.1), whole liver, brain, the *gastrocnemius* muscle and spinal cord was removed. While liver, muscle and brain were simply withdrawn, spinal cord was rinsed out of the

spinal canal with PBS. All organs were immediately snap-frozen and stored in liquid nitrogen.

For subsequent histological experiments, biopsies from the g*astrocnemius* muscle and the *rectus femoris* muscle were taken as well as the whole spine including the spinal cord. All organs for histological stains were immediately stored and fixed in 4% paraformaldehyde at 4°C. For the proceeding of histochemistry see chapter 3.13.

3.11 Molecular biology methods

3.11.1 Isolation of genomic DNA

To isolate clean and intact genomic DNA from both, tail-tip biopsies and fibroblast cell lines, always the ChargeSwitch® gDNA Mini Tissue Kit (*Invitrogen*) was used according to the manufacturer´s protocol. With the help of magnetic beads this kit provides a fast and extensive cleanup of genomic DNA even from tissues like tail-tips. The very clean genomic DNA is essential for the sensitive genomic quantitative real-time PCR.

3.11.2 Photometric determination of the DNA concentration

A NanoDrop ND-1000 Spectrophotometer (*Peqlab*) was used to determine the DNA concentration. Therefore, a 1.5 µl DNA sample was pipetted onto the end of a fiber optic cable and a second fiber optic cable was brought into contact with the liquid. Absorption was measured at wavelengths of 260 nm and 280 nm utilizing a pathlength of 0.2 mm, and the DNA concentration and purity was calculated by the software. The ratio of the measured absorption at the wavelength of 260 nm and 280 nm gives the grade of purity of the DNA. The ratio is recommended to range between 1.8 and 2.0. Higher values suggest contamination with RNA, while lower values point to contamination with proteins or ethanol. Measurements were performed in triplicates and the concentration calculated as mean of the single values.

3.11.3 Fluorimetric determination of the DNA concentration

For highly sensitive methods, like gene copy number determination, it is necessary to have very pure DNA and to know the exact concentration of it. To avoid any misleading concentration measurements due to RNA contaminations, the Quant-iT™ PicoGreen® dsDNA reagent (*Invitrogen*) was used according to the manufacturer´s protocol. With this kit and the help of a microplate reader it is possible to determine the exact DNA concentration.

3.11.4 Isolation of total RNA from mouse organs

To isolate total RNA from mouse organ biopsies the RNeasy Kit (*Qiagen*) and the QIAshredder (*Qiagen*) were used according to the manufacturer's protocols. For the isolation of total RNA out of fatty organs like brain or spinal cord, some preparative steps with Qiazol® according to the manufacturer´s protocol were included before starting with the RNeasy protocol. Always the optional DNase I digest was carried out using the RNase-Free DNase kit (*Qiagen*) according to the protocol included in the RNeasy kit.

3.11.5 Isolation of total RNA from primary fibroblast cell cultures

The isolation of total RNA from fibroblasts was carried out by the operating protocol of the used RNeasy Mini kit. Prior to the first cell lysis step, which was performed directly on the petri dishes, the medium was removed from the monolayer.

3.11.6 Determination of the RNA concentration

The standard method to quantify the RNA concentration is the measurement of the photometric absorbance at a wavelength of 260 nm (A260). Since at 260 nm also proteins, free nucleotides and DNA contribute to the absorbance signal, the pure photometric determination of the RNA is not very exact. To avoid misleading results, it was made use of a dye called RiboGreen®, which is fluorescent if it is specifically bound to RNA molecules and therefore helps to determine the exact RNA concentration. Furthermore the Quant-iT™ RiboGreen® RNA Assay Kit (*Invitrogen*) not only prevents to interpret contaminated RNA solutions, but also it aids to measure very low RNA concentration very exactly.

3.11.7 Photometric RNA concentration analysis

Similar to the DNA concentration determination, a NanoDrop ND-1000 Spectrophotometer (*Peqlab*) was used to determine the RNA concentration. Therefore, a 1.5 µl RNA sample was pipetted onto the end of a fiber optic cable and a second fiber optic cable was brought into contact with the liquid. Absorption was measured at wavelengths of 260 nm and 280 nm utilizing a pathlength of 0.2 mm, and the RNA concentration and purity was calculated by the software. The ratio of the measured absorption at the wavelength of 260 nm and 280 nm gives the grade of purity of the DNA. The ratio is recommended to range between 1.8 and 2.1. Higher values suggest contamination with degraded RNA or free nucleotides, whereas lower values point to contamination with proteins. Measurements were performed in triplicates and the concentration calculated as mean of the single values.

3.11.8 Fluorimetric RNA concentration analysis with RiboGreen® dye

Whenever RNA expression of treated fibroblasts or murine tissues was investigated, the expression of the transcript of interest was normalized to the total RNA amount. For this purpose, it was crucial to know the exact total RNA concentration. To ensure the knowledge of the exact RNA concentration, the Quant-iT™ RiboGreen® RNA Assay Kit (*Invitrogen*) was used according to the manufacturer´s protocol. This kit utilizes the feature that RiboGreen is non-fluorescent when free in solution, but when it is bound to RNA, the fluorescence of the dye increases more than 1000fold. The assay was set up in 96-well plates (Black, flat bottom, medium binding, #655076, *Greiner bio-one*). Fluorescence of the RNA-RiboGreen®-complexes was determined on a TECAN Safire^2 monochromator-based microplate reader (*Tecan*). All RNA stocks were analyzed in triplicates and the concentration calculated as mean value of these measurements.

3.11.9 Reverse transcription (cDNA synthesis)

All RNA expression experiments are based on the mRNA expression, but actually not directly RNA is measured by realtime-PCR attempts, but so called cDNA molecules are the templates for expression analysis. Do generate double-stranded complementary DNA (cDNA), the reverse transcription is the biomolecular technique of choice. It is taken advantage of the fact that most mRNA molecules possess a 3' poly-A-tail, and oligo-dT primers are used as starter molecules for the reverse transcriptase. The whole cDNA synthesis method was performed with the QuantiTect Rev. Transcription Kit (*Qiagen*) and oligo-dT primers (*Operon*).

3.11.10 Polymerase chain reaction (PCR)

One of the most commonly used biological technique worldwide is the polymerase chain reaction (PCR), which allows the enzymatic amplification of specific single-stranded DNA regions (Mullis and Faloona 1987). This technique utilizes the capacity of a DNA-dependent DNA polymerase to synthesize copies from a denatured, single-stranded DNA template, starting from sequence specific oligonucleotides (primers). The primers specifically hybridize to the complementary sequence in the DNA template and are elongated at their free 3'-hydroxy group. The program of cycles including repeated DNA denaturation, primer hybridization, and DNA synthesis is performed in a thermocycler. To sustain the maintenance of a functioning DNA-polymerase, the thermo stable T_{aq}-polymerase (from *Thermophilus aquaticus*) (*Invitrogen*) was used.

The standard PCR conditions, which were used, if not mentioned otherwise are:
10 min at 95°C denaturation followed by 34 cycles of 30 sec at 95°C, 30 sec at annealing temperature shown in table 4, 30 sec at 72°C. The final extension step was at 72°C for

10 min. The PCR products were resolved on an 1-2 % agarose gel (see chapter 3.11.14). For the used primers see chapter 3.7.

Table 7 Components used for a standard PCR

Component	Volume/reaction (µl)
Master mix	
Sterile water	variable
1.25 mM dNTP	4
10xPCR Buffer	2.5
25mM $MgCl_2$	1
Primer for	1
Primer rev	1
(Betain 1M)	(5µl)*
Taq polymerase	0.3
Template	
50 ng genomic DNA	variable*
Total volume	**25**

* Betain was only added to SMA_B genotyping PCR

3.11.11 Analysis of the number of transgenic *SMN2* copies by quantitative real-time PCR

Since *SMN2* is the main modifier of SMA, the knowledge of the exact transgene *SMN2* copy number in SMA model mice, is of crucial importance. The real-time PCR based copy number determination of SMN2 transgenes is newly developed method and therefore the details are presented in the “results”-part of this work (see 4.3.1.1).

3.11.12 Analysis of gene expression by quantitative real-time PCR

Quantitative real-time PCR of transcript levels in fibroblasts total RNA was extracted from every 10 cm cell culture dish using the RNeasy Kit (*Qiagen*) and QIAshredder according to the manufacturer’s protocols. DNase digest was included by use of the RNase-Free Dnase I set (*Qiagen*). Exact concentration of isolated RNA was precisely determined on a TECAN Safire² microplate reader using the RiboGreen® RNA quantitation kit (*Molecular Probes*). After reverse transcription of RNA into cDNA as described elsewhere (chapter 3.11.9), quantitative real-time PCR was performed on a LightCycler 1.5 instrument using Fast Start DNA Master SYBR Green I (*Roche*). Primers were chosen to bind in *SMN* exon 5 (5’-CCA CCA CCC CAC TTA CTA TCA-3’) (primer #1449) and *SMN* exon 7/8 (5’-ATC AAG AAG AGT TAC CCA TTC CA-3’) (primer #3054) for amplification of FL transcripts, and in *SMN* exon 5 (5’-CCA CCA CCC CAC TTA CTA TCA-3’) (primer #1449) and at the *SMN* exon6/exon8 border (5’-GCT CTA TGC CAG CAT TTC CAT A-3’) (primer #1450) in order to amplify truncated Δ7 transcripts. The

quantification program was followed by a melting step to detect the melting points for every PCR product. Analysis of the PCR curves was performed with the second derivative maximum method of the LightCycler software. All sample measurements were repeated at least three times and results are given as mean ± SEM.

3.11.13 Analysis of gene expression by one-step reverse transcription - quantitative real-time PCR

It is possible to perform the reverse transcription of RNA into cDNA followed by quantitative real-time PCR using cDNA as template in one and the same tube. To do so, a specific amount of RNA is incubated with all reagents required for reverse transcription (including the reverse transcriptase) and all reagents required for subsequent PCR (including the DNA-dependent DNA polymerase). The reaction mix is incubated at conditions, which allow the reverse transcriptase to become active and to synthesize cDNA. Then, by heating up the reaction mix, the reverse transcriptase is inactivated. Thereafter, the DNA-dependent DNA polymerase is activated and the quantitative real-time PCR takes place. One-step reverse transcription - quantitative real-time PCR is less time-consuming than separate reactions and minimizes pipette steps.

One-step reverse transcription - quantitative real-time PCR was performed on RNA samples derived from fibroblasts, which were previously transfected either with siRNA against different HDAC or with plasmids containing either HDAC2, HDAC8, HDAC11 or GFP as a control. The used OneStep RT-PCR Kit (*Qiagen*) is designed for sensitive one-step RT-PCR using any RNA template. For all quantified transcripts (except HDAC8, see Table 4) the pre-designed real-time QuantiTect Primer Assays (*Qiagen*) were chosen.

Analysis of the real-time raw data and normalization of *SMN* data with β-*actin* data for each sample was performed using the Sequence Detection Software, version 1.7 (*Applied Biosystems*). All sample measurements were repeated at least twice and results are given as mean ± standard error of the mean (SEM).

3.11.14 Agarose gel electrophoresis for separation of DNA fragments

The phosphate groups of the sugar-phosphate-backbone of DNA molecules are negatively charged. This attribute is used in the gel electrophoresis of DNA fragments. Depending on the fragment size, DNA molecules migrate at different speeds through the agarose gel matrix pores to the positively charged electric pole. The shorter fragments will more easily fit through the pores of the gel and migrate faster, while larger ones will have more difficulty and thus migrate slower. Additionally, the speed of migration depends on the current applied to the gel and the size of the pores of the gel. To

separate DNA fragments, which have different size, gel electrophoresis can be performed.

Not only for the genotyping of mice, but also to control the right size of PCR amplicons from newly established real-time PCR assays, agarose gel electrophoresis was performed. The routinely used agarose concentration of the gels was 1.5 %. 1.5 g of agarose (*Sigma*) was dissolved in 100 ml TBE buffer by boiling in a microwave. After a short cool-down step, 5 µl ethidium bromide solution (1%, *AppliChem*) was added and mixed. Thereafter, the liquid gel was poured into an appropriate gel tray and equipped with a comb. After solidifying of the agarose gel, the whole tray was transferred to a gel electrophoresis chamber. The gel was covered with a layer of TBE buffer, PCR samples were supplemented with DNA loading buffer and pipetted into the gel slots. DNA fragment separation was carried out at 75 V for ~30 min. To estimate the length of the PCR products a 100 bp DNA ladder (*Invitrogen*) was run together with the samples in an extra lane on the gel. The ethidium bromide-DNA fragments were visualized with UV light (wavelength 254 nm) on a ChemiDoc XRS Imaging system (*Biorad*).

3.12 Proteinbiochemical and immunological methods

3.12.1 Extraction of proteins from mouse organs

After the respective laboratory mouse was humanely sacrificed - either by decapitation (young mice) or by gasification on dry ice (adult mice) - its body was opened and quickly the organs of interest were removed. The freshly prepared organs were either used directly for protein or RNA (see chapter 3.11.4) extraction or snap frozen in liquid nitrogen.

To extract protein from mouse organs, about 300 mg of the respective organ was transferred into 150 µl of RIPA buffer (*Sigma*) and thoroughly homogenized using a T-10 Basic Ultra Turrax Homogeniser (*IKA*). All steps were performed on ice to avoid enzymatic degradation of RNA or proteins. To get rid of debris and DNA contamination the homogeneous organ solution was transferred into a centrifuge and spin down at 12,000 rpm at 4°C for 20 min. After centrifugation the protein containing supernatant was transferred into a new reaction tube. The proteins were either used directly for subsequent experiments or stored at -80°C.

3.12.2 Extraction of proteins from primary fibroblast cell cultures

To harvest protein from fibroblast cell lines, the D-MEM culture medium was removed, and cells were washed twice in 1 x PBS buffer (without Ca^{2+}, Mg^{2+}). To lyse the fibroblasts, 50 µl RIPA buffer (*Sigma*) was added directly on a 10 cm petri dish. To complete the lysis, dishes were kept on ice for 20 min. Thereafter, to get rid of debris and DNA contamination the homogeneous cell solution was transferred into a 1.5 ml reaction tube and then into a centrifuge and spin down at 12,000 rpm at 4°C for 20 min. After centrifugation the protein containing supernatant was transferred into a new reaction tube. The proteins were either used directly for subsequent experiments or stored at -80°C.

3.12.3 Protein contents determined according to the Bradford method

To quantify the protein concentration, it was made use of the method developed by Bradford (Bradford 1976). This technique utilizes the Bradford-dye capacity to bind proteins. If bound to protein, the dye shits it absorption maximum from 470 nm to 595 nm.

To determine the protein concentration 2 µl of each protein sample to be analyzed was incubated in 500 µl Bradford solution for 10 min on room temperature. Then the absorption of the samples was measured at a wavelength of 595 nm. With the help of a standard curve, which was prepared from bovine serum albumin (BSA) and which was previously programmed into the spectrophotometer the protein concentrations of the unknown samples were calculated.

3.12.4 Discontinuous denaturing polyacrylamide gel electrophoresis (SDS-PAGE)

To separate proteins according to their molecular weight, it is necessary to linearize the proteins by the use of the anionic detergent SDS (sodium dodecylsulfate). Since SDS applies a negative charge to the linearized protein, its endogenous charge is masked and all proteins in a protein solution are separated by their molecular weight (Laemmli 1970).

In a first step, the 12% PAA separation gel was prepared between two glass plates (distance 0.5 mm). 70% ethanol was added on top of the gel until solidification. After polymerization, the ethanol was removed and the stacking PAA gel was added on top of the separation gel between the two glass plates. The stacking gel contains less PAA than the separation gel, which results in larger gel pores. Moreover, the stacking gel is prepared with a Tris-buffer that differs from the Tris-buffer used for the separation gel in its concentration and pH. The main function of the stacking gel is to focus all of the

proteins into a single sharp band shortly after penetration into the gel. Proteins are then resolved in the separation gel, which possesses much smaller pores. As soon as an electric current is applied across the gel, the negatively charged proteins start to migrate. Short proteins will more easily fit through the pores in the gel, while larger ones will have more difficulty and migrate slower. The usage of a system with discontinuous buffers and gel pores enhances the sharpness of the protein bands. Before 7.5 µg of each protein sample were transferred into the slots of the PAA gel, samples were supplemented with Laemmli buffer and boiled at 95°C for 5 min to enhance denaturation. In a separate lane, marker proteins of known molecular weight were run (Precision Plus Protein All Blue Standards, *Biorad*) to estimate the molecular weight of the unknown proteins in the samples. Gel electrophoresis was performed at 50-120 V in an electrophoresis chamber using 1 x electrophoresis buffer.

3.12.5 Transfer of proteins to nitrocellulose membrane by wet blotting (Western blot)

To observe or to quantify protein expression, the method of Western blotting was utilized. As a first step to make proteins available for antibody detection, they were moved from within the SDS gel onto a nitrocellulose membrane [Protran BA 83 Cellulosenitrat (E), *Whatman*]. Prior to use, the membrane was equilibrated in transfer buffer, after that placed face-to-face on the gel, and a gel sandwich was prepared together with two fiber pads and two filter pads all soaked in transfer buffer. This gel sandwich was put into a cassette, which then was placed into a transfer module of a Mini Trans-Blot Cell (*Biorad*). Wet blotting was carried out at a current of 30 V overnight at 4°C. Thus, due to the incubation with SDS negatively charged proteins moved onto the membrane and adhered there, while maintaining the size specific organization they had within the gel. As a result of this blotting process, proteins were exposed on a thin surface layer for detection.

3.12.6 Ponceau staining of proteins on nitrocellulose membranes

To control the correct protein transfer after wet blotting over night, the nitrocellulose membrane was stained in a Ponceau solution for 30 s. The Ponceau dye staines the positively charged amino acid side chains red. For a good transfer, a homogenous protein band pattern is expected, but also air bubbles could be detected, making the whole blot useless. To go on with the immunostaining of the membrane (see chapter 3.12.7), the membrane was washed in TBS-Tween buffer several times to remove Ponceau dye again.

3.12.7 Immunostaining of membranes with antibodies and detection of signals with chemiluminescence reagent

After the wet blot protein transfer, all proteins are bound unspecifically to the nitrocellulose membrane. To avoid background signals due to unspecific interactions of the respective antibodies with the nitrocellulose membrane, the membrane was blocked in 6% blocking solution containing non-fat dry milk in TBS Tween buffer for 3 h (after Ponceau staining). This was followed directly by the incubation with the respective primary antibody against the target protein of interest (see Table **8**). Therefore, the primary antibody was diluted in 5 ml 1-2% non-fat dry milk in TBS Tween in a 50 ml reaction tube and after that incubated with the nitrocellulose membrane for the respective incubation time on a roller shaker at 4°C. To remove the unbound primary antibody rests, the membrane was washed subsequently for 5 x 5 min in TBS Tween. Then the secondary antibody, which binds specifically to the primary antibody and is linked to a reporter enzyme, the horseradish peroxidase, is incubated together with the membrane as described for the primary antibody. After a second washing step, dectection of the samples that are labeled and bound to the protein of interest was performed via chemiluminescent detection. For this purpose Western blots were incubated with 8 ml SuperSignal® West Pico Chemiluminescent Substrate (*Pierce*) for 5 min. This is a substrate, which will fluoresce when exposed to horseradish peroxidase on the secondary antibody. The light was then detected by photographic film (Hyperfilm ECL, *Amersham*) and the image analyzed by densitometry to evaluate the relative amount of protein staining and to quantify the results in terms of optical density.

Table 8 Antibody conditions used for Western blot analysis

Antibody	Dilution and incubation time
anti β-Actin, monoclonal mouse (*Sigma*)	1:20,000 for 1 h
anti-SF2/ASF, monoclonal mouse (kindly provided by A. Krainer, Cold Spring Harbor Laboratories)	1:200 overnight
anti-SRp20, monoclonal mouse (*Santa Cruz*)	1:100 for 24 h
anti-SMN, monoclonal mouse (*BD Transduction Laboratories*)	1:3,000 for 1 h
anti-Htra2-β1, polyclonal rabbit	1:1,000 for 2h
anti-cMYC, monoclonal mouse (*Invitrogen*)	1:1,000 for 1h
anti-HDAC2 (*Santa Cruz*)	1:1,000 overnight
anti-HDAC8 polyclonal rabbit (*MBL*)	1:1,000 for 2h

anti-acetyl Histone H3 K9, monoclonal mouse (*Upstate*)	1:1,000 for 2h
anti-β-Tubulin, (*Sigma*)	1:2,000 for 1h
anti-GADD45α monoclonal mouse (*Abnova*)	1:1,000 overnight

3.12.8 Chromatin Immunoprecipitation

Chromatin Immunoprecipitation (ChIP) gives a picture of the protein-DNA interactions that occur inside the nucleus of living cells or tissues. Here ChIP was used to determine the histone 3 acetylation status of lysine residue 9 (acetyl-H3K9). After treating cells with HDACis, the DNA-protein complexes were crosslinked and therefore fixed by applying formaldehyde to the cells. After crosslinking, the cells were lysed and the DNA was sheared into pieces 0.2-1 kb in length by sonication. Then anti-acetyl-H3K9 antibody-based immunoprecipitation was performed. After the protein-DNA complexes were pulled-down, the cross-linking was reversed and the amount of eluted DNA was quantified by real-time PCR. From the quantitative real-time PCR, conclusions may be drawn to the histone acetylation status of the respective genomic region. The same procedure was repeated with the use of an anti-HDAC8 antibody in order to assess the amount of HDAC8 protein bound to the *SMN2* promoter region. A more detailed describtion is given in the following:

After protein-DNA cross-linking with formaldehyde (300,000 fibroblast cells in 500 µl PBS + 12.5 µl 36.5% formaldehyde for 8 min at room temperature), cells were washed in PBS (2 x 0.5 ml ice-cold PBS) and pelleted (10 min at 470 x g at 4°C). The cell-pellet was resuspended in cell lysis buffer (130 µl buffer B (*Diagenode*) for 5 min on ice). To shear the chromatin into 500-1,000 bp long fragments, the cell lysate was sonicated using the Bioruptor (*Diagenode*) with the following parameters: 12 cycles of 30 sec “on” and 30 sec “off” each at “high” power.

Chromatin Immunoprecipitation (ChIP) was performed by using the LowCell# ChIP Kit™ (*Diagenode*) according the manufacturer’s protocol. With the help of protein A-coated paramagnetic beads respective antibodies were labeled in a first step and afterwards used for chromatin pull-down. After the cleanup of DNA, DNA concentration was fluorometrically measured by use of the Quant-iT™PicoGreen® dsDNA kit (*Invitrogen*), according to the manufacturer’s manual.

Table 9 Antibody conditions for ChIP experiments

Antibody	**amount for 300,000 cells and incubation time**
anti-H3K9ac polyclonal rabbit (*Diagenode*)	2 µg overnight
anti-HDAC8 polyclonal rabbit (*MBL*)	2 µg overnight
anti-acetyl Histone H3 K9, monoclonal mouse (*Upstate*)	2 µg overnight

For the quantification of the DNA amount of the *SMN2* promoter region, which was eluted from the respective ChIP experiment, a real-time PCR in the Taqman apparatus was performed. Therefore the PowerSYBR green master mix (2x) from *Applied Biosystems* was used. The mentioned master mix contains Taq-polymerase and SYBR-green, which is needed for a quantitative real-time PCR. The exact compound and conditions for the *SMN2* promoter real-time PCR are given in the subsequent tables.

Table 10 Compunds for the SMN2 promoter real-time PCR

Mastermix for Real-Time	**25µl**
SYBR-MM [2x]	12.5 µl
Primer 1 [10 pmol]	0.5 µl
Primer 2 [10 pmol]	0.5 µl
DNA (20ng)	e.g. 3.5 µl
H_2O	8 µl

Table 11 Conditions for real-time *SMN2* promoter PCR

	temperature	**time**	**Mode**
1x	50 °C	2 min	Activation of Taq
1x	95 °C	10 min	Denaturation
40x	95 °C	15 sec	Denaturation
	60 °C	45 sec	Annealing
	70 °C	45 sec	Taq activity/ fluorescent measurement

3.13 Histochemistry

Before whole mouse organs or biopsies were embedded in paraffin, they were fixed in 2% paraformaldehyd (PFA) over night and afterwards dehydrated with the help of an infiltration machine (*Leica*). Embedded samples were cut with the help of microtome (*Leica*) into 8 µm thick sections.

3.13.1 Nissl staining

Cresyl violet is a basic dye, which stains cell bodies and nuclei. Cross sections of the spine of mice were stained with the Nissl staining method in order to visualize cell bodies and nuclei of neurons, using the following steps:

1. depariffinization in Xylol	3 min
2. rehydration in a downward ethanol series	
100% ethanol	3 min
96% ethanol	3 min
70% ethanol	3 min
50% ethanol	3 min
PBS	5 min
3. staining in Cresyl Violet acetate	10 min

4. wash in $aqua_{bidest.}$
5. wash in high diluted acetic acid (2-3 drops acetic acid in 100 ml H_2O)
6. wash in $aqua_{bidest.}$

After the last washing step was finished, the sections were mounted in Vectashield mounting medium.

3.13.2 Hematoxylin and eosin staining

The hematoxylin and eosin (H&E) staining method involves application of the basic dye hematoxylin, which colors basophilic structures blue-purple, whereas the alcohol-based acidic eosin Y colors eosinophilic structures bright pink. The cellular basophilic structures contain nucleic acids, such as the ribosomes and the chromatin-rich cell nucleus, and the cytoplasmatic regions rich in RNA. Structures which contain intracellular or extracellular protein and most of the cytoplasm are stained by eosin. H&E staining was used for muscle overview stainings. Subsequently a detailed H&E staining protocol is given:

1. deparaffinization in Xylol	30 min
2. rehydration in a downward ethanol series	
100% ethanol	1 min
96% ethanol	1 min
70% ethanol	1 min
PBS	1 min
Water	1 min
3. staining in hematoxylin	6 min
4. short wash in water	
5. wash in water	15min
6. short wash in $aqua_{bidest.}$	
7. staining in eosin	1 min
8. short wash in water	6-7 times
9. 70% ethanol	1 min
10. 96% ethanol	1 min
11. 100% ethanol	1 min
12. Xylol	1 min
13. embedding in *Entellan*	

3.13.3 Immunohistochemistry

For preparation, muscle biopsies from the *gastrocnemius* muscle were embedded in 4% low melting agarose (*Cambrex*). In order to perform immunostainings of the neuromuscular junctions, always relatively thick (200 µm) vibratome sections were prepared. To visualize neuromuscular junctions (NMJ) anti-Neurofilament M antibody (*Millipore*), which recognizes the neurofilaments and tetramethylrhodamin-labelled α-bungarotoxin (α-BTX) (*Invitrogen*), which binds to acetylcholine receptors in the NMJs, were used, following the below-mentioned protocol.

Table 12 Stepwise protocol for immunostaining of neuromuscular junctions. Used material and respective conditions.

Substances	**Conditions**
Day 1	
Washing: in PBS	3 x 5 min
Blocking: in 4%BSA in PBS	1 h
Staining: anti-Neurofilament M (145kDa) rabbit	1:350 dilution

in 2% BSA/PBS/1%Triton X	overnight (wet board) at 4°C
Day 2	
Washing: in PBS	3 x 5 min
Staining: donkey anti-rabbit Cy2 (Dianova) and α-BTX in 2% BSA/PBS/1%Triton X	1:40 dilution 1:500 dilution For 4 h (wet board) at 4°C
Washing: in PBS	3 x 5 min
Mounting Medium w/o : Mounting medium with Dapi	1:4 dilution

3.13.4 Analysis of the motor neuron, NMJ and muscle stainings

- **Motor neuron count**

After the whole spine (including bones and spinal cord) was cut into 8 µm cross section and stained with Nissl-staining (as previously described in chapter 3.13.1), the cross sections from the lumbar region were analyzed under the light microscope. To avoid counting the same motor neurons several times, not subsequent sections, but every third or fourth section was analyzed. The obvious shape and size of the motor neurons and their specific localization in the anterior horns of the spinal cord, allowed a restricted and specific motor neuron count. The motor neurons of 20 cross sections each derived from 3 SAHA treated P5 SMA, 3 untreated P5 SMA, 3 SAHA treated P5 heterozygous, and 3 untreated P5 heterozygous animals were counted. The same was repeated for P10 mice. The motor neurons were counted by eye and subsequently evaluated.

- **NMJ evaluation**

Immunohistologically labeled neuromuscular junctions (NMJs) were visualized under a fluorescence microscope. Two-channel pictures (red: α-BTX, green: neurofilament M) were taken from NMJs. The surface area of each NMJ was measured with the help of *AxioVision Rel.4.7* computer software (*Zeiss*). 100 NMJs were measured for each respective animal. The muscle biopsies for the NMJ stainings derived from 3 SAHA treated P10 SMA, 3 untreated P10 SMA, 3 SAHA treated P10 heterozygous, and 3 untreated P10 heterozygous animals. The NMJ evaluation was subsequently analyzed by the use of statistic software (*MS Excel, SigmaPlot*).

- **Muscle fiber evaluation**

The *musculus rectus femoris* was stained with the H&E staining method. Under a light microscope an overview of the muscle structure was clearly visible. Comparable to the NMJ evaluation, the surface area of each muscle fiber was measured with the help of *AxioVision Rel.4.7* computer software (*Zeiss*). 100 muscle fibers were measured for each respective animal. The muscle biopsies for the muscle fiber stainings derived from 3 SAHA treated P10 SMA, 3 untreated P10 SMA, 3 SAHA treated P10 heterozygous, and 3 untreated P10 heterozygous animals. The muscle fiber evaluation was subsequently analyzed by the use of statistic software (*MS Excel, SigmaPlot*).

3.14 Statistical methods

Whenever the significance of the RNA expression levels after HDACi treatment as well as the changed protein levels were tested, it was done by the use of a directional student's t-test for uncorrelated samples. This significance test was performed for both, cell-derived protein and RNA levels after *in vitro* treatment and tissue-derived protein and RNA levels after *in vivo* treatment. In all cases, three levels of statistical significance were distinguished: $p<0.05$, $p<0.01$, and $p<0.001$.

To evaluate the significant variance in the number of born SMA_B mice compared to the expected number of SMA mice, a chi-square (χ^2) test was performed.

A Wilcoxon-rank-sum test was performed in order to determine the significance in the increase of survival (the shift of the Kaplan-Meier curves) of the SMA mice after SAHA treatment.

4 Results

In 96% of all patients with proximal spinal muscular atrophy (SMA) the homozygous loss of the *survival motor neuron gene 1* (*SMN1*) is either caused by a deletion or a gene conversion of *SMN1* into its almost identical copy gene *SMN2* (Wirth et al. 1999). The absence of the *SMN1* gene causes the degeneration of the α-motor neurons in the anterior horns of the spinal cord and thereby causes a progressing atrophy of the voluntary muscles. All SMA patients retain at least one copy of the *SMN2* gene, which is the main modifying gene of SMA. This is reflected by the fact that the disease severity inversely correlates with the *SMN2 copy* number (Brahe 2000; Burghes 1997; Feldkotter et al. 2002). The *SMN2* gene is incapable to produce enough full-length *SMN2* mRNA/protein; only ~10% of all *SMN2* transcripts are spliced correctly, including all exons, whereas ~90% of the *SMN2* transcripts lack exon 7 (Gennarelli et al. 1995; Lefebvre et al. 1995; Lorson et al. 1999).

For a potential SMA therapy the main target is the *SMN2* copy gene. Different strategies in modifying the *SMN2*-derived SMN protein level are possible. Two main policies are the elevation of the expression level of *SMN2* and the correction of the splicing of the *SMN2* pre-mRNA. The attempt that we performed was the epigenetic modification of the *SMN2* gene by means of histone deacetylase inhibitors (HDACi). In our laboratory we could prove that the FDA approved drug valproic acid (VPA), which functions as an HDACi, is able to up-regulate SMN expression *in vitro* and *in vivo* in SMA carriers and patients (Brichta et al. 2003; Brichta et al. 2006a). Recently, the favorable effect of VPA for a potential SMA therapy was further underlined by the *in vivo* findings in an SMA mouse model (Tsai et al. 2008a).

However, there is still a need for new potential SMA neurotherapeutics, since a clinical trial showed that VPA is able to increase SMN levels in only one third of SMA patients, whereas one third did not respond to the regimen and one third of patients even showed a down-regulation of the SMN expression (Brichta et al. 2006b). The results from a recent open label trial of VPA in 42 subjects with SMA revealed that this HDACi was well-tolerated, but no significant positive effect on the SMA progression has been observed. Nevertheless, weight gain and carnitine depletion has been found to be significant adverse effects (Swoboda et al. 2009). We focused our search for HDACi first on new substances from different chemical groups: the benzamide M344, the peptide depsipeptide (FK228) and the hydroxamic acid suberoylanilide hydroxamic acid (SAHA). The goal was the identification of new potential SMA therapeutics. Moreover, the broad range of undesirable side effects of unspecific pan-HDACis leads us to concentrate our search on a specific HDAC which regulates *SMN2* expression and a respective HDACi.

4.1 *In vitro* experiments with histone deacetylase (HDAC) inhibitors in fibroblast cell lines derived from SMA patients and SMA mouse models

4.1.1 Treatment of SMA fibroblast cultures with M344

M344 (IUPAC name: 4-(Diethylamino)-N-[7-(hydroxyamino)-7-oxoheptyl]benzamide) has 1999 been synthesized as an amide analogue of trichostatin A (TSA) by Jung et al.(Jung et al. 1999). It has been shown that M344 is a potent histone deacetylase inhibitor (HDACi) (IC_{50} = 100 nM), which induces terminal cell differentiation and causes an increase in hyperacetylated histone H4 and H3 (Jung et al. 1999; Takai et al. 2006). M344 has been proven to be an antiproliferative agent, which is able to suppress the growth of human endometrial and ovarian cancer cells by inducing cell cycle arrest and apoptosis (Takai et al. 2006). Because of its high potency in inhibiting HDACs, M344 was chosen for *in vitro* testing in SMA patient derived fibroblast cells, with regard to investigate M344´s potency in up-regulating the *SMN2* expression.

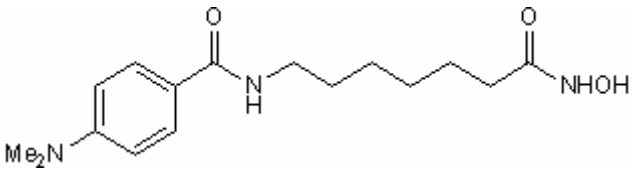

Figure 11 Chemical structure of the benzamide M344

In our laboratory, a collection of more than 100 primary fibroblast cell lines derived from epidermal skin biopsies of SMA patients, carriers and controls, is available. The rapid growth and the stable reproduction rate turn these fibroblasts into an important tool for *in vitro* testing of potential SMA neurotherapeutics. Cell lines from SMA type I (ML17; 2 *SMN2* copies), type II (ML20; 2 *SMN2* copies) and type III (ML12; 3 *SMN2* copies) patients were chosen to perform *in vitro* tests with M344. As preliminary work the optimal time period for M344 treatment was assessed by SMN protein level quantification (via western blotting) after 12, 24, 32, 48, 64, 80 and 96 h (M. Rießland, Diploma Thesis). For M344 treatment the optimal and most effective treatment period was 64 h and therefore chosen for all subsequent experiments.

4.1.1.1 Impact on *SMN2* RNA levels

In order to quantify the transcript amounts, first whole RNA of treated and untreated fibroblast cultures was precisely measured on a microplate reader using the RiboGreen®

dye. After that an exact amount of 150 ng was reverse transcribed. To avoid misleading results from the risk of altered housekeeper gene expression after HDACi treatment, the *SMN2* mRNA levels to the total RNA amount.

To assess whether M344 has an impact on the expression level of *SMN2*, the total amount of both *SMN2* transcripts, FL-*SMN2* and Δ7-*SMN2*, was quantified. The diagrammatic presentation of the quantified mean values for FL-*SMN2* and Δ7-*SMN2* is shown in Figure 12 a and b, respectively. In all three different cell lines a more than 1.6-fold up-regulation of the full-length transcript was observed after the treatment with 30 µM of M344 compared to the mock-treated cells (Figure 12). Interestingly, this elevation was not observed on the Δ7-*SMN2* levels. Whereas in ML20 the Δ7-*SMN2* remained nearly unchanged, in ML12 and ML17 a significant down-regulation starting from M344 concentrations of 5 µM was noticed. After treatment with 50 µM M344 the Δ7-*SMN2* level in ML12 went down to ~64% compared to the mock treated expression level. An even higher effect was found in ML17, where the Δ7-*SMN2* amount decreased to ~56% after treatment with 5 µM M344 (Figure 12b). This data suggests that not only the basic expression level of *SMN2* can be elevated by M344 treatment, but that also the splicing pattern of the *SMN2* pre-mRNA is reversed by its regimen. This reversion is clearly shown in Figure 12c. For each cell line in nearly every concentration of M344 a significant increase of the FL-*SMN2*/Δ7-*SMN2* ratio points towards the strong reversion of the splicing pattern. This reversion of the splicing pattern would be another beneficial effect of M344 in terms of looking for a future potential SMA neurotherapeutic agent.

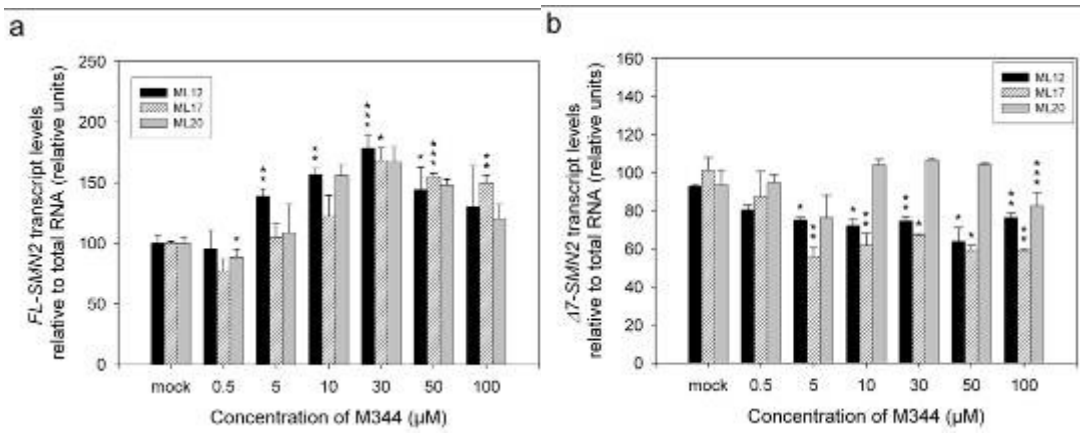

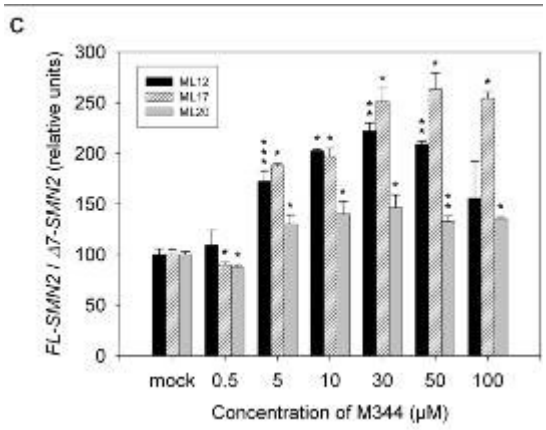

Figure 12 Up-regulation of *SMN2* mRNA in fibroblasts derived from SMA patients treated with increasing concentrations of M344 (0.5–100 µM) for 64h. Quantitative real-time PCR results are summarized as bar graphs. **a** Mean values (± SEM) for FL-*SMN2* relative to total RNA amount in cell lines ML12, ML17 and ML20. **b** Mean values (± SEM) for Δ7-*SMN2* relative to total RNA amount in cell lines ML12, ML17 and ML20. Δ7-*SMN2* levels were nearly unchanged or even reduced, suggesting an efficient reversion of the splicing pattern contributing to the significantly increased FL-*SMN2* levels. **c** Increasing FL-*SMN2*/Δ7-*SMN2* ratios in all cell lines, pointing out the strong reversion of the splicing pattern (* $p < 0.05$; ** $p < 0.01$; *** $p < 0.001$).

4.1.1.2 SMN and splicing factor protein level change under M344

To assess the impact of M344 on protein level, semiquantitative Western blotting was applied using β-Tubulin as internal control. All experiments were carried out in triplicates, using at least three different passages of the respective fibroblast cell line.

Whole protein extracts were first measured by the Bradford method; equal amounts of protein (7.5 µg) were loaded onto SDS PAGE gel and after electrophoresis, blotted on nitrocellulose membranes. The signal-intensity of the subsequently performed immunostainings was densitometrically quantified.

On protein level every tested fibroblast line responded to the 64 h M344 treatment in an up-regulation of the SMN protein level. The SMN protein amounts were significantly and dose-dependently up-regulated, reaching maximum values in the respective cell line ranging between 3- and 7-fold at concentrations of 30 to 50 µM (Figure 13 a and b). Importantly, a significant augmentation of SMN up to 1.5- to 3-fold could already be noticed at a very low concentration of only 5 µM M344.

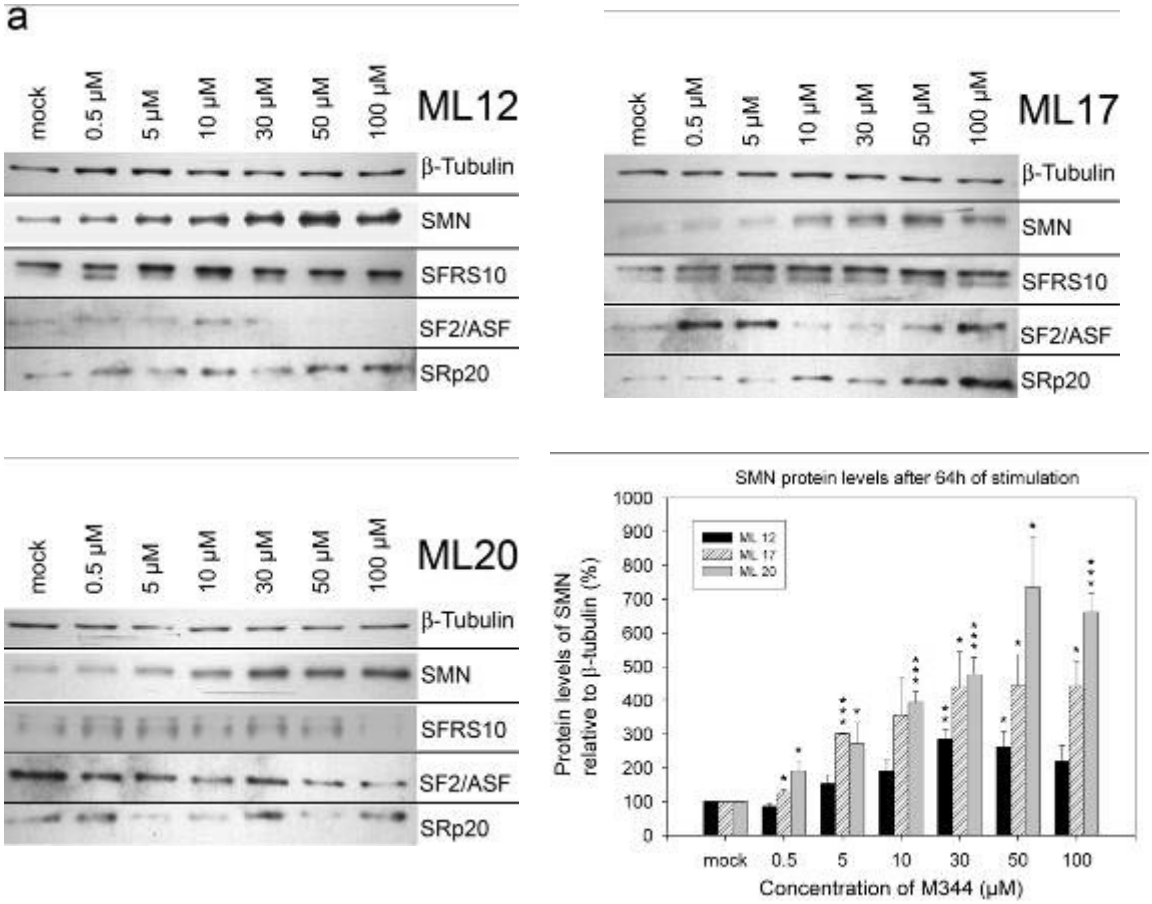

Figure 13 Increase of SMN and alteration of splicing factor protein levels in fibroblast cell lines from SMA patients after treatment with increasing concentrations of M344 (0.5–100 µM) for 64 h. **a** Western blots loaded with equal protein amounts were simultaneously stained with anti-β-tubulin, anti-SFRS10, anti-SF2/ASF, anti-SRp20 and anti-SMN. The pictures show representative Western blot analyses of cell cultures ML12, ML17 and ML20. **b** Mean SMN protein levels (± SEM) in ML12, ML17 and ML20 relative to β-tubulin (* $p < 0.05$; ** $p < 0.01$; *** $p < 0.001$)

Since it was noticed that M344 is able to reverse the splicing pattern of *SMN2* pre-mRNA, the question arose, if the splicing factor which is mainly involved in *SMN2* splicing correction, namely SFRS10, could be expressed differentially under M344 treatment. For that purpose quantitative Western blot analyses were performed, including the SR-like splicing factor SFRS10 (Hofmann et al. 2000), the SR splicing factor SF2/ASF, which is known to be involved in *SMN* pre-mRNA splicing (Cartegni and Krainer 2002) and the SR splicing factor SRp20, which was excluded to act in that way (Hofmann et al. 2000).

Whereas SF2/ASF protein levels were subjected to big fluctuations below and above baseline (Figure 14 a), SFRS10 showed a clear up-regulation in two of the three cell lines, while a slight down-regulation was observed for the remaining one at 50 and 100 µM M344 (Figure 14b).

Strikingly, both SFRS10 and SRp20 protein levels were augmented in a significant manner at the respective M344 concentrations. ML12 turned out to have a 3-fold

increase of SFRS10 at 30 µM M344 and ML17 even showed a 4.3-fold elevated expression at 50 µM. ML20 revealed only a very weak dose-dependent response. Nevertheless, even ML20 reached a highly significant increase of SFRS10 protein at 10 µM of M344 (Figure 14c).

The response to M344 treatment in SRp20 protein expression varied drastically inter-individually. ML12 showed a 4-fold increase starting from 10 µM M344 and its maximum elevation at 50 µM M344 culminated in a 7-fold protein concentration. In contrast to ML12, ML20 reached its maximum SRp20 expression of only 200% at 30 µM M344.

To draw a conclusion from these protein-expression data, M344 has a high impact not only on transcriptional activation of *SMN2* but also it is able to reverse the *SMN2* pre-mRNA splicing pattern via up-regulation of the mainly involved splicing factor SFRS10. Furthermore, the HDAC inhibitory function of M344 leads to the expression elevation of the *SMN2* unrelated splicing factor SRp20, indicating an unspecific impact of M344 on this protein.

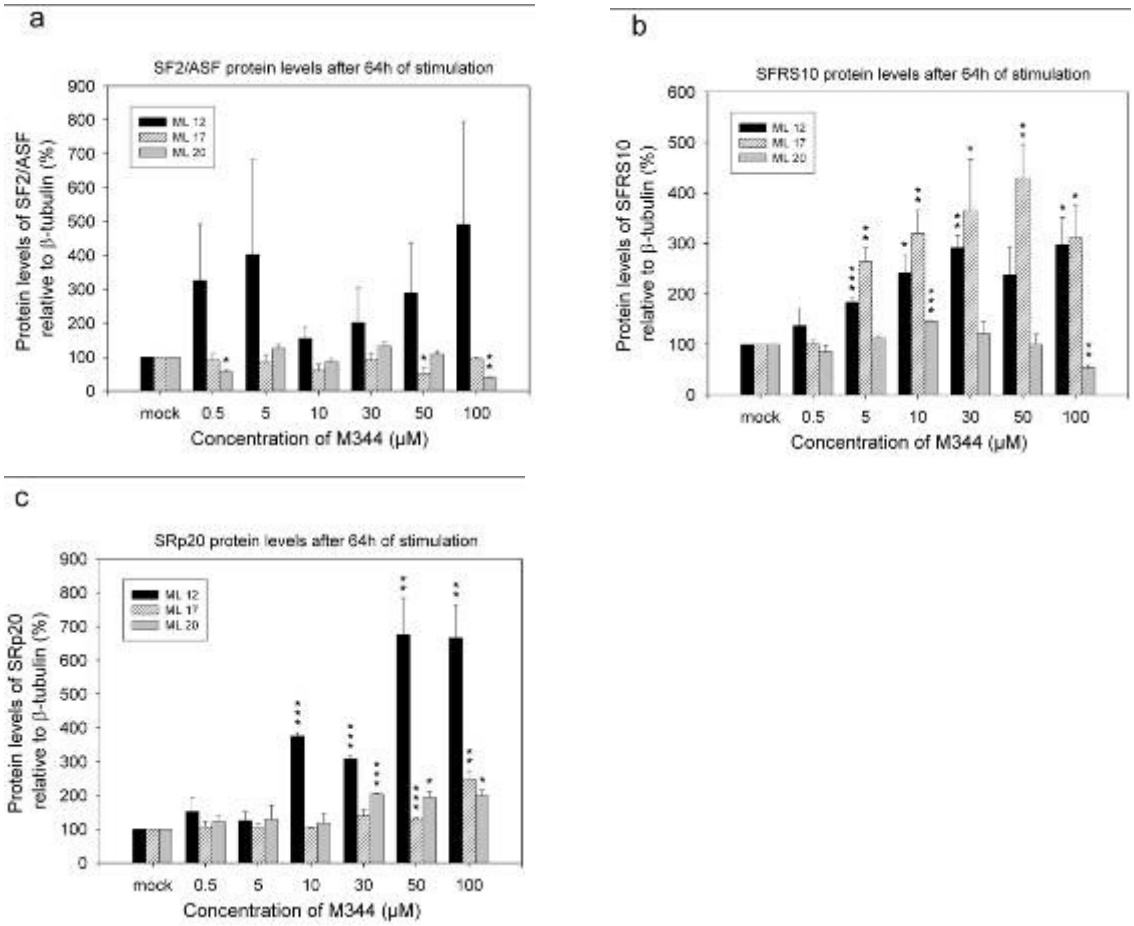

Figure 14 Regulation of the splicing factors **a** SF2/ASF, **b** SFRS10 and **c** SRp20 in the human SMA fibroblast lines ML12, ML17 and ML20 treated with increasing amounts of M344 for 64 h. SFRS10 and SRp20 protein levels are clearly elevated, while SF2/ASF is subject to expression fluctuations or nearly unchanged (* $p < 0.05$; ** $p < 0.01$; *** $p < 0.001$).

4.1.1.3 Change of the number of gems

The SMN protein is localized in subnuclear structures called gems (Liu and Dreyfuss 1996). Since the SMN protein level is strongly elevated under the M344 treatment, the next point to be investigated was the subcellular localization of SMN. To follow up the hypothesis that M344 is able to augment the number of gems, these structures were visualized by SMN immunofluorescence staining and counted. The nuclei were counterstained with 4′,6-Diamidino-2-phenylindol (DAPI). The number of gems per 100 cells was compared between the mock (DMSO) and the M344 (10 µM was chosen as a mean dosage, which showed remarkable responses in the respective cell lines) treated fibroblasts. M344 treatment revealed for each cell line a significant elevation of the number of gems per 100 cells (Figure 15a). Moreover, it was observed that the percentage of cells without gems decreased, whereas the percentage of cells with a low number of nuclear gems (one or two gems) remarkably increased, whereas only a few cells with a higher number of gems was found (Figure 15b). This suggests that the number of gems increased not only in cells, which prior to the M344 treatment contained gems, but that a great proportion of the monitored cells produced gems *de novo*.

Strikingly, a clear correlation between the degree of SMN protein amount up-regulation and the elevation of nuclear gem was found for every cell line. On protein level ML12 revealed the weakest increase after M344 stimulation of about 3-fold (Figure 13b), the same range of increase was observed on gem level (~3.3-fold). The highest impact in SMN protein expression was observed for ML20 (~7-fold) (Figure 13b). Consistent with this result, the highest increase (~30-fold Figure 15a) of observed gems was also found here. The intermediate up-regulation of SMN (~4.3-fold) in ML17 was reflected on gem level, where a significant 5.4-fold increase was found (Figure 15a).

Noteworthy, for all tested cell lines it could be stated that the respective line, which contained in an untreated state relatively low amounts of gems showed the highest response in up-regulating gem numbers.

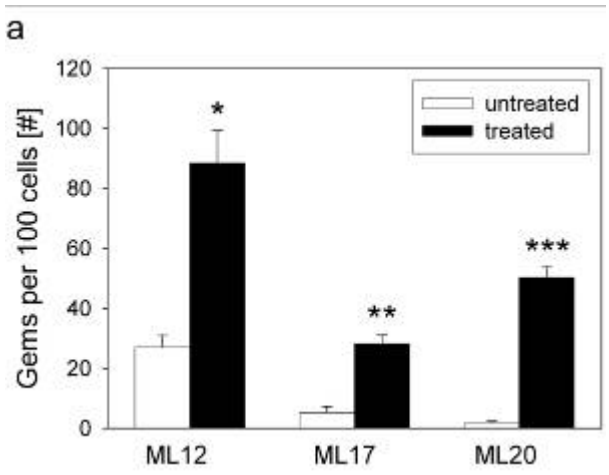

b

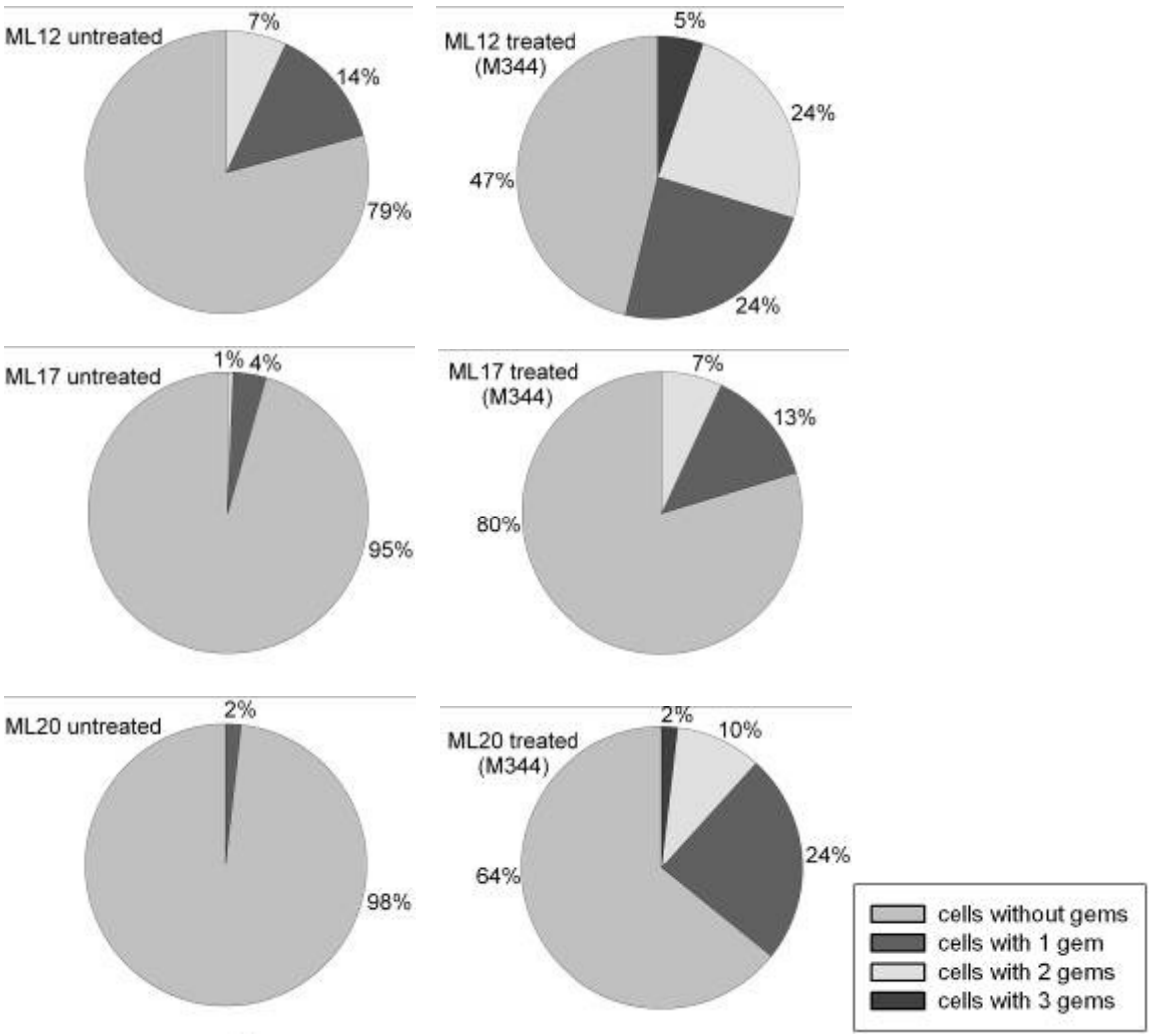

c

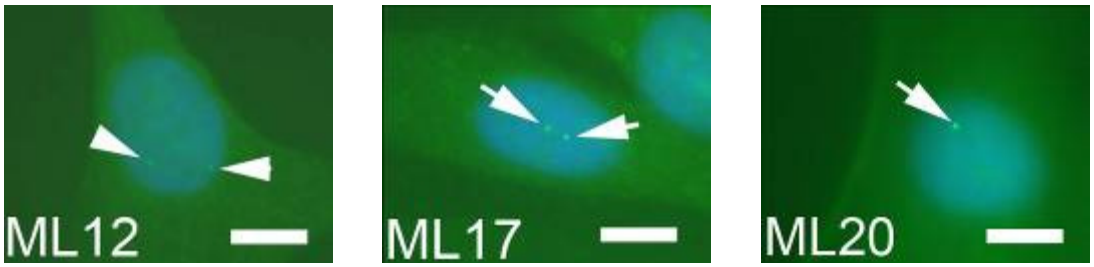

Figure 15 a Inter-individual comparison of the gem number/100 cells in untreated and M344-treated cell lines. For each cell line, a clear response on M344 treatment resulting in a significant elevation of the number of gems was observed (* $p < 0.05$; ** $p < 0.01$; *** $p < 0.001$). **b** Pie charts representing the percentages of cells without or with a certain number of gems in untreated or M344-treated fibroblasts. **c** Representative microscopy images of nuclear gems (marked with white arrows) from every treated cell line. Gems were stained with anti-SMN-FITC antibody, whereas the nuclei in blue were counterstained with DAPI. White bar = 10µm.

4.1.1.4 Cytotoxicity of M344 in SMA fibroblasts

Because it has to be considered that pan-HDAC inhibitors like M344 may have many unfavorable side effects in cell treatment, an MTT (thiazolyl blue tetrazolium bromide) assay was performed, which determines the viability of cells (Mosmann 1983).

The decrease of the fluorometric absorption of the formazan crystals, which are produced by living cells out of the MTT substrate, reached a significant level compared to mock treated cells at concentrations of M334 starting from 50 µM (Figure 16). This in turn indicates an increased cytotoxicity of M344 for fibroblasts for the concentrations 50 and 100 µM.

However, since M344 showed a high impact on SMN expression (3- to 6-fold up-regulation) at already considerably lower concentrations (5-30 µM), this substance could still be considered as a potential SMA therapeutic agent.

To date M344 is not FDA approved and so it remains elusive whether this HDACi might be used in a prospective SMA therapy. Until then M344 remains an experimental drug and we did not imply M344 for *in vivo* testing.

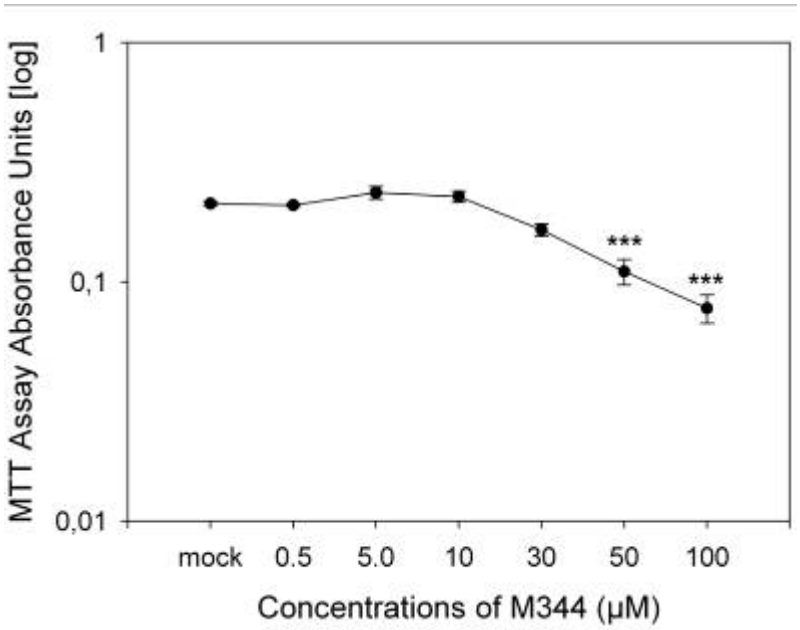

Figure 16 MTT cell viability assay in ML12 demonstrating Cytotoxicity of M344 at concentrations higher than 30 µM, implicating increasing cell death of cultured SMA fibroblasts at these M344 amounts (treatment time 64 h) (*** $p < 0.001$)

4.1.2 Treatment of SMA fibroblast cultures with FK228 (Depsipeptide)

Chromobacterium violaceum is producing the HDAC inhibitor FK228 (formerly named FR901228), also known as depsipeptide. FK228 is a very potent pan-HDACi, which predominantly inhibits HDAC class I (Furumai et al. 2002). Depsipeptide shows a potent *in vivo* antitumor activity against both human tumor xenografts and murine tumors (Ueda et al. 1994a; Ueda et al. 1994b). *Gloucester Pharmaceuticals, Inc.* holds the patent for FK228 and started recently several phase 2 clinical trails for different cancer entities (www.gloucesterpharma.com). This company graciously provided us with a limited amount of FK228 for a small *in vitro* testing setup.

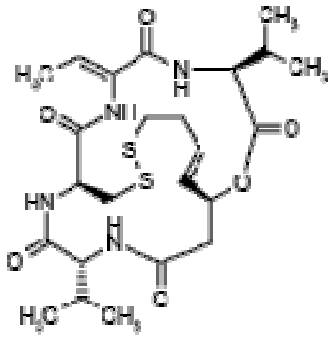

Figure 17 Chemical structure of FK228 (Depsipeptide)

Two human SMA type I fibroblast cell lines (ML16 3 *SMN2* copies and ML17; 2 *SMN2* copies) and one murine (MEF14, derived from an embryo SMA_B mouse strain (Monani et al. 2000), carrying the genotype $Smn^{-/-}$ $SMN2^{tg/tg}$) fibroblast cell line were tested for SMN2 expression changes after FK228 treatment. Because of the limited amount of FK228, the numbers of gems were quantified only in the human cell lines.

As preliminary work the optimal time period for FK228 treatment was assessed by SMN protein level quantification after 12, 24, 32, 48, 64, 80 and 96 h (data not shown). For FK228 treatment the optimal and most effective treatment period was 48 h for the murine fibroblast line and 64 h for the human cell lines and therefore chosen for all subsequent experiments.

4.1.2.1 Impact on *SMN2* RNA levels

To answer the question whether FK228 has an effect on the expression level of *SMN2*, the total amount of both *SMN2* transcripts, FL-*SMN2* and Δ7-*SMN2*, was quantified. As mentioned earlier, since HDACi may influence the expression of housekeeping genes, total RNA amount was taken as internal control. Therefore, the RNA derived from FK228 treated and untreated fibroblast cultures were precisely measured with the help of a microplate reader using the RiboGreen® dye. Subsequently exactly 150 ng RNA were reverse transcribed.

Using real-time RT PCR, it was shown that the RNA expression levels of the full length *SMN* (FL-*SMN*) are elevated by FK228 treatment in SMA-fibroblast cells. FK228 is a very potent HDACi, indicated by its high effect on the SMN expression level starting at low nanomolar doses. In the murine cell line MEF14 a significant increase of FL-*SMN* to over 170% was observed at only 10 nM FK228. Generally, every treated cell line responded positively to the FK228 regimen. The *FL*-SMN level was up-regulated to ~300% in ML17 at 50 and 100 nM, to ~140% in ML16 and MEF14 to 185% at 100 nM see Figure 18). This respective figure shows the diagrammatic presentation of the quantified mean values for FL-*SMN2*, Δ7-*SMN2* and the ratio between both, respectively. The most pronounced response revealed the cell line ML17 (SMA type I), with a 3-fold elevation of the FL-*SMN* level at relatively low FK228 concentrations of 50 and 100 nM. The inter-individual differences of human SMA fibroblast cell lines become very clear, comparing the FL-*SMN* expression change after FK228 treatment of ML16 and ML17. Although both cell lines were derived from type I SMA patients, ML16 responded at none of the FK228 concentrations in a significant manner, although this cell line showed weak elevated FL-*SMN* levels (Figure 18a), however to only ~140%. The murine SMA cell line (MEF14), presented a significant augmentation of the FL-*SMN* level at nearly all concentrations with a maximum increase to 185% at 100 nM. These data indicate that human *SMN2* is activated by FK228 also in a heterologous background, such as the mouse.

Strikingly, for all investigated cell lines the Δ7-*SMN2* level declined concordantly with FK228-treatment. In ML16 the decrease of the Δ7-*SMN2* amount reached significance already at a concentration of 10 nM FK228. Moreover, at a concentration of 500 nM the Δ7-level dropped to ~44%. For ML17 the amount of the Δ7-*SMN2* transcripts remained nearly unchanged at all concentrations, except at the highest concentration of 500 nM, where it revealed significantly reduced levels (~43%). The murine SMA fibroblast cell line showed a comparable reaction to the FK228 regimen on Δ7-*SMN2* level. An obvious decline of the Δ7-*SMN2* transcript level was observed, starting to be

significant at a FK228 concentration of 50 nM. A severe reduction of the Δ7-*SMN2* amount to ~42% was detectable at the highest concentration of 500 nM FK228.

The up-reglation of FL-*SMN2* on one side and the down-regulation of Δ7-*SMN2* on the other side resulted in an elevation of the FL-*SMN2*/Δ*7SMN2* ratio. Nearly in all cell lines and at every concentration of FK228 a significant increase of this ratio was observed (Figure 18c).

Taken together, the positive shift in FL-*SMN2* and the decline on Δ7-*SMN2* level obviously suggests an impact on the splicing of the *SMN2* pre-mRNA. This influence might be direct or indirect, by the up-regulation of a respective splicing factor, which reverses Δ7-*SMN2* towards FL-*SMN2* transcripts. However, the decline of both *FL-SMN2* and Δ*7-SMN2* transcripts observed for the highest FK228 concentrations at 250 nM and 500 nM suggests a certain cytotoxicity of FK228. The cytotoxicity will therefore be analyzed in chapter 4.1.2.4.

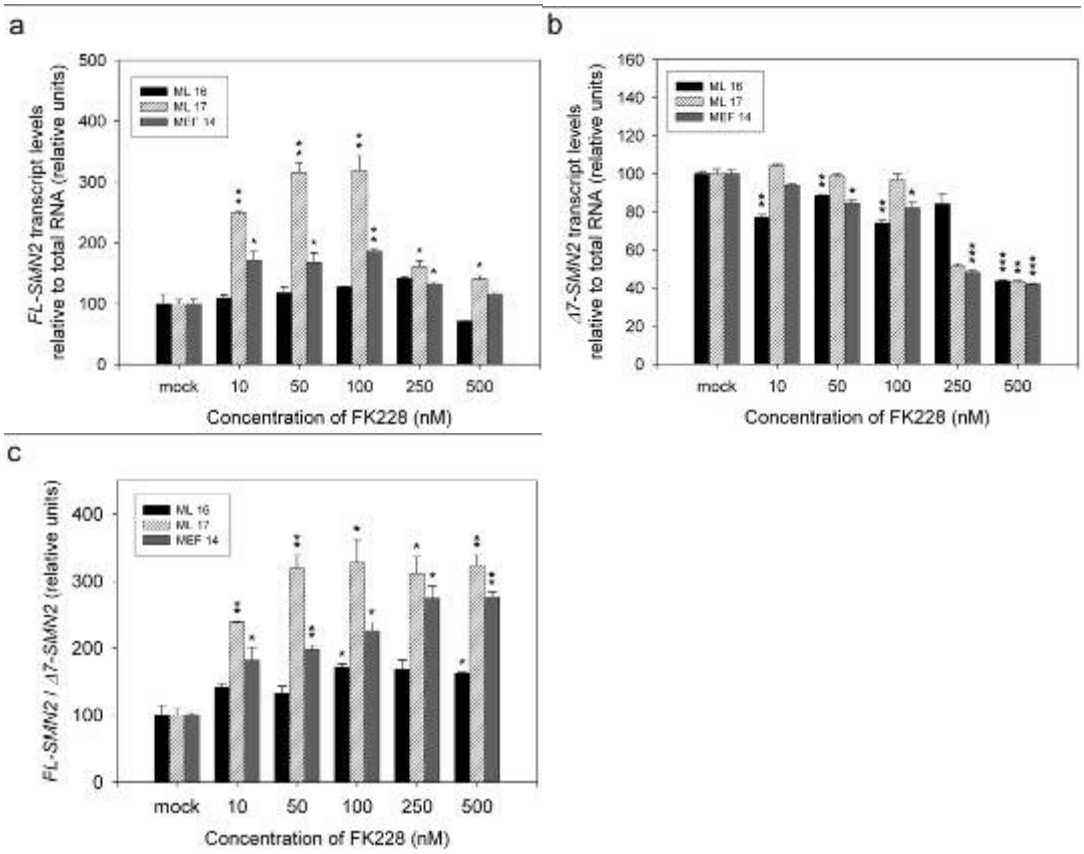

Figure 18 Up-regulation of *SMN2* mRNA in fibroblasts derived from SMA patients and on murine embryonic fibroblast line (MEF14) derived from a SMA mouse ($Smn^{-/-}$;$SMN2^{tg/tg}$) treated with increasing concentrations of FK228 (10–500 nM). Quantitative real-time PCR results are summarized as bar graphs. **a** Mean values (± SEM) for FL-*SMN2* relative to total RNA amount **b** Mean values (± SEM) for Δ7-*SMN2* relative to total RNA. Δ7-*SMN2* levels were nearly unchanged or even clearly reduced, suggesting an efficient reversion of the splicing pattern contributing to the significantly increased FL-*SMN2* levels. **c** Increasing FL-*SMN2*/Δ7-*SMN2* ratios in all cell lines, pointing out the reversion of the splicing pattern (* $p < 0.05$; ** $p < 0.01$; *** $p < 0.001$).

4.1.2.2 SMN and SFRS10 protein level change under FK228

To assess the impact of FK228 on the protein level of SMN, quantitative Western blots were performed. Since it was evident from the preceding RNA expression experiments that FK228 might influence the splicing of *SMN*2, the protein expression of the main splicing factor of *SMN2*, namely SFRS10, which is known to be capable to reverse the splicing pattern, quantitative Western blots of this factor was also performed.

In all three different tested cell lines, FK228 had a significant impact on the SMN protein level. Comparably to the previous observations regarding the elevation of the FL-*SMN2* transcript level, human ML17 and the murine MEF14 revealed the highest increase in SMN protein level (Figure 19).

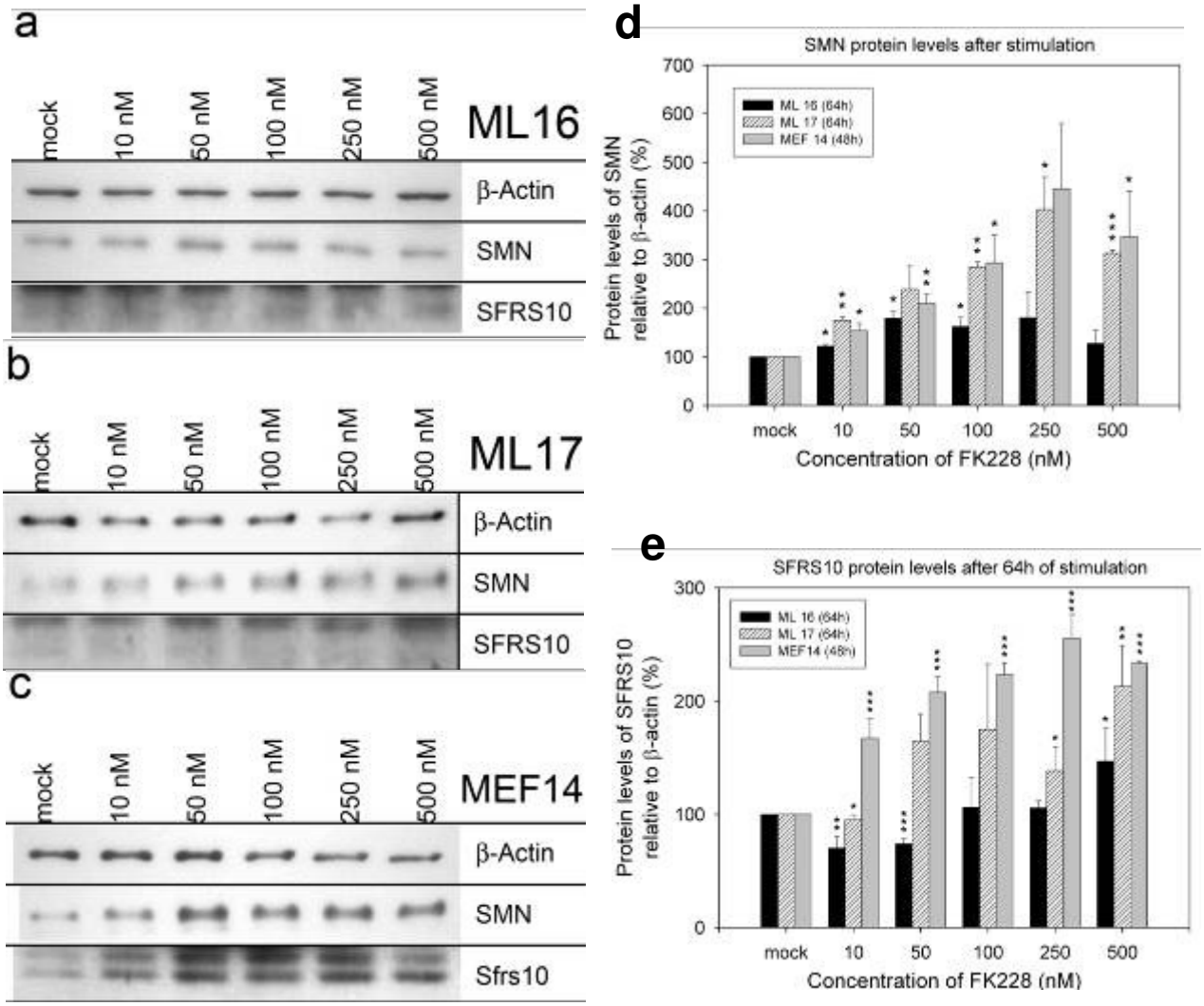

Figure 19 Increase of SMN and alteration of SFRS10 protein levels in fibroblast cell lines from SMA patients and SMA mouse model after treatment with increasing concentrations of FK228 (10–500 nM) for 64 h (48h for murine fibroblasts). **a, b, c** Western blots loaded with equal protein amounts were simultaneously stained with anti-β-Actin , anti-SFRS10 and anti-SMN. The pictures show representative Western blot analyses of cell cultures ML16, ML17 and Mef14.
d Mean SMN protein levels (± SEM) in ML16, ML17 and MEF14 relative to β-Actin **e** Mean SFRS10 protein levels (± SEM) in ML16, ML17 and MEF14 relative to β-Actin (* $p < 0.05$; ** $p < 0.01$; *** $p < 0.001$)

The human fibroblast line ML16 responded with an up-regulation of the SMN protein amount to maximum level of ~180% at a FK228 concentration of 250 nM. ML16 already revealed a significant augmentation to ~122% at the lowest FK228 concentration of 10 nM. Moreover, 50 nM of FK228 elevated SMN protein levels to ~179% compared to the mock-treated cells. The other human cell line ML17 responded to the FK228 regimen with a far higher elevation of SMN protein. 250 nM FK228 led to the maximum up-regulation of SMN protein amount of more than 4-fold. Interestingly, starting at the lowest concentration of 10 nM FK228, ML17 reacted in a significant increase of SMN to more than 175%. The murine fibroblast line revealed a 4.4-fold up-regulation of SMN at 250 nM. Here, the highest significant increase to ~347% was detected at a concentration of 500 nM FK228.

The most important splicing factor of the *SMN2* transcript is SFRS10. This factor was subjected to quantitative Western blot analysis, in order to explain the reason for the reversion of the splicing pattern (see chapter 4.1.2.1). Strikingly, all tested cell lines responded to FK228 treatment in an elevation of SFRS10. The ML17 and MEF14 revealed a high up-regulation of SFRS10 (ML17; 213% at 500 nM FK228; MEF14; 256% at 250 nM), the cell line ML16 responded to low FK228 concentrations in a decline of SFRS10 levels. Starting at 100 nM FK228 ML16 showed also a SFRS10 augmentation, reaching 147% at 500 nM FK228.

Taken these results together, it is obvious that FK228 mediated up-regulation of the SFRS10 level results in a shift of the splicing pattern towards *SMN2* exon 7 inclusion. The ratio of FL-*SMN* to Δ7-*SMN* strongly correlates with the SFRS10 protein level. This is observable for every tested cell line.

4.1.2.3 Change of the number of gems

It is well known that SMN proteins form nuclear aggregates, called gems. The respective number of these gems most likely reflects the amount of functioning SMN protein in the cell. Therefore, immunochemistry-stainings in human SMA fibroblasts was performed. Unfortunately the limited amount of the test substance FK228, restricted the treatment for the immunochemistry experiments to only the two human cell lines ML16 and ML17.

Nevertheless, comparable to the already reported expression results, ML16 reacted in a weak but significant increase of gems from 5.16±2.13 gems/100 nuclei to 22.8±1.51 gems/100nuclei, whereas ML17 revealed a ~6-fold up-regulation in gem numbers (from 7.23±3.5 gems/100 nuclei to 45.87±4.59 gems/100nuclei).

Additionally, the 50 nM FK228-treatment was observed to increase the percentage of cells with a low number of nuclear gems (one or two gems) remarkably, whereas the cell number without gems decreased. This means that the number of gems increased most likely not only in cells, which prior to the FK228 treatment contained gems, but that the treated cells produced new gems.

These findings suggest that the elevation seen on RNA and protein level is reflected in the amount of subnuclear gems.

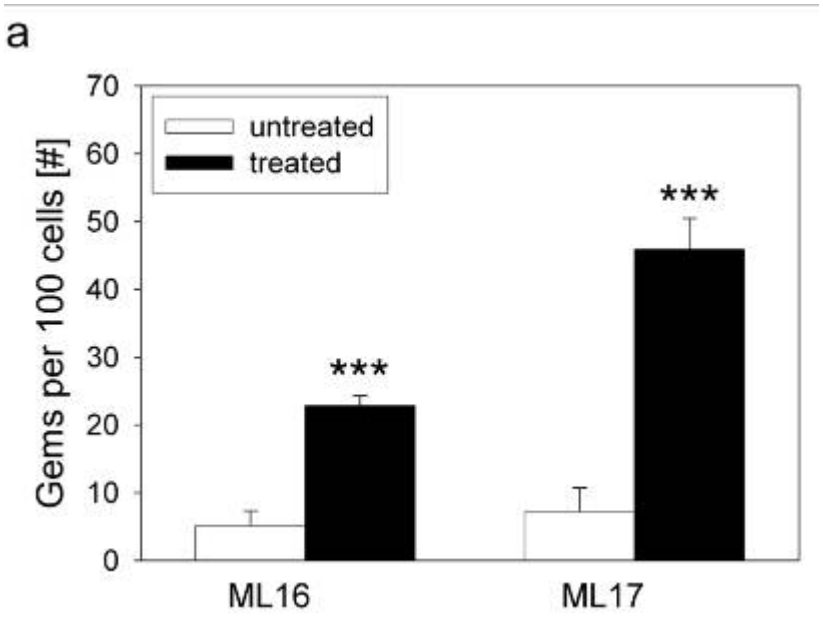

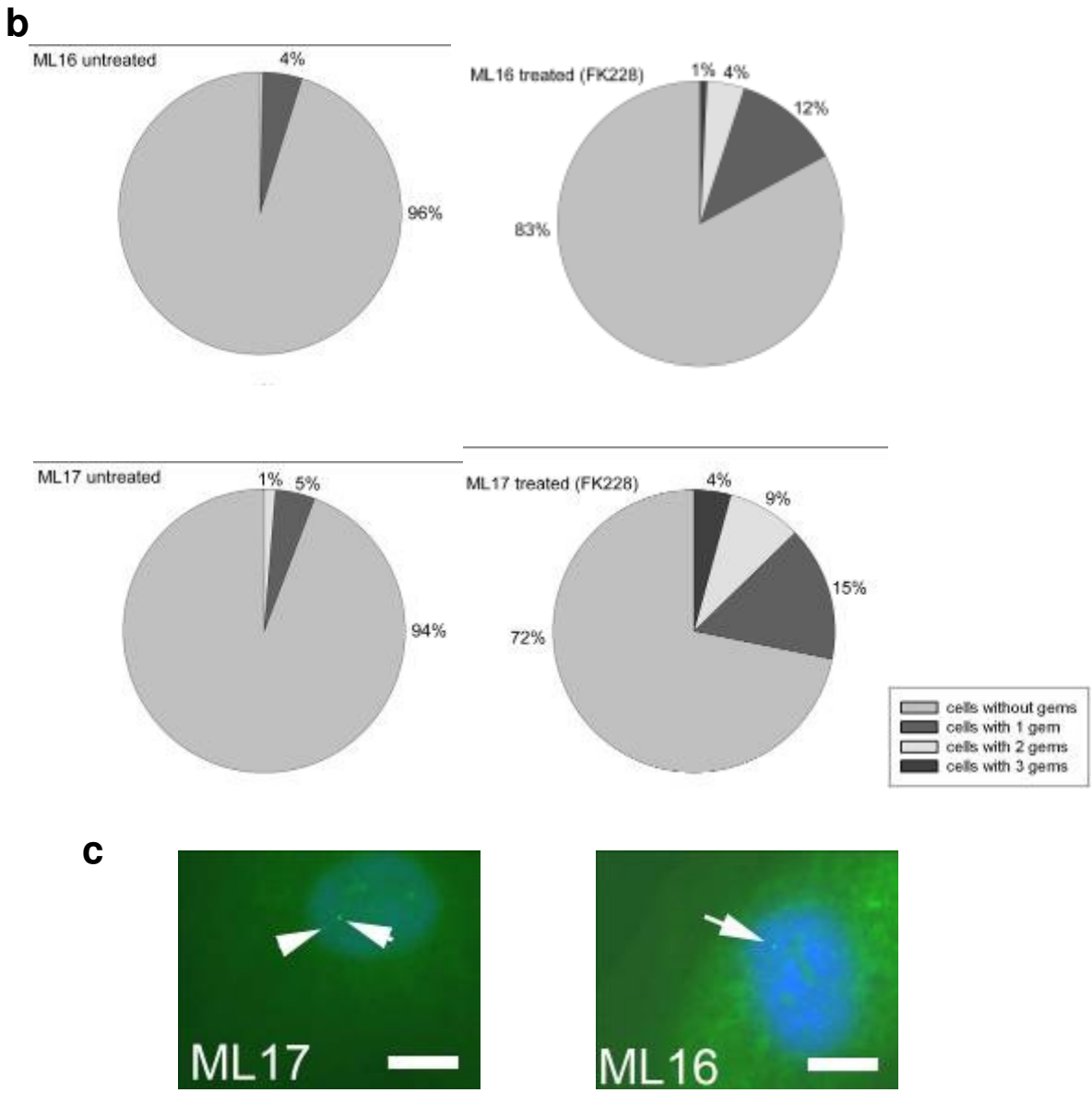

Figure 20 a Inter-individual comparison of the gem number/100 cells in untreated and FK228-treated cell lines. For each cell line, a clear response on FK228 [50 nM] treatment resulting in a significant elevation of the number of gems was observed (*** $p < 0.001$). **b** Pie charts representing the percentages of cells without or with a certain number of gems in untreated or FK228-treated fibroblasts. **c** Representative microscopy images of nuclear gems (marked with white arrows) from every treated cell line. Gems were stained with anti-SMN-FITC antibody, whereas the nuclei in blue were counterstained with DAPI. White bar = 10µm.

4.1.2.4 Cytotoxicity of FK228 in SMA fibroblasts

To test for cytotoxicity of FK228, a cell viability test, the so-called MTT-assay was applied. After treating the cells with FK228, the capability of the cell to convert MTT (thiazolyl blue tetrazolium bromide) into formazan crystals was assessed, which determines the viability of cells (Mosmann 1983).

The test for cytotoxicity revealed an unfavorable effect of the fibroblast lines. The test substance FK228 is known to be a very potent HDACi, starting to be efficient at low nanomolar concentrations. However, virtually all treatment concentrations of FK228 showed a negative effect on cell survival, making a future use of FK228 as a potential SMA neurotherapeutic drug questionable. Because of the observed high *in vitro* cytotoxicity, FK228 was not chosen to be tested for a future animal trail. Still, the *in vitro* data helped to gain insight into the *SMN2* activation via HDACi treatment, since FK228 was shown to activate *SMN2* even on a heterologous background, such as the mouse.

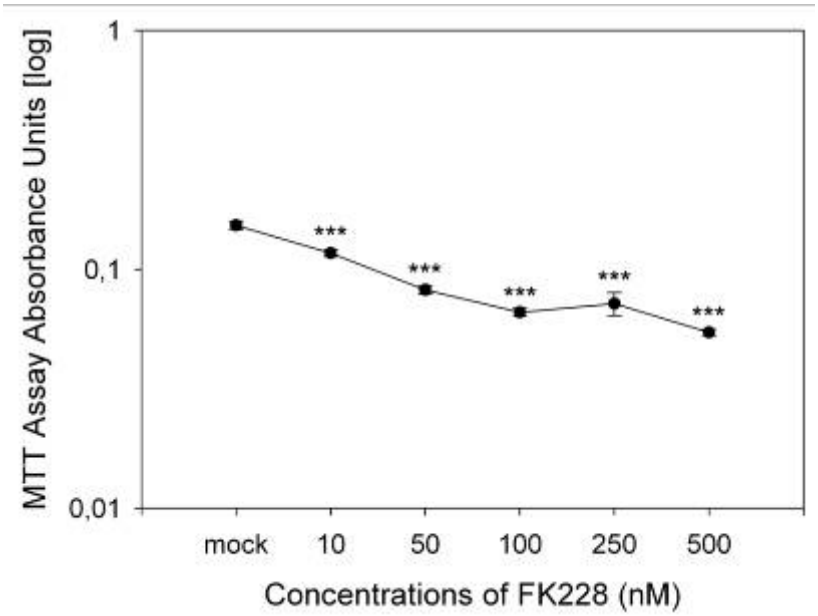

Figure 21 MTT cell viability assay in ML16 demonstrating cytotoxicity of FK228 at concentrations starting from 10 µM, implicating increasing cell death of cultured SMA fibroblasts at these FK228 amounts (treatment time 64 h) (*** $p < 0.001$)

4.2 Identification of the specific histone deacetylase (HDAC) regulating the expression of *SMN2*

With regard to a prospective SMA therapy, it would be crucial to identify an applicable drug, which bears only a passable amount of unfavorable side effects. Since pan-HDACi, such as VPA, FK228, M344, or SAHA unspecifically inhibit virtually all classes of HDACs, they most probably influence a wide variety of genes. This assumption is supported by the previously described results that the expression of up to 22% of genes can be altered by HDAC inhibitors (Peart et al. 2005). Thus, several side effects by the unspecific up-regulation of genes are consequently expected. At least for the long-term used HDACi VPA a number of unfavorable side effects have been described (reviewed in (Gerstner et al. 2008)).

4.2.1 Effects of histone deacetylase (HDAC) knock-down experiments on *SMN2* expression

To identify the specific HDAC, which is able to regulate the *SMN2* expression, a siRNA knock-down approach was applied. Therefore, to find the HDAC specifically regulating the *SMN2* gene the *SMN1* deleted SMA patient fibroblast line ML17 was selected. ML17 was subjected to siRNA knock-down approaches. Each HDAC was knocked down one after the other. The knock-down (KD) efficiency was controlled by real-time PCR (appendix Figure 56). After the knock-down of each HDAC, the whole protein extracts were first measured by the Bradford method; equal amounts of protein (7.5 µg) were loaded onto SDS PAGE gel and after electrophoresis, semi-quantitative Western blotting was applied using β-Actin as internal control. These experiments were carried out in triplicates.

Beside inter-individual fluctuations of the SMN protein level, exclusively the knock-down of HDAC8 resulted in a significant up-regulation of the SMN level (Figure 22 and Figure 23). After the quantification of three independent knock-down experiments of all Zn^{2+}-dependent classical HDAC from class I, II and IV, solely HDAC8 KD revealed a SMN protein elevation to ~150% ($p<0.05$), suggesting a specific role of HDAC8 in *SMN2* regulation (Figure 23).

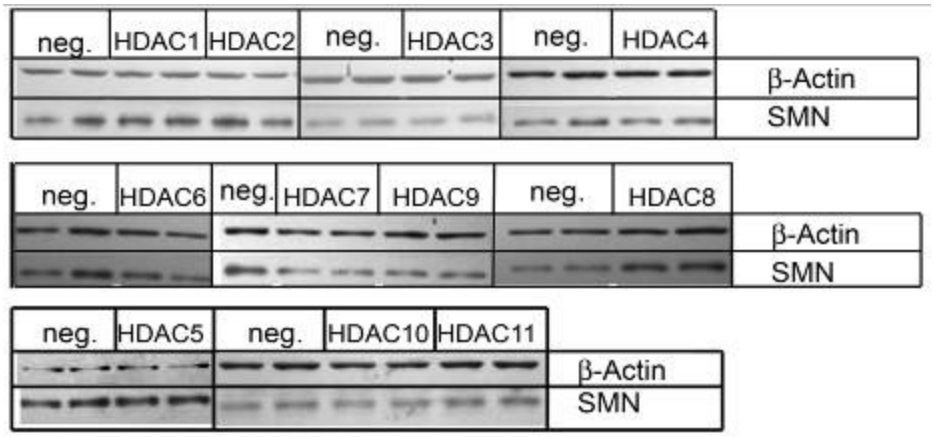

Figure 22 Representative Western blots of β-Actin and SMN protein after 48h knock-down of each classical HDAC (classes I,II,IV) in SMA-fibroblast cell line ML17. After knock-down of HDAC8, SMN protein level was significantly elevated.

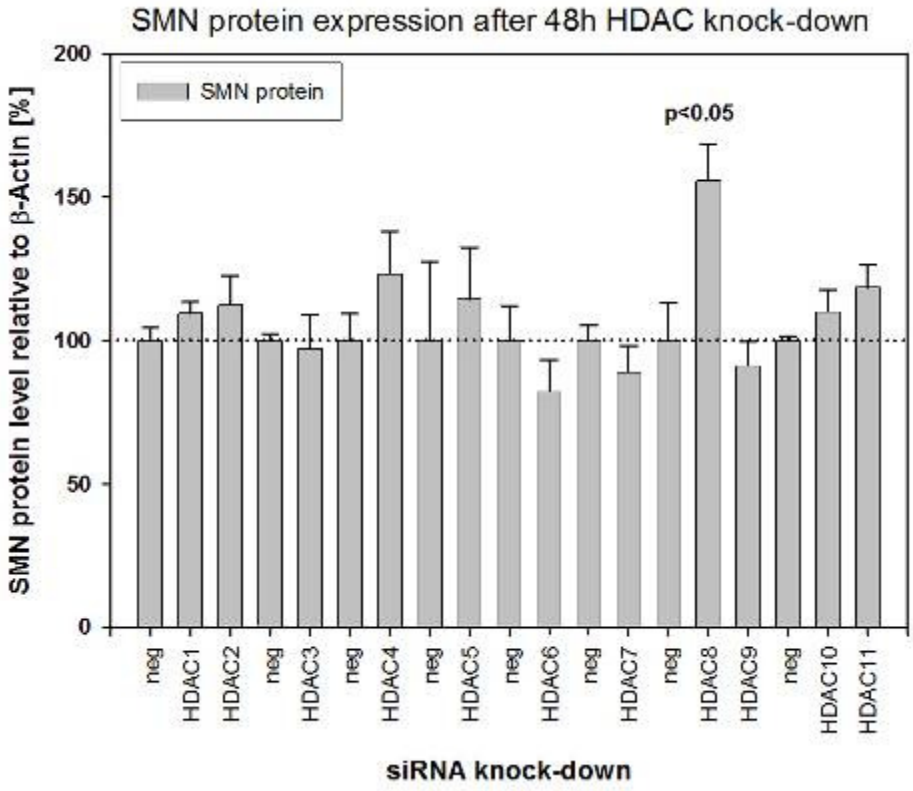

Figure 23 SMN protein quantification (relative to β-Actin) after 48h knock-down of each classical HDAC (classes I,II,IV). After knock-down of HDAC8, SMN protein level was significantly elevated. Quantification of triplicate knock-down in SMA fibroblast cell line ML17.

4.2.2 Chromatin immunoprecipitation of HDAC8 in the promoter region of *SMN2*

Since the knock-down of HDAC8 was found to up-regulate the expression of SMN protein, the question was addressed whether the HDAC8 protein is bound to the promoter region of *SMN2.* Therefore the previously characterized promoter region of SMN2 (Kernochan et al. 2005) has been investigated. The *SMN1*-deleted SMA patient derived fibroblast line ML17 was chosen to perform a chromatin immunoprecipitation (ChIP) experiment. To do so, all proteins bound to the respective promoter region were cross-linked to the DNA by the addition of paraformaldehyde. After this step the DNA was sheared by sonication and the respective protein-DNA complexes were immunoprecipitated with the help of an anti-HDAC8 antibody. After reversion of the cross-linking and elution of the DNA from the HDAC8 proteins, a quantitative real-time PCR was performed with specific primers amplifying the respective *SMN2* promoter regions (Figure 24).

The quantification of the *SMN2* promoter DNA fragments, which were bound by HDAC8 proteins revealed definitive binding in comparison to unspecific binding (represented by the unspecific IgG antibody ChIP-experiment). The amount of HDAC8, which was bound to the ~2500 bp upstream of the transcription initiation site located human *SMN2* promoter region 1 (HuSP1), was 3-fold higher than the HDAC8 level, which was bound to HuSP3 and HuSP4, which are located in the close vicinity to the transcription start site (TSS). Moreover, HuSp2 (~1200 bp upstream TSS) revealed a 2-fold higher binding of HDAC8 compared to HuSP3 and HuSP4 (Figure 25).

To summarize, these findings indicate that HDAC8 is natively bound to the *SMN2* promoter in SMA patient derived fibroblasts. Moreover, it was obvious that the amount of HDAC8 was increasing with the distance to the transcription initiations site.

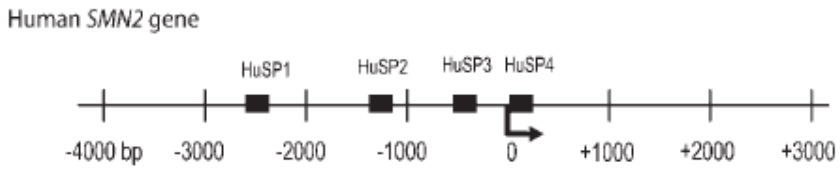

Figure 24 Schematic overview of the location of primer sets, which were spaced at ~500–1000 bp intervals. The arrow indicates the transcription initiation site taken from (Kernochan et al. 2005)

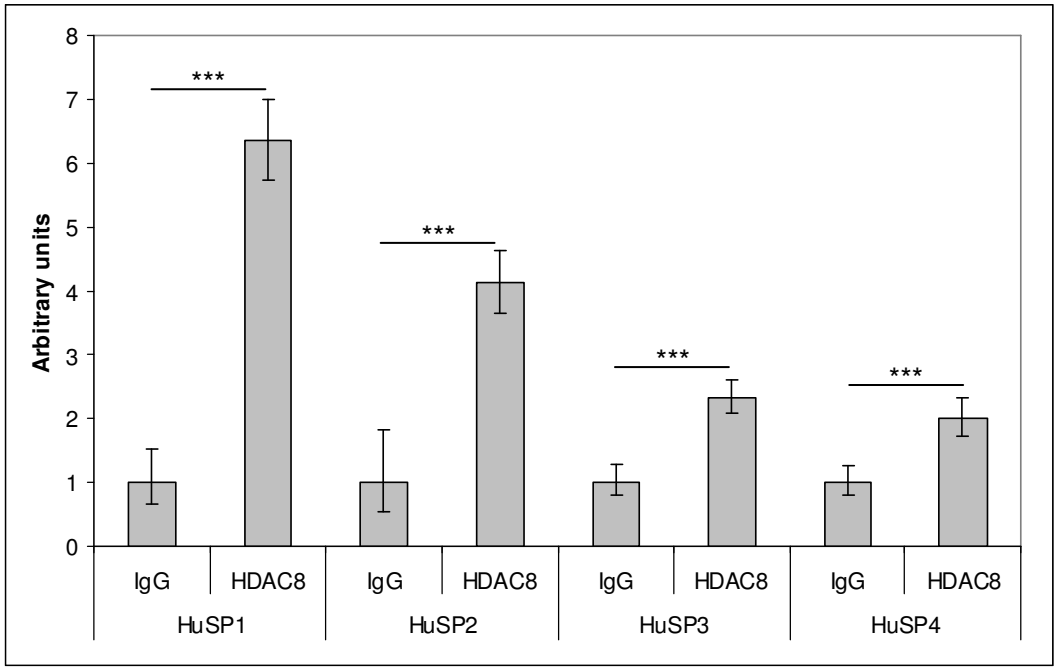

Figure 25 Diagrammatic representation of the ChIP-based quantification of the amount of HDAC8-protein bound to the respective *SMN2* promoter region. Measured in triplicates in SMA-fibroblast line ML17. IgG served as unspecific background binding control. (*** $p < 0.001$)

4.2.3 HDAC overexpression experiments in SMA fibroblasts and the effect on *SMN2* expression

Since it was found that HDAC8 knock-down is capable to up-regulate *SMN2* expression and that HDAC8 protein is bound in the promoter region of SMN2, the next topic to investigate whether the up-regulation of HDAC8 may consequently down-regulate the *SMN2* expression. Thus, to overexpress HDAC8, ML17 was transfected with an expression vector containing the myc-tagged cDNA of human HDAC8.

24h after transfection of the plasmid containing the myc-tagged cDNA of human HDAC8, the quantification of the subsequent semi-quantitative Western blot revealed a HDAC8 concentration dependent down-regulation of the SMN protein amount. Compared to the transfection of 4 µg GFP-tagged control plasmid, the expression of the transfected HDAC8 increased concentration dependently. A clear inverse correlation of the SMN protein level and the HDAC8 expression was observed. While the GFP-plasmid transfected cells showed 0% expression of myc-HDAC8, the expression raised from ~20% (2µg HDAC8 plasmid) over ~50% (4µg HDAC8 plasmid) to ~140% (8µg HDAC8 plasmid). However, the amount of SMN protein dropped concordantly with the elevation of HDAC8. The ~140% overexpression of HDAC8 led to the decline of SMN protein level to ~50% compared to the GFP-transfected cells.

Taken together these results strongly suggest that HDAC8 is able to regulate the *SMN2* expression. The amount of overexpressed HDAC8 reflects the level of SMN protein decrease, since both values correlate inversely.

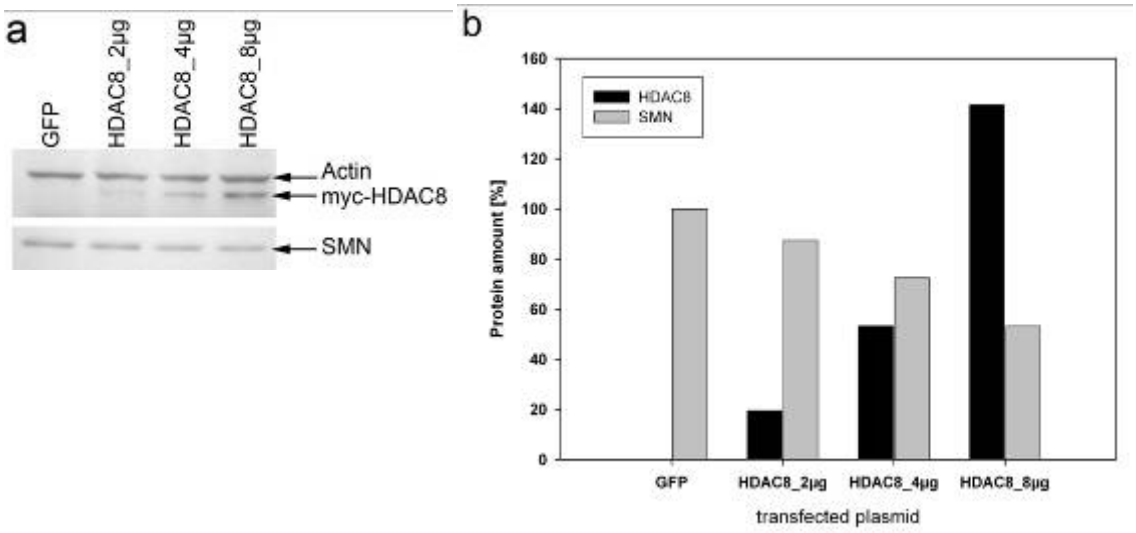

Figure 26 Overexpression of HDAC8 down-regulates the SMN protein level. GFP (control plasmid) and HDAC8 (myc-tagged) overexpression for 24h in ML17. **a)** Picture of Western Blot. **b)** diagrammatic representation of overexpression results.

4.2.4 Treatment of SMA fibroblasts with the HDAC8 specific inhibitor PCI-34051

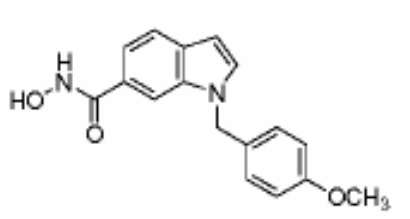

Figure 27 Chemical structure of PCI-34051

Since the previous HDAC knock-down and overexpression experiments (chapter 4.2.1 and 4.2.3) suggested that HDAC8 is regulating the *SMN2* expression, the possibility to chemically inhibit the specific function of HDAC8 raised. Hence, recently a novel HDAC8-specific inhibitor has been developed (Balasubramanian et al. 2008). It has been stated that HDAC8-specific inhibitor namely PCI-34051 has a >200-fold selectivity over the other HDAC isoforms. Moreover, PCI-34051 has been shown to induce caspase-dependent apoptosis in cell lines derived from T-cell lymphomas or leukemias (Balasubramanian et al. 2008). Additionally it has been proven that high HDAC8 expression was associated with poor prognostic markers and poor overall survival in patients with neuroblastoma. However, the treatment of neuroblastoma cell lines as well as short-term-culture neuroblastoma cells with with PCI-34051 was proven to inhibit cell proliferation and clone formation and to induce differentiation (Oehme et al. 2009). Since the *in vitro* functionality of PCI-34051 has extensively been proven and the previous findings suggested the HDAC8 mediated down-regulation of *SMN2,* PCI-34051 was applied for testing in SMA fibroblasts.

4.2.4.1 Impact on *SMN2* RNA levels

To investigate the impact of PCI-34051 on the *SMN2* expression, the total amount of both *SMN2* transcripts, FL-*SMN2* and Δ7-*SMN2*, was quantified. Again the total RNA amount was taken as internal control. After the dye-based precise measurement of the RNA concentration, exactly 150 ng RNA were reverse transcribed. After the most efficient treatment time was determined via a time-course experiment, the RNA was prepared after 6 h of PCI-34051 treatment.

The chosen SMA patient fibroblast line and the murine SMA-like fibroblast line revealed no increase of *SMN2* transcripts. A very weak up-regulation was observed for the human cell line, where FL-*SMN2* level increased to 120%. However, this augmentation did not reach statistical significance. Furthermore, no obvious impact of PCI-34051 treatment on the Δ7-*SMN2* was observed.

Taken together, the HDAC8-specific inhibitor is not capable to elevate the *SMN2* transcript level in a significant manner. Neither the FL-*SMN2* nor the Δ7-*SMN2* level was significantly elevated by PCI-34051 treatment.

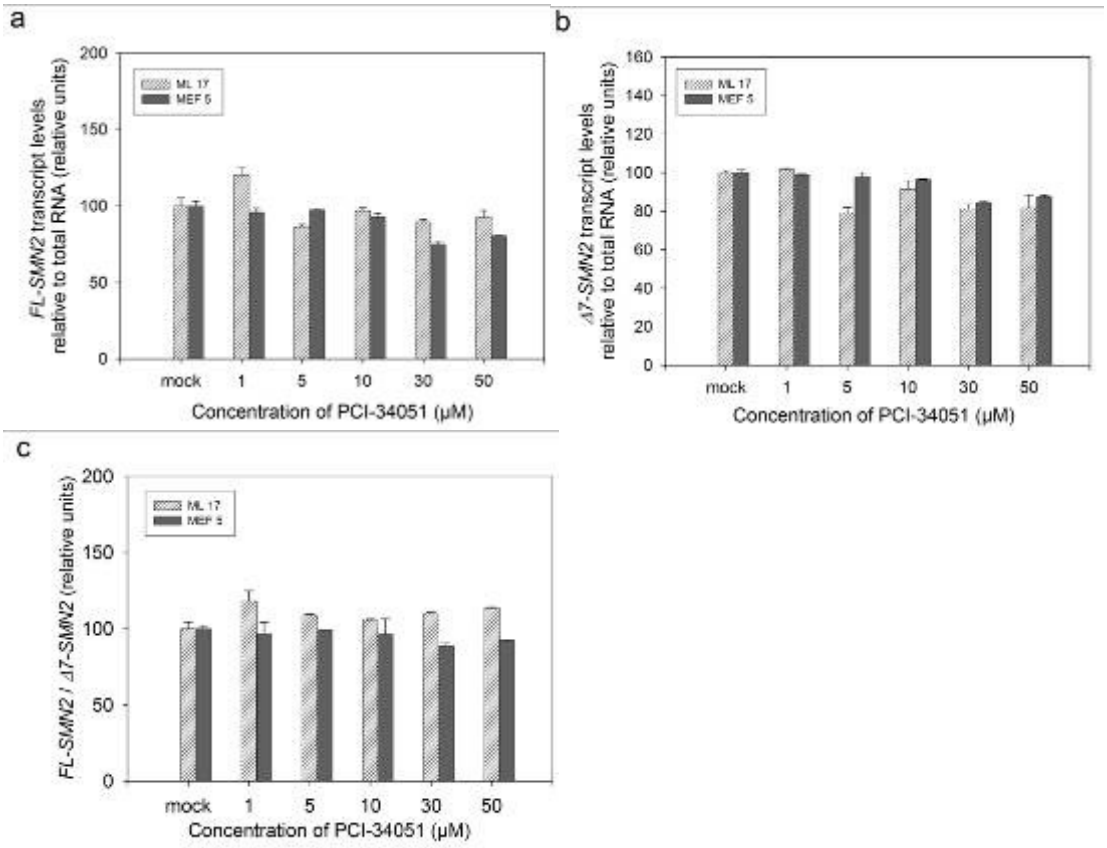

Figure 28 *SMN2* mRNA expression in fibroblasts derived from a SMA patient (ML17) and one murine embryonic fibroblast line (MEF14) derived from a SMA mouse ($Smn^{-/-}$;$SMN2^{tg/tg}$) treated with increasing concentrations of PCI-34051 (1–50 µM). Quantitative real-time PCR results are summarized as bar graphs. **a** Mean values (± SEM) for FL-*SMN2* relative to total RNA amount **b** Mean values (± SEM) for Δ7-*SMN2* relative to total RNA. **c** No obvious change in FL-*SMN2*/Δ7-*SMN2* ratios in all cell lines, revealed no impact on the splicing pattern. None of the observed regulations was significant.

4.2.4.2 SMN and SFRS10 protein level change under PCI-34051

In order to check whether the HDAC8-specific inhibitor PCI-34051 is capable to up-regulate the SMN protein expression, semi-quantitative Western blots were performed, with β-Actin as internal control. Additionally the effect of PCI-34051 on the SFRS10 protein level was assessed, since this protein is known to be the major splicing factor to restore the SMN2 splicing (Hofmann et al. 2000).

The quantification of the SMN protein levels derived from the treated cell lines ML17 (human) and MEF5 (murine) revealed only a limited capacity of PCI-34051 to elevate the SMN protein amount. While the human fibroblast line ML17 responded positively to PCI-34051 treatment, the murine cell line however revealed no obvious change in the SMN protein level. ML17 showed an up-regulation of SMN to ~150% at all tested concentrations. The highest significant elevation of the SMN level under PCI-34051 treatment was to ~185% at a concentration of 30 µM. However, the SFRS10 protein level was not noticed to be significantly elevated. MEF5 revealed no response to PCI-34051 on Sfrs10 level, whereas ML17 responded in a weak up-regulation to a maximum level of 147% (at 10 µM PCI-34051) (Figure 29). Small individual fluctuations of the SFRS10 expression resulted in a failure of the weak increase to reach statistical significance.

To summarize the protein expression data of ML17 and MEF5 under PCI-34051 treatment, it is noteworthy that this HDAC8-specific inhibitor is able to augment the SMN protein level in the human SMA patient derived fibroblast line to a mean elevation to ~150%. This is of particular interest, because the knock-down experiments of HDAC8 resulted in exactly the same degree of SMN protein augmentation (Figure 23).

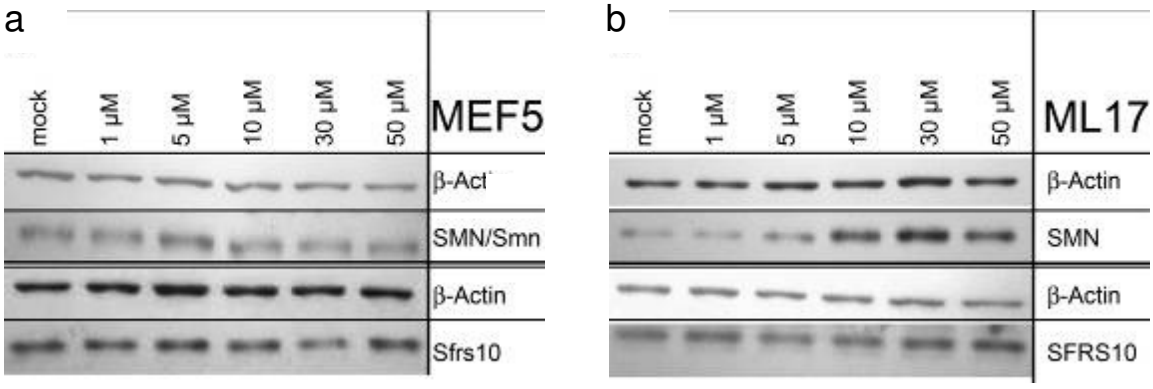

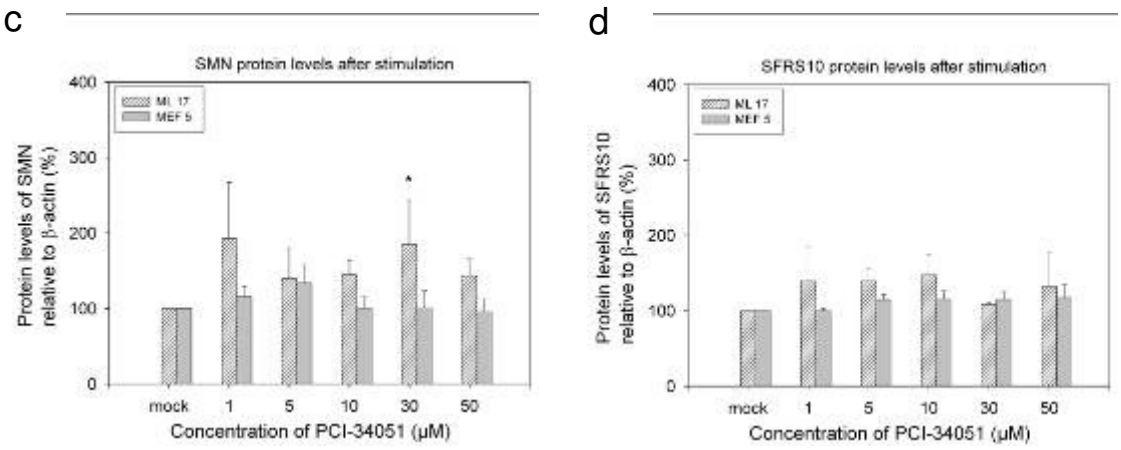

Figure 29 Impact of PCI-34051 on SMN and SFRS10 protein levels in fibroblast cell lines from SMA patient and SMA mouse model after treatment with increasing concentrations of PCI-34051 (1–50 µM) for 6 h **a, b** Western blots loaded with equal protein amounts were simultaneously stained with anti-β-Actin , anti-SFRS10 and anti-SMN. The pictures show representative Western blot analyses of cell cultures ML17 and MEF5. **c** Mean SMN protein levels (± SEM) in ML17 and MEF5 relative to β-Actin **d** Mean SFRS10 protein levels (± SEM) in ML17 and MEF5 relative to β-Actin (* $p < 0.05$)

4.2.4.3 Cytotoxicity of PCI-34051 in SMA fibroblasts

A MTT-assay, which is a cell-viability test, was performed to assess PCI-34051 for cytotoxic effects. After treating ML17 for 6h with PCI-34051, a MTT-assay was performed.

At none of the applied treatment concentration the SMA patient derived fibroblast line ML17 showed any signs of cytotoxicity (Figure 30). This favorable *in vitro* toxicity profile of PCI-34051 suggests a possibly good tolerance in prospective *in vivo* studies. Hence, the HDAC8-specific HDACi PCI-34051 might be a good candidate for further *in vivo* trails.

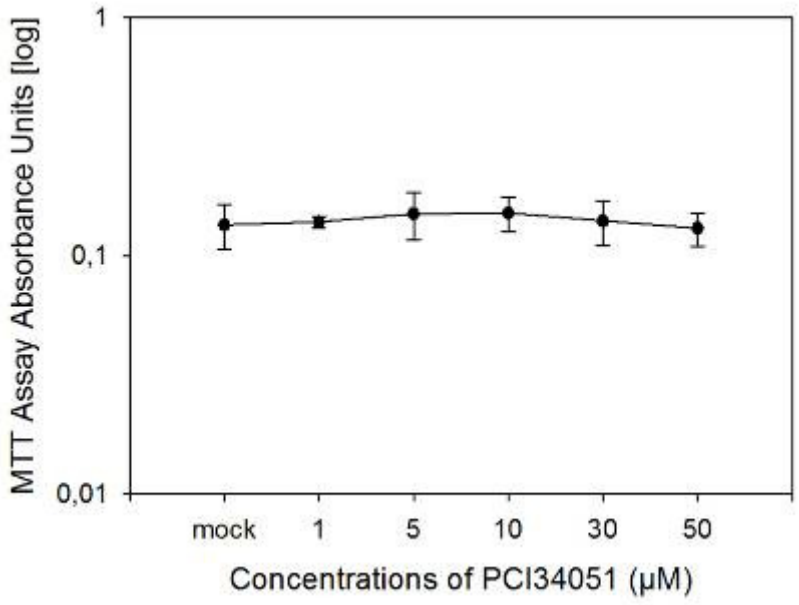

Figure 30 MTT cell viability assay in ML17 demonstrating virtually no cytotoxicity of PCI34051, implicating a good tolerance by the fibroblasts at the used PCI34051 amounts (treatment time 6h)

4.3 *In vivo* treatment of SMA mouse models with the histone deacetylase (HDAC) inhibitor suberoylanilide hydroxamic acid (SAHA)

4.3.1 SAHA treatment of the SMA_B mouse model

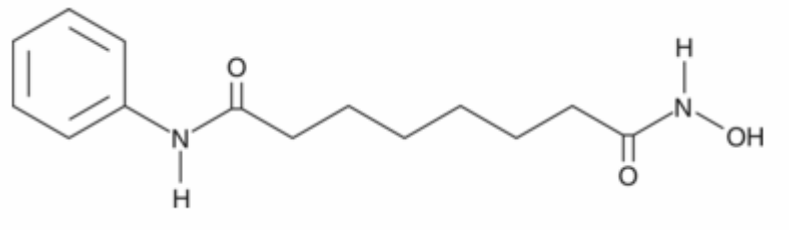

Figure 31 Chemical structure of suberoylanilide hydroxamic acid (SAHA)

Suberoylanilide hydroxamic acid (SAHA, Figure 31) or vorinostat (marketing name *Zolinza*) is a histone deacetylase inhibitor (HDACi), which inhibits virtually all classical HDACs (Hahnen et al. 2008). SAHA was the first HDACi approved (in 2006) by the U.S. Food and Drug Administration (FDA) for the treatment of cutaneous T cell lymphoma (CTCL) (www.merck.com/finance/annualreport/ar2006/pipeline.html). SAHA has been shown to reduce glioma progression *in vivo* (Eyupoglu et al. 2005). A recent study has been shown that SAHA re-activates human immunodeficiency virus (HIV) replication in peripheral blood mononuclear cells from individuals treated effectively with highly active antiretroviral therapy (HAART) indicating to have both an *in vitro* and *in vivo* effects against latently HIV infected T-cells (Contreras et al. 2009). Moreover, it has been proven that the oral therapy with SAHA ameliorates motor deficits in a mouse model of Huntington's disease (Hockly et al. 2003). Additionally, in the same study it has been clearly shown that SAHA crosses the blood-brain barrier, which is essential for prospective SMA therapy (Hockly et al. 2003).

Strikingly, our group could previously show that SAHA is able to up-regulate SMN on protein and RNA level *in vitro* in cell culture and *ex vivo* using cultured hippocampal brain slices derived from rat and human (Hahnen et al. 2006a), therefore, this drug was chosen for an *in vivo* attempt to ameliorate the SMA phenotype in SMA-like mice.

4.3.1.1 Determination of the transgene copy-number in the SMA_B mouse model

In order to determine the exact number of *SMN2* transgenes, we developed a novel real-time PCR method. Similar to humans (Burghes 1997; Feldkotter et al. 2002), also in mice the number of *SMN2* transgenes influences the SMA phenotype. Since there are multiple mouse models for SMA with the genotype $Smn^{-/-}$; $SMN2^{tg/tg}$ carrying one to several *SMN2* integrates per allele (Hsieh-Li et al. 2000; Monani et al. 2000), it is absolutely crucial to know the respective copy number of the human transgene to compare phenotypes. The exact knowledge about the *SMN2* copy number is all-important in therapeutical approaches.

Quantitative Southern blotting is a very time consuming and complicated method to assess the transgene number and is rather inexact.

Real-time PCR is the method of choice to quantify gene copy numbers. Previously several groups have been able to quantify transgene copy numbers in plants (Prior et al. 2006), zebrafish (Ji et al. 2005) or mice (Martins and Krawetz 2004). These groups relied on external probes to exactly quantify their real-time PCRs. To avoid the sometimes very high costs and the effort to design labelled probes, we designed exactly matching primer pairs, in order to use PowerSYBR© green alone to quantify the gene copy numbers with the Taqman method.

In our attempt to determine the *SMN2* copy numbers, $Smn^{+/-}$;$SMN2^{tg/+}$ mice were crossbred with FVB wild-type mice. Mouse tail-tip-DNA was highly purified using a magnetic bead system from Invitrogen (Material and methods part 3.11.1). After qualitative PCR of the transgene, using the endogenous single-copy murine gene apoliprotein b (ApoB) (Bilbao et al. 2003) as internal control, the dCt (delta *Cycle Threshold*) value of *SMN2tg* and *ApoB* was determined with the Taqman and PowerSYBR© green method. For each *SMN2tg* positive sample the dCt showed the same value, indicating that every mouse was heterozygous for the transgene, as expected. These DNAs were pooled and served as reference for later transgene copy determinations. Each significant ddCt (delta delta *Cycle Threshold*) value of ~1 was assigned as homozygous mouse carrying two copies of the human transgene. For a better understanding, the data of the different Ct (*Cycle Threshold*) values are marked in a typical real-time PCR run results in Figure 32 below.

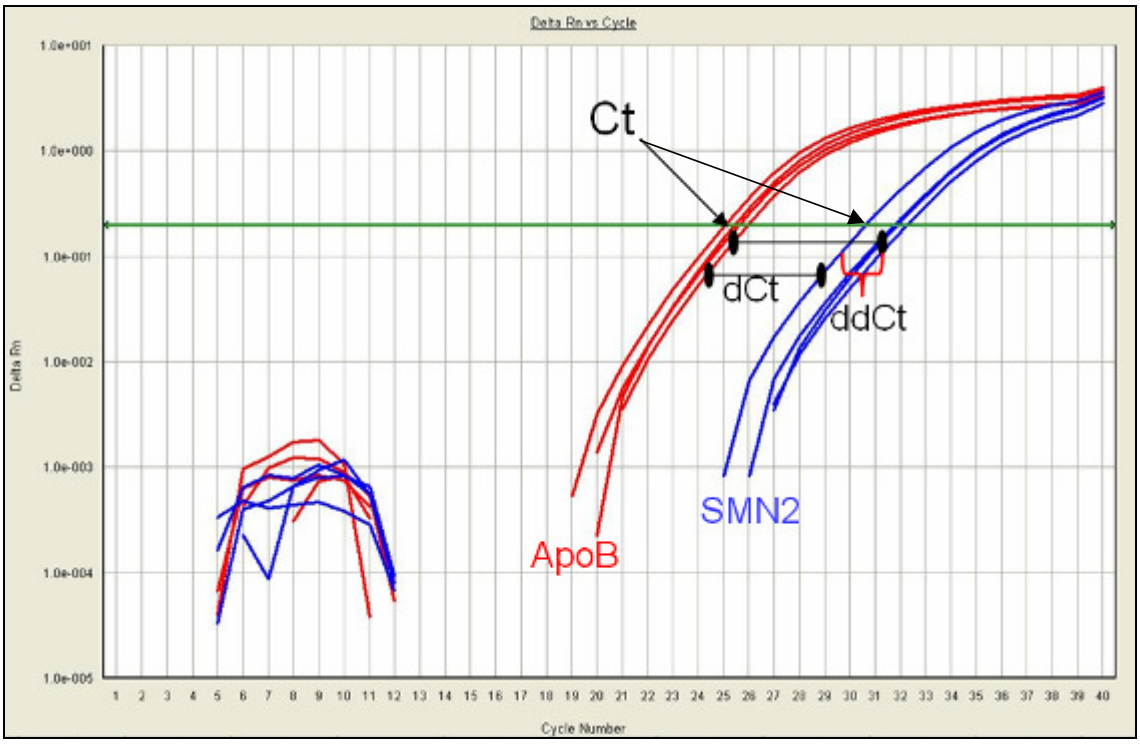

Figure 32 Overview of the values taken from the real-time PCR runs, as a basis for computer based calculations. The exponential amplification curves (red for ApoB and blue for SMN2) cross the threshold line (in green) at the respective Ct value (*Cycle Threshold*). The difference between the Ct values of ApoB and SMN2 build the delta Ct value of both (dCt). Thus, the difference of two dCt values derived from individual DNA samples build the ddCt value (delta delta *Cycle Threshold*).

Production of pool-DNA

Fourteen highly purified mouse tail-tip-DNA derived from offspring genotyped positive for the human transgene of FVB wildtype mice crossed with *Smn*$^{+/-}$;*SMN2*$^{tg/tg}$ mice was in two steps diluted to 5 ng/µl. Ten nanograms of these DNA samples were pooled in order to produce a "single-copy" internal reference of the human transgene. With both, the samples and the DNA-pool a quantitative real-time PCR was performed. Afterwards each dCt value (relating to the endogenous single-copy murine gene apoliprotein b (ApoB)) of the single heterozygous DNAs was compared to dCt value of the pool-DNA. In Figure 33 the diagrammatic presentation of the single DNAs in comparison to the pooled DNA is shown.

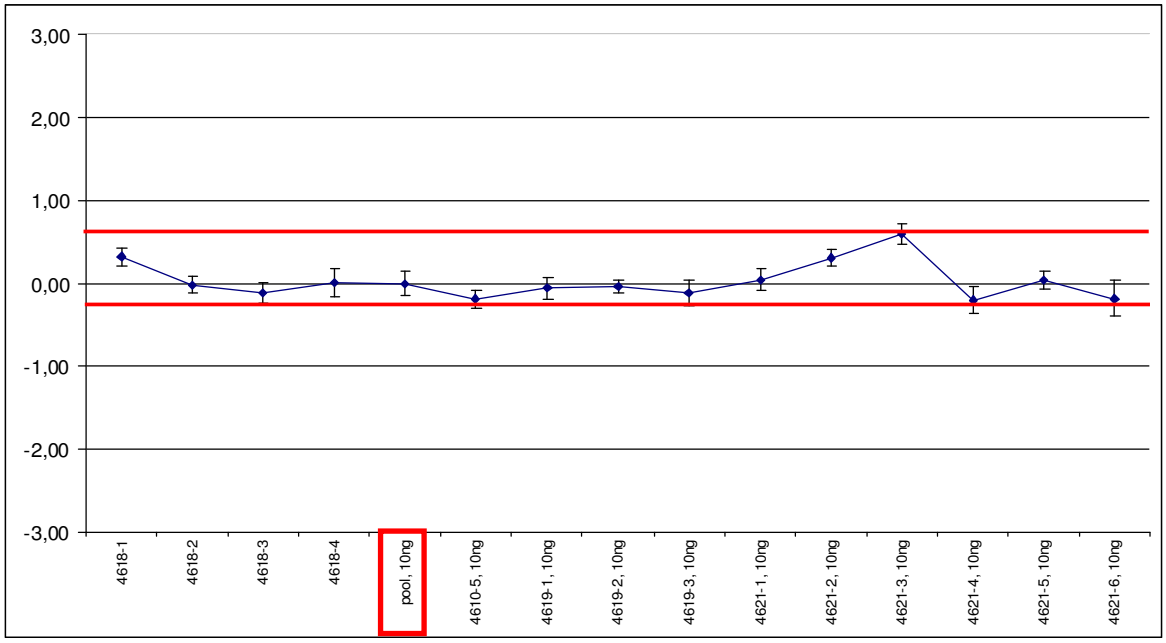

Figure 33 Diagrammatic compairison of the real-time PCR measured ddCt values (*SMN2* in relation to *ApoB*) of the different genomic DNAs of heterozygous SMA_B mice serving as pool-DNA. All ddCt-values are given in relation to the ddCt value of the pool-DNA.

.

Quantification of SMN2 copies in homozygous and heterozygous SMA_B mice

Each mouse tail tip DNA derived from the offspring of *SMN2*$^{tg/wt}$ crossed with *SMN2*$^{tg/wt}$ animals was first qualitatively genotyped via normal PCR. With the 84 transgene-positive samples, a quantitative real-time PCR was performed, using *ApoB* as internal control and the pool-DNA as reference. As expected, 28 of 84 mice showed 2 *SMN2* copies and are thus homozygous for the transgene. According to Mendelian inheritance, one fourth (25%) of the mice carrying the human *SMN2* transgene were genetically homozygote.

shows the bar diagram representing ddCt values for each sample, significant outliers of +0.8 or more indicating 2 *SMN2* copies and are marked in red.

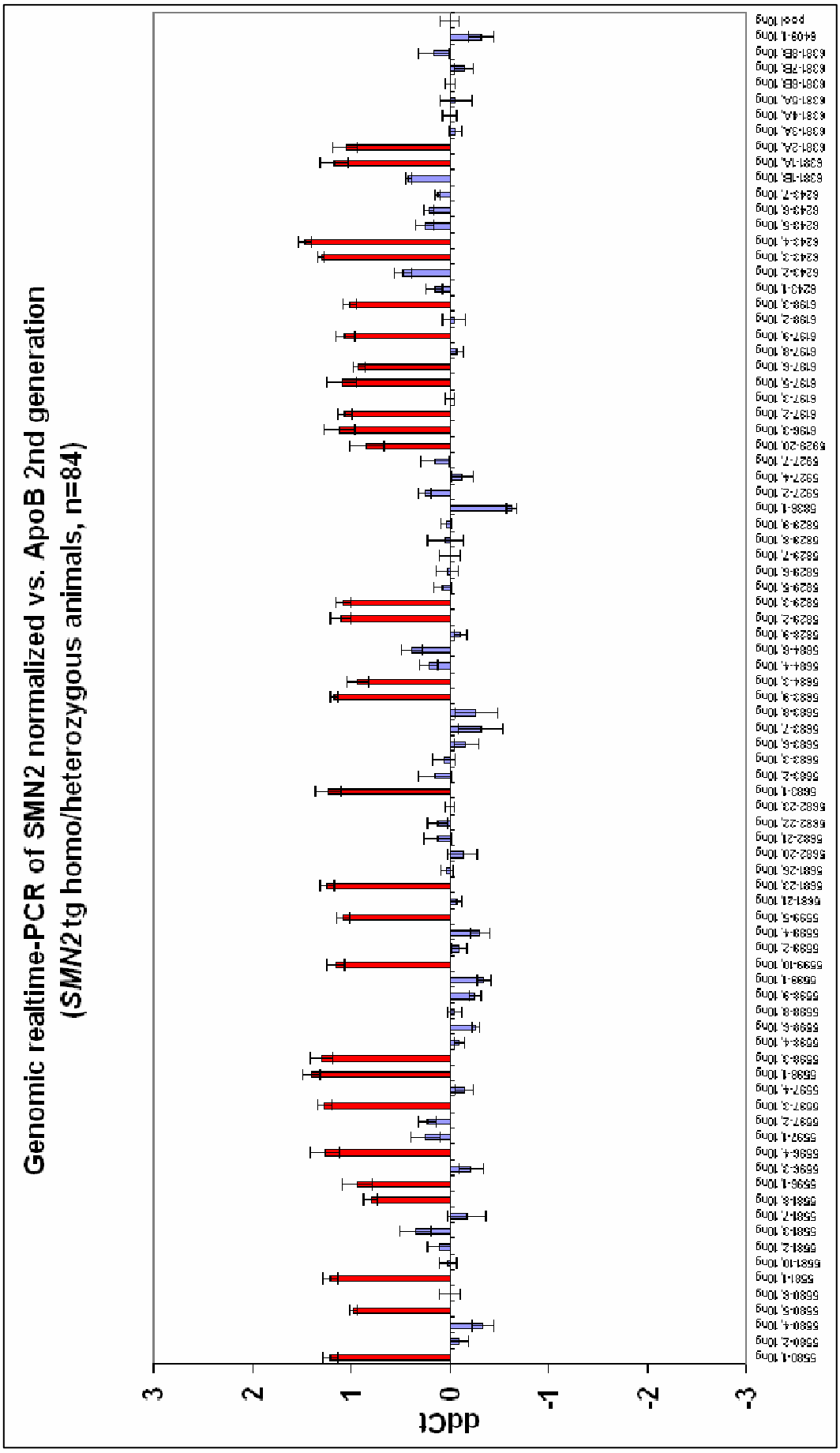

Figure 34 ddCt values of 84 SMA_B mice: *SMN2tg* gene in relation to *ApoB* as internal control. Blue bars represent ddCt values corresponding to heterozygous *SMN2tg* copy state, whereas red bars represent DNAs derived from *SMN2tg* homozygous animals.

4.3.1.2 Effects of SAHA treatment in the SMA_B mouse model

As a first mouse model of SMA the severe affected SMA type I mouse was chosen. This mouse model was generated in the year 2000 by the group of Arthur Burghes, and will therefore be subsequently entitled SMA_B mouse (Monani et al. 2000) (see chapter 1.3.1.2). These severely affected SMA-like mice were observed to live for 5 days, making it applicatory for the investigation of the potency of SAHA to prolong the survival of these respective animals. Importantly, the mice described in the original publication were on a C57BL6/J inbred strain background.

The mice finally used for the experiments were kindly provided by a collaborator of Arthur Burghes, Michael Sendtner. However, those animals were on a FVB/N in bred strain background. Importantly, the SMA_B mice on the FVB/N background were so far uncharacterized in terms of survival and SMA progression.

The high impact of the different background was unexpected, but led to the following observations.

After exactly determining the number of *SMN2* transgene copies of the potential breeder pair animals (see chapter 4.3.1.1), mice carrying the genotype $Smn^{-/+};SMN2^{tg/tg}$ were bred with each other. Following a mendelian inheritance, ¼ of the offspring was expected to carry a $Smn^{-/-};SMN2^{tg/tg}$ –genotype, which would resemble the expected SMA-like mice. However, SMA-like animals with this respective genotype were never observed to be born. Five breeder pairs produced 35 offspring with an average litter size of 7.2±1.2, but none of the theoretically expected 9 SMA-like animals was observed (Table 13).

In order to proof whether SAHA could prevent the SMA-like animals from prenatal death, the pregnant mother mice were treated from gestational day 15 on either with SAHA or with its respective solvent. Since SAHA is a hydrophobic substance, which is impossible to be solved in water, SAHA was solved in water supplemented with the carrier substance hydroypropyl-β-cyclodextran (HP-β-CD). Given the fact that a 20 g mouse drinks 3 ml water per day, this dosage equals 200 mg SAHA per kg body weight per day, which was previously described to be well tolerated in wild-type mice and shown to increase H3/H4 acetylation levels in the CNS (Hockly et al. 2003).

Strikingly, prenatal SAHA treatment resulted in a first observation of born living SMA-like animals. In contrast, the treatment with the solvent alone failed to result in a significant change in the number of born SMA mice, although one SMA-like animal was detected, which died at postnatal day one. The five observed SMA-like mice, which were born under SAHA treatment, survived for 2 (two mice), 8, 11, and 14 days, respectively

(Figure 35). This suggests a beneficial effect of SAHA on the *in utero* progression of SMA (Table 13).

Table 13 Observed discrepancy between expected number of SMA mice and *de facto* born amount of SMA-like animals. P-values suggest that the treatment of pregnant mice leads to a higher *in utero* survival rate of SMA-like mice.

Substance	# SMA-mice expected	# SMA-mice observed	p-value (χ^2-test)
water control	9	0	0,012
HP-β-CD	8	1	0,042
SAHA	12	5	**0,119**

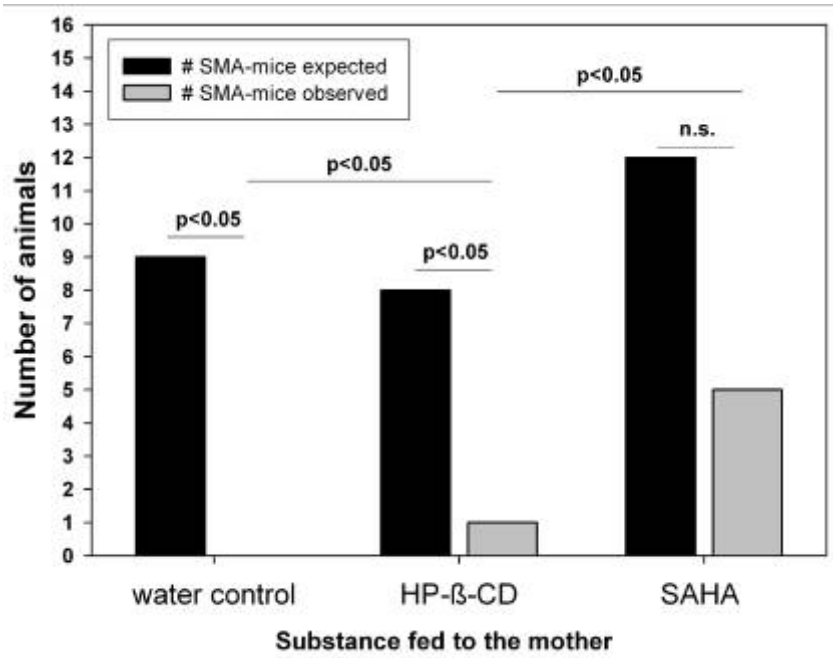

Figure 35 Number of born SMA mice increases after SAHA treatment of the pregnant mothers

Moreover, the SMA_B mice revealed a severely reduced fertility starting at breeder pair age of 6 months (Figure 36). Since SMA is a neuromuscular disorder leading to impairment in motor abilities, it was necessary to find a SMA-like mouse model, which reaches an age where motor abilities may be assessed.

Hence, the adversities in the breeding performance of the SMA_B mice, and the fact that the SMA_B mice on FVB/N background are so severely affected that they die prenatally, suggested the urgent need for a different mouse model.

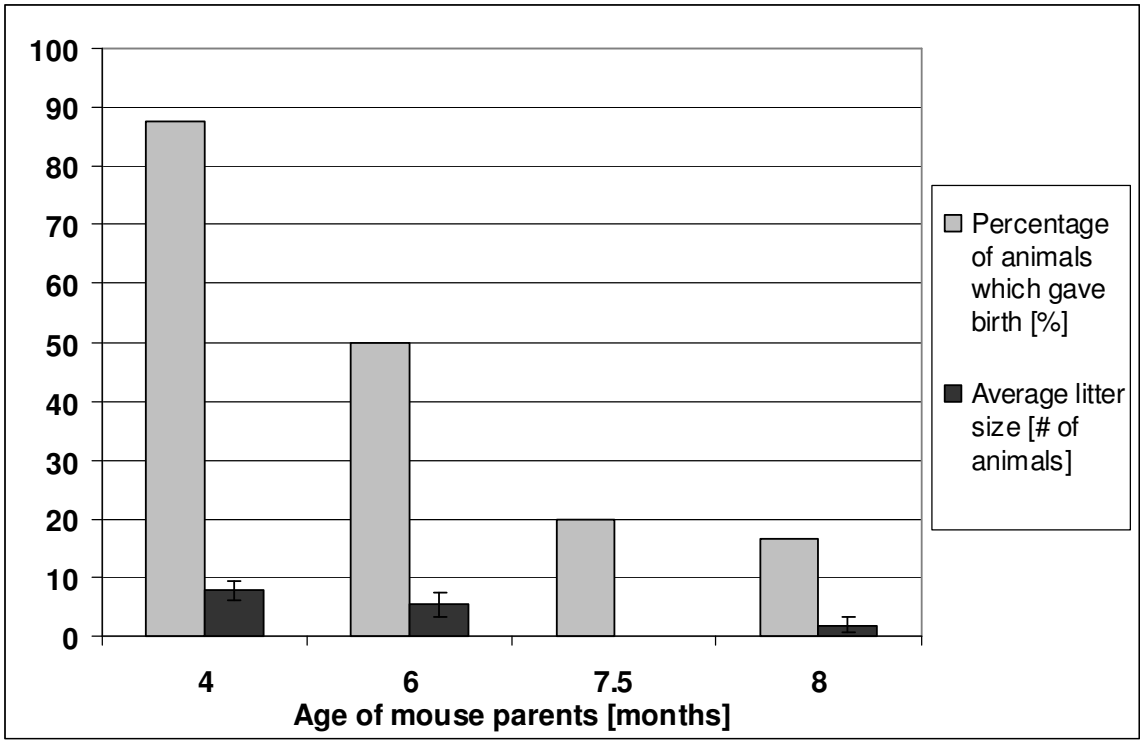

Figure 36 *Smn*$^{-/+}$;*SMN2*$^{tg/tg}$ animals show a severely reduce fertility starting at 6 months of age.

4.3.2 SAHA treatment of the SMA_H mouse model

As previously described, the SMA_B mouse model revealed multiple disadvantages for a proper study of the effect of SAHA in an *in vivo* model. The group of Hung Li generated a alternative mouse model in the year 2000. This mouse model is subsequently referred to as the SMA_H mouse (Hsieh-Li et al. 2000). The SMA_H mouse model was purchased from the Jackson´s Laboratory.

The *SMN2* copy number strongly influences the severity of SMA. Thus, although homozygously knocked-out for the murine *Smn* gene, the SMA_H mice are viable and fertile, if they carry the *SMN2* transgene also in a homozygous manner. This main phenotypic difference between the SMA_B and SMA_H mice is based on the difference of the respective transgene. While each transgene allele of the SMA_B mice carries one *SMN2* copy, each transgene of the SMA_H mice carries two *SMN2* copies. This feature protects $Smn^{-/-};SMN2^{tg/tg}$ animals from developing a SMA phenotype.

Since it was known that the SMA_H carry four SMN2 copies in a homozygous state, the transgene copy number of the four purchased founder animals was proven by the already described method (chapter 4.3.1.1). Here the DNA of the transgene-homozygous SMA_B mice served as a “heterozygous” control for the SMA_H mice.

Since the $Smn^{-/-};SMN2^{tg/tg}$ animals are viable and fertile, these mice were bred with $Smn^{+/-};SMN2^{wt/wt}$ mice, providing a 50% chance to receive $Smn^{-/-};SMN2^{tg/wt}$ animals, which present a SMA-like phenotype. This was a major advantage to produce large amounts of SMA-like mice. As described in the following chapters, SMA-like mice were virtually detected in every respective litter, living to a mean age of ~9.9 days.

4.3.2.1 Establishment of the treatment concentration and application method

Since this was the first time that SAHA was used in newborn mice, in a first step the right application method and adequate treatment concentration had to be determined. Previously published data suggested a SAHA concentration of 200 mg per kg per day in an adult mouse (Hockly et al. 2003) to be well tolerated.

SAHA is not soluble in water. Drinking water was supplemented with hydroypropyl-β-cyclodextran (HP-β-CD), to use that substance as a carrier. The maximum amount of SAHA to be solved in HP-β-CD-water is 2 g per 1 l. This results in a maximum treatment concentration of 12,5 mg per kg mouse, providing an applicable liquid volume of 12.5 µl to administer to a 2 g mouse.

Initially 13 SMA mice and 13 healthy littermates were orally fed with 12.5 µl HP-β-CD-supplied water twice daily (procedure see Figure 37b) starting from postnatal day

one. Since this treatment regimen revealed no significant impact on the survival time of both, SMA-like mice and littermates (see Figure 38b); next litters were also treated with 12.5 mg/kg SAHA solved in HP-β-CD-water two times a day. This respective concentration of SAHA had no significant impact on the mean survival of the SMA-like mice. However, 12.5 mg/kg/2xdaily orally applied SAHA revealed no toxic effect neither in SMA nor in heterozygous mice (Figure 38d).

Thus, to apply the previously published treatment concentration of 200 mg/day, SAHA had to be dissolved in dimethyl sulfoxide (DMSO), because of the relatively low solution capability of HP-β-CD-water. Both application methods, the oral and the subcutaneous (s.c.) administration of 12.5 µl DMSO twice per day revealed no significant decline of the median survival of SMA mice or littermates (see Figure 38a,c, subcutaneous injection procedure see Figure 37a). One single oral application of 200 mg/kg SAHA solved in DMSO was not tolerated by the newborn mice (P1). SMA-like mice and their healthy littermates died one day after the treatment (Figure 38g). Moreover, the oral application of 50 mg/kg/2xday (solved in DMSO) revealed no improvement in the survival time of the SMA-like mice. However, the 50 mg/kg/2xday (solved in DMSO) treatment showed a significant toxicity in the treated heterozygous littermates, since ~80% of the control littermates died during the treatment period (see Figure 39f). Also no improvement in the survival time of the SMA-like mice was observed in the animals, which were subjected to the subcutaneous application of 25 mg/kg/2xday (solved in DMSO). Repeated injections of SAHA (solved in DMSO) in the neck of young mice resulted in a severe necrosis of the respective tissue. Furthermore, the s.c. application of SAHA (25 mg/kg/2xday (solved in DMSO)) was followed by a detrimental effect on the mean lifespan of the heterozygous littermates, indicating a severe intolerance to s.c. application of SAHA (Figure 39e).

Despite the above mentioned side effects, the oral application of 25 mg/kg/2xday SAHA showed a significant improvement in the mean survival of the severe affected SMA-like mice. Thus, the oral application of 25 mg/kg/2xday SAHA revealed no significant reduction in the mean survival of heterozygous littermates. Hence, the oral treatment with a dosage of 25 mg/kg/2xday SAHA was extended to a treatment of 42 SMA-like animals and 38 healthy littermates (see chapter 4.3.2.1).

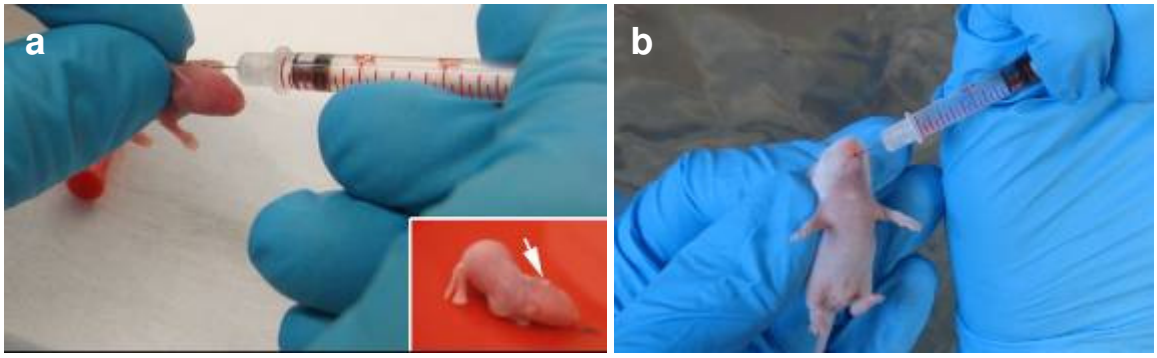

Figure 37 a Subcutaneous injection of SAHA (solved in DMSO). Lower right corner: the white arrow marks the location of SAHA escape and onset of necrosis. **b** oral application of SAHA (solved in DMSO) with the help of a feeding needle (blunt ended syringe).

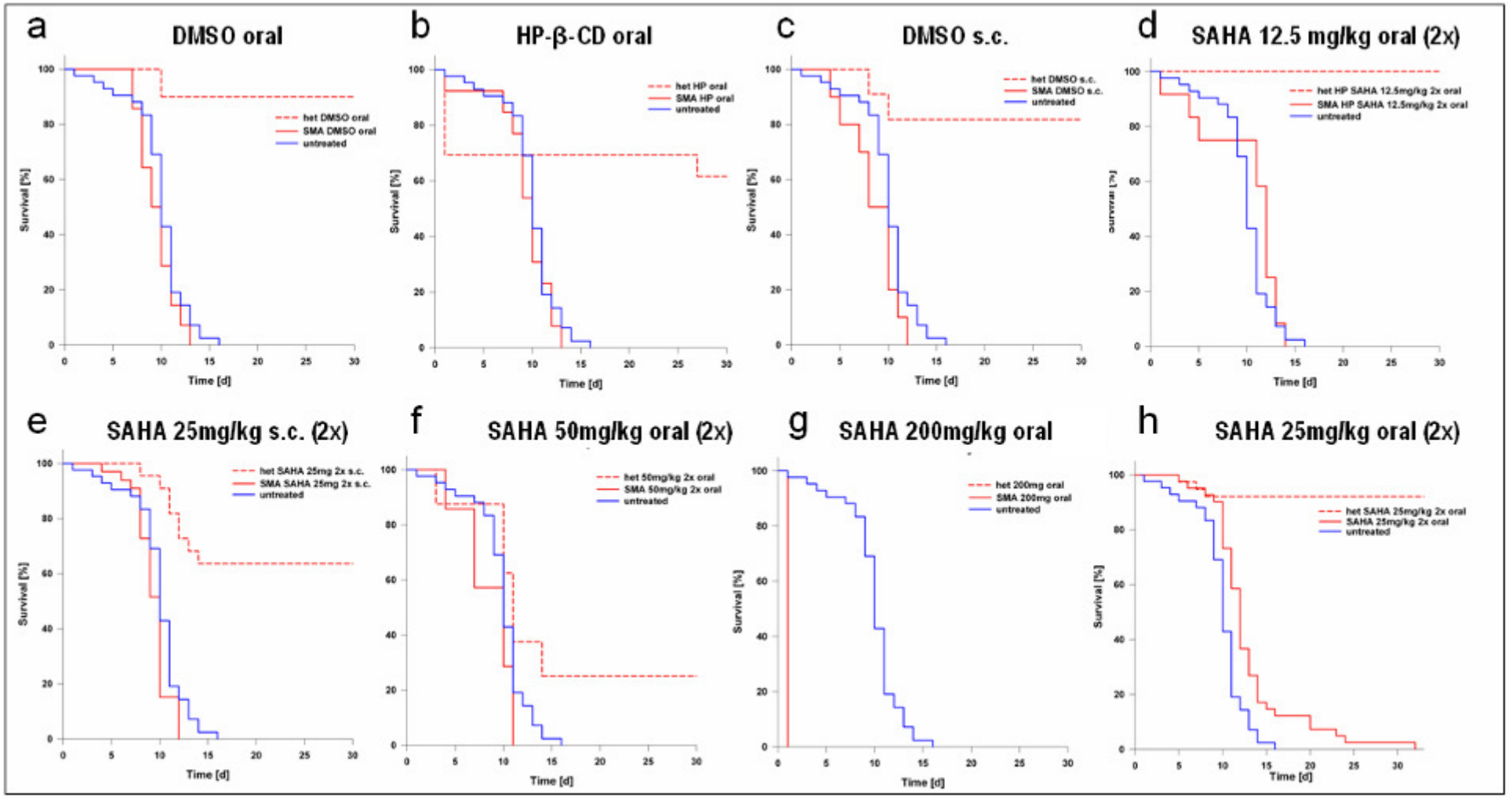

Figure 38 Overview of the survival analyses of the differentally treated SMA mice and their heterozygous littermates in comparison to untreated SMA mice (blue line).All mice were treated with a liquid volume of 6.5 µl per gram mouse regardless of substance and application method **a**) oral DMSO treatment has no impact on survival of SMA mice or littermates (p=0,192), **b**) oral HP-β-CD treatment has no impact on survival of SMA mice or littermates (p=0,354), **c**) subcutaneous DMSO treatment shows unfavourable side effects on SMA mice (p=0,0721), **d**) oral SAHA (solved in HP-β-CD) treatment has no impact on survival of SMA mice or littermates (p=0,243), **e**) subcutaneous SAHA (25mg/kg twice daily) treatment shows unfavourable side effects on SMA mice p=0,0291 and on heterozygous littermates, **f,g**) oral SAHA (50mg/kg twice daily for f) (200mg/kg once daily for g) treatment reveals high toxicity for SMA (p<0.0001) (f) p=0,181) and heterozygous (p<0.0001) mice, **h**) oral SAHA (solved in DMSO, 25mg/kg twice daily) treatment reveals a significant increase in survival of SMA mice (p=0,000509); red dashed line=heterozygous treated; red line=SMA treated; blue line=SMA untreated; s.c.=subcutaneous; 2x=twice daily; HP-β-CD=hydroxpropyl-β-cyclodextrin.

4.3.2.2 Effects of SAHA treatment on survival of the SMA_H mice

Since the adequate SAHA treatment regimen was determined, in all subsequent experiments SMA-like mice and their unaffected littermates were treated twice daily with 25 mg/kg SAHA solved in DMSO by oral application with a feeding needle.

The mean survival of the untreated SMA_H mice was 9.905 days (boxplot in Figure 39a). The treated group of SMA-like mice revealed a mean survival of 12.905 days, which indicates a significant increase in the mean survival time of 30.288% ($p<0.001$). Noteworthy, the mouse representing the longest survivor in the untreated group lived for 16 days, while ~10% of the SAHA treated animals lived 16 days or longer: one mouse died at the age of 16 days, two mice lived for 20 days, one mouse for 23 days, one mouse for 24 days, and one mouse lived for 32 days (Figure 39b). However, the single mouse under SAHA treatment, which reached an age of 32 days, developed a severe necrosis of the tail and the hind limbs (Figure 40). Therefore this mouse had to be sacrificed at day 32. Remarkably, the onset of a necrosis of the hind limbs and the tail was also observed for the treated SMA mice, which survived for 20 days or longer. Thus, it is important to mention that the necrosis is not an effect of SAHA, but rather a known feature of progressing SMA (Araujo Ade et al. 2009). Necrosis was never observed in SAHA-treated littermates. Hence, the SMA-like mice developed the necrosis, because they reached under SAHA treatment a far longer survival than the untreated ones. Untreated SMA mice did not develop necrosis, since they have a severely reduced life-expectancy. Importantly the mean survival of the treated SMA mice was shifted significantly. Both, the rank-sum t-test and the Mann-Whitney rank sum test for significance clearly revealed that the difference in the median values between the two groups is greater than would be expected by chance; there is a statistically significant difference ($p <0.001$), suggesting that SAHA is reducing the progression of SMA development.

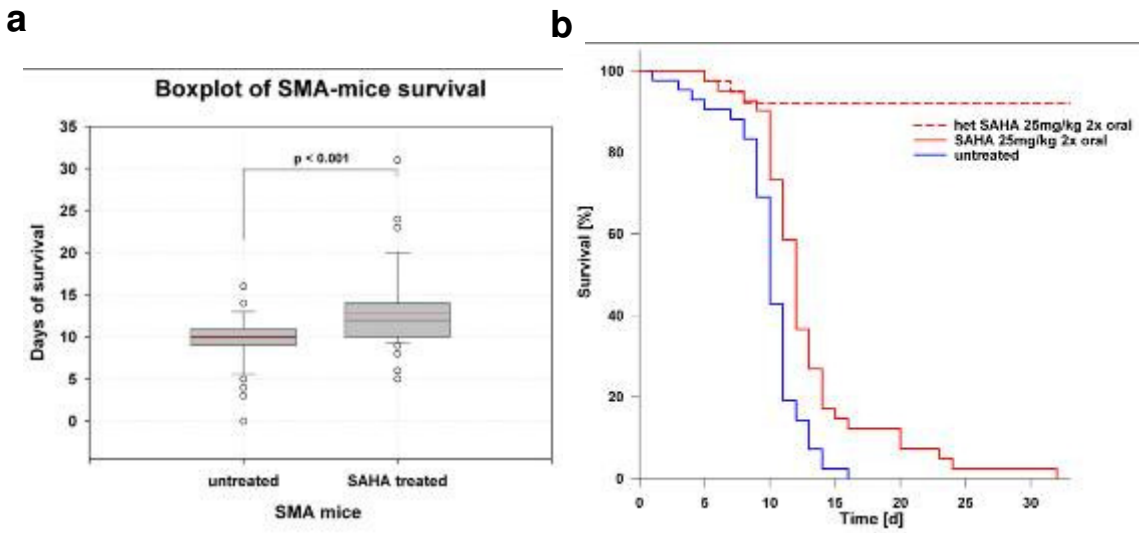

Figure 39 Comparison of the mean survival of SMA mice SAHA-treated vs. untreated presented in boxplot (mean value=red line; median value=black line) in **a)** and in a Kaplan-Meier-curve in **b)** red dashed line=heterozygous treated (n=38); red line=SMA treated (n=42); blue line=SMA untreated (n=42)

Figure 40 SAHA-treated SMA mouse developing a necrosis of tail and hind limbs at the age of 25 days. This mouse had to be scarified at an age of 32 days.

4.3.2.3 Effects of SAHA treatment on body weight of SMA_H mice

To characterize the progression of SMA and the development of the SMA-like animals with or without SAHA treatment, the weight of each mouse was determined daily. Every single animal was weighed each morning before the first application of SAHA.

Interestingly, all mice regardless of the respective genotypes show the same weight gain up to postnatal day 3, where the mean weight ranges from ~2.1 to ~2.3g. However, from this time point on, the weight of the SAHA-treated heterozygous control littermates increases in an almost linear manner. In contrast to this continuous augmentation, the mean weight of both, the untreated and the SAHA-treated SMA-like mice reveal a rather slow elevation up to postnatal day 8. The treated SMA-like mice show a mean weight of ~4g at P9, whereas the untreated ones reach a mean weight of 3.6g at the same age. From P10 to P12, the mean weight of the untreated SMA-like mice and the SMA-like mice under SAHA regimen shows slight fluctuations, but remain static just under ~4g. However, for comparison, the SAHA-treated heterozygous littermates reveal a mean weight of 8.1g at P12, which is twice the amount of SMA-like animals at this respective age. Strikingly, from P12 on the untreated SMA-like animals continuously lose weight until P16, where the last untreated mouse died. In contrast to the decline of mean weight in the untreated SMA-like mice, the SAHA-treated mice showed an increase in mean weight to a maximum level of ~5.5g at P16. The obvious steep ascent of the weight progression curve from P14 to P15 or from P24 to P25 in Figure 41 of the SAHA-treated SMA-like mice is explainable by the fact that some mice died around that age (Kaplan-Meier-Curve Figure 39b), after they lost some weight. Therefore, only the long-surviving SAHA-treated SMA-like mice make up the mean weight value from P15 onward. The mean weight of the SAHA-treated SMA-like mice surviving longer than 14 days stays nearly unchanged around ~5g. The steep ascent in the weight curve from P24 to P25 again resembles the death of a mouse, which lost weight before dying. The weight progression of the long-survivor SMA-like mouse stagnated until this mouse had to be sacrificed because of the progressing necrosis of the hind limbs (see Figure 40 and chapter 4.3.2.2).

Taken together, these data indicate that SAHA treatment prolongs the survival of SMA-like mice but does not normalize the weight progression of these animals. Thus, the weight progression of the treated SMA-like mice rather stays static, comparable to the untreated SMA-like mice. Therefore, a dwarf-like phenotype was observed for the SAHA-treated SMA-like mice of an older age. These animals were only half as large as their heterozygous littermates at an age of 14 days. This discrepancy was even higher at later ages (see Figure 42).

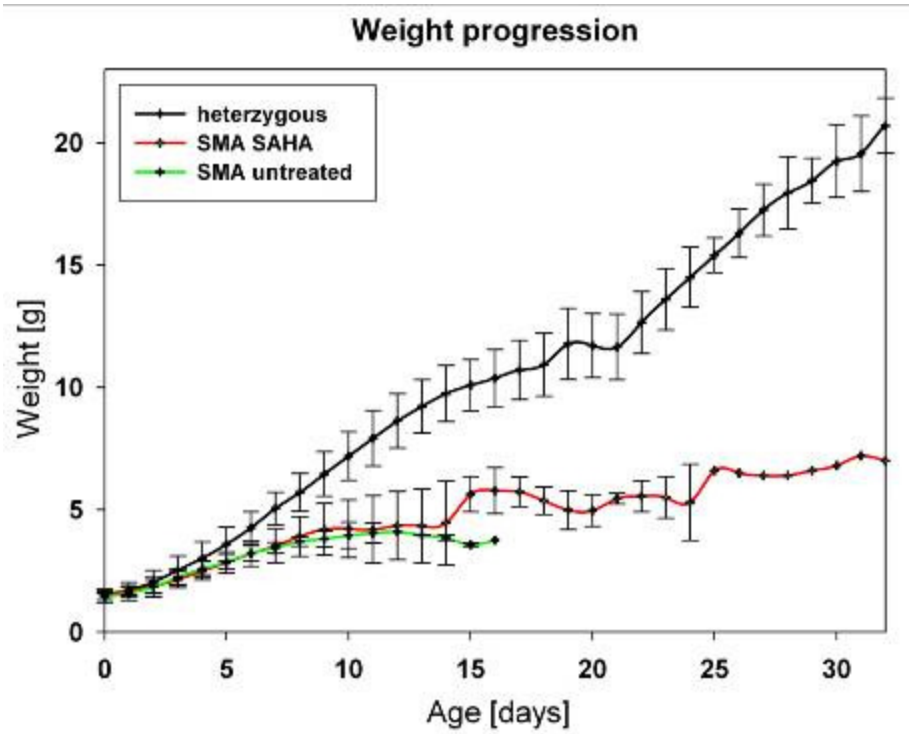

Figure 41 Diagrammatic representation of the mean weight progression of SAHA-treated heterozygous mice (n=38), SAHA-treated SMA-like mice (n=42) and untreated SMA-like mice (n=42). red line=SMA-like mice treated, green line=SMA-like mice untreated, black line=heterozygous SAHA-treated.

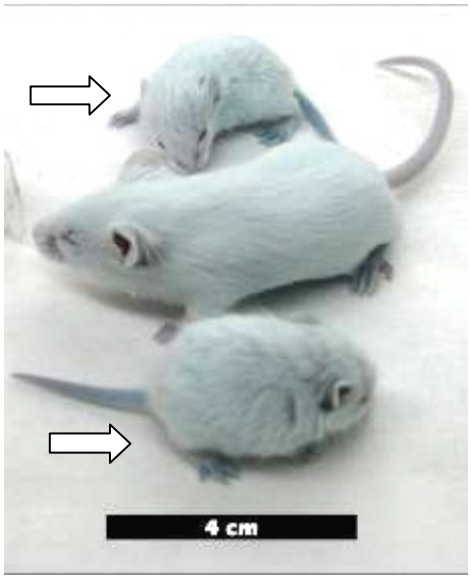

Figure 42 This photo resembles the obvious size difference between two SAHA-treated SMA mice (marked with arrows) and one SAHA-treated heterozygous littermate. All mice were at an age of 14 days. The size discrepancy was even higher at later ages.

4.3.2.4 Effects of SAHA treatment on motor ability of SMA_H mice

Since SMA is a motor neuron disease, severely affecting the motoric abilities of patients, a potential prospective therapy should ameliorate motor impairments. Therefore, the effect of SAHA treatment on the motor abilities of SMA-like mice was chosen as major outcome criterion of the SAHA treatment experiment.

As a first motor test the commonly used so-called righting-reflex-test was performed (Avila et al. 2007). Since the neonatal SMA-like mice showed no differences in their ability to right compared to the healthy littermates (appendix Figure 59) the so-called tube test was performed instead. It was especially developed to be performed with neonates (El-Khodor et al. 2008). In brief, to perform a tube test each pup was placed one by one headfirst into a vertical 50 ml reaction tube, thereafter, depending on the motor ability, meaning the spreading of the hind limbs, each mouse was rated from 4 (best tube score wide spreading) to 1 (bad tube score, hind limbs in a clasped position) (see Figure 43). The worst tube score of 0 was noted when the mouse was not able to hold onto the tube (for a detailed description see chapter 3.10.2).

Interestingly, the motor performance of all neonates, regardless of their genotype and treatment situation, developed similar from P0 to P2. As expected, the motor abilities of the SAHA-treated heterozygous animals were developing normal and reached a mean tube score of ~4 at P8. From this age onward, virtually every SAHA-treated heterozygous mouse performing the tube test was rated with a tube score of 4. However, the motor abilities of the SAHA-treated SMA-like mice developed similar to that of their heterozygous littermates and reached a mean tube score of ~3.8 at P6. The mean tube score of the untreated SMA-like mice reached a value of ~2 at P2, which is concordant with the observations of the treated SMA-like and heterozygous mice. Strikingly, the untreated SMA-like animals showed from P2 on a clear stagnation in their motor performance development. Beside some fluctuations, the mean tube score of the untreated SMA-like mice showed no significant increase, but was oscillating between values of 2 to 2.5. From P9 to P13 the mean tube score of the untreated SMA-like mice revealed a very steep decline from ~2.5 to ~0. This reflects the progression of SMA, which was previously described by the survival time evaluation (see chapter 4.3.2.2) and the characterization of the weight progression (see chapter 4.3.2.3).

However, the SAHA treatment is able to ameliorate the motor impairment of SMA-like mice. The SAHA-treated SMA-like and the heterozygous animals showed a very similar development of motor ability. Noteworthy, the motor development of the SAHA-treated SMA-like mice was delayed for one day. The heterozygous mice revealed a mean tube score of ~3.7 at postnatal day 5, whereas the SAHA-treated SMA-like mice

reached this tube score only at P6. This developmental delay was also observed for the time points P3 to P6. Although the SAHA-treated SMA-like mice revealed a decline in motor performance starting at P9, their achieved tube score was always significant higher than the tube score of the untreated SMA-like mice. The observed fluctuations in tube score values are again explainable by the fact that, some SAHA-treated SMA-like mice became moribund and therefore revealed deterioration in motor performance shortly before death (see Figure 44).

As a concluding remark, it is noteworthy to state that SAHA treatment ameliorates the motor impairment of SMA-like mice. The SAHA-treated SMA-like mice do not show a full rescue of the motor ability deterioration, but compared to untreated SMA-like mice those mice reveal a significant improvement of motor ability.

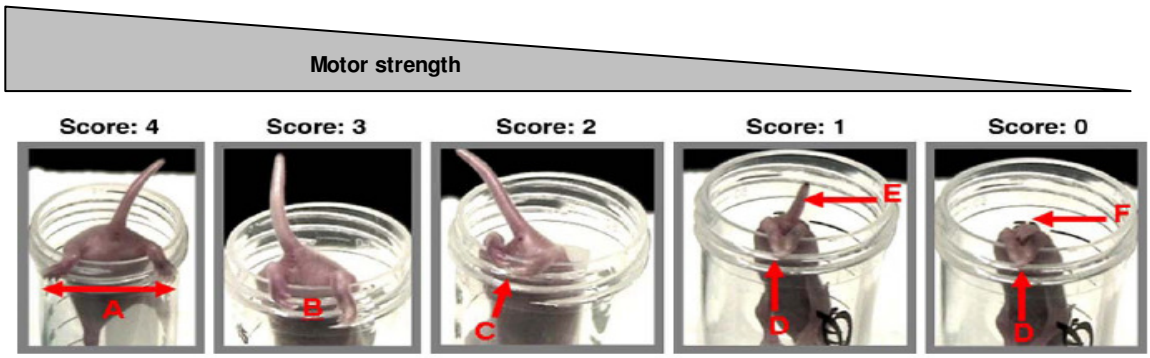

Figure 43 Overview of the tube test scoring scale. Tube score of 4 indicates normal hind-limb separation with tail raised (A); score of 3, hind limbs are closer together but they seldom touch each other (B); score of 2, hind limbs are close to each other and often touching (C); score of 1, hind limbs are almost always in a clasped position (D) with the tail raised (E); a score of 0 indicates failure to hold onto the tube. (Taken from (El-Khodor et al. 2008)).

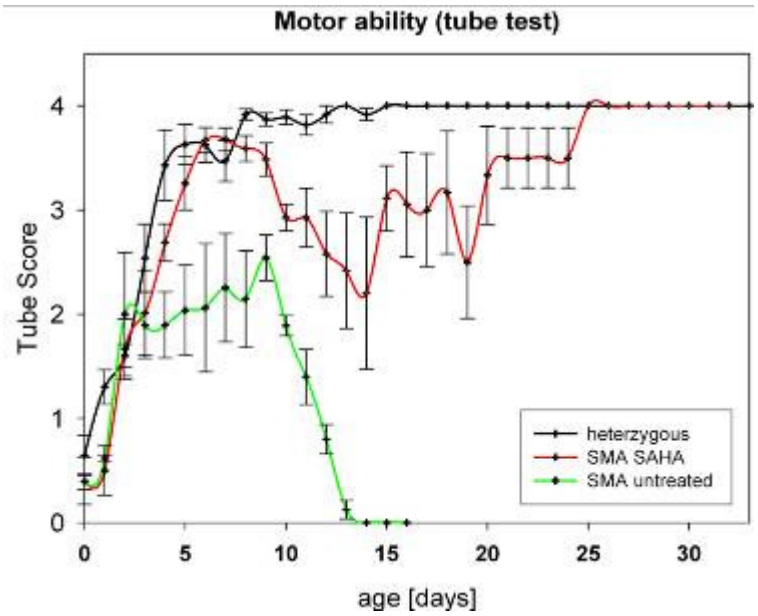

Figure 44 Diagrammatic representation of the mean motor ability progression of SAHA-treated heterozygous mice (n=38), SAHA-treated SMA-like mice (n=42) and untreated SMA-like mice (n=42). red line=SMA-like mice treated, green line=SMA-like mice untreated, black line=heterozygous SAHA-treated.

4.3.2.5 Effects of SAHA treatment in the SMA_H mouse model on *SMN2*tg expression

In order to evaluate the impact of SAHA treatment on the *Smn/SMN2* expression *in vivo,* mice were sacrificed by decapitation either at day P5 or P10. SAHA-treated SMA-like mice (*Smn*$^{-/-}$*; SMN2*$^{tg/wt}$), or SAHA-treated heterozygous littermates (*Smn*$^{+/-}$*; SMN2*$^{tg/wt}$) were opened by abdominal incision and subsequently RNA or protein was prepared out of the respective organs (see chapters 3.11.4 and 3.12.1). Therefore, whole liver, whole brain, the *gastrocnemius* muscle and spinal cord were removed. All animals, which were used were orally treated with SAHA twice daily, started at P1; the last treatment took place 1 hour prior to decapitation. All data, which will be discussed in the following are based on organ extracts derived from 3 SAHA treated P5 SMA, 3 untreated P5 SMA, 3 SAHA treated P5 heterozygous, and 3 untreated P5 heterozygous animals were counted. The same organ extracts were derived from respective P10 mice.

- SMN protein levels

In order to investigate the impact of SAHA on protein level, semi-quantitative Western blotting was performed using β-actin as internal control. All experiments were carried out with the protein extracts from liver, brain, the *gastrocnemius* muscle and spinal cord derived from the respective mice.

First the whole protein extracts were measured by the Bradford method, subsequently 7.5 µg protein were loaded onto SDS PAGE gel and after electrophoresis, a Western blot was performed. The results of the densitrometrical analysis were evaluated and depicted in a histogram. Here the SMN signal-intensity was quantified in relation to the internal control β-actin. Due to the high grade of homology between the murine Smn and the human SMN protein, the used antibody is not able to distinguish between both, therefore the term SMN stands for both proteins, which may be derived from *Smn*$^{+/-}$*; SMN2*$^{tg/wt}$-mice.

Strikingly, in all tissues derived from SAHA-treated SMA-like animals an up-regulation of SMN protein level was observed. Importantly, SMN protein levels derived from neuronal tissues, such as spinal cord in P5, as well as brain in P10 SAHA-treated SMA-like animals showed a positive response to SAHA. This finding proofs that SAHA not only crosses the blood-brain barrier, but also is able to augment the SMN expression in the main SMA-target tissues. In the spinal cord of P5 SMA-like mice SAHA treatment increased the mean SMN level significantly 2.7-fold compared to untreated, the age matched heterozygous animals showed a significant ~1.5-fold increase (Figure 45a). Similar to this finding, the SAHA regimen resulted in a slightly and not significant

increase of the mean SMN protein level of ~15% in the spinal cord of P10 mice. The SAHA treatment of heterozygous P10 mice revealed a non-significant down-regulation of the SMN amount from ~300% to ~240% (relative to untreated SMA) in the spinal cord (Figure 46a).

In contrast, the SMN protein level derived from the brain tissue of heterozygous P5 and P10 mice revealed a non-significant positive response to the SAHA regimen. Also the ~18%-increase of SMN in the SAHA-treated SMA mice reached no statistical significance (Figure 45b). However, the in SMN protein level derived from the brain tissue of treated P10 mice a massive significant augmentation to ~550% was identified (Figure 46b).

The muscle tissue of all treated animals responded in massive up-regulations of the SMN-protein levels. In the case of the P5 mice, the SMA-like animals showed a massive and significant 17.6-fold increment, whereas the heterozygous littermates responded in a 2.3-fold augmentation of the mean SMN level (Figure 45c). Moreover, the SMN protein level derived from P10 SMA-like mice displayed a significant 3.5-fold up-regulation under SAHA treatment, while the heterozygous control mice presented a non-significant ~1.3-fold augmentation of the respective SMN amount (Figure 46c).

Lastly, the SMN amount derived from the liver of P10 remained unchanged in the heterozygous mice, whereas it was ~30% up-regulated by SAHA in the P10 SMA-like mice. Nevertheless, neither in the untreated nor in the SAHA-treated P5 SMA-animals a SMN protein band was detected (Figure 45d). However, the P5 heterozygous mice responded in a ~100% up-regulation in the SMN-protein level, indicating a response to SAHA regimen.

To summarize these data, it was proven that SAHA is able to up-regulate the SMN expression in all tested tissue, except the liver. Moreover, it is obvious that SAHA crosses the blood-brain barrier, confirming earlier reports (Hockly et al. 2003). Thus, SAHA treatment is capable of incrementing the SMN expression in neuronal tissues, such as brain and spinal cord. This issue is of particular interest, since the α-motor neurons are the primary target tissue of a prospective SMA therapy. However, the SAHA regimen could not elevate the SMN level of tissues derived from SMA-like mice to the respective levels of heterozygous animals. This suggests that SAHA treatment could not lead to a full protection of SMA, but may ameliorate the disease progression. This speculation is concordant with the previously described results from the survival and motor test analysis.

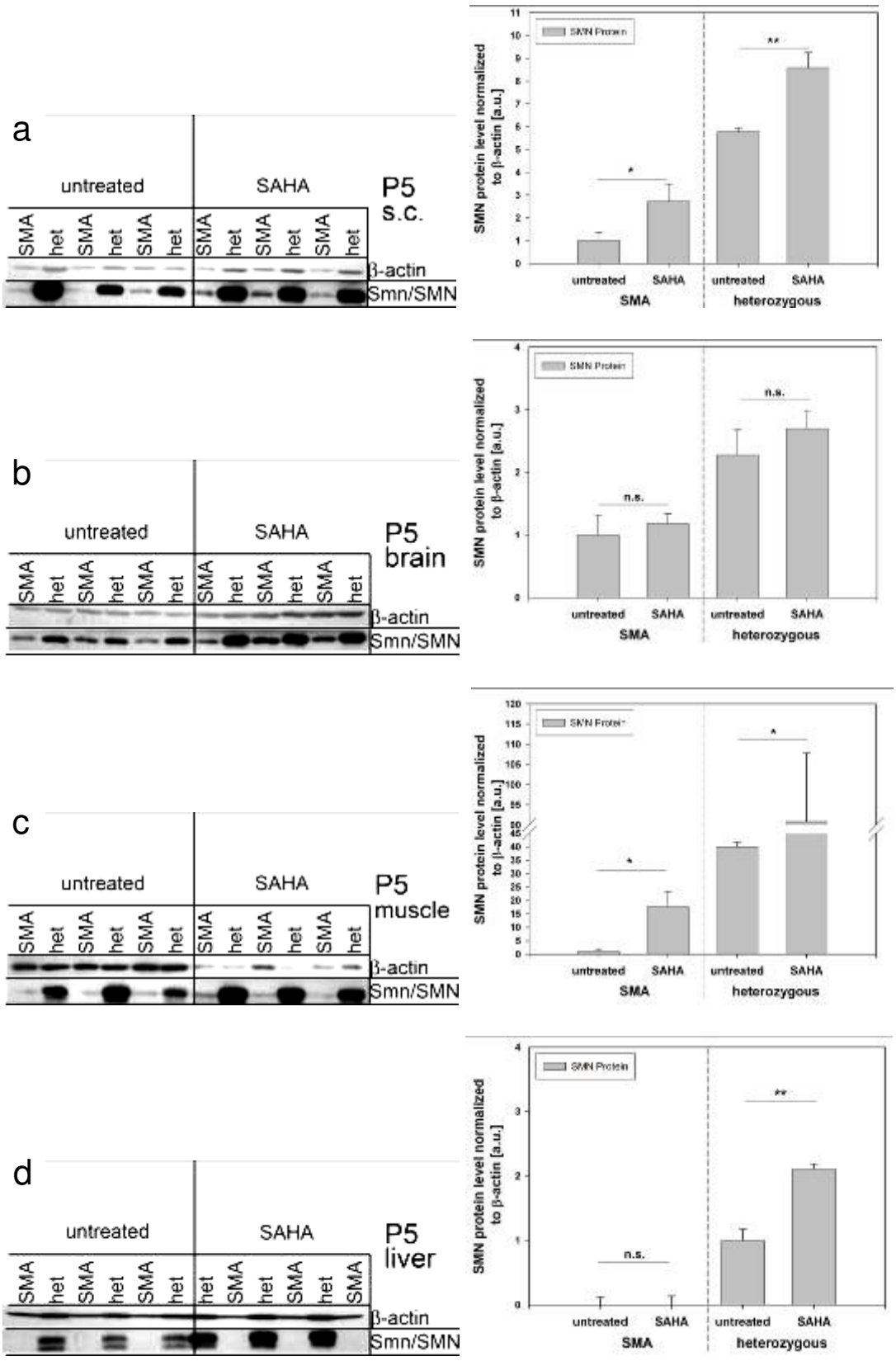

Figure 45 Impact of *in vivo* SAHA treatment on SMN expression in P5 mice. Western blots loaded with equal protein amounts were simultaneously stained with anti-β-actin and anti-SMN. The pictures show representative Western blot analyses and the diagrammatic representation of the semi-quantitative protein quantification. Mean SMN protein levels (± SEM) in **a)** spinal cord, **b)** brain, **c)** muscle, **d)** liver relative to β-actin (* $p < 0.05$; ** $p < 0.01$; *** $p < 0.001$) SMA=SMA-like mouse; het=heterozygous mouse

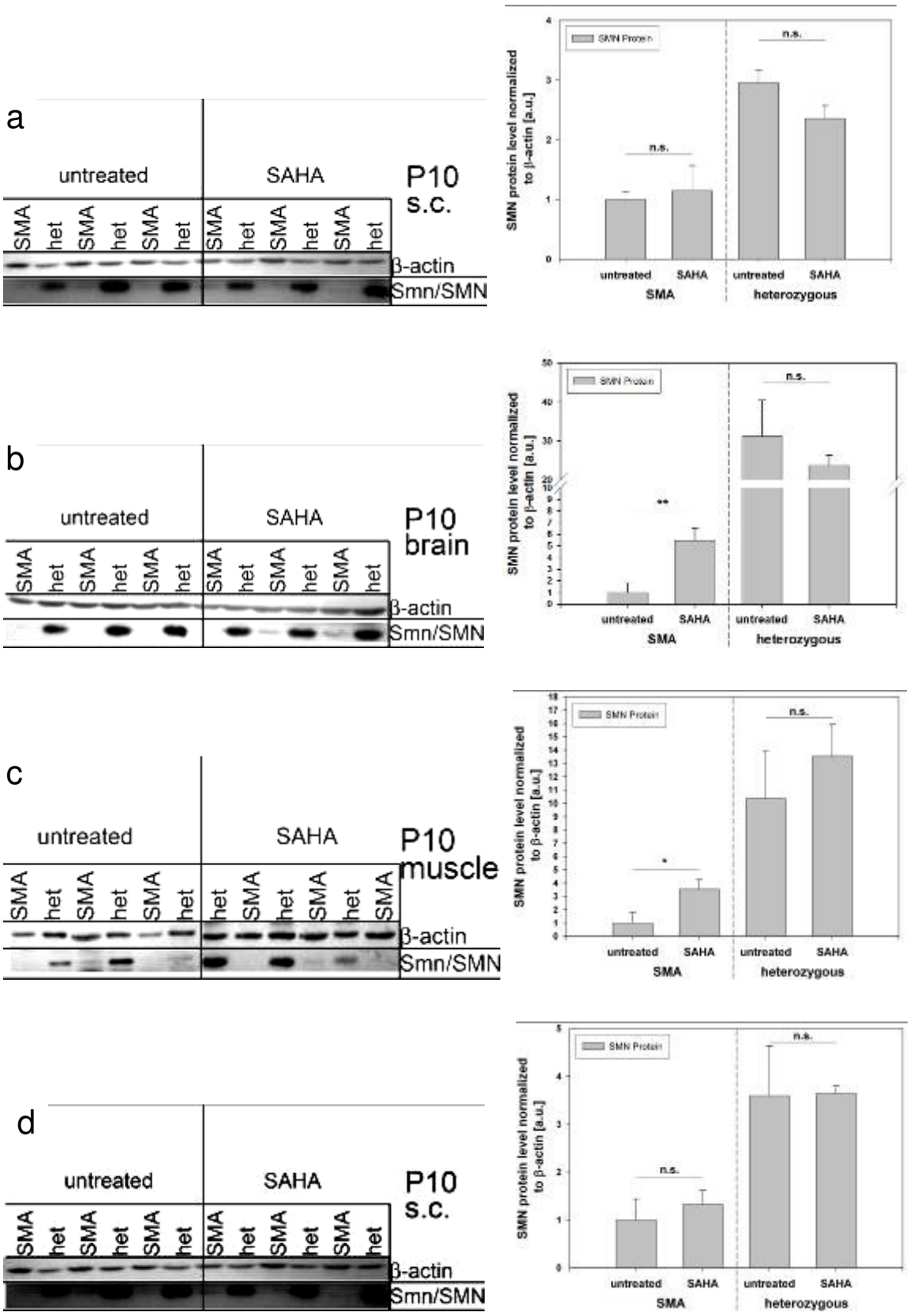

Figure 46 Impact of *in vivo* SAHA treatment on SMN expression in P10 mice. Western blots loaded with equal protein amounts were simultaneously stained with anti-β-actin and anti-SMN. The pictures show representative Western blot analyses and the diagrammatic representation of the semi-quantitative protein quantification. Mean SMN protein levels (± SEM) in **a)** spinal cord, **b)** brain, **c)** muscle, **d)** liver relative to β-actin (* $p < 0.05$; ** $p < 0.01$; *** $p < 0.001$) SMA=SMA-like mouse; het=heterozygous mouse

- Sfrs10 protein levels

Since it is well known that the splicing factor SFRS10 is competent to reverse the splicing pattern of *SMN2* pre-mRNA in human (Hofmann et al. 2000), semi-quantitative Western blots of the murine orthologue (Sfrs10) were performed, to address the question whether the expression of this factor is up-regulated by SAHA treatment in mice. Again, the protein expression of β-actin served as an internal control.

The Sfrs10 protein level in the spinal cord of SMA-like mice was not significantly changed under SAHA treatment, neither in the P5 nor in the P10 animals. In case of the heterozygous mice, a doubling of the Sfrs10 protein level was observed for the P5 mice, while the protein level in P10 spinal cord showed no change (Figure 47a and Figure 48a). Thus, the Sfrs10 level of the spinal cord seemed to be subjected to individual fluctuations.

Neither in the brain derived Sfrs10 protein level of P5 nor in the respective protein level of P10 mice any impact of SAHA was detected. This finding was true for both, the SMA-like and the heterozygous mice (Figure 47b and Figure 48b).

These findings suggest that SAHA treatment has no direct effect on the Sfrs10 expression in neuronal tissues.

Strikingly, the muscle tissue revealed a significant positive response to SAHA in all tested mice. While the P5 SMA-like mice displayed a 4-fold up-regulation, their heterozygous littermates revealed a 3.3-fold augmentation (Figure 47c). Moreover, the Sfrs10 protein level in the muscle of P10 SMA-like mice increased ~2-fold under SAHA regimen, whereas the heterozygous mice showed ~1.5-fold increment (Figure 48c).

However, the Sfrs10 level of the liver of P5 SMA-like mice was too low, to be detected by Western blotting. Nevertheless, the heterozygous P5 mice displayed a weak down-regulation after SAHA treatment of ~25% (Figure 47d). The SAHA treatment of P10 SMA-like mice resulted in a significant 6.9-fold augmentation of the Sfrs10 level in the liver tissue. Still, the heterozygous mice manifest no significant change in the Sfrs10 amount in the liver (Figure 48d).

To summarize these results, SAHA has no influence on the Sfrs10 expression in the brain and the spinal cord of SMA-like mice. Nevertheless, SAHA is able to act in neuronal tissues, since Sfrs10 was 2-fold elevated in the spinal cord of heterozygous P5 mice. However, SAHA treatment elevates the Sfrs10 level in the liver of P10 SMA-like mice, whereas the P5 SMA-like mice display virtually no expression of Sfrs10. Importantly, the muscle tissue of every SAHA-treated responded in a significant augmentation of the Sfrs10 level. Noteworthy, the Sfrs10 expression in the liver and in the muscle was observed to be strongly correlated with the respective genotype. Thus, the SMA-like mice showed a significant lower expression of Sfrs10 than the

heterozygous mice. This indicates an unexpected and not previously described expression correlation of SMN/Smn and Sfrs10 in mice.

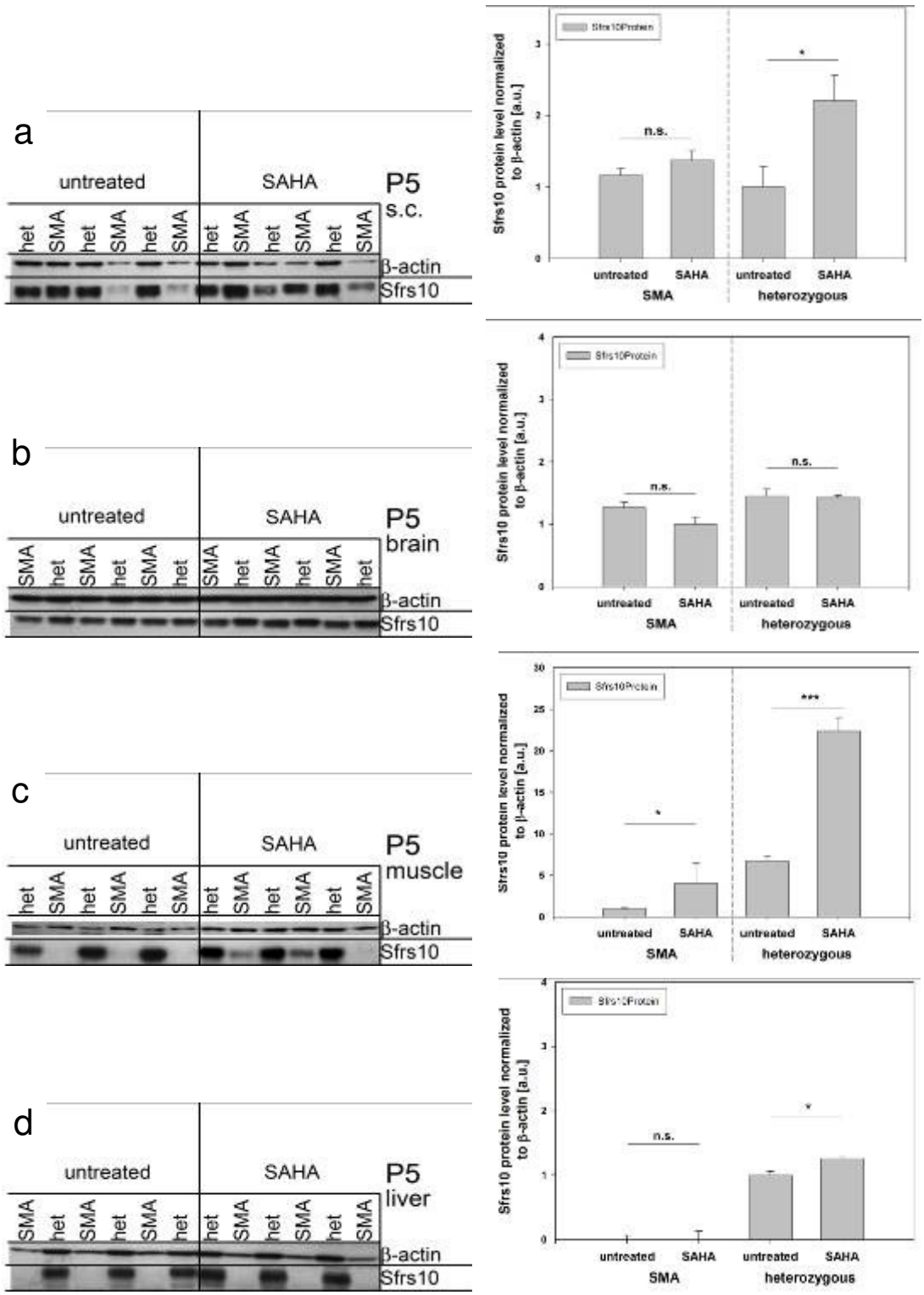

Figure 47 Impact of *in vivo* SAHA treatment on Sfrs10 expression in P5 mice. Western blots loaded with equal protein amounts were simultaneously stained with anti-β-actin and anti-Sfrs10. The pictures show representative Western blot analyses and the diagrammatic representation of the semi-quantitative protein quantification. Mean Sfrs10 protein levels (± SEM) in **a)** spinal cord, **b)** brain, **c)** muscle, **d)** liver relative to β-actin (* $p < 0.05$; ** $p < 0.01$; *** $p < 0.001$) SMA=SMA-like mouse; het=heterozygous mouse

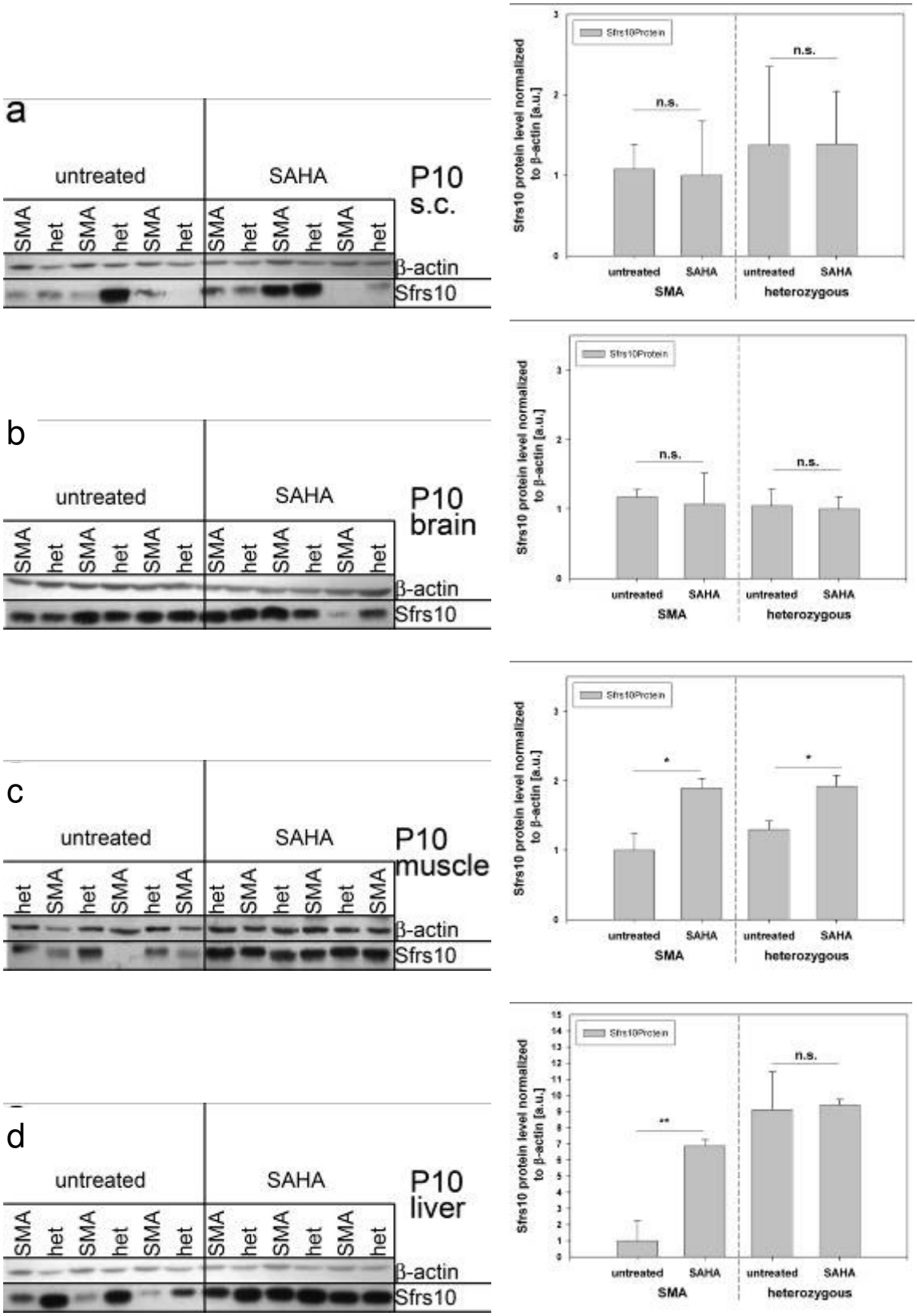

Figure 48 Impact of *in vivo* SAHA treatment on Sfrs10 expression in P10 mice. Western blots loaded with equal protein amounts were simultaneously stained with anti-β-actin and anti-Sfrs10. The pictures show representative Western blot analyses and the diagrammatic representation of the semi-quantitative protein quantification. Mean Sfrs10 protein levels (± SEM) in **a)** spinal cord, **b)** brain, **c)** muscle, **d)** liver relative to β-actin (* $p < 0.05$; ** $p < 0.01$; *** $p < 0.001$) SMA=SMA-like mouse; het=heterozygous mouse

- SMN RNA expression levels

To address the question if SAHA has an *in vivo* effect on the expression level of *SMN2*, the total amount of both *SMN2* transcripts, FL-*SMN2* and Δ7-*SMN2*, was quantified. Since it is known that HDACis may influence the expression of housekeeping genes, total RNA amount was taken as internal control. To do so, the RNAs derived from the respective murine organs of the untreated or SAHA treated SMA-like or heterozygous mice were precisely determined on a microplate reader using the RiboGreen® dye. Afterwards a total of exactly 150 ng RNA was subjected to reverse transcription.

The interpretation of the real-time RT-PCR revealed a substantial effect of the SAHA regiment on the *SMN2* transgene expression. The used primer for the real-time PCR were especially designed to detect only the FL- or the Δ7-*SMN2* transcript, which was only derived from the human *SMN2* transgene, regardless whether the respective mouse was heterozygous for the murine *Smn* gene. For a better comparison, the respective transcript levels of the untreated mice were always set to 1. The relative amount of the transcript levels of the SAHA-treated animals was therefore normalized to 1.

The FL-*SMN2* expression levels of the P5 heterozygous littermates were subjected to a down-regulation after SAHA treatment in the brain, muscle and spinal cord, whereas the liver revealed a significant 20% up-regulation. Moreover, the SAHA treatment resulted in down-regulations of the Δ7-*SMN2* levels in all tested organs derived from heterozygous P5 mice (Figure 49a). In contrast, the P5 SMA-like mice responded in virtually all organs in a weak up-regulation of both FL- and Δ7-*SMN2* to the SAHA regimen, solely the spinal cord derived Δ7-*SMN2* transcript amount was reduced to ~80%, which was statistically not significant (Figure 49b). This might suggest an impact of Sfrs10 on the splice-reversion. Contrary to the P5 mice, the SMA-like as well as the heterozygous P10 mice showed a massive response to the SAHA regimen. The FL-*SMN2* level was twofold augmented after SAHA treatment in virtually every tested tissue. Moreover, the muscle tissue of the heterozygous P10 mice displayed a 16-fold increase in FL-*SMN2* amount (Figure 49c). Only the Δ7-SMN2 level of the P10 heterozygous mice remained nearly unchanged in the brain and the liver. In contrast, the Δ7-*SMN2* amounts were significantly elevated due to the SAHA regimen (Figure 49c). The P10 SMA-like mice, revealed a massive augmentation of both, the FL- and the Δ7-*SMN2* transcript level in nearly all tested tissues. Except the FL-*SMN2* level of the brain and the Δ7-*SMN2* amount derived from the liver were not elevated significantly (Figure 49d). All other transcript amounts were twofold significantly augmented under SAHA regimen. Again, the *gastrocnemius* muscle derived transcripts were vastly increased (>10-fold) (Figure 49d).

To summarize the results of the transcript quantification, it is important to state that the P10 animals revealed a far higher response to the SAHA treatment on the transcript level than the P5 mice. Interestingly, no significant impact on the splicing reversion was detectable. Interestingly, the P10 mice, regardless of the genotype, revealed a massive increase of both FL-*SMN2* and Δ7-*SMN2* amounts, suggesting that the transcription *per se* is activated but no reversion of the splicing is facilitated. Also on protein level muscles revealed a 4 to 10-fold increase in the SMA-like mice. These findings suggest that this respective tissue is quite prone to the SAHA regimen. Importantly, transcript levels derived from the brain as well as from the spinal cord show elevations, although less pronounced than in muscle. This finding underlines the potential of SAHA to cross the blood-brain barrier, an essential feature for a potential SMA drug.

a

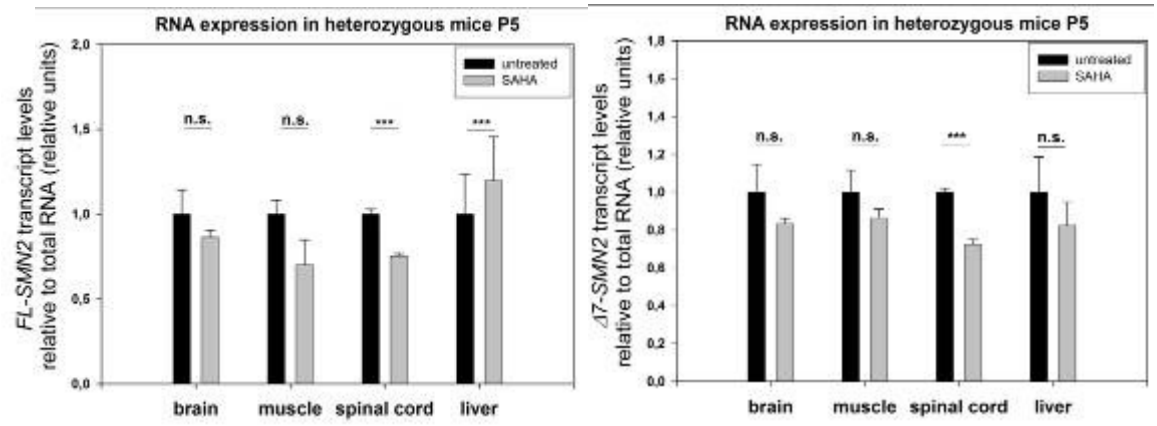

b

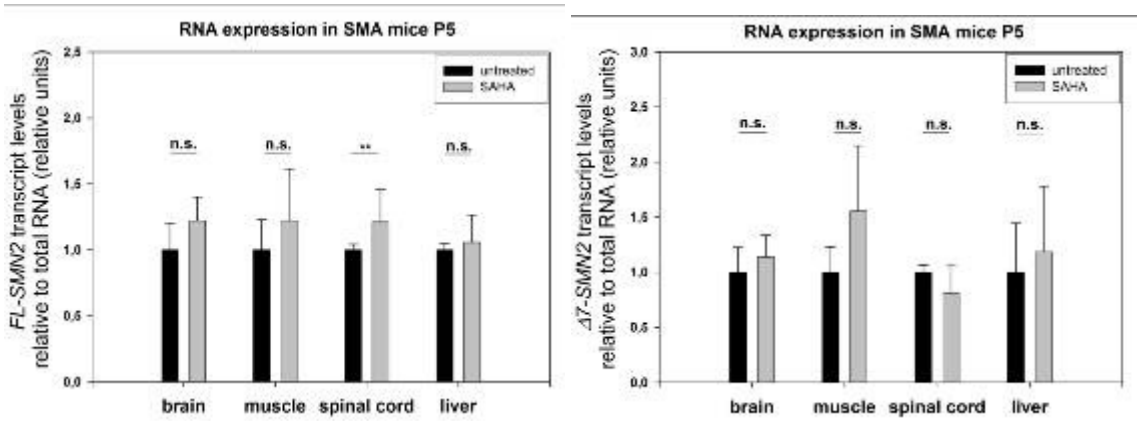

c

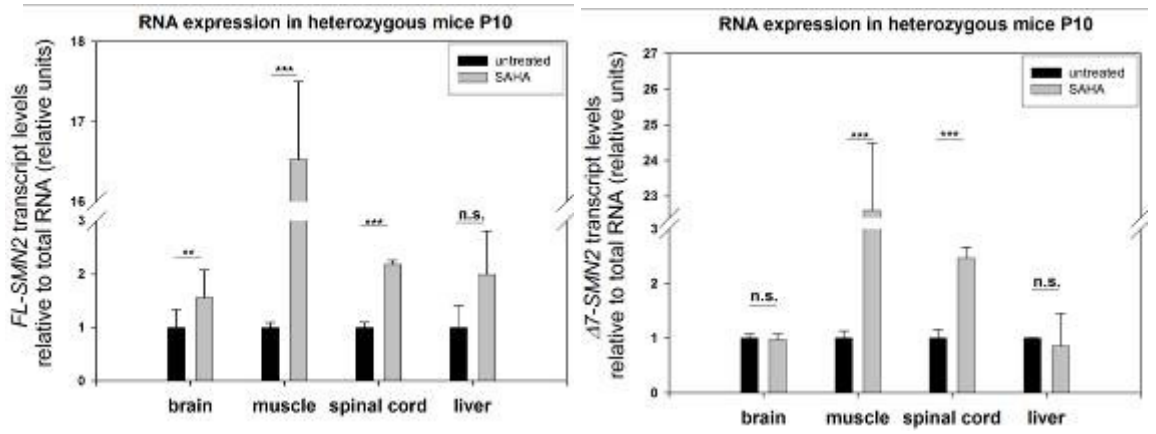

d

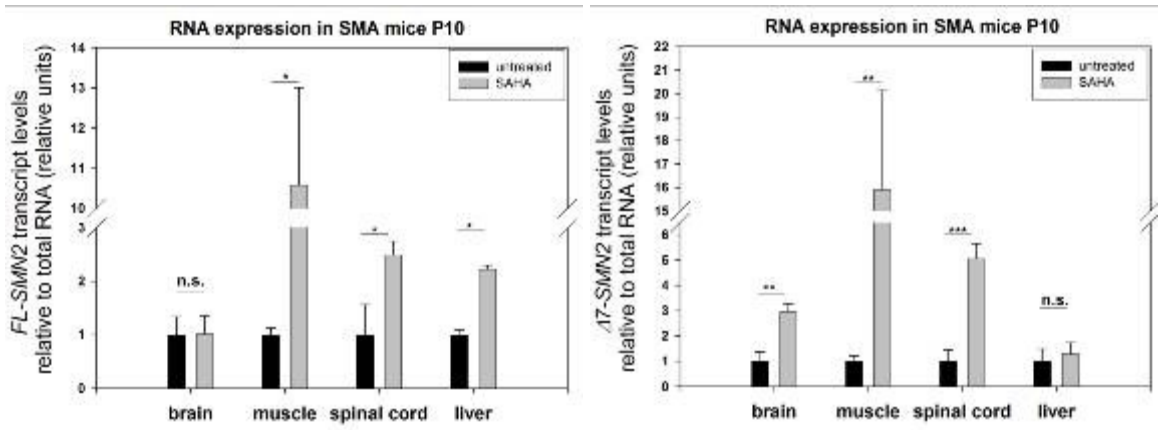

Figure 49 *SMN2* mRNA levels derived from brain, muscle, spinal cord and liver of SMA-like mice and heterozygous littermates treated with SAHA. Quantitative real-time PCR results are summarized as bar graphs. Mean values (± SEM) for FL-*SMN2* and Δ7-*SMN2* relative to total RNA amount in heterozygous P5 mice **a)**, in SMA-like P5 mice **b),** in heterozygous P10 mice **c)** and in SMA-like P10 mice **d).** (* $p < 0.05$; ** $p < 0.01$; *** $p < 0.001$).

4.3.2.6 Histological changes in the SMA_H mouse model after SAHA treatment

- Change in number of motor neurons

The primary feature of SMA is the deterioration of the α-motor neurons in the anterior horns of the spinal cord, which causes the subsequent muscular atrophy. A potential drug for SMA therapy should be able to ameliorate this phenotype and protect the α-motor neurons from the progressing deterioration. To check whether SAHA is capable to rescue the α-motor neurons, these neurons were quantified in P5 and P10 SMA-like mice and heterozygous littermates. To do so, motor neurons of 20 cross-sections derived from each 3 SAHA-treated P5 SMA, 3 untreated P5 SMA, 3 SAHA-treated P5 heterozygous, and 3 untreated P5 heterozygous animals were counted and the mean number of motor neurons per anterior horn was evaluated. Therefore, cross-sections of the spine derived from the lumbar region of the respective mouse were generated and stained by *Nissl* staining. The specific localization in the anterior horns of the spinal cord and the specific size and shape of the α-motor neurons allowed a clear discrimination between the α-motor neurons and the surrounding remaining neurons (Figure 50).

The evaluation of the number of α-motor neurons in the spinal cord revealed in five days old mice no significant difference between heterozygous mice and SMA-like animals. This is true for untreated as well as SAHA-treated mice. Moreover, no obvious discrepancy between SAHA-treated and untreated mice was observed, regardless of the respective genotype. The mean number of α-motor neurons in each anterior horn region ranged between 12 and 13 (Figure 51).

In contrast, the SAHA-treated as well as the untreated P10 heterozygous mice displayed ~18 α-motor neurons in each anterior horn cross-section. In untreated SMA-like mice of the same age the progression of SMA was reflected by a significant reduction of the mean number of motor neurons down to ~8. The P10 SMA-like mice under SAHA regimen showed a significantly higher mean value of motor neurons of ~14, suggesting a neuroprotective effect of SAHA. However, the SAHA treatment did not fully rescue the deterioration of the motor neurons, since the difference between the mean values of the untreated or SAHA-treated heterozygous P10 mice and the SAHA-treated SMA-like P10 mice is still significant. Nevertheless, the mean value of the number of motor neurons of the P10 SAHA-treated SMA-like animals was virtually equal to the mean number of motor neurons in P5 heterozygous mice (Figure 51).

Taken together, these findings indicate that SAHA ameliorates the deterioration of motor neurons, but is not able to fully rescue the SMA progression. SAHA treatment is

able to “stabilize” the mean number of motor neurons at the level of P5 old heterozygous mice, and thus can only delay the neuronal impairment observed in SMA-like mice.

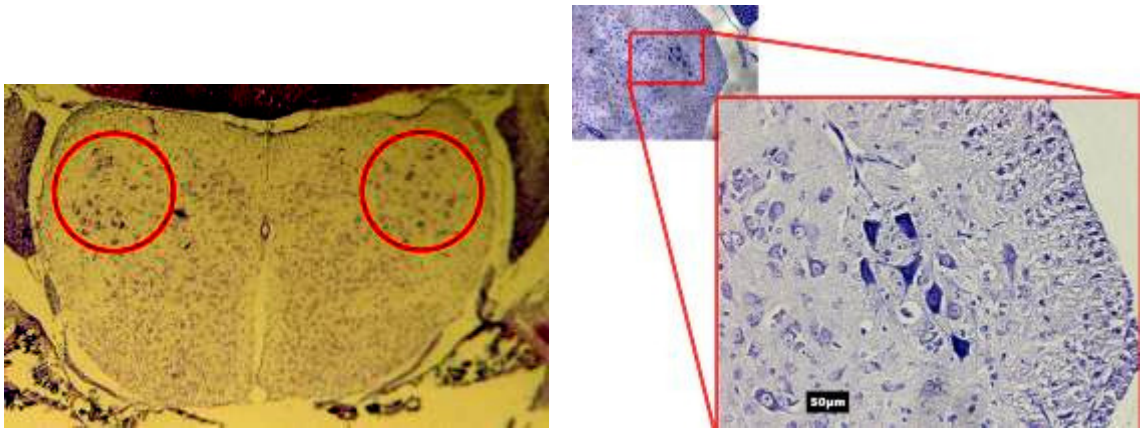

Figure 50 Nissl stainings of cross-sections derived from the lumbar region of spines **a)** overview of a cross-section of the spine of an untreated heterozygous mouse. The red circles highlight the localization of the α-motor neurons in the anterior horns. **b)** depiction of the characteristic shape and size of α-motor neurons in the anterior horns of the spinal cord. Cross-section of an untreated P5 SMA-like mouse.

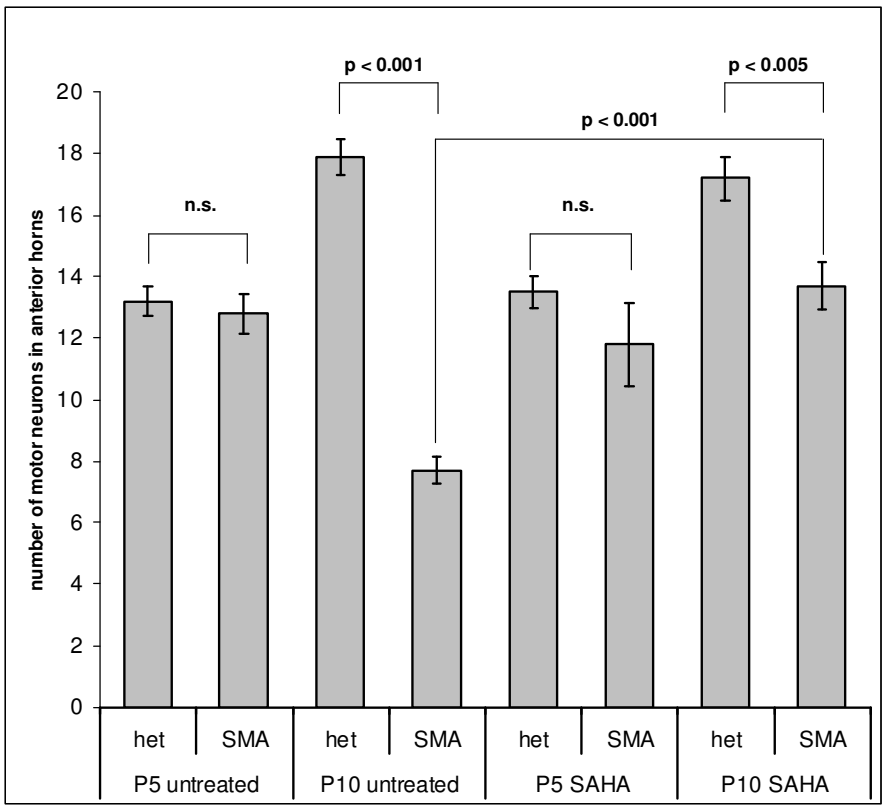

Figure 51 Diagrammatic representation of the α-motor neuron counts of cross-sections derived from P5 SAHA-treated and untreated SMA-like and heterozygous mice as well as P10 SAHA-treated and untreated SMA-like and heterozygous mice. For each age, each treatment status and each genotype n=3. The mean values of 20 cross-sections per animal were used.

- Change in size of motor neuron junctions (NMJs)

The axon terminals of a motor neuron together with the motor end plate of a muscle are called neuromuscular junctions (NMJs) synapses. It has been shown that in SMA-like mice, in which SMN protein levels are severely reduced, the maturation of the NMJs is seriously impaired. Furthermore, it has been proven that the size of the NMJs is severely reduced in murine SMA mouse models (Kariya et al. 2008). Thus, to investigate the effect of SAHA regimen on the size of the NMJs, the area of the NMJs was measured (in μm^2). To do so, 200µm thick longitudinal sections of the *gastrocnemius* muscle were stained with anti-Neurofilament M (green), which labels the neurons and α-Bungarotoxin (labeled with rhodamine: red), which binds to the muscular acetycholine-receptors (AChR). The surface area of each NMJ was measured with the help of *Axio Vision* computer software (*Zeiss*). 100 NMJs were measured in that way for each respective animal: 3 SAHA treated P10 SMA, 3 untreated P10 SMA, 3 SAHA treated P10 heterozygous, and 3 untreated P10 heterozygous animals. Only mice at P10 were chosen, assuming the highest discrepancy between SMA-like and heterozygous mice. This assumption was based on the finding that the motor neuron number is significantly reduced at that respective age (Figure 51).

As expected the mean NMJ-size showed no difference between the heterozygous untreated and heterozygous SAHA-treated mice. The mean surface area sizes ranged between 230 and 240μm^2. However, the untreated SMA-like mice revealed a severely reduced area size of 100μm^2, indicating the progression of SMA. Notably, the SAHA-treated SMA-like mice displayed a significantly higher mean NMJ size of 160μm^2. Nevertheless, SAHA treatment was not capable to fully rescue the NMJ phenotype, since the difference between of the mean NMJ size of the untreated or SAHA-treated heterozygous mice and the SAHA-treated SMA-like mice remained significant (Figure 53).

Taken together, these results suggest that SAHA treatment ameliorates the NMJ-phenotype of SMA-like mice. However, the SAHA regimen is not sufficient to fully protect the NMJ size to be reduced.

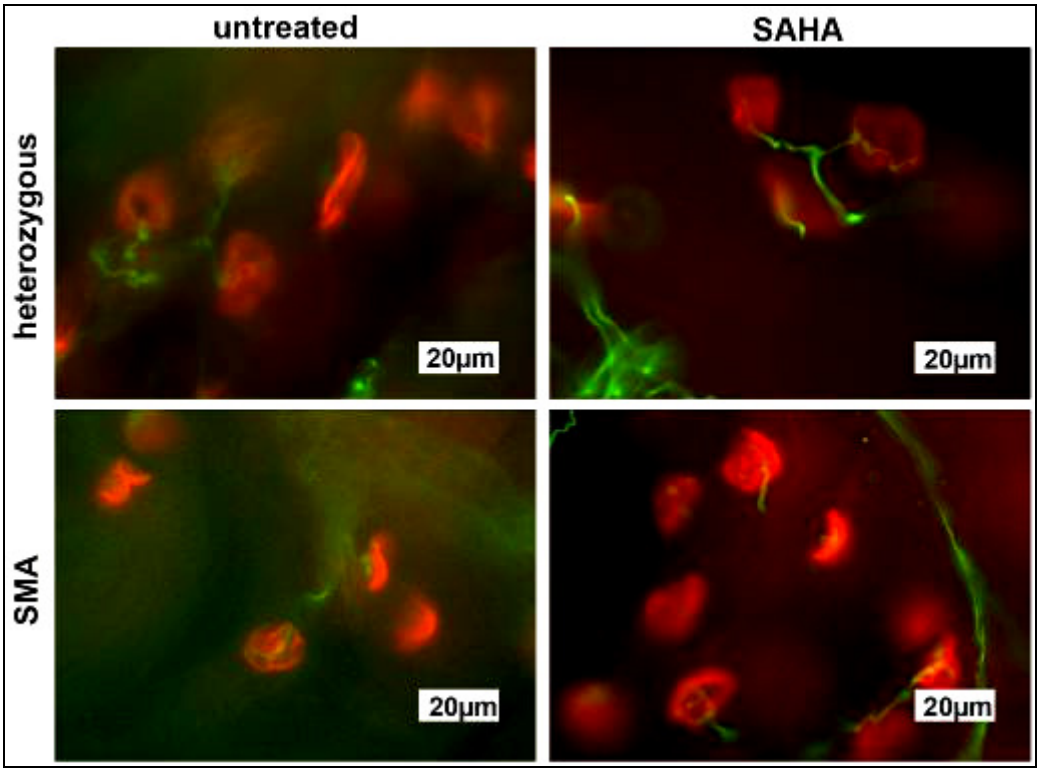

Figure 52 Representative microscopic illustration of the immunofluorescence staining of the NMJs derived from longitudinal sections of the *gastrocnemius* muscle of an untreated heterozygous mouse, a SAHA-treated heterozygous mouse and an untreated SMA-like mouse and a SAHA-treated SMA-like mouse. (red: α-BTX-rhodamine, stains Ach-receptors; green: anti-neurofilament M (labeled with AlexaFlour 488), stains neurofilament M-ptoteins)

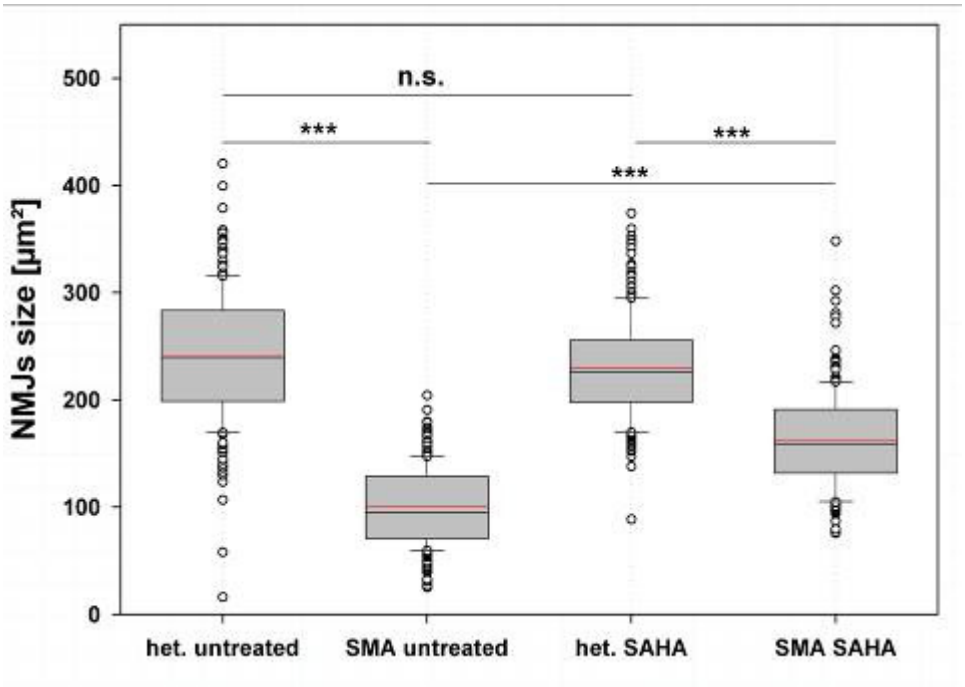

Figure 53 Boxplot of surface area sizes of NMJs measured in longitudinal-sections derived from P10 SAHA-treated and untreated SMA-like and heterozygous mice, For each treatment status and each genotype n=3. 100 NMJs per mouse were measured. (mean value=red line; median value=black line).

- Change in size of muscle fibers

One major hallmark of SMA is - as the name says - the atrophy of the proximal muscles. It has been described that mouse models of SMA show a reduction of the muscle fiber size in the hind limb muscles (Gavrilina et al. 2008a). Since the previously described data from motor ability tests, motor neuron counts and NMJ characterization suggest that SAHA might influence the SMA phenotype also on the muscular level, change in the size of muscle fibers were evaluated. Therefore, cross-sections of the *rectus femoris* muscle were stained with an H&E staining. Like previously described the surface area of each sliced muscle fiber was measured with the help of *Axio Vision* computer software (*Zeiss*). The surface area size of 100 muscle fibers was measured in that way for each respective animal: 3 SAHA treated P10 SMA, 3 untreated P10 SMA, 3 SAHA treated P10 heterozygous, and 3 untreated P10 heterozygous animals. Like for the NMJ-characterization, only mice at P10 were chosen, assuming the highest discrepancy between SMA-like and heterozygous mice. This assumption was based on the finding that motor ability, motor neuron number as well as NMJ surface area sizes were significantly reduced at that respective age (Figure 44, Figure 51 and Figure 53).

Expectedly, the mean surface area sizes of the untreated and the SAHA-treated heterozygous mice showed virtually no difference and was ~280µm² for both. Nevertheless, the untreated SMA-like mice showed a severe reduction in the surface area size down to ~125µm², which resembled the profound progression of SMA. Strikingly, the SAHA-treated SMA-like mice revealed a significantly augmented mean muscle fiber size of ~190µm². Comparable to the already described findings, SAHA treatment was also not able to fully rescue the muscle fiber size phenotype, since the difference between the mean muscle fiber size of the untreated or SAHA-treated heterozygous mice and the SAHA-treated SMA-like mice were still significantly different (Figure 55).

To summarize these results, SAHA treatment ameliorates the muscle fiber size phenotype in SMA-like mice, most likely as a secondary effect, by protecting the α-motor neurons from deterioration. However, as already described for the motor neuron and the NMJ phenotype, the muscle fiber phenotype is not fully rescued by the SAHA regimen, since there was a significant discrepancy between the treated or untreated heterozygous and the SAHA-treated SMA-like mice detectable (Figure 55).

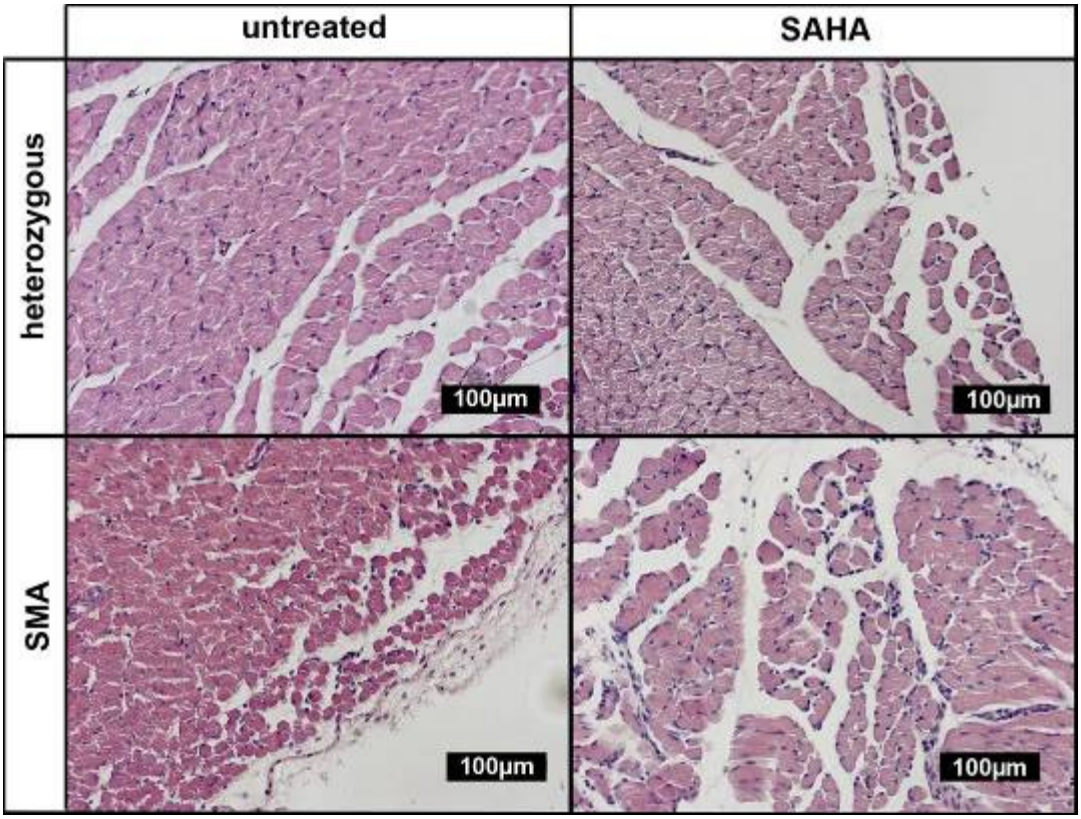

Figure 54 Representative microscopic illustration of the H&E staining of the muscle fibers derived from cross-sections of the *rectus femoris* muscle of an untreated heterozygous mouse, a SAHA-treated heterozygous mouse and an untreated SMA-like mouse and a SAHA-treated SMA-like mouse. The surface area size of the muscle fibers of the untreated SMA-mouse is obviously smaller than the surface area sizes of a SAHA-treated SMA-mouse.

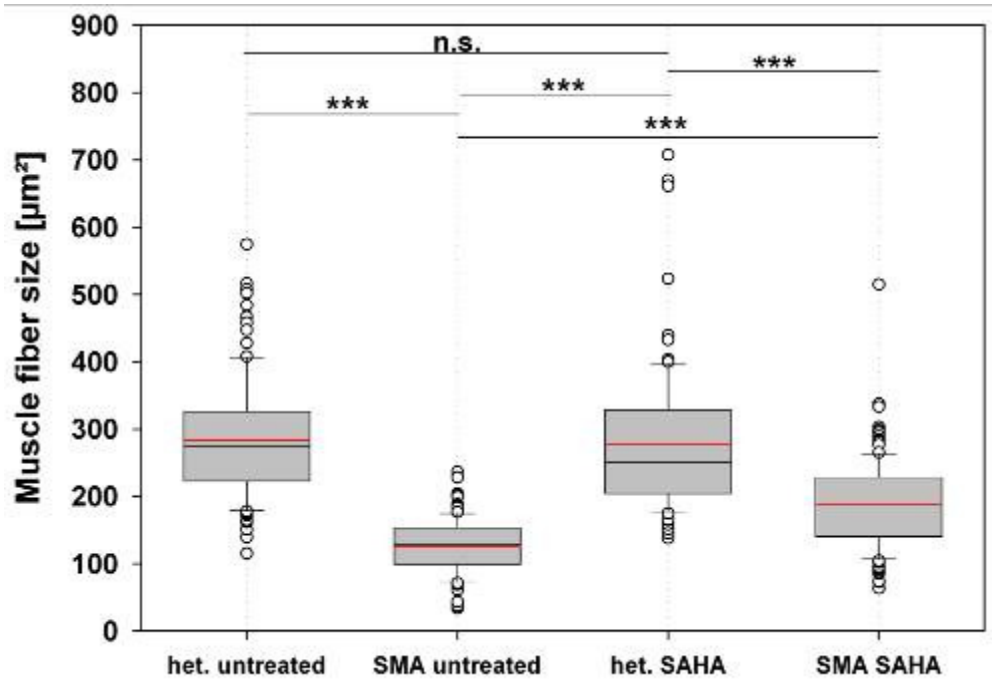

Figure 55 Boxplot of surface area sizes of muscle fiber sizes measured in cross-sections derived from P10 SAHA-treated and untreated SMA-like and heterozygous mice. For each treatment status and each genotype n=3. 100 muscle fibers per mouse were measured. (mean value=red line; median value=black line).

5 Discussion

It has been shown that 96% of all patients with proximal spinal muscular atrophy (SMA) lack the *survival motor neuron gene 1* (*SMN1*), which is either caused by a deletion or a gene conversion of *SMN1* into its almost identical copy gene *SMN2* (Wirth et al. 1999). The loss of the *SMN1* gene causes SMA. A unique feature of SMA is that all patients with this hereditary disease carry at least one copy of the main disease modifying gene, the *SMN2* gene. It has been described that the disease severity inversely correlates with the *SMN2 copy* number (Brahe 2000; Burghes 1997; Feldkotter et al. 2002). However, the *SMN2* is not able to fully compensate the loss of *SMN1* in SMA patients. Because of a silent nucleotide exchange in exon 7 of *SMN2* an exonic splicing enhancer is destroyed (Lorson and Androphy 2000; Lorson et al. 1999) and an exonic splicing silencer is newly created (Kashima and Manley 2003). Thus, the pre-mRNA of *SMN2* is predominantly wrongly spliced. Only ~10% of the *SMN2* transcripts are spliced like the *SMN1* transcripts, producing fully functional full-length *SMN2* mRNA/protein, whereas ~90% of the *SMN2* transcripts lack exon 7 (Gennarelli et al. 1995; Lefebvre et al. 1995; Lorson et al. 1999).

The *SMN2* gene is therefore the main target gene for a potential SMA therapy. The activation of transcription of *SMN2* and the correction of the splicing pattern by *in vitro* or *ex vivo* treatment with histone deacetylase inhibitors, has been described to elevate the SMN protein level (Brichta et al. 2003; Chang et al. 2001; Garbes et al. 2009; Hahnen et al. 2005).

In the present work the epigenetic modification of the *SMN2* gene by means of histone deacetylase inhibitors (HDACi) was performed. Previously, our group could show that the well-known HDACi valproic acid (VPA) is capable to up-regulate SMN expression *in vitro* and *in vivo* in SMA carriers and patients (Brichta et al. 2003; Brichta et al. 2006a). Moreover, the favorable effect of VPA in terms of a potential SMA therapy has recently been proven by *in vivo* findings in an SMA mouse model (Tsai et al. 2008a).

Nevertheless, the search for more potential SMA neurotherapeutics is ongoing, since a recent clinical trial of VPA in SMA patients revealed minimal positive effect on the SMA progression suggesting the need for alternatives to VPA (Swoboda et al. 2009).

Therefore, in this study the search was focused on new HDACi substances from different chemical groups: the benzamide M344 and the bicyclic tetrapeptide depsipeptide (FK228).

5.1 *In vitro* experiments with the pan-HDACis M344 and FK228

The *in vitro* treatment of SMA patient derived fibroblast cell lines revealed that the novel compounds M344 and FK228 have the ability to extensively stimulate the expression of *SMN2*. A massive 3- to 7-fold up-regulation of the SMN protein level was determined at concentrations ranging between 30 and 50 µM M344 after 64 h of treatment; whereas the peptide FK228 was acting in far lower doses on the SMN protein level. Here, FK228 revealed its highest impact (~4-fold) on the SMN protein level at 250 nM. Interestingly, the *SMN2*-activating ability of FK228 was also found in a murine embryonic fibroblast line (MEF14), which was derived from SMA_B-like mouse (*Smn*$^{-/-}$;*SMN2*$^{tg/tg}$). In the MEF14 250 nM of FK228 caused a 4-fold up-regulation of the SMN protein. This finding was of particular interest, since this revealed the first proof that FK228 is able to activate the *SMN2* expression in a heterologous background such as the mouse. Also M344 was shown to act at quite low concentrations like 5 µM, where a 1.5- to 4-fold augmentation of SMN was still measured. While M344 had a significant impact on the elevation of the SMN protein level, FK228 failed to augment the SMN level extensively in ML16. This finding suggests that cell lines differ in their response to diverse HDACis inter-individually. This hypothesis is supported by the previously described findings that the pan-HDACi VPA augmented SMN levels in only one third of the treated SMA patients, whereas one third responded in a decline of the SMN protein level and the last third has been found to be non-responders to VPA regimen (Brichta et al. 2006a). The search for biomarkers concerning a susceptibility to VPA treatment is of particular interest and therefore research subject in our laboratory. However, the weak response of ML16 to the FK228 treatment suggests a similar mode of predisposition for a respective FK228 regimen.

Concordantly, the up-regulation of the SMN protein level under FK228 and M344 treatment resulted in a marked increase of nuclear gems, particularly for M344. These nuclear dot-like structures are widely understood to resemble functioning enrichments of SMN proteins (Liu and Dreyfuss 1996; Liu et al. 1997; Young et al. 2000). Thus, it is of particular interest that both test substances were able to elevate the number of gems. Moreover, it was obvious that the increase in the number of gems strongly correlated with the effect, which was found on SMN protein level. Noteworthy, not only the mean number of gems per 100 nuclei increased, but also the number of cells, which contain gems, was augmented. This indicates a profound up-regulation of gems numbers in virtually every treated fibroblast, suggesting an augmentation of functioning SMN complexes.

Interestingly, although several other HDACis such as sodium butyrate, valproic acid, phenylbutyrate, suberoylanilide hydroxamic acid and LBH589 (Andreassi et al. 2001; Brichta et al. 2003; Chang et al. 2001; Garbes et al. 2009; Hahnen et al. 2006c; Sumner et al. 2003) have in the last years been reported to activate *SMN2,* none of these compounds were members of the chemical groups of benzamides (M344) or tetrapeptides (FK228). The most potent HDACi in terms of elevating the SMN protein level is the hydroxamate LBH589, as shown in our laboratory (Garbes et al. 2009). However, M344 was shown in this work to elevate the SMN protein level ~7-fold, which is the second highest augmentation of SMN by HDACi treatment. The 4-fold increase of SMN after FK228 treatment resembles a similar effect like the treatment with 1 mM VPA (Brichta et al. 2003).

Beside the effect of M344 and FK228 on the SMN protein level, also the effect on the *SMN2* transcript level was investigated. Quantitative analysis of *SMN2* mRNA revealed considerably increased FL-*SMN2* transcript levels. In contrast, Δ7-*SMN2* levels were almost unchanged or even reduced, suggesting an efficient reversion of the splicing pattern of *SMN2* pre-mRNA by M344 and FK228 treatment. The effect on the reversion of the pre-mRNA splicing pattern of FK228 was even higher than the observed effect of M344. Interestingly, the Δ7-*SMN2* transcript level decreased at the highest treatment concentrations of FK228 of 250 and 500 nM to 50% of the mock treated amounts. This indicates a very strong reversion of the splicing pattern. Because of the observed reversion of the *SMN2* pre-mRNA splicing, the expression of the splicing factor SFRS10, which is well known to be capable to revert the *SMN2* splicing (Hofmann et al. 2000), the protein level of this respective factor was investigated. SFRS10 protein levels were indeed elevated under the regimen with M344 as well as with FK228, supporting the hypothesis of splice reversion by SFRS10. The impact of the HDACi treatment was reflected in the reversion of the splicing pattern in virtually all tested cell lines. However, the high levels of FL-*SMN2* RNA and protein can be explained only by additional transcription activation of *SMN2*. Similar to the results obtained for other HDAC inhibitors (Brichta et al. 2003; Brichta et al. 2006a), the effect especially of M344 observed on the SMN protein level is much higher than the effect seen on RNA level.

This is not an unexpected finding, since *SMN* transcript levels are quite uniformly expressed among all tissues whereas the protein level reveals marked differences (Coovert et al. 1997; Lefebvre et al. 1997). Moreover, recent data could proof that the HDACi LBH589 is capable to stabilize the SMN protein by reducing its ubiquitinylation as well as favoring incorporation into the SMN complex (Garbes et al. 2009). A similar mechanism could also be activated by the treatment with M344 and FK228. Both, M344 and FK228 are potent pan-HDAC (Hahnen et al. 2008), therefore it is obvious that these

substances are also changing the expression levels of other genes. In a recent microarray based study it has been described that the unspecific inhibition of virtually all present HDACs alters the transcription of up to 22% of all investigated genes (Peart et al. 2005). Therefore it was not unexpected that M344 was found to up-regulate SRp20, another splicing factor, which is not involved in *SMN2* splicing. Hence, the ability of M344 to stimulate the expression of a number of splicing factors should be considered for further potential therapies of other diseases. Moreover, these data underline the unspecific transcriptional activation by HDAC inhibitors in general and in particular of M344. With regard to a prospective SMA therapy, it is important to mention that severe side effects caused by some HDACis are relatively rare as it is well-known from valproic acid, which is successfully used in epilepsy treatment for more than three decades. In contrast to SFRS10 and SRp20, SF2/ASF expression is subject to fluctuations and not clearly influenced by M344 treatment. This observation differs from the finding of increased SF2/ASF levels found after treatment with valproic acid and demonstrates that diverse HDAC inhibitors act on a varying spectrum of target genes. Moreover, a reduction of cell viability of fibroblasts was detected at high M344 concentrations above 30 µM. In agreement with this observation, SMN2 protein levels decreased at doses of 50 µM (ML12) and 100 µM (ML17 and ML20) M344, respectively. Additionally, significantly increased SMN protein levels with maximum levels ranging between 3- to 6-fold were already determined at low concentrations of 5–30 µM M344, which is below the drug amounts causing increased cell death. Thus, M344 remains highly promising for a future application in an SMA therapy. In contrast to this finding, FK228 revealed a significant cytotoxicity starting from the lowest concentration of 10 nM. Nevertheless, the cytotoxicity found in ML16 was reflected by the weak response of this cell line to the FK228 regimen. Because of the unfavorable toxicity profile of FK228, a further *in vivo* animal trial was neglected.

Since also M344 has never been described to be tested *in vivo,* we also rejected to deepen our research efforts on this particular substance. In contrast, we focused our search for new substances, which might be able to elevate the SMN level, on compounds, which are FDA-approved or at least subjected to clinical trials. Nevertheless, the *in vitro* experiments using FK228 and M344 gave deep insight into the epigenetic regulations of *SMN2* expression. Moreover, it was proven that the HDACi FK228 is able to up-regulate *SMN2* expression in human cells and on a heterologous background such as mouse fibroblasts. For the first time it was shown that substances belonging to the chemical classes of benzamides (M344) and bicyclic tetrapeptides (FK228) are able to elevate SMN levels in SMA fibroblast lines.

5.2 Identification of HDAC8 to be specifically involved in *SMN2* expression regulation

It has been described that the unspecific inhibition of virtually all classic HDACs by the use of pan-HDACis alters the expression of up to 22% of all genes (Peart et al. 2005). In that study the pan-HDACis SAHA and FK228 have been described to regulate unspecifically the expression of about one fourth of all tested transcripts. However, the microarray chip analysis, which has been performed after treating Jurkat cells with the respective substances, revealed that the gene set, which was regulated by both HDACis, was highly overlapping but not identical (Peart et al. 2005). This suggests that different pan-HDACis, although unspecifically targeting all classic HDACs, might have slight differences in their functional outcome. While one HDACi might activate a whole pathway, the other one might down-regulate the activation. Moreover, it has recently been shown that certain HDACs additionally to the epigenetic modifications exhibit important cytoplasmatic functions by controlling the acetylation status and function of numerous cytoplasmatic proteins and transcription factors (Yang and Seto 2008). Therefore, not only the altered transcription but also direct regulation of numerous proteins should be considered when applying HDACis.

With regard to a prospective therapeutic use of HDACis in SMA, it remains quite questionable to apply unspecific HDACis to patients, since numerous unfavorable side effects might emerge. Hence, for the long-term used unspecific HDACi VPA a number of unfavorable side effects have been described (reviewed in (Gerstner et al. 2008)).

To avoid the majority of side effects, which arises by the unspecific up-regulation of genes, an HDACi should be identified, which specifically is able to up-regulate *SMN2* expression. Therefore, the identification of the specific HDAC, which controls the *SMN2* expression, was attempted in this work.

To identify the HDAC, which regulates the *SMN2* expression, a siRNA based knock-down approach was applied. To specifically investigate the *SMN2* protein expression, a *SMN1* deleted SMA fibroblast line was subjected to the knock-down approach. After knocking-down each of the eleven classical HDACs, the SMN protein amount was quantified. Interestingly, the only significant up-regulation of the SMN protein level was observed after the knock-down of HDAC8. This finding was of particular interest, since the literature so far stated that HDAC2 is the main HDAC to regulate *SMN2* expression (Kernochan et al. 2005). However, this respective study proposed HDAC2 to be the *SMN2* regulating enzyme because of the finding that HDAC2 binds to the promoter region of *SMN2* in transgenic murine NSC34 cells. Nevertheless, HDAC2 binding has been observed to be enriched in the close proximity (0 to 500 bp

upstream) to the transcription initiation site of *SMN2,* whereas we found HDAC8 to be most enriched in the *SMN2* promoter regions upstream to the transcription initiation site. This suggests a possible simultaneous action of HDAC8 and HDAC2. Moreover, it has been postulated that HDAC2 binds the murine *Smn* promoter during embryonic development, which is associated with a significant decline in the acetylation status of the histones bound to this respective region (Kernochan et al. 2005). However, the function of HDAC8 has not been investigated in this respective study. Noteworthy, it has been observed in our laboratory (PhD thesis of L. Brichta and (Hahnen et al. 2006b)) that the benzamide MS-275 is not able to up-regulate SMN. Nevertheless, MS-275 is known to inhibit HDAC1, HDAC2 and HDAC3, but not HDAC8 (Witt et al. 2009). Therefore, HDAC8 might be suspected to play an important role in the expression regulation of *SMN2.* To prove the possibility of HDAC8 to be involved in the histone deacetylation in the promoter region of *SMN2*, ChIP experiments were performed. Hence, the ChIP experiment revealed that HDAC8 is obviously bound to the *SMN2* promoter region. This finding indicated that HDAC8 is able to regulate the expression of *SMN2* by histone deacetylation in its promoter region upstream of the transcription initiation site of *SMN2*. To gain a deeper insight into the capability of HDAC8 to regulate the *SMN2* expression, HDAC8 overexpression experiments were applied. Therefore, a plasmid containing the human HDAC8 cDNA was transfected into *SMN1* deleted SMA fibroblast cells. As expected the overexpression of HDAC8 was able to reduce the SMN protein level in a concentration dependent manner. In contrast, the overexpression of HDAC2 and HDAC11 (as negative control) did not reveal any decrease of SMN protein level (appendix Figure 57). The higher the amount of expressed HDAC8 was the lower was the SMN protein level. This correlation suggested a role of HDAC8 in regulating the SMN protein level.

HDAC8 was identified and characterized for the first time in the year 2000 by three independent groups (Buggy et al. 2000; Hu et al. 2000; Van den Wyngaert et al. 2000). It has been described that HDAC8 is able to deacetylate histone H3 and H4 *in vitro* and to repress transcription (Hu et al. 2000). More recently, it has been shown that the specific inhibition of HDAC8 induces apoptosis in T-cell lymphomas (Balasubramanian et al. 2008). In the present year a knock-out mouse model of HDAC8 has been described. Knock-out of HDAC8 in mice led to specific disturbances in the skull morphogenesis (Haberland et al. 2009). Moreover, this study revealed 838 genes to be up-regulated and 928 genes to be down-regulated after HDAC8 knock-out in the mouse at least twofold. However, the expression of the murine *Smn* gene was not affected. This finding might be explained by the fact that SMN is *per se* highly expressed during embryogenesis, or that HDAC8 might not control the expression of the murine *Smn* gene. The main impact of

the HDAC8 knock-out was observed in the neural crest cells, which resemble a subpopulation of cells derived from the ectoderm. Interestingly, the ectoderm forms also the neural tube, which later during embryogenesis develops among others into motor neurons. This might give evidence for speculations about a neuron specific role of HDAC8.

However, if HDAC8 is the main HDAC to be involved in *SMN2* expression regulation, it would be important to find a HDAC8 specific inhibitor for a prospective SMA treatment. Therefore, we focused on the search for a compound, which is capable to specifically inhibit the function of HDAC8. It has recently been shown that the substance PCI-34051 is able to specifically inhibit the function of HDAC8. Moreover, researchers have been able to induce apoptosis in T-cell lymphomas by the specific inhibition of HDAC8 by the hydroxamate PCI-34051 (Balasubramanian et al. 2008).

The murine SMA-like fibroblast line MEF5 ($Smn^{-/-}$;$SMN2^{tg/tg}$) and the human SMA fibroblast line ML17 were treated with PCI-34051 in order to investigate its capability to up-regulate the *SMN2* expression. Interestingly, the human cell line responded in an up-regulation of the protein level to a maximum level of ~185%, whereas the murine reacted only in a not significant increase to only ~120%. This fact might be explainable by the heterologous background of *SMN2.* While in the native situation the promoter region of the human *SMN2* is regulated by the deacetylation of HDAC8, in the artificial situation where the *SMN2* transgene is located in the genetic murine environment, HDAC8 may not regulate the *SMN2* transgene expression. Strikingly, PCI-34051 up-regulates the mean SMN protein for virtually every tested concentration to ~150%, which resembles the elevation of the protein level after the knock-down of HDAC8. Moreover, the specificity of PCI-34051 was proven by an *in vitro* HDAC activity test. The test showed clearly that PCI-34051 was not able to fully inhibit the total function of a HDAC extract from rat liver, whereas the pan-HDACs M344, FK228 and SAHA were able to fully deplete the function (appendix Figure 58). Unexpectedly, the FL-*SMN2* transcript level was not significantly elevated by PCI-34051 treatment in ML17. Moreover, the human cell line revealed no change in Δ7-*SMN2* levels, whereas the murine cell line MEF5 neither displayed an increase in FL- nor in Δ7-*SMN2* levels. Additionally, the protein level of the main splicing factor capable to restore the *SMN2* splicing namely SFRS10 (Hofmann et al. 2000), revealed no elevation under PCI-34051 regimen. This finding might be explained by the fact that the specificity of PCI-34051 prevents the unspecific up-regulation of the splicing factor SFRS10. However, this might explain also the weak effect of PCI-34051 on the FL-*SMN2* as well as the SMN protein level.

The attempt was performed to avoid negative side effects by the specific inhibition of the respective HDAC that regulates *SMN2* expression. However, the specific enzyme

inhibition led to the reduction of "positive side effects" seen in the treatment with unspecific HDACis, such as up-regulation of genes that help to correct the *SMN2* pre-mRNA splicing or, which stabilize the SMN protein. Several pan-HDACis have been shown to possess the "positive side effects" to restore the *SMN2* splicing (Brichta et al. 2003; Hahnen et al. 2006c; Hahnen et al. 2005), to stabilize SMN protein and to protect SMN from degradation (Garbes et al. 2009). Thus, prospective animal trials might help to gain insight into the advantages and disadvantages of a potential therapy by the use of specific or unspecific histone deacetylase inhibitors.

5.2.1 *In vitro* findings with regard to the current state of research

To date several diverse attempts have been undertaken to increase the SMN protein level *in vitro.* Virtually all research groups made use of cell lines derived from SMA patients (overview of *in vitro* drug-attempts to elevate SMN is given in Table 14).

It has been proven that the cell cycle inhibitor hydroxyurea is able to elevate the SMN level ~1.9-fold in lymphoblastoid cell lines from SMA patients. As the underlying mechanism of action transcriptional activation and splicing correction has been proposed (Grzeschik et al. 2005). The antibiotics aclarubicin and diverse aminoglycosides have been assessed in fibroblast cell lines derived from SMA patients. Aclarubicin has been observed to restore the SMN protein level, via splicing correction, to levels comparable to healthy controls (Andreassi et al. 2001). Various aminoglycosides have been shown to augment the number of gems 20-fold by the skipping of the stop codon of *SMN2* (Mattis et al. 2006). Phosphatase inhibitors like Na-vanadate and diverse quinazolines have been shown to elevate the protein level 2- to 3-fold by transcriptional activation (Jarecki et al. 2005). Moreover, Na-vanadate has been observed to correct the splicing and therefore to increase the activity of a specific luciferase reporter assay 6- to 8-fold (Zhang et al. 2001). The transcriptional activation of *SMN2* in SMA fibroblasts by the cytokines interferone β and γ has been shown to restore the SMN protein level to control levels (Baron-Delage et al. 2000). The nonsteroidal anti-inflammatory drug indoprofen has been found to activate the transcription of *SMN2* in SMA fibroblasts and thereby to modestly elevate the SMN level ~1.13-fold (Lunn et al. 2004). Moreover, the inhibition of the proteasomal degradation of SMN by MG-132 in SMA fibroblasts resulted in a 1.5-fold increase of the SMN levels (Chang et al. 2004). Also a 1.5-fold SMN protein elevation has been described for fibroblasts treated with the β_2-adrenergic agonist salbutamol. This increase has been discussed to be accomplished by the transcriptional activation of *SMN2* and by the activation of the cyclic adenosine monophosphate (cAMP) pathway (Angelozzi et al. 2008).

Additionally, several HDACis have been shown to possess capability to up-regulated the SMN protein level in SMA cell lines. Sodium butyrate has been observed to elevate the SMN protein level in lymphoblastoid cell lines from SMA patients by transcriptional activation and splicing correction ~3-fold (Chang et al. 2001). VPA has been proven to augment SMN levels in SMA fibroblasts by transcriptional activation, splicing correction and protein stabilization up to ~4-fold (Brichta et al. 2003). The FDA-approved drug 4-phenylbutyrate has been shown to activate *SMN2* transcription and therefore to augment the SMN protein level ~1.9-fold (Andreassi et al. 2004). Our group could previously show that SAHA and LBH589 are also able to massively increase the SMN level *in vitro* (Garbes et al. 2009; Hahnen et al. 2006c). In SMA fibroblasts it has been proven that SAHA activates the transcription and restores the splicing of *SMN2* and thereby elevates the SMN level ~3-fold (Hahnen et al. 2006c). LBH589 in contrast, has been shown to act on the transcriptional activation, the splicing correction and the protein stabilization of SMN, and therefore to tremendously increase SMN levels up to 10-fold (Garbes et al. 2009).

To compare these previously reported results with the results obtained during this work, it is of high interest that the two tested pan-HDACis M344 and FK228 are able to increase the SMN protein levels in human and murine (FK228) SMA fibroblast lines ~7- and ~4-fold, respectively. Moreover, it was proven that both substances act via transcriptional activation and splicing correction of *SMN2.* Additionally, it can be stated that M344 is second and FK228 is the third most potent substance to increase the SMN protein level. Furthermore, both compounds were found to elevate gem levels in SMA patient cell lines, indicating the production of functional SMN protein. Moreover, for the first time it was shown that an isoenzyme specific HDACi is able to increase the SMN level. Here it was proven that the HDAC8 specific HDACi PCI-34051 is capable to activate the transcription of *SMN2* and thus to increase the SMN protein level up to 1.8-fold.

Table 14 Overview of diverse drugs shown to elevate the SMN protein level *in vitro* in comparison to the results discussed in this thesis (marked in grey). Results are summarized from given publications

Mechanism of action	Compound	Experimental setup (*in vitro*)	Modification of SMN	Maximum SMN protein increase	Original publication
Histone deacetylase inhibition	M344	Fibroblast cell lines from SMA patients	Transcriptional activation, Splicing correction	~7-fold	This thesis, (Riessland et al. 2006)
	FK228	Fibroblast cell lines from SMA patients and mice	Transcriptional activation, Splicing correction	~4-fold	This thesis
Histone deacetylase 8 inhibition (specific)	PCI-34051	Fibroblast cell lines from SMA patients and mice	Transcriptional activation	~1.8-fold	This thesis
Histone deacetylase inhibition	Sodium butyrate	Lymphoblastoid cell lines from SMA patients	Transcriptional activation, Splicing correction	~ 3-fold	(Chang et al. 2001)
	Valproic acid (VPA)	Fibroblast cell lines from SMA patients and motor neurons derived from rat stem cells	Transcriptional activation, Splicing correction, Protein stabilization	~4-fold	(Brichta et al. 2003) (Hahnen et al. 2006c)
	4-Phenylbutyrate	Fibroblast cell lines from SMA patients	Transcriptional activation	~1.9-fold	(Andreassi et al. 2004)
	Suberoylanilide hydroxamic acid (SAHA)	Fibroblast cell lines from SMA patients and rat motor neurons	Transcriptional activation, Splicing correction	~3-fold	(Hahnen et al. 2006c)
	LBH589	Fibroblast cell lines from SMA patients	Transcriptional activation, Splicing correction, Protein stabilization	~10-fold	(Garbes et al. 2009)
Cell cycle inhibitor	Hydroxyurea	Lymphoblastoid cell lines from SMA patients	Transcriptional activation, Splicing correction	~1.9-fold	(Grzeschik et al. 2005)
Antibiotics	Aclarubicin	Fibroblast cell lines from SMA patients	Splicing correction	restoration to control levels (healthy individuals)	(Andreassi et al. 2001)
	Aminoglycosides	Fibroblast cell lines from SMA patients	Skipping of stop codon	~20-fold elevation in number of gems	(Mattis et al. 2006)
Phosphatase inhibitor	Na-vanadate	fibroblast cell lines from SMA patients, NSC34 motor neuron like cells containing anSMN-Luciferase-modified construct	Splicing correction	6-8-fold increase in Luciferase reporter activity	(Zhang et al. 2001)
	Quinazolines	fibroblast cell lines from SMA patients, NSC34 motor neuron like cells containing anSMN-Luciferase-modified construct	Transcriptional activation	2-3-fold	(Jarecki et al. 2005)
Cytokine	IFN-β and IFN-γ	Fibroblast cell lines from SMA patients	Transcriptional activation	restoration to control levels ~4-fold induction of transcription	(Baron-Delage et al. 2000)
Nonsteroidal anti-inflammatory drug	Indoprofen	Fibroblast cell lines from SMA patients	Transcriptional activation	1.13-fold	(Lunn et al. 2004)
Proteasome inhibitor	MG-132	Fibroblast cell lines from SMA patients	inhibition of proteasomal degradation	1.5-fold	(Chang et al. 2004)
β2-adrenergic agonist	Salbutamol	Fibroblast cell lines from SMA patients	Transcriptional activation, cAMP pathway activation	1.5-fold	(Angelozzi et al. 2008)

5.3 *In vivo* characterization of SAHA treatment in mouse models for SMA

It has been widely described that the deterioration of the α-motor neurons in the anterior horns of the spinal cord leads to a progressive muscle weakness and following atrophy (Zerres and Rudnik-Schoneborn 1995). Nonetheless, in the past years a debate has been ongoing, whether either the motor neurons or the muscles are the primary affected tissue. Finally, the attempt to rescue the severe SMA phenotype in a *Smn*$^{-/-}$;*SMN2*$^{tg/tg}$ (SMA_B) mouse model, by overexpressing *SMN1* muscle- or neuron-specific, has shown that the onset of SMA can be hindered by neuron specific *SMN1* expression (Gavrilina et al. 2008b). This was the final proof that the main target cells for a potential SMA therapy are the α-motor neurons. However, so far the common way to test the efficiency of new compounds to up-regulate the *SMN2* expression is to administer the respective substances in cell culture to SMA fibroblasts or SMA patient derived lymphoid cell lines (Brichta et al. 2003; Chang et al. 2001). This way of *in vitro* testing may not be the method of choice, since very recent studies have been proven that the HDACi VPA is not able to elevate SMN protein levels in *Smn*$^{-/-}$;*SMN2*$^{tg/tg}$ murine fibroblast lines, whereas the same substance elevates the SMN level in neural precursor cells (NSCs) of the identical genotype (Hauke et al. 2009; Rak et al. 2009). This indicates that the up-regulation of SMN expression could most likely differ between cell types. Although the SMA-like murine fibroblast lines showed no up-regulation under VPA regimen, a recent study has proven that VPA is able to ameliorate the SMA phenotype in type III-like SMA mice. In this respective study it has been shown that VPA treated mice show better motor function, less degeneration of spinal motor neurons, less muscle atrophy and better neuromuscular junction innervations than non-treated SMA-like animals (Tsai et al. 2008b). Moreover, the study has displayed an up-regulation of the SMN protein level in the spinal cord of VPA-treated SMA-like mice.

In order to test whether the *in vitro* influence of suberoylanilide hydroxamic acid (SAHA) can be confirmed also *in vivo*, SAHA was tested in SMA-like mice. Since we have been able to show earlier that SAHA, a pan-HDACi (Hahnen et al. 2008), is able to elevate SMN levels *in vitro* in SMA patient derived cells and *ex vivo* using cultured hippocampal brain slices derived from rat and human (Hahnen et al. 2006a). In view of a prospective SMA therapy in humans it was also of essential importance that SAHA was recently approved (in 2006) by the U.S. Food and Drug Administration (FDA) for the treatment of cutaneous T cell lymphoma (CTCL) (www.merck.com/finance /annualreport/ar2006/pipeline.html). Therefore, this substance would be feasible to directly apply to SMA patients. Additionally, it has been shown that SAHA crosses the

blood-brain barrier and that the oral therapy with SAHA in a mouse model of Huntington's disease ameliorates motor deficits of the animals (Hockly et al. 2003).

A type I SMA_B mouse model was chosen to apply an *in vivo* study of SAHA treatment. The respective mouse model has been reported to live for a mean survival time of ~5 days (Monani et al. 2000). This relatively short survival time was a favourable feature of the mouse model, since the major outcome measurement of the SAHA animal trial was survival time. However, the transgenic mice, which were characterized in the original publication, were on a C57BL/6J background. The SMA_B mouse model we obtained from Prof. Dr. M. Sendtner was in contrast on a FVB/N background. A high impact of the inbred strain background on the SMA-phenotype was detected, since no living SMA-like animals were born. It is well-known that the inbred strain background has a high impact on the phenotype of transgenic or knock-out animals. A recent example for this characteristic is the HDAC8 knock-out mouse model. These animals were viable on a mixed background (SV129/C57BL/6/CD1), whereas on a pure C57BL/6 background they showed 100% prenatal lethality (Haberland et al. 2009). Additionally, several studies have been shown that strain related differences have led to estimates that 1-2% of the genes may vary in expression between the six brain regions, which were investigated in the particular projects of C57BL/6 and 129SvEv mice (Pavlidis and Noble 2001; Sandberg et al. 2000). These findings underline the differences in gene expression in neuronal tissues of different mouse strains, which might lead to variable SMA phenotypes in the respective mouse models. Moreover, it has been published that the C57BL/6 background ameliorates the SMA-phenotype in SMA_H mice. In this case it has been stated that the mice on pure C57BL/6J background live for 13±2 months (Tsai et al. 2008b), while the survival on FVB/N background was only 9.9 days (own observations).

However, the oral SAHA treatment of the pregnant mothers of severely affected SMA_B-mice, starting at gestational day 15, resulted in an elevation of living born SMA-like animals. This reflected the capacity of SAHA to ameliorate the severe SMA phenotype *in utero*. However, only an amelioration of the SMA phenotype was observed, since all animals died soon after birth. With regard to a potential SMA therapy the treatment of a pregnant mother with HDAC inhibitors had to be performed very carefully, since it is well known that these substances, like VPA, are severely teratogenic in human in the first trimester of pregnancy (Alsdorf and Wyszynski 2005; Kultima et al. 2004; Wyszynski et al. 2005). To avoid the maternal treatment and to assess the outcome of SAHA regimen on the motor ability of the SMA-like mice, another SMA mouse model was applied. The used SMA_H mouse model carries in contrast to the SMA_B mouse model 2 *SMN2* transgenes (concatemers) per transgene integrate, whereas the SMA_B mouse model carries only one per integrate. First, the SMA_H mouse model, which was also on a

FVB/N background, had to be comprehensively characterized in our mouse facility. It was proven that heterozygous transgenic mice on a null *Smn* background (*Smn*$^{-/-}$;*SMN2*$^{tg/wt}$) develop a severe SMA phenotype and show a mean survival of ~9.9 days. Contrary to the homozygous transgenic SMA_B mice on a null *Smn* background, the homozygous transgenic SMA_H mice on a null *Smn* background (*Smn*$^{-/-}$;*SMN2*$^{tg/tg}$) were viable and fertile, but display necrosis of the tail and the ears later in life. Therefore, one major advantage of the SMA_H mouse model is that the breeding of one homozygous transgenic SMA_H mouse on a null *Smn* background (*Smn*$^{-/-}$;*SMN2*$^{tg/tg}$) with one homozygous knock-out SMA_H mouse (*Smn*$^{+/-}$;*SMN2*$^{wt/wt}$) gives rise to 50% SMA-like animals (*Smn*$^{-/-}$;*SMN2*$^{tg/wt}$). Whereas in the case of SMA_B mice, the breeding of two *Smn*$^{+/-}$;*SMN2*$^{tg/tg}$ mice results in only 25% SMA-like (*Smn*$^{-/-}$;*SMN2*$^{tg/tg}$) mice in each litter. This high percentage of offspring developing a SMA-like phenotype accelerated the *in vivo* treatment approaches. Moreover, the SMA-like mice revealed a progressing SMA, which was reflected by the deterioration of α-motor neurons in the anterior horns of the spinal cord and by the progressive decline of motor ability compared to healthy littermates. These advantageous features, which were firstly characterized in this work, make the SMA_H mouse model the best SMA mouse model for the *in vitro* characterization of potential SMA drugs. This opinion is substantiated by the following comparison of the commonly used SMA mouse models.

The phenotypic appearance of the so far described mouse models for SMA is quite diverse. It has been shown that the introduction of a mutated *SMN* transgene (*SMN*^{A111G}) leads to the complete rescue of the SMA phenotype. *Smn*$^{-/-}$;*SMN2*$^{tg/tg}$;*SMN*$^{A111Gtg/wt}$-mice have a normal life expectancy and show no symptoms of SMA (Workman et al. 2009). Another *SMN* missense mutation (*SMN*^{A2G}) has been proven to lessen the SMA phenotype. *Smn*$^{-/-}$;*SMN2*$^{tg/tg}$;*SMN*$^{A2Gtg/wt}$-mice live for ~15 months and display first of SMA after ~3.5 month of life (Monani et al. 2003). A SMA mouse model, which is frequently used for *in vivo* drug testing, is the *Smn*$^{-/-}$;*SMN2*$^{tg/tg}$;*SMNΔ7*$^{tg/tg}$ mouse. These animals have been shown to present first symptoms of SMA after ~9 days of life and die at the age of ~14 days. These SMA type I-like mice are on FVB/N background and carry homozygously the *SMN2* and the *SMNΔ7* (the cDNA of *SMNΔ7*) transgene on a null *Smn* background (Le et al. 2005). These animals are well suitable for drug testing but have two disadvantages: 1. The *SMNΔ7* transgene is artificial and does not reflect the natural situation in SMA patients, 2. Due to the fact that *Smn*$^{-/-}$;*SMN2*$^{tg/tg}$;*SMNΔ7*$^{tg/tg}$ mice die at the age of ~14 days, it is necessary to breed *Smn*$^{-/+}$;*SMN2*$^{tg/tg}$;*SMNΔ7*$^{tg/tg}$ animals, which results in only 25% of SMA-like mice per litter.

Interestingly, in this study it was proven that the inbred strain background has a major influence on the SMA phenotype of SMA-like mice. *Smn*$^{-/-}$;*SMN2*$^{tg/tg}$ (SMA_B) on

100% C57BL/6 background have been described to live for ~5 days and display first symptoms of SMA at ~2-3 days of life (Monani et al. 2000). However, in this work it was observed that the animals with exactly the same genotype on 100% FVB/N background are prenatally lethal. Moreover, it has been published that (SMA_H) SMA-like mice on 100% C57BL/6 background display a mild form of SMA (type III) and live for ~13 month. We could prove that SMA-like mice carrying the same genotype but on 100% FVB/N background display a SMA type I-like phenotype, show first symptoms at P5 and die at the age of 9.9 days. Since *Smn*$^{-/-}$;*SMN2*$^{tg/tg}$ (SMA_H) mice are fertile and live longer than ~1.5 year, it is possible to breed them with *Smn*$^{-/+}$;*SMN2*$^{wt/wt}$ mice and thus to produce 50% SMA-like mice (*Smn*$^{-/-}$;*SMN2*$^{tg/wt}$) per litter. This feature makes the SMA_H –like mice the best SMA mouse model for drug screenings.

Table 15 Overview of commonly used SMA mouse models. The two mouse models, which were used and characterized in this thesis, are marked in grey.

Genotype	*SMN2* copies per integrate	SMA type	Inbred stain background	Mean survival	Age of onset of SMA	SMA-like animals per litter	First characterization of phenotype
Smn-/-;SMN2tg/wt (SMA_B)	1	I	FVB/N	Prenatal lethality		25%	This thesis
Smn-/-;SMN2tg/wt (SMA_H)	2	I	FVB/N	~9.9 days	~5 days	50%	This thesis, and (Hsieh-Li et al. 2000)
Smn-/-;SMN2tg/wt (SMA_H)	2	I, II, III	FVB/N	Heterogeneous	Heterogeneous	50%	(Hsieh-Li et al. 2000)
Smn-/-;SMN2tg/wt (SMA_H)	2	III	C57BL/6	13±2 months	6 months	50%	(Tsai et al. 2008b)
Smn-/-;SMN2tg/tg (SMA_B)	1	I	C57BL/6	~5 days	~2-3 days	25%	(Monani et al. 2000)
	8 *SMN2* copies	No SMA	C57BL/6	Complete rescue of the phenotype		25%	
Smn-/-;*SMN2*tg/tg; *SMNΔ*7tg/tg	1	I	FVB/N	~14 days	~9 days	25%	(Le et al. 2005)
*Smn-/-;SMN2tg/tg; SMN*A2Gtg/wt	1	III	FVB/N	~15 months	~3.5 months	25%	(Monani et al. 2003)
*Smn-/-;SMN2tg/tg; SMN*A111Gtg/wt or *Smn-/-;SMN2tg/wt; SMN*A111Gtg/wt	1	No SMA	FVB/N	Complete rescue of the phenotype		25%	(Workman et al. 2009)

After finding the right SAHA treatment concentration and application method - such as the oral application of 25 mg/kg SAHA twice daily - the SAHA regimen revealed a significant amelioration of SMA progression. The SAHA regimen significantly prolonged the mean survival time of the SMA-like mice by more than 30%. Interestingly, ~10% of the treated SMA-like mice lived longer than the longest surviving untreated SMA mouse. However, some of the SAHA-treated mice died within the first days of life. On the one hand these mice might have died due to severe side effects of SAHA, since also ~10% of the heterozygous, healthy littermates died under SAHA regimen. On the other hand these findings might indicate that some mice respond beneficial to SAHA, whereas

others might be non-responders. Similar observations have been described for the VPA treatment in SMA patients. In that case only one third of the treated individuals reacted with an up-regulation of the SMN protein level in blood, one third revealed no reaction, and one third even displayed a down-regulation of the SMN level (Brichta et al. 2006a). The reason for the difference in response to VPA is so far unknown, but currently under investigation in our laboratory. A similar difference in responders and non-responders might explain the heterogeneity of the life prolonging effect of SAHA. However, even in the SAHA responders, SAHA treatment was not capable to restore the lifespan to normal.

It is obvious that SAHA treatment was not able to restore the normal development, since the weight of the treated SMA-like mice correlated stronger with the weight of the untreated SMA-like mice than with the normal weight gaining healthy littermates. The treated SMA-like mice showed a stagnation of weight improvement starting around day P10. This resulted in a dwarf-like appearance of the long-surviving SMA-like mice. Moreover, some of the long-surviving SAHA-treated SMA-like mice showed a severe necrosis of the hind limbs. Remarkably, onset of necrosis was only observed for the treated SMA mice, which survived for 20 days or longer. Importantly, the necrosis is not an effect of SAHA, but rather a characteristic of progressive SMA as previously reported (Araujo Ade et al. 2009). Untreated SMA-like mice did not develop necrosis, since they have a severely reduced life-expectancy. The motor abilities were significantly improved under the SAHA regimen. The applied motor function test (tube test (El-Khodor et al. 2008)) revealed that the SAHA-treated SMA-like mice have a significantly better motor function than the untreated SMA-like mice. The motor function of the treated SMA-like mice developed comparable to the healthy littermates, but declined at later stages, resembling the progression of SMA in some of the animals. Nevertheless, the untreated SMA-like mice never reached the level of motor ability of heterozygous animals. The decline of motor function started earlier in life and therefore reflects the severe progression of SMA. Also the motor function deficits of the SMA-like mice were ameliorated but not restored by the SAHA regimen.

It was detected that SAHA stimulated the *SMN2* transcript expression in virtually all tested organs, such as brain, liver, spinal cord and muscle. Interestingly, both splice variants FL-*SMN2* and Δ7-*SMN2* were up-regulated by SAHA. This indicates that Sfs10, the main splicing factor known to be able to correct the *SMN2* pre-mRNA splicing (Hofmann et al. 2000), which was also up-regulated in some tested tissues, does not significantly influence the *SMN2* splicing in these mice. The *SMN2* transcript levels appeared far higher up-regulated (especially in the muscle tissue) in the P10 than in the P5 mice, regardless of their respective genotypes. This might be explained by a long-

term effect of SAHA treatment. Additionally, the SMN protein level was also significantly augmented under SAHA treatment in virtually all tissues derived from SMA-like mice but never reached the SMN protein level found in heterozygous mice. Of particular importance was the finding that SAHA increased the SMN level also in neuronal tissues, underlining its ability to cross the blood-brain barrier. This would be essential for a prospective SMA drug.

Furthermore, histological examinations revealed that the SAHA regimen reduces the loss of spinal motor neurons, improves the size of neuromuscular junctions and most likely as a secondary effect is able to increase the surface area size of cross sections of muscle fibers. All histological improvements of the phenotype resembled an amelioration of the SMA progression, but also revealed that SAHA treatment is not able to restore the phenotypic appearance of the investigated healthy littermates. This finding holds true for every investigated feature of the SMA-like animals: lifespan, weight progression, motor ability, SMN expression, degeneration of motor neurons, size of neuromuscular junctions, and size of muscle fibers. The SMA effect in each of these features was ameliorated by SAHA treatment, but the appearance of the healthy heterozygous animals was never reached. The lack of potency of SAHA to fully rescue the SMA-like phenotype is explainable by its relatively short half-life time. SAHA has been described to have a half-life time in humans of ~2 h, whereas in mice ~45 min (Duvic et al. 2007; Venkatesh et al. 2007). However, higher dosages of SAHA were not tolerated by the mice. Nevertheless, the very clear favorable function of SAHA might be realized not only by the activation of *SMN2* but by an additional neuroprotective property of SAHA. It has previously been described that SAHA possesses neuroprotective efficacy (Hockly et al. 2003).

So far, several *in vivo* approaches have been performed in order to ameliorate the SMA phenotype in a mouse model for SMA (overview in Table 16). The attempts to prolong the survival of SMA-like mice are quite versatile.

Three independent studies have been focused on the SMA-like mice treatment with different HDACis, namely the pan-HDACis sodium butyrate (NaBu), trichostatin A (TSA) and valproic acid (VPA). NaBu treatment has been shown to prolong survival (+39%) and to ameliorate muscular atrophy of tails. Treatment of mothers has been shown to overcome embryonic lethality (Chang et al. 2001). TSA has been found to increase the SMN level 2-fold and to attenuate weight loss. Additionally, TSA elevated the myofiber size and number and anterior horn cell size. TSA-treated mice showed better motor behavior and a 19% increased survival (Avila et al. 2007). A more recent study revealed that the TSA treatment plus nutritional support extended median survival of spinal muscular atrophy mice by 170%. Treated mice have been observed to continue

to gain weight, maintain stable motor function, and retain intact neuromuscular junctions long after TSA was discontinued. These findings are of particular interest, since feeding problems are known for SMA patients as well as SMA-like mice, to worsen the SMA phenotype (Narver et al. 2008a). VPA-treated SMA type III-like mice revealed better motor function, larger motor-evoked potentials, less degeneration of spinal motor neurons, less muscle atrophy and better neuromuscular junction innervation (Tsai et al. 2008b). VPA has been shown to elevate SMN levels ~1.4-fold in spinal cord. Since the chosen mice showed a very mild form of SMA, the impact of VPA treatment on the survival was not determined.

Two attempts to force the read-through of the premature stop-codon in Δ7-*SMN2* mRNA and therefore facilitate the production of a more stable protein (by the addition of 5 amino acids) have been performed. Geneticin (G418) has been shown to improve motor function and up-regulate SMN ~3-fold. Nevertheless, an increase in survival has not been observed (Heier and DiDonato 2009a). The experimental compound TC007 has been shown to increase survival by 30%, increase the number of ventral horn cells and improve motor function (Mattis et al. 2009b).

It has been proven that treatment of pregnant mothers of very severely affected SMA-like mice with the nonsteroidal anti-inflammatory drug indoprofen, overcomes embryonic lethality. This finding has been explained by the observation that indoprofen up-regulates the transcription of *SMN2* (Lunn et al. 2004).

During the annual meeting of the "*Families of SMA*" preliminary data have been presented regarding the treatment of SMA-like mice with the phosphatase inhibitor quinazoline D157495. This substance has been shown to increase the survival to 400%.

Two studies have been concentrating on the idea to correct the splicing of *SMN2* pre-mRNA by the use of antisense oligonucleotides (ASOs). In one study one ASO has been used, which was able to bind with one side specifically to the *SMN2* sequence (in intron 6) and was able to recruit SFRS10 to the other side. Therefore, SFRS10 has been shown to restore the SMN2 splicing. This ASO was directly injected into the central nervous system (CNS) of SMA-like mice. The treated mice showed an increased weight gain and a 2-fold elevated SMN level (Baughan et al. 2009b). Another study made use of a steric block ASO. Here it has been shown that this ASO did not recruit a splicing factor, but rather blocked an intronic suppressor element (Williams et al. 2009a). After injecting the respective ASOs directly into the CNS, the SMA-like mice revealed an increase in weight gain and a partial correction of motor deficits (righting reflex).

The previously discussed *in vivo* approaches to ameliorate the SMA phenotype in mice were all based on the possibility to positively influence the *SMN2* gene, either by transcriptional activation, or by splicing correction, or by forcing a read-through of the

premature stop-codon. However, several attempts were performed to treat SMA-like mice without targeting the *SMN2* transgene. These *SMN2* independent approaches are discussed in the following.

The delivery of recombinant follistatin, which is a natural antagonist of myostatin and known to increase skeletal muscle mass, has been shown to lessen the disease severity in a SMA-like mouse. The treated SMA-like mice revealed an increased muscle mass, increase in number of ventral horn cells, a 30% longer survival and motor function improvement, whereas the SMN level remained unchanged (Rose et al. 2009a)

By the use of lentiviral gene transfer, researchers have been succeeded to introduce a human *SMN1* gene copy into the motor neurons of SMA-like mice. The respective animals revealed an increase in weight gain and motor neuron survival. Additionally, the SMN expression has been shown to be restored to normal in the motor neurons. Treated SMA-like mice were observed to live 20% to 38% longer (Azzouz et al. 2004).

A recent study has proven that the intrathecal introduction of neuronal stem cells into SMA-like mice increased motor neuron survival and weight gain, improved the muscular phenotype and the motor function. Additionally, the treated mice were shown to live ~40% longer and the stem cell introduction has been proven to act neuroprotectively (Corti et al. 2008).

Moreover, it has been observed that the transplantation of wild-typic bone marrow into a SMA mouse model (*HSA-Cre; Smn*$^{fl7/fl7}$ (Muscle specific *Smn* exon 7 KO)) was able to improve the myopathic phenotype (muscular regeneration) and the motor performance (+85%) (Salah-Mohellibi et al. 2006). However, no increase in the SMN expression was observed.

Interestingly, researchers have found out that regular physical exercises increase the mean survival by 57.3%. Moreover, it has been shown that trained mice revealed increased motor neuron survival, *SMN2* splicing correction, improvement in muscular phenotype and a certain neuroprotection (Grondard et al. 2005).

To compare these findings with the present study, it is noteworthy that SAHA treatment resulted in the fourth highest increase of survival, which was ever observed by the treatment with a chemical compound. Moreover, the SAHA-treated SMA-like mice revealed increased muscle mass, increase in number of motor neurons, motor function improvement and bigger neuromuscular junction size. Additionally, the SAHA treatment of mothers is able to overcome embryonic lethality. SAHA regimen resulted in a profound increase of SMN levels in all tested tissues except the liver. The ~17-fold increase of the SMN amount in the muscle was the highest ever observed. Strikingly, this compound

was shown to ameliorate the SMA phenotype in two different mouse models for SMA, highlighting its potency.

To summarize these results, SAHA was proven to ameliorate the SMA progression in two different SMA mouse models. However, SAHA treatment was not capable to protect against the onset of SMA. For future *in vivo* approaches for a SMA therapy it would be necessary, to identify substances, which are well tolerated by the test animals and moreover have a longer half-life time than SAHA in order to reduce the number of disturbing applications of the test substance. Importantly, SAHA turned out to efficiently ameliorate the SMA phenotype in type I-like SMA mouse models. Since SAHA is a FDA-approved drug, it is worth to be examined in clinical trials with SMA patients. These findings are of particular interest, since recent studies revealed only modest beneficial improvement in SMA patients, which were treated with valproic acid (Swoboda et al. 2009). SAHA is therefore the only alternative FDA-approved HDACi, which was shown to ameliorate the SMA phenotype in SMA-like mice. Moreover, SAHA is the only FDA-approved second generation HDACi shown to significantly increase the mean lifespan of SMA-like animals.

Table 16 Overview of *in vivo* approaches to ameliorate the SMA phenotype of diverse SMA mouse models in comparison to the results discussed in this thesis (marked in grey). Results are summarized from the given publications.

Mechanism of action	Compound	SMA mouse model	Increase in mean survival	Effect on SMA progression	SMN protein increase	Original publication
Histone deacetylase inhibition (activation of *SMN2* transcription and/or splicing)	Suberoylanilide hydroxamic acid (SAHA)	SMA_H (*Smn*-/-;*SMN2*tg/tg) (on FVB/N) SMA_B (*Smn*-/-;*SMN2*tg/wt) (on FVB/N)	30% Treatment of mothers overcomes embryonic lethality	Increased muscle mass, increase in number of ventral horn cells, motor function improvement, treatment of mothers overcomes embryonic lethality, bigger neuromuscular junction size	~17-fold in muscle ~2-5-fold mean increase	This thesis
Histone deacetylase inhibition (activation of *SMN2* transcription and/or splicing)	Sodium butyrate (NaBu)	SMA_H (*Smn*-/-;*SMN2*tg/wt) (on FVB/N)	39%	Treatment of mothers overcomes embryonic lethality, muscular atrophy of tails is ameliorated	Slightly increased (not quantified)	(Chang et al. 2001)
	Valproic acid (VPA)	SMA_H (*Smn*-/-;*SMN2*tg/wt) (on C57BL/6)	Not determined	better motor function, larger motor-evoked potentials, less degeneration of spinal motor neurons, less muscle atrophy, and better neuromuscular junction innervation	~1.4-fold	(Tsai et al. 2008b)
	Trichostatin A (TSA)	*Smn*-/-;*SMN2*tg/tg;SMNΔ7tg/tg	19%	Increased myofiber size and number, better motor behavior, attenuated weight loss, increased anterior horn cell size	1.5-2-fold	(Avila et al. 2007)
	Trichostatin A (TSA) plus nutrition	*Smn*-/-;*SMN2*tg/tg;SMNΔ7tg/tg	170%	Increased myofiber size, weight gain, maintained stable motor function, retained intact neuromuscular junctions, long-lived mice show necrosis	Not determined	(Narver et al. 2008a)
Read-through of stop codon	TC007	*Smn*-/-;*SMN2*tg/tg;SMNΔ7tg/tg	~30%	Increase in number of ventral horn cells, motor function improvement	~2-4-fold	(Mattis et al. 2009a)
	Geneticin (G418)	*Smn*-/-;*SMN2*tg/tg;SMNΔ7tg/tg	No increase (due to toxicity)	Motor function improvement	~3-fold	(Heier and DiDonato 2009b)
Nonsteroidal anti-inflammatory drug (Transcriptional activation)	Indoprofen	SMA_B (*Smn*-/-;*SMN2*tg/wt) (on C57BL/6/FVB/N)	Treatment of mothers overcomes embryonic lethality		Not determined	(Lunn et al. 2004)
Phosphatase Inhibitor (Transcriptional activation)	Quinazoline (D157495)	Humanized SMA mouse (B2-strain, (AGG-TTT)) (not published)	400%	Motor function improvement (not published)	(not published)	(DiDonato et al. 2009, FSMA meeting)
Oligonucleotides (splicing correction)	Bifunctional RNA (high affinity to SFRS10)	*Smn*-/-;*SMN2*tg/tg;SMNΔ7tg/tg, SMA_H (*Smn*-/-;*SMN2*tg/wt) (on C57BL/6)	"trend towards increased life expectancy"	Increase in weight gain	~2-fold	(Baughan et al. 2009a)
	Steric block antisense oligonucleotide	*Smn*-/-;*SMN2*tg/tg;SMNΔ7tg/tg	Not determined	Increase in weight gain, partial correction of motor deficits (righting reflex)	~2-3-fold	(Williams et al. 2009b)
Induction of muscle growth	Recombinant follistatin	*Smn*-/-;*SMN2*tg/tg;SMNΔ7tg/tg	30%	Increased muscle mass, increase in number of ventral horn cells, motor function improvement	unchanged	(Rose et al. 2009b)

Lentiviral gene transfer	Lentivector expressing human SMN	*Smn*-/-;*SMN2*tg/tg;SMNΔ7tg/tg	20% to 38%	Increase in weight gain, increased motor neuron survival	Restoration in motor neurons	(Azzouz et al. 2004)
Stem cell therapy	Neuronal stem cells	*Smn*-/-;*SMN2*tg/tg;SMNΔ7tg/tg	~40%	Increased motor neuron survival, improvement in muscular phenotype, neuroprotection, motor function improvement, Increase in weight gain	~2-fold	(Corti et al. 2008)
Transplantation	Bone marrow transplantation (wt)	*HSA-Cre; Smnfl7/fl7* (Muscle specific *Smn* KO)	Not determined	Improvement of myopathic phenotype (muscular regeneration), improvement of motor performance (+85%)	Not determined	(Salah-Mohellibi et al. 2006)
Physical training	Exercises (running)	SMA_H (*Smn*-/-;*SMN2*tg/tg) (on FVB/N)	57.3%	Increased motor neuron survival, splicing correction, improvement in muscular phenotype, neuroprotection	Not determined	(Grondard et al. 2005)

5.4 Future prospects

The results, which were observed and discussed in this work, give rise to several possible future prospects.

Since it was found that the inbred strain background of the SMA-like mice has a major influence on the severity of the disease, one project, which has already been started in our laboratory, addresses the question what modifies the SMA phenotype. Therefore, the SMA_H mice on FVB/N background will be crossed back onto pure C57BL/6 background. During back crossing, the phenotypic appearance of the animals will be characterized with regard to the percentage of the respective backgrounds. Finally, an array-based expression profile comparison of the 100% FVB/N and the 100% C57BL/6 SMA_H mice will give information about possible modifying factors. The identification of modifiers of the SMA disease severity is of particular interest, since these factors could serve as new targets for a potential SMA therapy.

HDAC8 was identified in this work as the main HDAC involved in the expression regulation of *SMN2.* Since the HDAC8-specific inhibitor PCI-34051 was able to elevate the SMN level in SMA fibroblast cells, a further proof of principle is currently ongoing in our laboratory to prove the capability of other HDAC8 specific inhibitors to augment SMN levels. Moreover, it would be interesting whether the crossbreeding of SMA-like mice with HDAC8 knock-out mice, would ameliorate the SMA phenotype. Since the ubiquitous HDAC8 knock-out has been shown to be lethal at P0 (Haberland et al. 2009), a inducible conditional knock-out in the motor neurons would most likely be the suitable tool to investigate the impact on *SMN2* in the SMA-like mice. To assess the *in vivo* impact of the lack of the different HDACs on the *SMN2* expression, it would be worth to crossbreed all motor neuron specific knock-out mice of the HDAC class I one by one to SMA-like mice and investigate the change in the SMA phenotype.

Since this study proved that the prenatal treatment with SAHA overcomes prenatal lethality of a very severe SMA mouse model, it might be worth to combine a prenatal and a postnatal SAHA treatment in the milder SMA_H mouse model. The prenatal treatment might increase the *SMN2* expression during the embryonic development and therefore support the development and especially the maintenance of the motor neurons in SMA-like mice. It has been shown that the combination of HDACi treatment plus nutritional support ameliorates the SMA phenotype more than HDACi treatment alone (Narver et al. 2008b). Also physical exercises have been shown to lessen the SMA phenotype in SMA-like mice (Grondard et al. 2005). Thus, the combination of SAHA treatment, physical training and nutritional support might be the optimal therapeutic strategy for SMA-like

mice. Moreover, the treatment of the vascular problems, which result in severe necrosis, might prolong the survival of SMA-like mice.

This combination therapy might be the optimal care for SMA-like animals and thus lead to the best effect in SMA amelioration.

5.4.1 Future prospects for potential SMA therapy

The findings gained in this study together with previously described data open different possible strategies for prospective SMA therapies. Since all SMA patients retain the *SMN2* the activation of this gene is a unique opportunity for a SMA therapy. As already discussed, several compounds have been described to be capable to massively augment the *SMN2* transcription and to correct the splicing of *SMN2.* Since some of these drugs, like phenylbutyrate, VPA and SAHA are FDA-approved and therefore clinically available, they are very promising candidates for a SMA therapy. Since first clinical trials with VPA revealed only a very modest effect on SMA progression, it is crucial to find further potential SMA drugs (Swoboda et al. 2009). Moreover, the FDA-approved drugs aclarubicin and indoprofen revealed positive effects on *SMN2* splicing correction and SMN protein stabilization, respectively. Therefore, it is of highest interest to find out whether a combination therapy with e.g. SAHA together with aclarubicin and indoprofen would lead to an amelioration of the SMA phenotype. However, the combination of these drugs has to be monitored quite carefully, since there is an obvious potential for the development of unfavorable side effects.

Moreover, several therapy strategies are possible without targeting the *SMN2* gene. One theoretically possible strategy is the *SMN1* gene replacement. In mouse experiments it has been shown that the lentivector *SMN1* gene transfer into SMA-like mice increased their survival by 3-5 days (Azzouz et al. 2004). However, it is questionable, whether this method is applicable for a human therapy. Another possible approach has recently been discussed in more detail. The growing field of stem cell research might help to find a way to introduce stem cells (or induced pluripotent stem cells) into the spinal cord of SMA patients in order to produce new motor neurons. Recently, it was proven that it is possible to generate induced pluripotent stem cells (iPSCs) from skin SMA fibroblast cells. Researchers used these cells to generate motor neurons that showed selective deficits compared to those derived from an unaffected control. Therefore, these cells were proposed as a new, promising resource to study disease mechanisms, screen new drug compounds and develop new therapies (Ebert et al. 2009). Additionally, it was recently shown that the intrathecal introduction of neuronal stem cells into SMA-like mice ameliorated the SMA phenotype, revealed a

neuroprotective effect and the treated mice were shown to live ~40% longer (Corti et al. 2008).

Interestingly, the FDA-approved drug riluzole has been shown to act as a neuroprotective agent, reducing the death of neurons and therefore attenuating the SMA progression in a SMA-like mouse (Haddad et al. 2003). Since recent clinical trials have been proven that this compound is well tolerated by SMA patient, it could be another drug to be evaluated in a combination therapy for SMA (Russman et al. 2003).

Since SMA is a progressing disease, the starting time point of the therapy is absolutely crucial. Soon after onset of disease and if a patient still possesses a sufficient amount of functional motor neurons, it is necessary to apply directly a therapy to maintain the neuron integrity with neuroprotective agents or by the elevation in SMN levels. However, if a patient already lacks functional motor neurons, stem cell therapy is the only possible therapy. Nevertheless, supporting muscle strength e.g. by the induction of muscle growths, and supplying nutritional support may help every SMA patient, regardless of the status of the disease.

Probably the best approach for a potential SMA therapy would be the combination of substances, which activate the *SMN2* expression, correct the splicing of *SMN2*, stabilize the *SMN* protein and act neuroprotectively. Moreover, this therapy should be combined with so-called aggressive ancillary care (nutritional support). SAHA has been shown to be neuroprotective (Hockly et al. 2003). Additionally, in this study it was proven that SAHA was able to activate the *SMN2* expression and to elevate the SMN level. Thus, we propose to use SAHA in clinical trials with SMA patients.

6 Summary

Proximal spinal muscular atrophy (SMA) is a common autosomal recessive neuromuscular disorder and the leading hereditary cause of death in early childhood. To date, no cure is available. The disease determining gene for SMA is the *survival motor neuron gene 1* (*SMN1*). *SMN1* produces full length transcripts only (FL-*SMN*), whereas the majority (~90%) of transcripts derived from the copy gene *SMN2* lack exon 7 (Δ7-*SMN2*) due to alternative splicing. Although the amount of fully-functional *SMN2*-derived FL-SMN protein is not sufficient to overcome the absence of *SMN1* and to prevent disease onset, *SMN2* has been shown to be the main disease modifying gene. *SMN2* is present in all SMA patients, which all lack functional *SMN1.* Therefore, and due to its disease modifying property, *SMN2* became the most interesting target for a potential SMA therapy. It has been proven that epigenetic modification by histone deacetylase inhibitors (HDACis) successfully activates the transcription of *SMN2.* Additionally, HDACi treatment has been shown to modulate the splicing pattern of *SMN2* by the up-regulation of the splicing factor SFRS10, resulting in increased FL-*SMN* levels. The elevation of the SMN protein level has been proven to ameliorate disease progression *in vitro*, *ex vivo* and *in vivo*.

In the present work two newly identified second generation HDAC inhibitors of different chemical classes, namely M344 (benzamide) and FK228 (tetrapeptide, also known as depsipeptide, or romidepsin), were shown to be able to elevate SMN and SFRS10 protein levels in fibroblast cell lines derived from SMA patients. Moreover, it was proven by quantitative real-time PCR that both HDACis up-regulated the FL-*SMN2* transcript amounts and revealed no change or even a decrease in the Δ7-*SMN2* level indicating a reversion of the splicing pattern. The ability to correct the *SMN2* splicing was confirmed by the finding that both substances were able to elevate SFRS10 protein levels. Semi-quantitative Western blot analysis revealed that the treatment with M344 resulted in an up to 7-fold and with FK228 in an up to 4.4-fold augmentation of the SMN protein level. FK228 proved its efficacy to elevate SMN levels also in a murine fibroblast line derived from a SMA-like mouse, indicating potency to modulate *SMN2* expression regardless of the genetic background. Moreover, fluorescence microscopy revealed that both substances were able to increase the number of subnuclear gems, indicating the elevated production of fully-functional SMN proteins. However, the performed MTT-assays revealed for both substances an *in vitro* toxicity profile, which restrained further *in vivo* characterization.

In order to identify the respective HDAC isoenzyme mainly involved in *SMN2* expression regulation, all eleven classical HDACs were knocked-down by siRNA. Only

after the knock-down of HDAC8, the SMN protein level was significantly up-regulated. Thus, HDAC8 overexpression experiments were performed, which could clearly prove that HDAC8 activity regulates the SMN protein expression. Furthermore, chromatin immunoprecipitation experiments revealed that HDAC8 binds to the promoter region of *SMN2*, resembling the involvement in the epigenetic regulation of *SMN2* expression. This finding was confirmed by treating *SMN1* deleted fibroblasts with HDAC8 specific inhibitor (PCI-34051). Real-time PCR expression analysis and semi-quantitative Western blots revealed that the up-regulation of SMN by PCI-34051 resembled the elevation of SMN by the knock-down of HDAC8. Moreover, a cell viability assay revealed virtually no cytotoxicity. The great advantage of using an isoform specific HDACi in a potential SMA therapy is the reduction of unfavorable side effects.

To identify a potential drug for a prospective SMA therapy, it is necessary to confirm its potency *in vivo*. Previously, our group has shown for the first time that the FDA-approved drug suberoylanilide hydroxamic acid (SAHA) is able to elevate the SMN level *in vitro* (SMA fibroblasts) and *ex vivo* (rat and human hippocampal brain slices). Thus, this work proved that SAHA is a potent and non-toxic candidate drug for SMA treatment, since the *in vivo* characterization of this compound revealed a beneficial effect on disease progression in two different SMA mouse models. First, since the *SMN2* copy number is crucial for the severity of SMA, a real-time PCR based assay was developed to precisely determine the *SMN2* copy number of SMA-like mice. In the very severe SMA mouse model SAHA treatment of the pregnant mother mice could prevent embryonic lethality of the SMA-like mice. In another SMA mouse model, which was here characterized for the first time in detail, the direct application of SAHA to the SMA-like mice revealed a significant amelioration of the SMA progression. The mean lifespan was increased by ~30%, from 9.9 to 12.9 days. Moreover, the SAHA-treated SMA-like mice showed better motor function abilities. Additionally, in histochemical attempts it was shown that SAHA-treated SMA-like mice revealed less degeneration of the α-motor neurons in the anterior horns of the spinal cord and larger muscle fibers. Immunofluorescence stains could prove that SAHA-treated SMA-like mice showed an increase in neuromuscular junction size. Furthermore, real-time PCR approaches as well as semi-quantitative Western blotting displayed that SAHA treatment elevated SMN protein and transcript levels in the brain, spinal cord, muscle and liver. Although SAHA was able to ameliorate the SMA phenotype, it was not able to fully rescue the mice from disease progression.

Since SAHA is an FDA-approved drug and was shown to ameliorate the SMA progression, it can be considered as an attractive candidate for a potential SMA therapy.

7 Zusammenfassung

Proximale spinale Muskelatrophie (SMA) ist eine häufige autosomal rezessive neuromuskuläre Erkrankung und die häufigste genetisch bedingte Kindestodesursache. Bis heute kann SMA nicht geheilt werden. Die Krankheit wird hervorgerufen durch den homozygoten Verlust des *survival motor neuron* Gens (*SMN1*). *SMN1* produziert ausschließlich Volllänge-Transkripte (VL-*SMN2*), wohingegen bei ~90% der Transkripte der Genkopie *SMN2*, bedingt durch alternatives Spleißen, das Exon 7 fehlt (Δ7-*SMN2*). Obwohl die Menge des vom *SMN2* Gen produzierten voll funktionstüchtigen VL-SMN Proteins nicht ausreicht, das Ausbrechen der Krankheit zu verhindern, ist dennoch *SMN2* das wichtigste krankheitsmodifizierende Gen. Zudem trägt jeder SMA Patient mindestens eine *SMN2* Kopie. Aus diesen Gründen wurde *SMN2* zum interessantesten Zielgen für eine potenzielle SMA Therapie. Es konnte gezeigt werden, dass durch epigenetische Modifizierung durch Histondeacetylase-Inhibitoren (HDACis), die *SMN2* Transkription aktiviert werden kann. Zudem konnte durch HDACi-Behandlung die Menge des Spleißfaktors SFRS10 heraufreguliert werden, was in einer Revertierung des *SMN2* Spleißmusters resultierte. Die Steigerung der SMN Proteinmenge milderte die Ausprägung der SMA *in vitro*, *ex vivo* und *in vivo*.

In der vorliegenden Arbeit konnte gezeigt werden, dass zwei neu identifizierte HDACis aus unterschiedlichen chemischen Substanzklassen, M344 (Benzamid) und FK228 (Tetrapeptid), in der Lage sind, sowohl die SMN, als auch die SFRS10 Proteinmenge in Fibroblastenkulturen von SMA Patienten heraufzuregulieren. Außerdem konnte mit Hilfe von quantitativer *real-time PCR* gezeigt werden, dass beide Substanzen eine Erhöhung der VL-*SMN2* Transkriptmenge und keine Veränderung oder sogar eine Abnahme der Δ7-*SMN2* Transkriptmenge verursachen, was für eine Revertierung des *SMN2* Spleißmusters spricht. Die Fähigkeit, das SMN2 Spleißmuster zu korrigieren, wurde durch die Beobachtung bestätigt, dass beide Substanzen in der Lage sind, die SFRS10 Proteinmenge zu erhöhen. Durch semiquantitative *Western blots* konnte gezeigt werden, dass die Behandlung mit M344 zu einer 7-fachen und mit FK228 zu einer 4,4-fachen Steigerung der SMN Proteinmenge führte. FK228 sorgte auch in einer murinen Fibroblastenkultur, die von einer SMA-Maus stammte, für eine Erhöhung der SMN Proteinmenge. Dies spricht dafür, dass FK228, unabhängig des genetischen Hintergrunds in der Lage ist, *SMN2* Expression zu aktivieren. Außerdem zeigten fluoreszenzmikroskopische Untersuchungen, dass beide Substanzen die Anzahl subnukleärer *gems* steigerten. Die Neubildung von *gems* spiegelt die erhöhte Produktion funktionstüchtiger SMN Proteine wider. Die *in vitro* Toxizitätsprüfung (MTT-Assay)

jedoch, stellte eine weitergehende *in vivo* Charakterisierung beider Substanzen vorerst zurück.

Um dasjenige HDAC-Isoenzym zu identifizieren, welches hauptsächlich in der Regulation der *SMN2* Expression involviert ist, wurde die Expression aller elf „klassischen HDACs“ mit Hilfe von siRNA ausgeschaltet (*knock-down*). Nur nach Ausschalten von HDAC8 zeigte sich die SMN Proteinmenge signifikant erhöht. Desweiteren konnte durch Überexpression von HDAC8 die SMN Proteinmenge herunterreguliert werden. Chromatin-Immunopräzipitationsexperimente bewiesen, dass HDAC8 in der Promoterregion des *SMN2* Gens bindet, was eine Beteiligung in der epigenetischen Regulation der *SMN2* Expression nahe legt. Diese Ergebnisse konnten durch die Behandlung von *SMN1*-deletierten Fibroblasten mit einem HDAC8-spezifischen Inhibitor (PCI-34051) bestätigt werden. *Real-time PCR* Expressionsanalyse und semiquantitative *Western blots* bestätigten, dass das Ausmaß der Heraufregulierung von SMN durch PCI-34051 dem entsprach, welches nach dem *knock-down* von HDAC8 beobachtet wurde. Die *in vitro* Toxizitätsprüfung (MTT-Assay) zeigte keinerlei Zytotoxizität. Der grundlegende Vorteil eines Isoform-spezifischen HDACis in einer potenziellen Therapie für SMA, läge in der Vermeidung von einem Großteil unerwünschter Nebenwirkungen.

Um ein potenzielles Medikament für eine SMA-Therapie zu identifizieren, ist es nötig, seine Wirksamkeit in *in vivo* Versuchen zu bestätigen. Vorausgehend konnte unsere Arbeitsgruppe zum ersten Mal zeigen, dass das von der *FDA* zugelassene Medikament *suberoylanilide hydroxamic acid* (SAHA) in der Lage ist, die SMN Mengen *in vitro* (SMA Fibroblasten) und *ex vivo* (Hirnschnittkulturen von Mensch und Ratte) zu erhöhen. Diese Arbeit zeigt, dass SAHA ein sehr potenter Wirkstoff für eine SMA-Therapie ist, da diese Substanz in der *in vivo* Charakterisierung sehr positiven Einfluss auf den Krankheitsverlauf in zwei unterschiedlichen Mausmodellen für SMA zeigte. Da die Anzahl der SMN2 Genkopien entscheidend für den Schweregrad der SMA ist, wurde zunächst eine *real-time PCR* basierende Methode entwickelt, mit der es möglich ist, die exakte *SMN2* Kopienanzahl zu bestimmen. In einem Mausmodell mit sehr schwerer SMA-Verlaufsform, konnte die SAHA-Behandlung der Muttertiere die embryonale Letalität der SMA-Mäuse verhindern. In einem weiteren SMA-Mausmodell, welches hier zum ersten Mal ausführlich beschrieben wurde, zeigte die direkte Applikation von SAHA in die SMA-Mäuse eine deutliche Abschwächung des Krankheitsverlaufs. Die durchschnittliche Lebensdauer der erkrankten Tiere konnte durch SAHA-Behandlung von 9,9 auf 12,9 Tage um ~30% verlängert werden. Darüber hinaus zeigten die SAHA-behandelten SMA-Mäuse im Vergleich zu unbehandelten bessere motorische Fähigkeiten. Histochemische Untersuchungen bewiesen, dass die mit SAHA

behandelten SMA-Mäuse eine verringerte Degeneration der α-Motoneuronen in den Vorderhörnern des Rückenmarks und durchschnittlich im Querschnitt größere Muskelfasern aufwiesen. Immunofloureszenz-Färbungen zeigten außerdem in den behandelten SMA-Tieren größere neuromuskuläre Endplatten als in den unbehandelten. Zudem wurde durch *real-time PCR* Expressionsanalysen und semiquantitative *Western blots* festgestellt, dass SAHA-Behandlung die *SMN2*/SMN2 Transkript- und Proteinmenge in Gehirn, Rückenmark, Muskel und Leber erhöhte. SAHA ist zwar in der Lage den Krankheitsverlauf abzuschwächen, aber nicht den Ausbruch der SMA komplett zu verhindern.

Da SAHA ein zugelassenes Medikament ist und hier gezeigt werden konnte, dass es den Krankheitsverlauf der SMA positiv beeinflussen kann, sollte der Wirkstoff als ein vielversprechender Kandidat für eine potenzielle SMA-Therapie in Erwägung gezogen werden.

8 Publications, lectures, poster contributions and awards

- **Original publications**

Garbes L, **Riessland M**, Holker I, Heller R, Hauke J, Trankle C, Coras R, Blumcke I, Hahnen E, Wirth B (2009b) LBH589 induces up to 10-fold SMN protein levels by several independent mechanisms and is effective even in cells from SMA patients non-responsive to valproate. Human Molecular Genetics 18: 3645-58

Hauke J, **Riessland M**, Lunke S, Eyupoglu IY, Blumcke I, El-Osta A, Wirth B, Hahnen E (2009) Survival motor neuron gene 2 silencing by DNA methylation correlates with spinal muscular atrophy disease severity and can be bypassed by histone deacetylase inhibition. Hum Mol Genet 18: 304-17

Riessland M, Brichta L, Hahnen E, Wirth B (2006) The benzamide M344, a novel histone deacetylase inhibitor, significantly increases SMN2 RNA/protein levels in spinal muscular atrophy cells. Hum Genet 120: 101-10

Hahnen E, Eyupoglu IY, Brichta L, Haastert K, Tränkle C, Siebzehnrübl FA, **Riessland M**, Hölker I, Claus P, Romstöck J, Buslei R, Wirth B, Blümcke I (2006) *In vitro* and *ex vivo* evaluation of second-generation histone deacetylase inhibitors for the treatment of spinal muscular atrophy. J Neurochem: 10.1111/j.1471-4159.2006.03868.x

Riessland M, Tomalik-Scharte D, Fuhr U (2004) Do data presented at an American Society for Clinical Pharmacology and Therapeutics meeting make it to full publication? Clinical Pharmacology and Therapeutics 75: 123-4

- **Review**

Wirth B, **Riessland M**, Hahnen E (2007) Drug discovery for spinal muscular atrophy. Expert Opin. Drug Discov 2: 437-451

- **Lecture contributions**

Riessland M, Brichta L, Hahnen E, Wirth B. (2006) The benzamide M344, a novel histone deacetylase inhibitor, significantly increases SMN2 RNA/protein levels in spinal muscular atrophy (SMA) cells. *Abstract book* (10th Annual International SMA Research Group Meeting, Montréal, Canada)

Garbes L, **Riessland M**, Holker I, Trankle C, Hauke J, Hahnen E Heller R, Wirth B (2009) What did we learn from *in vivo* and *in vitro* treatment with HDACi in SMA? *Abstract book* (13th Annual International SMA Research Group Meeting, Cincinnati, USA)

- **Poster contributions**

Hahnen E, Eyüpoglu IY, Brichta L, Siebzehnrübl FA, **Riessland M**, Tränkle C, Buslei R, Wirth B, Blümcke I. (2005) Therapy of spinal muscular atrophy : Hydroxamid acids increase survival of motor neuron protein levels. *Medgen* 17:113 (P234) (Annual Meeting of the German Society of Human Genetics, Halle)

Hahnen E, Eyüpoglu IY, Brichta L, Haastert K, Tränkle C, Siebzehnrübl FA, **Riessland M**, Holker I; Claus P, Romstöck J, Buslei R, Blümcke I, Wirth B. (2006) *In vitro* and *ex vivo* evaluation of second generation histone deacetylase inhibitors fort he treatment of spinal muscular atrophy. *Medgen* 18:113 (P291) (Annual Meeting of the German Society of Human Genetics, Heidelberg)

Riessland M, Brichta L, Hahnen E, Wirth B. (2006) The benzamide M344, a novel histone deacetylase inhibitor, significantly increases SMN2 RNA/protein levels in spinal muscular atrophy (SMA) cells. *Medgen* 18:113 (P293) (Annual Meeting of the German Society of Human Genetics, Heidelberg, Germany)

Riessland M, Brichta L, Hahnen E, Wirth B. (2007) The benzamide M344, a novel histone deacetylase inhibitor, significantly increases SMN2 RNA/protein levels in spinal muscular atrophy (SMA) cells. (20th course in "Medical Genetics", European School of Genetic Medicine, Bertinoro di Romagna, Italy)

Riessland M., Hahnen E., Wirth B. (2007) Rapid and reliable determination of transgene copy numbers in mice by SYBR green_based real_time PCR *Medgen* (P266) (Annual Meeting of the German Society of Human Genetics, Bonn, Germany)

Hauke J, **Riessland M**, Lunke S, Eyupoglu IY, Blumcke I, El-Osta A, Wirth B, Hahnen E (2009) *SMN2* gene silencing by DNA methylation correlates with SMA disease severity and can be bypassed by histone deacetylase inhibition. (Epigenetic World Congress, Berlin, Germany)

- **Best poster award**

Riessland M, Brichta L, Hahnen E, Wirth B. (2007) The benzamide M344, a novel histone deacetylase inhibitor, significantly increases SMN2 RNA/protein levels in spinal muscular atrophy (SMA) cells. (20th course in "Medical Genetics", European School of Genetic Medicine, Bertinoro di Romagna, Italy)

9 References

Alsdorf R, Wyszynski DF (2005) Teratogenicity of sodium valproate. Expert Opinion on Drug Safety 4: 345-53

Andreassi C, Angelozzi C, Tiziano FD, Vitali T, De Vincenzi E, Boninsegna A, Villanova M, Bertini E, Pini A, Neri G, Brahe C (2004) Phenylbutyrate increases SMN expression in vitro: relevance for treatment of spinal muscular atrophy. Eur J Hum Genet 12: 59-65

Andreassi C, Jarecki J, Zhou J, Coovert DD, Monani UR, Chen X, Whitney M, Pollok B, Zhang M, Androphy E, Burghes AH (2001) Aclarubicin treatment restores SMN levels to cells derived from type I spinal muscular atrophy patients. Hum Mol Genet 10: 2841-9

Angelozzi C, Borgo F, Tiziano FD, Martella A, Neri G, Brahe C (2008) Salbutamol increases SMN mRNA and protein levels in spinal muscular atrophy cells. J Med Genet 45: 29-31

Araujo Ade Q, Araujo M, Swoboda KJ (2009) Vascular perfusion abnormalities in infants with spinal muscular atrophy. Journal of Pediatrics 155: 292-4

Avila AM, Burnett BG, Taye AA, Gabanella F, Knight MA, Hartenstein P, Cizman Z, Di Prospero NA, Pellizzoni L, Fischbeck KH, Sumner CJ (2007) Trichostatin A increases SMN expression and survival in a mouse model of spinal muscular atrophy. J Clin Invest 117: 659-71

Azzouz M, Le T, Ralph GS, Walmsley L, Monani UR, Lee DC, Wilkes F, Mitrophanous KA, Kingsman SM, Burghes AH, Mazarakis ND (2004) Lentivector-mediated SMN replacement in a mouse model of spinal muscular atrophy. J Clin Invest 114: 1726-31

Balasubramanian S, Ramos J, Luo W, Sirisawad M, Verner E, Buggy JJ (2008) A novel histone deacetylase 8 (HDAC8)-specific inhibitor PCI-34051 induces apoptosis in T-cell lymphomas. Leukemia 22: 1026-34

Baron-Delage S, Abadie A, Echaniz-Laguna A, Melki J, Beretta L (2000) Interferons and IRF-1 induce expression of the survival motor neuron (SMN) genes. Mol Med 6: 957-68

Baughan TD, Dickson A, Osman EY, Lorson CL (2009a) Delivery of bifunctional RNAs that target an intronic repressor and increase SMN levels in an animal model of spinal muscular atrophy. Hum Mol Genet 18: 1600-11

Baughan TD, Dickson A, Osman EY, Lorson CL (2009b) Delivery of bifunctional RNAs that target an intronic repressor and increase SMN levels in an animal model of spinal muscular atrophy. Human Molecular Genetics 18: 1600-11

Bilbao R, Srinivasan S, Reay D, Goldberg L, Hughes T, Roelvink PW, Einfeld DA, Wickham TJ, Clemens PR (2003) Binding of adenoviral fiber knob to the coxsackievirus-adenovirus receptor is crucial for transduction of fetal muscle. Hum Gene Ther 14: 645-9

Bose JK, Wang IF, Hung L, Tarn WY, Shen CK (2008) TDP-43 overexpression enhances exon 7 inclusion during the survival of motor neuron pre-mRNA splicing. J Biol Chem 283: 28852-9

Bradford MM (1976) A rapid and sensitive method for the quantitation of microgram quantities of protein utilizing the principle of protein-dye binding. Anal Biochem 72: 248-54

Brahe C (2000) Copies of the survival motor neuron gene in spinal muscular atrophy: the more, the better. Neuromuscul Disord 10: 274-5

Brahe C, Clermont O, Zappata S, Tiziano F, Melki J, Neri G (1996) Frameshift mutation in the survival motor neuron gene in a severe case of SMA type I. Hum Mol Genet 5: 1971-6

Brichta L, Hofmann Y, Hahnen E, Siebzehnrubl FA, Raschke H, Blumcke I, Eyupoglu IY, Wirth B (2003) Valproic acid increases the SMN2 protein level: a well-known drug as a potential therapy for spinal muscular atrophy. Hum Mol Genet 12: 2481-9

Brichta L, Holker I, Haug K, Klockgether T, Wirth B (2006a) In-vivo activation of SMN in SMA carriers and patients treated with valproate. Ann Neurol 59: DOI:10.1002/ana.20836

Brichta L, Holker I, Haug K, Klockgether T, Wirth B (2006b) In vivo activation of SMN in spinal muscular atrophy carriers and patients treated with valproate. Ann Neurol 59: 970-5

Brzustowicz LM, Lehner T, Castilla LH, Penchaszadeh GK, Wilhelmsen KC, Daniels R, Davies KE, Leppert M, Ziter F, Wood D, et al. (1990) Genetic mapping of chronic childhood-onset spinal muscular atrophy to chromosome 5q11.2-13.3. Nature 344: 540-1

Buchthal F, Olsen PZ (1970) Electromyography and muscle biopsy in infantile spinal muscular atrophy. Brain 93: 15-30

Buggy JJ, Sideris ML, Mak P, Lorimer DD, McIntosh B, Clark JM (2000) Cloning and characterization of a novel human histone deacetylase, HDAC8. Biochemical Journal 350 Pt 1: 199-205

Buhler D, Raker V, Luhrmann R, Fischer U (1999) Essential role for the tudor domain of SMN in spliceosomal U snRNP assembly: implications for spinal muscular atrophy. Hum Mol Genet 8: 2351-7

Burghes AH (1997) When is a deletion not a deletion? When it is converted. Am J Hum Genet 61: 9-15

Burglen L, Lefebvre S, Clermont O, Burlet P, Viollet L, Cruaud C, Munnich A, Melki J (1996) Structure and organization of the human survival motor neurone (SMN) gene. Genomics 32: 479-82

Burlet P, Huber C, Bertrandy S, Ludosky MA, Zwaenepoel I, Clermont O, Roume J, Delezoide AL, Cartaud J, Munnich A, Lefebvre S (1998) The distribution of SMN protein complex in human fetal tissues and its alteration in spinal muscular atrophy. Hum Mol Genet 7: 1927-33

Burt EC, Towers PR, Sattelle DB (2006) Caenorhabditis elegans in the study of SMN-interacting proteins: a role for SMI-1, an orthologue of human Gemin2 and the identification of novel components of the SMN complex. Invert Neurosci 6: 145-59

Carrozza MJ, Utley RT, Workman JL, Cote J (2003) The diverse functions of histone acetyltransferase complexes. Trends Genet 19: 321-9

Cartegni L, Krainer AR (2002) Disruption of an SF2/ASF-dependent exonic splicing enhancer in SMN2 causes spinal muscular atrophy in the absence of SMN1. Nat Genet 30: 377-84

Carvalho T, Almeida F, Calapez A, Lafarga M, Berciano MT, Carmo-Fonseca M (1999) The spinal muscular atrophy disease gene product, SMN: A link between snRNP biogenesis and the Cajal (coiled) body. J Cell Biol 147: 715-28

Chan YB, Miguel-Aliaga I, Franks C, Thomas N, Trulzsch B, Sattelle DB, Davies KE, van den Heuvel M (2003) Neuromuscular defects in a Drosophila survival motor neuron gene mutant. Hum Mol Genet 12: 1367-76

Chang HC, Dimlich DN, Yokokura T, Mukherjee A, Kankel MW, Sen A, Sridhar V, Fulga TA, Hart AC, Van Vactor D, Artavanis-Tsakonas S (2008) Modeling spinal muscular atrophy in Drosophila. PLoS One 3: e3209

Chang HC, Hung WC, Chuang YJ, Jong YJ (2004) Degradation of survival motor neuron (SMN) protein is mediated via the ubiquitin/proteasome pathway. Neurochem Int 45: 1107-12

Chang JG, Hsieh-Li HM, Jong YJ, Wang NM, Tsai CH, Li H (2001) Treatment of spinal muscular atrophy by sodium butyrate. Proc Natl Acad Sci U S A 98: 9808-13

Chen Q, Baird SD, Mahadevan M, Besner-Johnston A, Farahani R, Xuan J, Kang X, Lefebvre C, Ikeda JE, Korneluk RG, MacKenzie AE (1998) Sequence of a 131-kb region of 5q13.1 containing the spinal muscular atrophy candidate genes SMN and NAIP. Genomics 48: 121-7

Cifuentes-Diaz C, Frugier T, Tiziano FD, Lacene E, Roblot N, Joshi V, Moreau MH, Melki J (2001) Deletion of murine SMN exon 7 directed to skeletal muscle leads to severe muscular dystrophy. J Cell Biol 152: 1107-14

Clemens MJ (2001a) Initiation factor eIF2 alpha phosphorylation in stress responses and apoptosis. Prog Mol Subcell Biol 27: 57-89

Clemens MJ (2001b) Translational regulation in cell stress and apoptosis. Roles of the eIF4E binding proteins. J Cell Mol Med 5: 221-39

Contreras X, Schweneker M, Chen CS, McCune JM, Deeks SG, Martin J, Peterlin BM (2009) Suberoylanilide hydroxamic acid reactivates HIV from latently infected cells. J Biol Chem 284: 6782-9

Coovert DD, Le TT, McAndrew PE, Strasswimmer J, Crawford TO, Mendell JR, Coulson SE, Androphy EJ, Prior TW, Burghes AH (1997) The survival motor neuron protein in spinal muscular atrophy. Hum Mol Genet 6: 1205-14

Corti S, Nizzardo M, Nardini M, Donadoni C, Salani S, Ronchi D, Saladino F, Bordoni A, Fortunato F, Del Bo R, Papadimitriou D, Locatelli F, Menozzi G, Strazzer S, Bresolin N, Comi GP (2008) Neural stem cell transplantation can ameliorate the phenotype of a mouse model of spinal muscular atrophy. J Clin Invest 118: 3316-30

Czeizel A, Hamula J (1989) A hungarian study on Werdnig-Hoffmann disease. J Med Genet 26: 761-3

de Ruijter AJ, van Gennip AH, Caron HN, Kemp S, van Kuilenburg AB (2003) Histone deacetylases (HDACs): characterization of the classical HDAC family. Biochemical Journal 370: 737-49

DiDonato CJ, Brun T, Simard LR (1999) Complete nucleotide sequence, genomic organization, and promoter analysis of the murine survival motor neuron gene (Smn). Mamm Genome 10: 638-41

DiDonato CJ, Chen XN, Noya D, Korenberg JR, Nadeau JH, Simard LR (1997) Cloning, characterization, and copy number of the murine survival motor neuron gene: homolog of the spinal muscular atrophy-determining gene. Genome Res 7: 339-52

DiDonato CJ, Morgan K, Carpten JD, Fuerst P, Ingraham SE, Prescott G, McPherson JD, Wirth B, Zerres K, Hurko O, et al. (1994) Association between Ag1-CA alleles and severity of autosomal recessive proximal spinal muscular atrophy. Am J Hum Genet 55: 1218-29

Doenecke D, Gallwitz D (1982) Acetylation of histones in nucleosomes. Mol Cell Biochem 44: 113-28

Duvic M, Talpur R, Ni X, Zhang C, Hazarika P, Kelly C, Chiao JH, Reilly JF, Ricker JL, Richon VM, Frankel SR (2007) Phase 2 trial of oral vorinostat (suberoylanilide hydroxamic acid, SAHA) for refractory cutaneous T-cell lymphoma (CTCL). Blood 109: 31-9

Eberharter A, Becker PB (2002) Histone acetylation: a switch between repressive and permissive chromatin. Second in review series on chromatin dynamics. EMBO Rep 3: 224-9

Ebert AD, Yu J, Rose FF, Jr., Mattis VB, Lorson CL, Thomson JA, Svendsen CN (2009) Induced pluripotent stem cells from a spinal muscular atrophy patient. Nature 457: 277-80

Eggert C, Chari A, Laggerbauer B, Fischer U (2006) Spinal muscular atrophy: the RNP connection. Trends Mol Med

El-Khodor BF, Edgar N, Chen A, Winberg ML, Joyce C, Brunner D, Suarez-Farinas M, Heyes MP (2008) Identification of a battery of tests for drug candidate evaluation in the SMNDelta7 neonate model of spinal muscular atrophy. Exp Neurol 212: 29-43

Eyupoglu IY, Hahnen E, Buslei R, Siebzehnrubl FA, Savaskan NE, Luders M, Trankle C, Wick W, Weller M, Fahlbusch R, Blumcke I (2005) Suberoylanilide hydroxamic acid (SAHA) has potent anti-glioma properties in vitro, ex vivo and in vivo. J Neurochem 93: 992-9

Fakan S, Leser G, Martin TE (1984) Ultrastructural distribution of nuclear ribonucleoproteins as visualized by immunocytochemistry on thin sections. J Cell Biol 98: 358-63

Feldkotter M, Schwarzer V, Wirth R, Wienker TF, Wirth B (2002) Quantitative analyses of SMN1 and SMN2 based on real-time lightCycler PCR: fast and highly reliable carrier testing and prediction of severity of spinal muscular atrophy. Am J Hum Genet 70: 358-68

Felsenfeld G, Groudine M (2003) Controlling the double helix. Nature 421: 448-53

Frugier T, Tiziano FD, Cifuentes-Diaz C, Miniou P, Roblot N, Dierich A, Le Meur M, Melki J (2000) Nuclear targeting defect of SMN lacking the C-terminus in a mouse model of spinal muscular atrophy. Hum Mol Genet 9: 849-58

Furumai R, Matsuyama A, Kobashi N, Lee KH, Nishiyama M, Nakajima H, Tanaka A, Komatsu Y, Nishino N, Yoshida M, Horinouchi S (2002) FK228 (depsipeptide) as a natural prodrug that inhibits class I histone deacetylases. Cancer Res 62: 4916-21

Garbes L, Riessland M, Holker I, Heller R, Hauke J, Trankle C, Coras R, Blumcke I, Hahnen E, Wirth B (2009) LBH589 induces up to 10-fold SMN protein levels by several independent mechanisms and is effective even in cells from SMA patients non-responsive to valproate. Hum Mol Genet

Gavrilina TO, McGovern VL, Workman E, Crawford TO, Gogliotti RG, DiDonato CJ, Monani UR, Morris GE, Burghes AH (2008a) Neuronal SMN expression corrects spinal muscular atrophy in severe SMA mice while muscle-specific SMN expression has no phenotypic effect. Hum Mol Genet 17: 1063-75

Gavrilina TO, McGovern VL, Workman E, Crawford TO, Gogliotti RG, DiDonato CJ, Monani UR, Morris GE, Burghes AH (2008b) Neuronal SMN expression corrects spinal muscular atrophy in severe SMA mice while muscle-specific SMN expression has no phenotypic effect. Human Molecular Genetics 17: 1063-75

Gennarelli M, Lucarelli M, Capon F, Pizzuti A, Merlini L, Angelini C, Novelli G, Dallapiccola B (1995) Survival motor neuron gene transcript analysis in muscles from spinal muscular atrophy patients. Biochem Biophys Res Commun 213: 342-8

Gerstner T, Bell N, Konig S (2008) Oral valproic acid for epilepsy--long-term experience in therapy and side effects. Expert Opin Pharmacother 9: 285-92

Gilliam TC, Brzustowicz LM, Castilla LH, Lehner T, Penchaszadeh GK, Daniels RJ, Byth BC, Knowles J, Hislop JE, Shapira Y, et al. (1990) Genetic homogeneity between acute and chronic forms of spinal muscular atrophy. Nature 345: 823-5

Glass CK, Rosenfeld MG (2000) The coregulator exchange in transcriptional functions of nuclear receptors. Genes Dev 14: 121-41

Graul AI, Sorbera LA, Bozzo J, Serradell N, Revel L, Prous JR (2007) The year's new drugs and biologics--2006. Drug News and Perspectives 20: 17-44

Gregoretti IV, Lee YM, Goodson HV (2004) Molecular evolution of the histone deacetylase family: functional implications of phylogenetic analysis. Journal of Molecular Biology 338: 17-31

Grondard C, Biondi O, Armand AS, Lecolle S, Della Gaspera B, Pariset C, Li H, Gallien CL, Vidal PP, Chanoine C, Charbonnier F (2005) Regular exercise prolongs survival in a type 2 spinal muscular atrophy model mouse. J Neurosci 25: 7615-22

Gronroos E, Hellman U, Heldin CH, Ericsson J (2002) Control of Smad7 stability by competition between acetylation and ubiquitination. Mol Cell 10: 483-93

Gruss C, Knippers R (1996) Structure of replicating chromatin. Prog Nucleic Acid Res Mol Biol 52: 337-65

Grzeschik SM, Ganta M, Prior TW, Heavlin WD, Wang CH (2005) Hydroxyurea enhances SMN2 gene expression in spinal muscular atrophy cells. Ann Neurol 58: 194-202

Gu W, Roeder RG (1997) Activation of p53 sequence-specific DNA binding by acetylation of the p53 C-terminal domain. Cell 90: 595-606

Gubitz AK, Feng W, Dreyfuss G (2004) The SMN complex. Exp Cell Res 296: 51-6

Haberland M, Mokalled MH, Montgomery RL, Olson EN (2009) Epigenetic control of skull morphogenesis by histone deacetylase 8. Genes and Development 23: 1625-30

Haddad H, Cifuentes-Diaz C, Miroglio A, Roblot N, Joshi V, Melki J (2003) Riluzole attenuates spinal muscular atrophy disease progression in a mouse model. Muscle Nerve 28: 432-7

Hahnen E, Eyupoglu IY, Brichta L, Haastert K, Trankle C, Siebzehnrubl FA, Riessland M, Holker I, Claus P, Romstock J, Buslei R, Wirth B, Blumcke I (2006a) In vitro and ex vivo evaluation of second-generation histone deacetylase inhibitors for the treatment of spinal muscular atrophy. J Neurochem 98: 193-202

Hahnen E, Eyupoglu IY, Brichta L, Haastert K, Trankle C, Siebzehnrubl FA, Riessland M, Holker I, Claus P, Romstock J, Buslei R, Wirth B, Blumcke I (2006b) In vitro and ex vivo evaluation of second-generation histone deacetylase inhibitors for the treatment of spinal muscular atrophy. Journal of Neurochemistry 98: 193-202

Hahnen E, Eyupoglu IY, Brichta L, Haastert K, Tränkle C, Siebzehnrübl FA, Riessland M, Hölker I, Claus P, Romstöck J, Buslei R, Wirth B, Blümcke I (2006c) *In vitro* and *ex*

vivo evaluation of second-generation histone deacetylase inhibitors for the treatment of spinal muscular atrophy. J Neurochem: 10.1111/j.1471-4159.2006.03868.x

Hahnen E, Eyupoglu IY, Brichta L, Siebzehnrubl FA, Riessland M, Trankle C, Buslei R, Wirth B, Blumcke I (2005) Therapy of spinal muscular atrophy: hydroxamic acids increases survival of motor neuron protein levels. Medgen 17: 113

Hahnen E, Forkert R, Marke C, Rudnik-Schoneborn S, Schonling J, Zerres K, Wirth B (1995) Molecular analysis of candidate genes on chromosome 5q13 in autosomal recessive spinal muscular atrophy: evidence of homozygous deletions of the SMN gene in unaffected individuals. Hum Mol Genet 4: 1927-33

Hahnen E, Hauke J, Trankle C, Eyupoglu IY, Wirth B, Blumcke I (2008) Histone deacetylase inhibitors: possible implications for neurodegenerative disorders. Expert Opin Investig Drugs 17: 169-84

Hahnen ET, Wirth B (1996) Frequent DNA variant in exon 2a of the survival motor neuron gene (SMN): a further possibility for distinguishing the two copies of the gene. Hum Genet 98: 122-3

Hasan S, Stucki M, Hassa PO, Imhof R, Gehrig P, Hunziker P, Hubscher U, Hottiger MO (2001) Regulation of human flap endonuclease-1 activity by acetylation through the transcriptional coactivator p300. Mol Cell 7: 1221-31

Hauke J, Riessland M, Lunke S, Eyupoglu IY, Blumcke I, El-Osta A, Wirth B, Hahnen E (2009) Survival motor neuron gene 2 silencing by DNA methylation correlates with spinal muscular atrophy disease severity and can be bypassed by histone deacetylase inhibition. Hum Mol Genet 18: 304-17

Heier CR, DiDonato CJ (2009a) Translational readthrough by the aminoglycoside geneticin (G418) modulates SMN stability in vitro and improves motor function in SMA mice in vivo. Human Molecular Genetics 18: 1310-22

Heier CR, DiDonato CJ (2009b) Translational readthrough by the aminoglycoside geneticin (G418) modulates SMN stability in vitro and improves motor function in SMA mice in vivo. Hum Mol Genet 18: 1310-22

Helmken C, Wirth B (2000) Exclusion of Htra2-beta1, an up-regulator of full-length SMN2 transcript, as a modifying gene for spinal muscular atrophy. Hum Genet 107: 554-8

Hockly E, Richon VM, Woodman B, Smith DL, Zhou X, Rosa E, Sathasivam K, Ghazi-Noori S, Mahal A, Lowden PA, Steffan JS, Marsh JL, Thompson LM, Lewis CM, Marks PA, Bates GP (2003) Suberoylanilide hydroxamic acid, a histone deacetylase inhibitor, ameliorates motor deficits in a mouse model of Huntington's disease. Proc Natl Acad Sci U S A 100: 2041-6

Hoffmann (1893) Dritter Beitrag zur Lehre von der hereditären progressiven spinalen Muskelatrophie
im Kindesalter. . *Dtsch Z Nervenheilk*. : 217-222

Hofmann Y, Lorson CL, Stamm S, Androphy EJ, Wirth B (2000) Htra2-beta 1 stimulates an exonic splicing enhancer and can restore full-length SMN expression to survival motor neuron 2 (SMN2). Proc Natl Acad Sci U S A 97: 9618-23

Hofmann Y, Wirth B (2002) hnRNP-G promotes exon 7 inclusion of survival motor neuron (SMN) via direct interaction with Htra2-beta1. Hum Mol Genet 11: 2037-49

Hsieh-Li HM, Chang JG, Jong YJ, Wu MH, Wang NM, Tsai CH, Li H (2000) A mouse model for spinal muscular atrophy. Nat Genet 24: 66-70

Hu E, Chen Z, Fredrickson T, Zhu Y, Kirkpatrick R, Zhang GF, Johanson K, Sung CM, Liu R, Winkler J (2000) Cloning and characterization of a novel human class I histone deacetylase that functions as a transcription repressor. Journal of Biological Chemistry 275: 15254-64

Hua Y, Zhou J (2004) Survival motor neuron protein facilitates assembly of stress granules. FEBS Lett 572: 69-74

Huang Y, Myers SJ, Dingledine R (1999) Transcriptional repression by REST: recruitment of Sin3A and histone deacetylase to neuronal genes. Nature Neuroscience 2: 867-72

Hubbert C, Guardiola A, Shao R, Kawaguchi Y, Ito A, Nixon A, Yoshida M, Wang XF, Yao TP (2002) HDAC6 is a microtubule-associated deacetylase. Nature 417: 455-8

Jablonka S, Schrank B, Kralewski M, Rossoll W, Sendtner M (2000) Reduced survival motor neuron (Smn) gene dose in mice leads to motor neuron degeneration: an animal model for spinal muscular atrophy type III. Hum Mol Genet 9: 341-6

Jarecki J, Chen X, Bernardino A, Coovert DD, Whitney M, Burghes A, Stack J, Pollok BA (2005) Diverse small-molecule modulators of SMN expression found by high-throughput compound screening: early leads towards a therapeutic for spinal muscular atrophy. Hum Mol Genet 14: 2003-18

Ji W, Zhou W, Abruzzese R, Guo W, Blake A, Davis S, Davis S, Polejaeva I (2005) A method for determining zygosity of transgenic zebrafish by TaqMan real-time PCR. Anal Biochem 344: 240-6

Jung M, Brosch G, Kolle D, Scherf H, Gerhauser C, Loidl P (1999) Amide analogues of trichostatin A as inhibitors of histone deacetylase and inducers of terminal cell differentiation. J Med Chem 42: 4669-79

Kariya S, Park GH, Maeno-Hikichi Y, Leykekhman O, Lutz C, Arkovitz MS, Landmesser LT, Monani UR (2008) Reduced SMN protein impairs maturation of the neuromuscular junctions in mouse models of spinal muscular atrophy. Hum Mol Genet 17: 2552-69

Kashima T, Manley JL (2003) A negative element in SMN2 exon 7 inhibits splicing in spinal muscular atrophy. Nat Genet 34: 460-3

Kawaguchi Y, Kovacs JJ, McLaurin A, Vance JM, Ito A, Yao TP (2003) The deacetylase HDAC6 regulates aggresome formation and cell viability in response to misfolded protein stress. Cell 115: 727-38

Kedersha NL, Gupta M, Li W, Miller I, Anderson P (1999) RNA-binding proteins TIA-1 and TIAR link the phosphorylation of eIF-2 alpha to the assembly of mammalian stress granules. J Cell Biol 147: 1431-42

Kelter AR, Herchenbach J, Wirth B (2000) The transcription factor-like nuclear regulator (TFNR) contains a novel 55-amino-acid motif repeated nine times and maps closely to SMN1. Genomics 70: 315-26

Kernochan LE, Russo ML, Woodling NS, Huynh TN, Avila AM, Fischbeck KH, Sumner CJ (2005) The role of histone acetylation in SMN gene expression. Hum Mol Genet

Kong L, Wang X, Choe DW, Polley M, Burnett BG, Bosch-Marce M, Griffin JW, Rich MM, Sumner CJ (2009) Impaired synaptic vesicle release and immaturity of neuromuscular junctions in spinal muscular atrophy mice. J Neurosci 29: 842-51

Kornberg RD, Klug A (1981) The nucleosome. Sci Am 244: 52-64

Kornberg RD, Lorch Y (1999) Twenty-five years of the nucleosome, fundamental particle of the eukaryote chromosome. Cell 98: 285-94

Kouzarides T (2000) Acetylation: a regulatory modification to rival phosphorylation? Embo J 19: 1176-9

Kovacs JJ, Murphy PJ, Gaillard S, Zhao X, Wu JT, Nicchitta CV, Yoshida M, Toft DO, Pratt WB, Yao TP (2005) HDAC6 regulates Hsp90 acetylation and chaperone-dependent activation of glucocorticoid receptor. Molecular Cell 18: 601-7

Krennhrubec K, Marshall BL, Hedglin M, Verdin E, Ulrich SM (2007) Design and evaluation of 'Linkerless' hydroxamic acids as selective HDAC8 inhibitors. Bioorganic and Medicinal Chemistry Letters 17: 2874-8

Kugelberg E, Welander L (1956) Heredofamilial juvenile muscular atrophy simulating muscular dystrophy. AMA Arch Neurol Psychiatry 75: 500-9

Kultima K, Nystrom AM, Scholz B, Gustafson AL, Dencker L, Stigson M (2004) Valproic acid teratogenicity: a toxicogenomics approach. Environmental Health Perspectives 112: 1225-35

Laemmli UK (1970) Cleavage of structural proteins during the assembly of the head of bacteriophage T4. Nature 227: 680-5

Le TT, Pham LT, Butchbach ME, Zhang HL, Monani UR, Coovert DD, Gavrilina TO, Xing L, Bassell GJ, Burghes AH (2005) SMNDelta7, the major product of the centromeric survival motor neuron (SMN2) gene, extends survival in mice with spinal muscular atrophy and associates with full-length SMN. Hum Mol Genet 14: 845-57

Lefebvre S, Burglen L, Reboullet S, Clermont O, Burlet P, Viollet L, Benichou B, Cruaud C, Millasseau P, Zeviani M, et al. (1995) Identification and characterization of a spinal muscular atrophy-determining gene. Cell 80: 155-65

Lefebvre S, Burlet P, Liu Q, Bertrandy S, Clermont O, Munnich A, Dreyfuss G, Melki J (1997) Correlation between severity and SMN protein level in spinal muscular atrophy. Nat Genet 16: 265-9

Liu Q, Dreyfuss G (1996) A novel nuclear structure containing the survival of motor neurons protein. Embo J 15: 3555-65

Liu Q, Fischer U, Wang F, Dreyfuss G (1997) The spinal muscular atrophy disease gene product, SMN, and its associated protein SIP1 are in a complex with spliceosomal snRNP proteins. Cell 90: 1013-21

Lorson CL, Androphy EJ (2000) An exonic enhancer is required for inclusion of an essential exon in the SMA-determining gene SMN. Hum Mol Genet 9: 259-65

Lorson CL, Hahnen E, Androphy EJ, Wirth B (1999) A single nucleotide in the SMN gene regulates splicing and is responsible for spinal muscular atrophy. Proc Natl Acad Sci U S A 96: 6307-11

Lorson CL, Strasswimmer J, Yao JM, Baleja JD, Hahnen E, Wirth B, Le T, Burghes AH, Androphy EJ (1998) SMN oligomerization defect correlates with spinal muscular atrophy severity. Nat Genet 19: 63-6

Lunn MR, Root DE, Martino AM, Flaherty SP, Kelley BP, Coovert DD, Burghes AH, Man NT, Morris GE, Zhou J, Androphy EJ, Sumner CJ, Stockwell BR (2004) Indoprofen upregulates the survival motor neuron protein through a cyclooxygenase-independent mechanism. Chem Biol 11: 1489-93

Lunn MR, Wang CH (2008) Spinal muscular atrophy. Lancet 371: 2120-33

Markowitz JA, Tinkle MB, Fischbeck KH (2004) Spinal muscular atrophy in the neonate. J Obstet Gynecol Neonatal Nurs 33: 12-20

Marks PA, Richon VM, Rifkind RA (2000) Histone deacetylase inhibitors: inducers of differentiation or apoptosis of transformed cells. J Natl Cancer Inst 92: 1210-6

Martins RP, Krawetz SA (2004) Using multiplexed real-time polymerase chain reaction to rapidly identify single-copy transgenic animals. Anal Biochem 329: 337-9

Mattis VB, Ebert AD, Fosso MY, Chang CW, Lorson CL (2009a) Delivery of a read-through inducing compound, TC007, lessens the severity of a SMA animal model. Hum Mol Genet

Mattis VB, Ebert AD, Fosso MY, Chang CW, Lorson CL (2009b) Delivery of a read-through inducing compound, TC007, lessens the severity of a SMA animal model. Human Molecular Genetics

Mattis VB, Rai R, Wang J, Chang CW, Coady T, Lorson CL (2006) Novel aminoglycosides increase SMN levels in spinal muscular atrophy fibroblasts. Hum Genet 120: 589-601

McWhorter ML, Monani UR, Burghes AH, Beattie CE (2003) Knockdown of the survival motor neuron (Smn) protein in zebrafish causes defects in motor axon outgrowth and pathfinding. J Cell Biol 162: 919-31

Melki J, Abdelhak S, Sheth P, Bachelot MF, Burlet P, Marcadet A, Aicardi J, Barois A, Carriere JP, Fardeau M, et al. (1990) Gene for chronic proximal spinal muscular atrophies maps to chromosome 5q. Nature 344: 767-8

Melki J, Burlet P, Clermont O, Pascal F, Paul B, Abdelhak S, Sherrington R, Gurling H, Nakamura Y, Weissenbach J, et al. (1993) Refined linkage map of chromosome 5 in the region of the spinal muscular atrophy gene. Genomics 15: 521-4

Melki J, Lefebvre S, Burglen L, Burlet P, Clermont O, Millasseau P, Reboullet S, Benichou B, Zeviani M, Le Paslier D, et al. (1994) De novo and inherited deletions of the 5q13 region in spinal muscular atrophies. Science 264: 1474-7

Miguel-Aliaga I, Culetto E, Walker DS, Baylis HA, Sattelle DB, Davies KE (1999) The Caenorhabditis elegans orthologue of the human gene responsible for spinal muscular atrophy is a maternal product critical for germline maturation and embryonic viability. Hum Mol Genet 8: 2133-43

Mohaghegh P, Rodrigues NR, Owen N, Ponting CP, Le TT, Burghes AH, Davies KE (1999) Analysis of mutations in the tudor domain of the survival motor neuron protein SMN. Eur J Hum Genet 7: 519-25

Monani UR, Lorson CL, Parsons DW, Prior TW, Androphy EJ, Burghes AH, McPherson JD (1999) A single nucleotide difference that alters splicing patterns distinguishes the SMA gene SMN1 from the copy gene SMN2. Hum Mol Genet 8: 1177-83

Monani UR, Pastore MT, Gavrilina TO, Jablonka S, Le TT, Andreassi C, DiCocco JM, Lorson C, Androphy EJ, Sendtner M, Podell M, Burghes AH (2003) A transgene carrying an A2G missense mutation in the SMN gene modulates phenotypic severity in mice with severe (type I) spinal muscular atrophy. J Cell Biol 160: 41-52

Monani UR, Sendtner M, Coovert DD, Parsons DW, Andreassi C, Le TT, Jablonka S, Schrank B, Rossol W, Prior TW, Morris GE, Burghes AH (2000) The human centromeric survival motor neuron gene (SMN2) rescues embryonic lethality in Smn(-/-) mice and results in a mouse with spinal muscular atrophy. Hum Mol Genet 9: 333-9

Montes J, Gordon AM, Pandya S, De Vivo DC, Kaufmann P (2009) Clinical outcome measures in spinal muscular atrophy. J Child Neurol 24: 968-78

Mosmann T (1983) Rapid colorimetric assay for cellular growth and survival: application to proliferation and cytotoxicity assays. J Immunol Methods 65: 55-63

Mullis KB, Faloona FA (1987) Specific synthesis of DNA in vitro via a polymerase-catalyzed chain reaction. Methods Enzymol 155: 335-50

Munsat TL, Davies KE (1992) International SMA consortium meeting. (26-28 June 1992, Bonn, Germany). Neuromuscul Disord 2: 423-8

Narver HL, Kong L, Burnett BG, Choe DW, Bosch-Marce M, Taye AA, Eckhaus MA, Sumner CJ (2008a) Sustained improvement of spinal muscular atrophy mice treated with trichostatin A plus nutrition. Ann Neurol 64: 465-70

Narver HL, Kong L, Burnett BG, Choe DW, Bosch-Marce M, Taye AA, Eckhaus MA, Sumner CJ (2008b) Sustained improvement of spinal muscular atrophy mice treated with trichostatin A plus nutrition. Annals of Neurology 64: 465-70

Nover L, Scharf KD, Neumann D (1989) Cytoplasmic heat shock granules are formed from precursor particles and are associated with a specific set of mRNAs. Mol Cell Biol 9: 1298-308

Oehme I, Deubzer HE, Wegener D, Pickert D, Linke JP, Hero B, Kopp-Schneider A, Westermann F, Ulrich SM, von Deimling A, Fischer M, Witt O (2009) Histone deacetylase 8 in neuroblastoma tumorigenesis. Clinical Cancer Research 15: 91-9

Oprea GE, Krober S, McWhorter ML, Rossoll W, Muller S, Krawczak M, Bassell GJ, Beattie CE, Wirth B (2008) Plastin 3 is a protective modifier of autosomal recessive spinal muscular atrophy. Science 320: 524-7

Owen N, Doe CL, Mellor J, Davies KE (2000) Characterization of the Schizosaccharomyces pombe orthologue of the human survival motor neuron (SMN) protein. Hum Mol Genet 9: 675-84

Pandey UB, Nie Z, Batlevi Y, McCray BA, Ritson GP, Nedelsky NB, Schwartz SL, DiProspero NA, Knight MA, Schuldiner O, Padmanabhan R, Hild M, Berry DL, Garza D, Hubbert CC, Yao TP, Baehrecke EH, Taylor JP (2007) HDAC6 rescues neurodegeneration and provides an essential link between autophagy and the UPS. Nature 447: 859-63

Paushkin S, Charroux B, Abel L, Perkinson RA, Pellizzoni L, Dreyfuss G (2000) The survival motor neuron protein of Schizosacharomyces pombe. Conservation of survival motor neuron interaction domains in divergent organisms. J Biol Chem 275: 23841-6

Paushkin S, Gubitz AK, Massenet S, Dreyfuss G (2002) The SMN complex, an assemblyosome of ribonucleoproteins. Curr Opin Cell Biol 14: 305-12

Pavlidis P, Noble WS (2001) Analysis of strain and regional variation in gene expression in mouse brain. Genome Biology 2: RESEARCH0042

Pazin MJ, Kadonaga JT (1997) What's up and down with histone deacetylation and transcription? Cell 89: 325-8

Pearn JH, Hudgson P, Walton JN (1978) A clinical and genetic study of spinal muscular atrophy of adult onset: the autosomal recessive form as a discrete disease entity. Brain 101: 591-606

Peart MJ, Smyth GK, van Laar RK, Bowtell DD, Richon VM, Marks PA, Holloway AJ, Johnstone RW (2005) Identification and functional significance of genes regulated by structurally different histone deacetylase inhibitors. Proc Natl Acad Sci U S A 102: 3697-702

Pellizzoni L (2007) Chaperoning ribonucleoprotein biogenesis in health and disease. EMBO Rep 8: 340-5

Pellizzoni L, Charroux B, Dreyfuss G (1999) SMN mutants of spinal muscular atrophy patients are defective in binding to snRNP proteins. Proc Natl Acad Sci U S A 96: 11167-72

Piazzon N, Rage F, Schlotter F, Moine H, Branlant C, Massenet S (2008) In vitro and in cellulo evidences for association of the survival of motor neuron complex with the fragile X mental retardation protein. J Biol Chem 283: 5598-610

Prior FA, Tackaberry ES, Aubin RA, Casley WL (2006) Accurate determination of zygosity in transgenic rice by real-time PCR does not require standard curves or efficiency correction. Transgenic Res 15: 261-5

Rajendra TK, Gonsalvez GB, Walker MP, Shpargel KB, Salz HK, Matera AG (2007) A Drosophila melanogaster model of spinal muscular atrophy reveals a function for SMN in striated muscle. J Cell Biol 176: 831-41

Rak K, Lechner BD, Schneider C, Drexl H, Sendtner M, Jablonka S (2009) Valproic acid blocks excitability in SMA type I mouse motoneurons. Neurobiology of Disease

Raker VA, Hartmuth K, Kastner B, Luhrmann R (1999) Spliceosomal U snRNP core assembly: Sm proteins assemble onto an Sm site RNA nonanucleotide in a specific and thermodynamically stable manner. Mol Cell Biol 19: 6554-65

Riessland M, Brichta L, Hahnen E, Wirth B (2006) The benzamide M344, a novel histone deacetylase inhibitor, significantly increases SMN2 RNA/protein levels in spinal muscular atrophy cells. Hum Genet 120: 101-10

Rochette CF, Gilbert N, Simard LR (2001) SMN gene duplication and the emergence of the SMN2 gene occurred in distinct hominids: SMN2 is unique to Homo sapiens. Hum Genet 108: 255-66

Rose FF, Jr., Mattis VB, Rindt H, Lorson CL (2009a) Delivery of recombinant follistatin lessens disease severity in a mouse model of spinal muscular atrophy. Human Molecular Genetics 18: 997-1005

Rose FF, Jr., Mattis VB, Rindt H, Lorson CL (2009b) Delivery of recombinant follistatin lessens disease severity in a mouse model of spinal muscular atrophy. Hum Mol Genet 18: 997-1005

Roth SY, Denu JM, Allis CD (2001) Histone acetyltransferases. Annu Rev Biochem 70: 81-120

Roy N, Mahadevan MS, McLean M, Shutler G, Yaraghi Z, Farahani R, Baird S, Besner-Johnston A, Lefebvre C, Kang X, et al. (1995a) The gene for neuronal apoptosis inhibitory protein is partially deleted in individuals with spinal muscular atrophy. Cell 80: 167-78

Roy N, McLean MD, Besner-Johnston A, Lefebvre C, Salih M, Carpten JD, Burghes AH, Yaraghi Z, Ikeda JE, Korneluk RG, et al. (1995b) Refined physical map of the spinal muscular atrophy gene (SMA) region at 5q13 based on YAC and cosmid contiguous arrays. Genomics 26: 451-60

Rudnik-Schoneborn S, Forkert R, Hahnen E, Wirth B, Zerres K (1996) Clinical spectrum and diagnostic criteria of infantile spinal muscular atrophy: further delineation on the basis of SMN gene deletion findings. Neuropediatrics 27: 8-15

Russman BS, Iannaccone ST, Samaha FJ (2003) A phase 1 trial of riluzole in spinal muscular atrophy. Arch Neurol 60: 1601-3

Salah-Mohellibi N, Millet G, Andre-Schmutz I, Desforges B, Olaso R, Roblot N, Courageot S, Bensimon G, Cavazzana-Calvo M, Melki J (2006) Bone marrow transplantation attenuates the myopathic phenotype of a muscular mouse model of spinal muscular atrophy. Stem Cells 24: 2723-32

Sandberg R, Yasuda R, Pankratz DG, Carter TA, Del Rio JA, Wodicka L, Mayford M, Lockhart DJ, Barlow C (2000) Regional and strain-specific gene expression mapping in the adult mouse brain. Proceedings of the National Academy of Sciences of the United States of America 97: 11038-43

Schlattner U, Tokarska-Schlattner M, Wallimann T (2006) Mitochondrial creatine kinase in human health and disease. Biochim Biophys Acta 1762: 164-80

Schmutz J, Martin J, Terry A, Couronne O, Grimwood J, Lowry S, Gordon LA, Scott D, Xie G, Huang W, Hellsten U, Tran-Gyamfi M, She X, Prabhakar S, Aerts A, Altherr M, Bajorek E, Black S, Branscomb E, Caoile C, Challacombe JF, Chan YM, Denys M, Detter JC, Escobar J, Flowers D, Fotopulos D, Glavina T, Gomez M, Gonzales E, Goodstein D, Grigoriev I, Groza M, Hammon N, Hawkins T, Haydu L, Israni S, Jett J, Kadner K, Kimball H, Kobayashi A, Lopez F, Lou Y, Martinez D, Medina C, Morgan J, Nandkeshwar R, Noonan JP, Pitluck S, Pollard M, Predki P, Priest J, Ramirez L, Retterer J, Rodriguez A, Rogers S, Salamov A, Salazar A, Thayer N, Tice H, Tsai M, Ustaszewska A, Vo N, Wheeler J, Wu K, Yang J, Dickson M, Cheng JF, Eichler EE, Olsen A, Pennacchio LA, Rokhsar DS, Richardson P, Lucas SM, Myers RM, Rubin EM (2004) The DNA sequence and comparative analysis of human chromosome 5. Nature 431: 268-74

Schrank B, Gotz R, Gunnersen JM, Ure JM, Toyka KV, Smith AG, Sendtner M (1997) Inactivation of the survival motor neuron gene, a candidate gene for human spinal muscular atrophy, leads to massive cell death in early mouse embryos. Proc Natl Acad Sci U S A 94: 9920-5

Setola V, Terao M, Locatelli D, Bassanini S, Garattini E, Battaglia G (2007) Axonal-SMN (a-SMN), a protein isoform of the survival motor neuron gene, is specifically involved in axonogenesis. Proc Natl Acad Sci U S A 104: 1959-64

Shafey D, Cote PD, Kothary R (2005) Hypomorphic Smn knockdown C2C12 myoblasts reveal intrinsic defects in myoblast fusion and myotube morphology. Exp Cell Res 311: 49-61

Singh NK, Singh NN, Androphy EJ, Singh RN (2006) Splicing of a critical exon of human survival motor neuron is regulated by a unique silencer element located in the last intron. Mol Cell Biol 26: 1333-46

Soares VM, Brzustowicz LM, Kleyn PW, Knowles JA, Palmer DA, Asokan S, Penchaszadeh GK, Munsat TL, Gilliam TC (1993) Refinement of the spinal muscular atrophy locus to the interval between D5S435 and MAP1B. Genomics 15: 365-71

Sterner DE, Berger SL (2000) Acetylation of histones and transcription-related factors. Microbiol Mol Biol Rev 64: 435-59

Strahl BD, Allis CD (2000) The language of covalent histone modifications. Nature 403: 41-5

Sumner CJ, Huynh TN, Markowitz JA, Perhac JS, Hill B, Coovert DD, Schussler K, Chen X, Jarecki J, Burghes AH, Taylor JP, Fischbeck KH (2003) Valproic acid increases SMN levels in spinal muscular atrophy patient cells. Ann Neurol 54: 647-54

Sun Y, Grimmler M, Schwarzer V, Schoenen F, Fischer U, Wirth B (2005) Molecular and functional analysis of intragenic SMN1 mutations in patients with spinal muscular atrophy. Hum Mutat 25: 64-71

Swoboda KJ, Scott CB, Reyna SP, Prior TW, LaSalle B, Sorenson SL, Wood J, Acsadi G, Crawford TO, Kissel JT, Krosschell KJ, D'Anjou G, Bromberg MB, Schroth MK, Chan GM, Elsheikh B, Simard LR (2009) Phase II open label study of valproic acid in spinal muscular atrophy. PLoS One 4: e5268

Takai N, Ueda T, Nishida M, Nasu K, Narahara H (2006) M344 is a novel synthesized histone deacetylase inhibitor that induces growth inhibition, cell cycle arrest, and apoptosis in human endometrial cancer and ovarian cancer cells. Gynecol Oncol 101: 108-13

Thompson TG, Morrison KE, Kleyn P, Bengtsson U, Gilliam TC, Davies KE, Wasmuth JJ, McPherson JD (1993) High resolution physical map of the region surrounding the spinal muscular atrophy gene. Hum Mol Genet 2: 1169-76

Tini M, Benecke A, Um SJ, Torchia J, Evans RM, Chambon P (2002) Association of CBP/p300 acetylase and thymine DNA glycosylase links DNA repair and transcription. Mol Cell 9: 265-77

Tsai LK, Tsai MS, Ting CH, Li H (2008a) Multiple therapeutic effects of valproic acid in spinal muscular atrophy model mice. J Mol Med 86: 1243-54

Tsai LK, Tsai MS, Ting CH, Li H (2008b) Multiple therapeutic effects of valproic acid in spinal muscular atrophy model mice. J Mol Med

Ueda H, Manda T, Matsumoto S, Mukumoto S, Nishigaki F, Kawamura I, Shimomura K (1994a) FR901228, a novel antitumor bicyclic depsipeptide produced by Chromobacterium violaceum No. 968. III. Antitumor activities on experimental tumors in mice. J Antibiot (Tokyo) 47: 315-23

Ueda H, Nakajima H, Hori Y, Fujita T, Nishimura M, Goto T, Okuhara M (1994b) FR901228, a novel antitumor bicyclic depsipeptide produced by Chromobacterium violaceum No. 968. I. Taxonomy, fermentation, isolation, physico-chemical and biological properties, and antitumor activity. J Antibiot (Tokyo) 47: 301-10

van Bergeijk J, Rydel-Konecke K, Grothe C, Claus P (2007) The spinal muscular atrophy gene product regulates neurite outgrowth: importance of the C terminus. Faseb J 21: 1492-502

Van den Wyngaert I, de Vries W, Kremer A, Neefs J, Verhasselt P, Luyten WH, Kass SU (2000) Cloning and characterization of human histone deacetylase 8. FEBS Letters 478: 77-83

Van Lint C, Emiliani S, Verdin E (1996) The expression of a small fraction of cellular genes is changed in response to histone hyperacetylation. Gene Expr 5: 245-53

Venkatesh PR, Goh E, Zeng P, New LS, Xin L, Pasha MK, Sangthongpitag K, Yeo P, Kantharaj E (2007) In vitro phase I cytochrome P450 metabolism, permeability and pharmacokinetics of SB639, a novel histone deacetylase inhibitor in preclinical species. Biol Pharm Bull 30: 1021-4

Viollet L, Bertrandy S, Bueno Brunialti AL, Lefebvre S, Burlet P, Clermont O, Cruaud C, Guenet JL, Munnich A, Melki J (1997) cDNA isolation, expression, and chromosomal localization of the mouse survival motor neuron gene (Smn). Genomics 40: 185-8

Vitte JM, Davoult B, Roblot N, Mayer M, Joshi V, Courageot S, Tronche F, Vadrot J, Moreau MH, Kemeny F, Melki J (2004) Deletion of murine Smn exon 7 directed to liver leads to severe defect of liver development associated with iron overload. Am J Pathol 165: 1731-41

von Deimling F, Scharf JM, Liehr T, Rothe M, Kelter AR, Albers P, Dietrich WF, Kunkel LM, Wernert N, Wirth B (1999) Human and mouse RAD17 genes: identification, localization, genomic structure and histological expression pattern in normal testis and seminoma. Hum Genet 105: 17-27

Walker MP, Rajendra TK, Saieva L, Fuentes JL, Pellizzoni L, Matera AG (2008) SMN complex localizes to the sarcomeric Z-disc and is a proteolytic target of calpain. Hum Mol Genet 17: 3399-410

Wen YD, Perissi V, Staszewski LM, Yang WM, Krones A, Glass CK, Rosenfeld MG, Seto E (2000) The histone deacetylase-3 complex contains nuclear receptor corepressors. Proceedings of the National Academy of Sciences of the United States of America 97: 7202-7

Werdnig (1891) Zwei frühinfantile hereditäre Fälle von progressiver Muskelatrophie unter dem Bilde
der Dystrophie, aber auf neurotischer Grundlage.
. Archiv für Psychiatrie und Nervenkrankheiten.: 437-480

Williams JH, Schray RC, Patterson CA, Ayitey SO, Tallent MK, Lutz GJ (2009a) Oligonucleotide-mediated survival of motor neuron protein expression in CNS improves phenotype in a mouse model of spinal muscular atrophy. Journal of Neuroscience 29: 7633-8

Williams JH, Schray RC, Patterson CA, Ayitey SO, Tallent MK, Lutz GJ (2009b) Oligonucleotide-mediated survival of motor neuron protein expression in CNS improves phenotype in a mouse model of spinal muscular atrophy. J Neurosci 29: 7633-8

Wirth B (2000) An update of the mutation spectrum of the survival motor neuron gene (SMN1) in autosomal recessive spinal muscular atrophy (SMA). Hum Mutat 15: 228-37

Wirth B (2002) Spinal muscular atrophy: state-of-the-art and therapeutic perspectives. Amyotroph Lateral Scler Other Motor Neuron Disord 3: 87-95

Wirth B, el-Agwany A, Baasner A, Burghes A, Koch A, Dadze A, Piechaczeck-Wappenschmidt B, Rudnik-Schoneborn S, Zerres K, Schonling J (1995) Mapping of the spinal muscular atrophy (SMA) gene to a 750-kb interval flanked by two new microsatellites. Eur J Hum Genet 3: 56-60

Wirth B, Herz M, Wetter A, Moskau S, Hahnen E, Rudnik-Schoneborn S, Wienker T, Zerres K (1999) Quantitative analysis of survival motor neuron copies: identification of subtle SMN1 mutations in patients with spinal muscular atrophy, genotype-phenotype correlation, and implications for genetic counseling. Am J Hum Genet 64: 1340-56

Wirth B, Pick E, Leutner A, Dadze A, Voosen B, Knapp M, Piechaczek-Wappenschmidt B, Rudnik-Schoneborn S, Schonling J, Cox S, et al. (1994) Large linkage analysis in 100 families with autosomal recessive spinal muscular atrophy (SMA) and 11 CEPH families using 15 polymorphic loci in the region 5q11.2-q13.3. Genomics 20: 84-93

Wirth B, Schmidt T, Hahnen E, Rudnik-Schoneborn S, Krawczak M, Muller-Myhsok B, Schonling J, Zerres K (1997) De novo rearrangements found in 2% of index patients with spinal muscular atrophy: mutational mechanisms, parental origin, mutation rate, and implications for genetic counseling. Am J Hum Genet 61: 1102-11

Witt O, Deubzer HE, Milde T, Oehme I (2009) HDAC family: What are the cancer relevant targets? Cancer Lett 277: 8-21

Wolstencroft EC, Mattis V, Bajer AA, Young PJ, Lorson CL (2005) A non-sequence-specific requirement for SMN protein activity: the role of aminoglycosides in inducing elevated SMN protein levels. Hum Mol Genet 14: 1199-210

Workman E, Saieva L, Carrel TL, Crawford TO, Liu D, Lutz C, Beattie CE, Pellizzoni L, Burghes AH (2009) A SMN missense mutation complements SMN2 restoring snRNPs and rescuing SMA mice. Hum Mol Genet 18: 2215-29

Wyszynski DF, Nambisan M, Surve T, Alsdorf RM, Smith CR, Holmes LB (2005) Increased rate of major malformations in offspring exposed to valproate during pregnancy. Neurology 64: 961-5

Yang L, Mei Q, Zielinska-Kwiatkowska A, Matsui Y, Blackburn ML, Benedetti D, Krumm AA, Taborsky GJ, Jr., Chansky HA (2003) An ERG (ets-related gene)-associated histone methyltransferase interacts with histone deacetylases 1/2 and transcription co-repressors mSin3A/B. Biochem J 369: 651-7

Yang XJ (2004) The diverse superfamily of lysine acetyltransferases and their roles in leukemia and other diseases. Nucleic Acids Res 32: 959-76

Yang XJ, Seto E (2008) The Rpd3/Hda1 family of lysine deacetylases: from bacteria and yeast to mice and men. Nature Reviews. Molecular Cell Biology 9: 206-18

Young PJ, DiDonato CJ, Hu D, Kothary R, Androphy EJ, Lorson CL (2002) SRp30c-dependent stimulation of survival motor neuron (SMN) exon 7 inclusion is facilitated by a direct interaction with hTra2 beta 1. Hum Mol Genet 11: 577-87

Young PJ, Le TT, Dunckley M, Nguyen TM, Burghes AH, Morris GE (2001) Nuclear gems and Cajal (coiled) bodies in fetal tissues: nucleolar distribution of the spinal muscular atrophy protein, SMN. Exp Cell Res 265: 252-61

Young PJ, Le TT, thi Man N, Burghes AH, Morris GE (2000) The relationship between SMN, the spinal muscular atrophy protein, and nuclear coiled bodies in differentiated tissues and cultured cells. Exp Cell Res 256: 365-74

Zerres K, Davies KE (1999) 59th ENMC International Workshop: Spinal Muscular Atrophies: recent progress and revised diagnostic criteria 17-19 April 1998, Soestduinen, The Netherlands. Neuromuscul Disord 9: 272-8

Zerres K, Rudnik-Schoneborn S (1995) Natural history in proximal spinal muscular atrophy. Clinical analysis of 445 patients and suggestions for a modification of existing classifications. Arch Neurol 52: 518-23

Zhang HL, Pan F, Hong D, Shenoy SM, Singer RH, Bassell GJ (2003) Active transport of the survival motor neuron protein and the role of exon-7 in cytoplasmic localization. J Neurosci 23: 6627-37

Zhang ML, Lorson CL, Androphy EJ, Zhou J (2001) An in vivo reporter system for measuring increased inclusion of exon 7 in SMN2 mRNA: potential therapy of SMA. Gene Ther 8: 1532-8

Zou J, Barahmand-pour F, Blackburn ML, Matsui Y, Chansky HA, Yang L (2004) Survival motor neuron (SMN) protein interacts with transcription corepressor mSin3A. J Biol Chem 279: 14922-8

10 Appendix

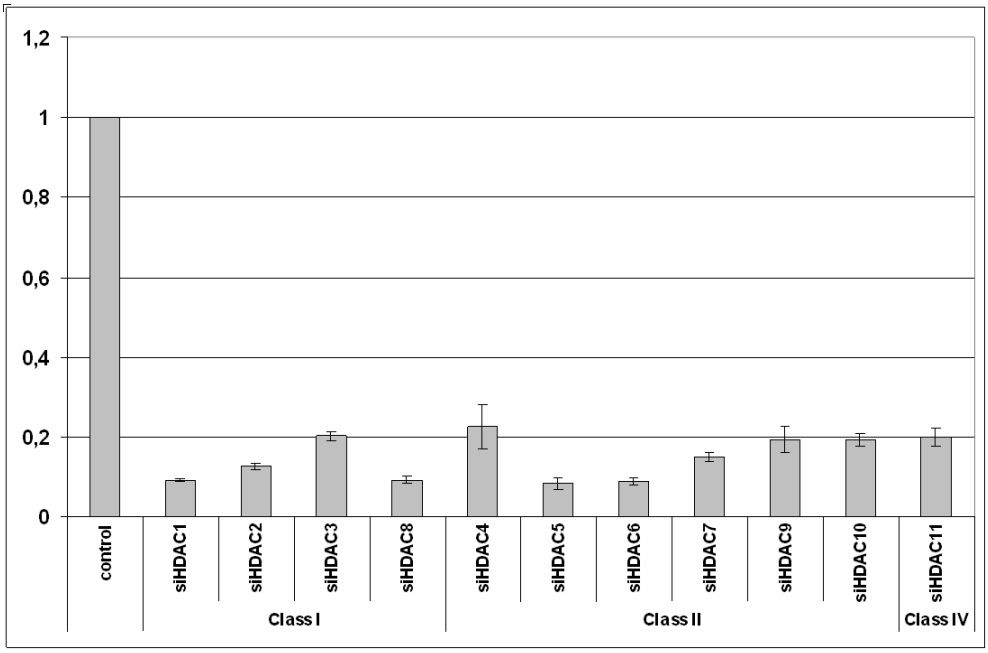

Figure 56 Diagrammatic representation of the knock-down efficiency of the respective siRNA approach. Knock-down efficiency was checked by quantitative real-time PCR, using primers for the respective targeted HDAC. Every knock-down was significant ($p<0.01$).

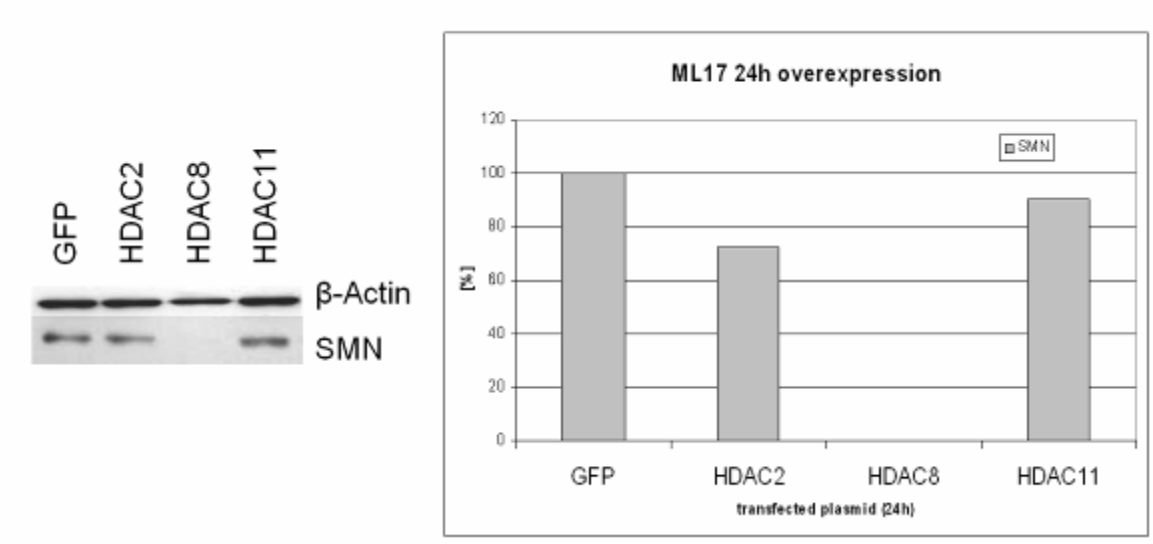

Figure 57 Western blot and the respective quantification after overexpression of GFP (as control transfection), HDAC2, HDAC8 and HDAC11 in ML17

	pIC_{50}
M344	6.52 ± 0.04
SAHA	6.30 ± 0.02
PCI-34051	4.23 ± 0.11
FK-228	8.07 ± 0.07
SB	3.10 ± 0.10
VPA#	2.14 ± 0.07

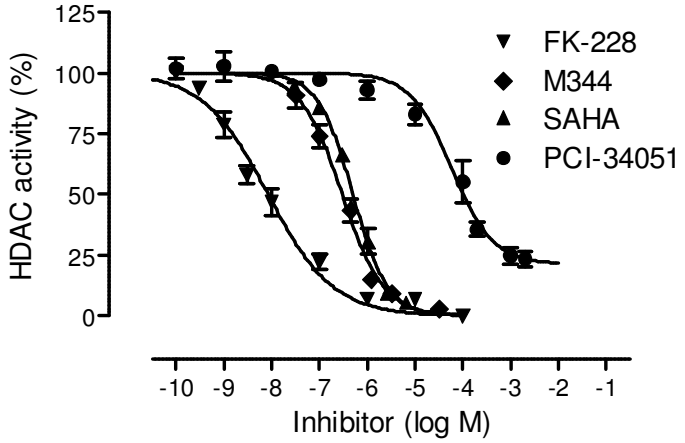

Figure 58 Fluorescent-based *in vitro* HDAC activity test to determine the inhibitory concentrations of the respective HDAC inhibitors. HDAC enzyme mixture was derived from rat liver extracts.

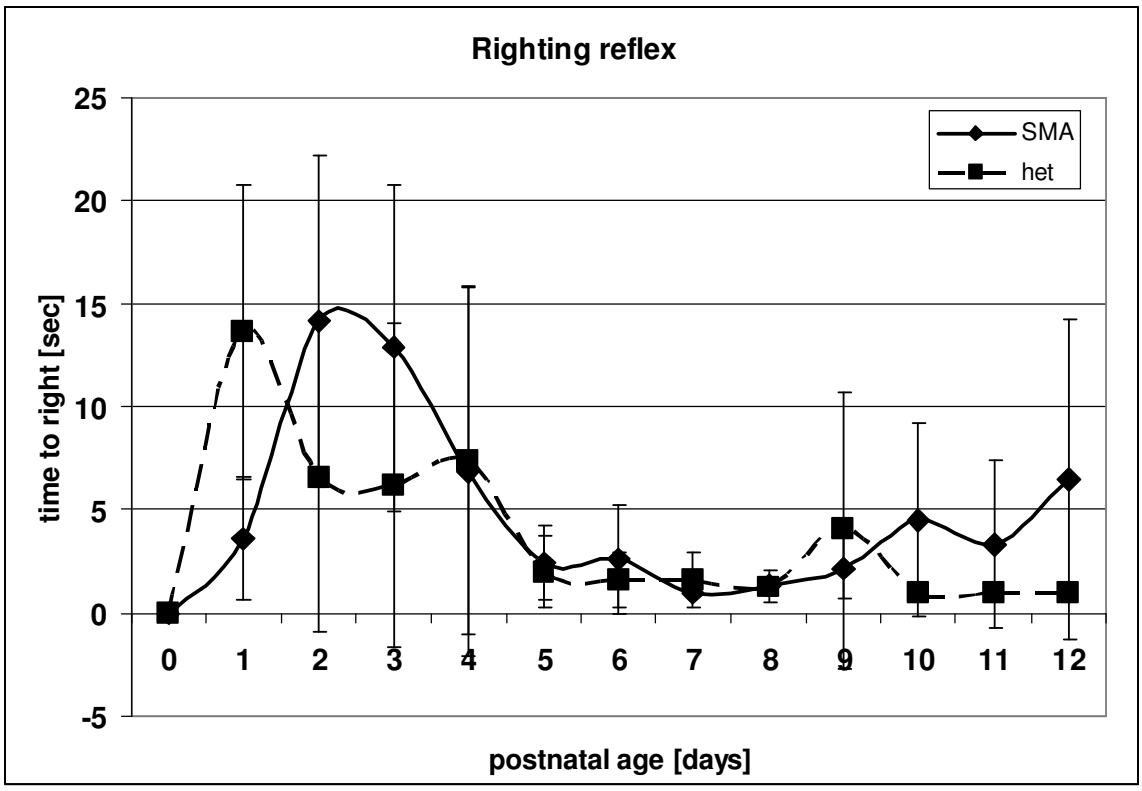

Figure 59 Motor ability experiment (righting reflex). Mice were placed on one side and time was measured until mice got back on four paws. Since the time [sec.] to right was not directly correlated with the genotype and subjected to massive fluctuations, the tube test was performed, to assess motor performance of the mice. (het=heterozygous (n=6), SMA=SMA-like mice(n=6))

Erklärung

Ich versichere, dass ich die von mir vorgelegte Dissertation selbständig angefertigt, die benutzten Quellen und Hilfsmittel vollständig angeben und die Stellen der Arbeit - einschließlich Tabellen, Karten und Abbildungen -, die anderen Werken im Wortlaut oder dem Sinn nach entnommen sind, in jedem Einzelfall als Entlehnung kenntlich gemacht habe; dass diese Dissertation noch keiner anderen Fakultät oder Universität zur Prüfung vorgelegen hat; dass sie - abgesehen von unten angegebenen Teilpublikationen - noch nicht veröffentlicht worden ist sowie, dass ich eine solche Veröffentlichung vor Abschluss des Promotionsverfahrens nicht vornehmen werde.
Die Bestimmungen der Promotionsordnung sind mir bekannt. Die von mir vorgelegte Dissertation ist von Prof. Dr. rer. nat. Brunhilde Wirth und Prof. Dr. rer. nat. Manolis Pasparakis betreut und in der Arbeitsgruppe von Prof. Dr. rer. nat. Brunhilde Wirth durchgeführt worden.

Teilpublikationen sind in Kapitel 8 angegeben.

Markus Rießland, Köln, den 28.09.2009